STUDIES ON STRESS INDUCED TAG ACCUMULATION IN MICROALGA *SCENEDESMUS* sp. IITRIND2

Ph.D THESIS

by

NEHA ARORA

DEPARTMENT OF BIOTECHNOLOGY
INDIAN INSTITUTE OF TECHNOLOGY ROORKEE
ROORKEE-247667, INDIA
MAY, 2018

STUDIES ON STRESS INDUCED TAG ACCUMULATION IN MICROALGA *SCENEDESMUS* sp. IITRIND2

A THESIS

Submitted in partial fulfilment of the
requirements for the award of the degree

of

DOCTOR OF PHILOSOPHY

in

BIOTECHNOLOGY

by

NEHA ARORA

DEPARTMENT OF BIOTECHNOLOGY
INDIAN INSTITUTE OF TECHNOLOGY ROORKEE
ROORKEE-247667, INDIA
MAY, 2018

INDIAN INSTITUTE OF TECHNOLOGY ROORKEE
ROORKEE

CANDIDATE'S DECLARATION

I hereby certify that the work which is being presented in the thesis entitled "**STUDIES ON STRESS INDUCED TAG ACCUMULATION IN MICROALGA *SCENEDESMUS* sp**. **IITRIND2**", in partial fulfilment of the requirements for the award of the degree of Doctor of Philosophy and submitted in the Department of Biotechnology of the Indian Institute of Technology Roorkee, Roorkee is an authentic record of my own work carried out during a period from July, 2014 to May, 2018 under the supervision of Dr. Vikas Pruthi, Professor, Department of Biotechnolgy, Indian Institute of Technology Roorkee, Roorkee.

The matter presented in the thesis has not been submitted by me for the award of any other degree of this or any other institute.

(**NEHA ARORA**)

This is to certify that the above statement made by the candidate is correct to the best of my knowledge.

(VIKAS PRUTHI)
Supervisor

Date:

Table of Contents

Chapter 1

Introduction and Review of literature

Chapter 2

Bioprospecting of novel indigenous high biomass and accumulating microalgal strains capable of growing in sea water

Chapter 3

Elucidation of molecular halotolerance mechanism of
***Scenedesmus* sp. using integrated omics approach**

Chapter 4

Assessing the robust growth and lipid accumulating characteristics of *Scenedesmus* sp. cultivated in natural sea water using small scale custom built photobioreactor

Chapter 5

Delineating the differential metabolic responses of *Scenedesmus* sp. during arsenic (III, V) mitigation

Chapter 6

Acknowledgements

To my life- coach, my father Dr. Gurpal Singh: because I owe it all to you.

First and foremost, I wish to thank my advisor, Dr. Vikas Pruthi, Professor, Department of Biotechnology, Indian Institute of Technology Roorkee for his continuous support, dedicated inspiration, patient guidance and constructive criticism throughout my Ph.D. His encouragement to carry out independent research has helped me to approach a problem with systemic thinking, data-driven decisions and raise new possibilities, aiding me to evolve as a better researcher.

My special word of thanks to Dr. Krishna Mohan Poluri, Assistant Professor, Department of Biotechnology, IIT Roorkee for his valuable teachings, cooperation, motivation and facilitating all the requirements during my Ph.D. which kept me going ahead.

I am also extremely indebted to Dr. Philip T. Pienkos, Strategic Project Lead, National Renewable Energy Laboratory (NREL), Golden, Colorado, USA for hosting me in his laboratory as a part of my B-ACER internship. His scientific inputs, valuable advice, guidance and extensive discussions around my work brought this thesis towards a completion. I owe a lot of gratitude to him and feel privileged to be associated with a person like him.

I owe a great deal of appreciation and gratitude to Dr. Michael T. Guarnieri, Researcher IV-Molecular Biology, NREL Dr. Ambarish Nag, Researcher IV-Data Science, NREL, Dr. Lieve Laurens, Senior Scientist NREL and Dr. Thomas Dempster, Arizona State University for their support throughout out my stay at Colorado and providing me experimental hands-on-training on different aspects of large scale algal cultivation and transcriptomics.

I gratefully acknowledge Dr. Dinesh Kumar (CBMR, Lucknow) for providing NMR facility and teaching me metabolomics. Besides, I would like to thank the Department of Biotechnology and Institute Instrumentation centre (IIC), IIT Roorkee for instrument facilities to carry out my research work.

I express my heartfelt gratitude to Dr. Parul Pruthi, my SRC committee members: Dr. Sanjoy Ghosh, Dr. Naveen K. Navani, Dr. M.R. Maurya; DRC Chairman: Prof. R. Prasad; Head of the Department: Prof. A.K. Sharma, all faculty members for their constant support.

I would also like to extend huge, warm thanks to Laurie Lavine for her love, care and moral support. My special thanks to Nick, Fanni and Luke for providing me a stimulating and fun filled environment during my stay at NREL. Words fail me to express my appreciation to Bratati Chowdhury and Vaibhav Singh for their support, generous care and being there for me during the happy and hard moments to push me and motivate me. I would also like to thank my good friends (Poonam, Juhi, Vandana, Shweta, Alok, Rashmi, Khushboo, Nipanshu, Sajal, Purva, Viabhav, Sheenam, Anupriya), all of my lab mates, Dr. Durgesh and Amit from CBMR, Lucknow for their valuable help and support.

I would also like to thank some people from my early days of my research tenure, Dr. Sanjay Gupta, Dr. Seema, Dr. Shalini, Dr. Poonam Dev and Dr. Manisha Nanda were among those who kept me going at the beginning.

A special note of thanks to office staff, Department of Biotechnology, campus administration and workers of my hostel, Kasturba Bhawan for making my stay comfortable in campus.

I gratefully acknowledge Department of Biotechnology (DBT) for providing me financial support that made my Ph.D. work possible. I'll like to acknowledge Indo-US Science Technology Forum (IUSSTF) for B-ACER internship (2016) to support my lab visit at NREL, Colorado, USA for a period of 6 months. I also thank, Science and Engineering Research Board (SERB) for providing me travel grant to attend EUBCE-2018, Copenhagen, Denmark.

I would like to pay high regards to my mother, brother Robin, sister Dr. Iteeka, sister-in-law, Deepanjali Srivastava and brother-in-law Dr. Abhishek Dashora for their sincere encouragement, unconditional support and inspiration all these years and lifting me uphill throughout my life. I owe everything to them. Last but not the least, I shall pay obeisance in the name of Almighty God and express my thanks and profound gratefulness for giving me strength to peruse my dreams.

<div align="right">Neha Arora</div>

Abstract

Energy crisis, water shortage and pollution are among the major challenges confronting the sustainable environmental existence. Currently, fossil fuels fulfil 80 % of the world's primary energy requirements of which 58 % is consumed by the transportation sector. Renewable energy derived from sustainable feedstocks can reduce the load on the fossil fuels and curb the greenhouse gasses (GHG) emissions. Biofuels specifically biodiesel production has increased over the years (2.8 billion gallons in 2016) due to its renewability, reduced carbon emissions, unburned hydrocarbons and particulate emissions as compared to petro diesel engines. Biodiesel is a mixture of fatty acid methyl esters (FAMEs) derived from plant oils, animal fats, and waste cooking oils. However, plant oil derived biodiesel cannot be sustainable as edible oils compete with the food consumption. Further, non-edible oils and waste cooking oils have high amount of free fatty acids (FFA) which are undesirable for biodiesel production. Non edible oils also demand large areas of land reserves and water resources, thus competing with food crops.

Additional to the fuel crisis, heavy metals disembogue into water bodies have also led to loss of aquatic life, bioaccumulation and biomagnification of toxins in the food chain. Removal of heavy metals from the water sources is critical as they are non-biodegradable, recalcitrant and can abolish the self-purification ability of aquatic bodies leading to toxic water supply. Among the heavy metals, arsenic (As) is one of the major toxin contaminating the groundwater in many countries including India, China, Vietnam, Bangladesh and Pakistan. United States Environmental Protection Agency (USEPA) has classified arsenic as Group 1 carcinogen based on human epidemiological data. European Union has fixed a maximum limit up to 10 μg ml^{-1} for As contamination. However, exposure to As even in low quantities (0.1 μg ml^{-1}) can increase the risk of skin, kidney, lung and bladder cancers. Currently various physico-chemical treatment methods are employed including ion-exchange, precipitation, solar distillation for removal of As from water bodies. However, methods listed above produce As laden discards which needs to be treated further before being finally discharged into water bodies.

In view of the current scenario, utilization of microorganisms specifically photosynthetic green microalgae has been considered as potential cell factories for the production of biodiesel and as prospective bioremediators. They have faster doubling time, require less land, high photosynthetic ability and biomass production as compared to energy crops such as rapeseed and soybean. Furthermore, they have a unique ability to adapt to various

environmental conditions ranging from fresh water to marine and even waste water along with mitigation of of CO_2. Under adverse conditions such as nutrient limitation, temperature, pH, light intensity, heavy metal etc. microalgae can accumulate up to 50-60 % of lipids (dry cell weight) making them as desirable feedstocks for biodiesel production. These stored lipids or triacylglycerol (TAGs) contain fatty acids ranging from C12-C24 that are identical to plant oils (Jatropha, Palm, and Soya). Moreover, microalgae have high metal binding capacity and they can remove arsenic by adsorbing the heavy metal onto its surface as its cell wall is composed of different functional groups which act as binding sites for heavy metals followed by intracellular metabolism.

Despite the great potential of microalgae for biodiesel and mitigation of arsenic, its utilization on large scale is still a long road ahead. To bridge this gap, reduction in the cost of algal production encompassing bioprospecting of potential high lipid accumulating strains, utilization of sea water for cultivating microalgae and integrating As removal with biodiesel production are quintessential. Further, understanding the molecular adaption mechanisms in response salt and metal stress in prospective oleaginous microalgal strains could lead to successful modifications in the expression of key lipid/salt/metal associated enzymes resulting in overall improved productivity. This could be achieved by through knowledge of algal-omics which can then be manipulated to achieve desirable outcomes. Keeping the above view in mind, the specific details of thesis chapters (1-5) are as follows:

Chapter 1 gives an overview on energy crisis and arsenic pollution with the role of microalgae as a potential feedstock for biodiesel production and as a budding tool for mitigating arsenic from the contaminated waters. A detailed literature survey of algal omics techniques (proteomics, metabolomics and lipidomics) and their role in identification of potential genetic engineering targets for boosting TAG accumulation have also been discussed.

Chapter 2 deals with the bioprospecting of indigenous high biomass and lipid accumulating microalgal strains capable of growing sea water. A total of four strains (*Scenedesmus* sp. IITRIND2, *Chlamydomonas debarayna* IITRIND3; *Chlorella* sp., and *Tetradesmus obliquus* IITRIND1) were isolated from a fresh water lake and three procured strains (*Chlorella minutissima*, *Scenedesmus abundans* and *Chlorella pyrendosia*) were evaluated for salt tolerance by cultivating in artificial sea water (ASW; 35 g/L sea salts). Among the isolated strains, *Scenedesmus* sp. IITRIND2 was able to grow in ASW and thus was chosen for further experiments. The microalga attained maximum lipid productivity of 83 ± 2 mg/L/d in ASW as compared to the Bold's basal media (BBM) (25 ± 1.2 mg/L/d). The increase

in the lipid content was balanced by a sharp decrease in its protein and carbohydrate content. Further, biochemical analysis evidenced that salinity induced oxidative stress resulted in reduced levels of photosynthetic pigments, elevated H_2O_2, thiobarbituric acid reactive substances, proline, glycine betaine, catalase and ascorbate peroxidase activity attributing to microalga's halotolerance. The FAME analysis revealed the dominance of C14:0, C16:0, C18:0, C18:1 and C18:2 fatty acids under halotolerant conditions. Further, the properties of biodiesel resulted under saline conditions were in compliance with ASTM D6751 and EN 14214 fuel standards indicating that the lipid augmented halotolerant algal strains capable of growing in sea water can be formulated as environmental sustainable and economic viable sources for biodiesel production.

Chapter 3 characterizes the halotolerance and TAG accumulating mechanism of *Scenedesmus* sp. IITRIND2 in response to ASW (35 g/L sea salts) as compared to control (0 g/L sea salts) by studying both physiological and molecular responses. On exposure to salinity, the microalga rewired its cellular reserves and ultrastructure, restricted the ions channels, modulated its surface potential along with secretion of extrapolysaccharide to maintain homeostasis and resolve the cellular damage. To gain further insights into the molecular responses under halotolerance conditions, an "integrated omics approach" comprising of metabolomics, proteomics and lipidomics studies was utilized. The obtained results were complemented with real time polymerase chain reaction (RT-PCR). The algal-omics studies suggested a well organised salinity driven metabolic adjustment by the microalga starting from increasing the negatively charged lipids, up regulation of proline and sugars accumulation followed by direction of carbon and energy flux towards TAG synthesis. Further, the algal-omics studies indicated both *de-novo* and lipid cycling pathways at work for increasing the overall TAG accumulation inside the microalgal cells. Such a salt response is unique and different from the well-known halotolerant microalga; *Dunaliella salina*, implying diversity in algal response with species. Based on the integrated algal-omics studies, four potential genetic targets belonging to two different metabolic pathways (salt tolerance and lipid production) were identified.

Chapter 4 illustrates the potential of *Scenedesmus* sp. IITRIND2 for carbohydrate and lipid accumulation by cultivating in natural sea water in a small-scale custom built photobioreactor. The microalga showed remarkable ability to cope up with different salinity environments under given temperature and light conditions. Such an adaptation was attributed

to the increase in neutral sugars, such as glucose, mannose, galactose, fucose and ribose, associated with both structural and storage (and potentially osmoprotectant) polymeric carbohydrates. The carbohydrate rearrangements may aid with rewiring the cellular components and membrane permeability in circumventing the detrimental effects of high salinity. The microalga showed high carbohydrate and lipid accumulation, signifying its potential for integrated bioethanol and biodiesel production. *(This work was a part of Bioenergy-Awards for Cutting Edge Research (B-ACER), 2016 carried out under the supervision of Dr. Philip T. Pienkos, Strategic Project Lead, NREL, CO, USA).*

Chapter 5 aims to integrate toxic and carcinogenic heavy metal arsenic (both III and V forms) removal coupled to biodiesel production by *Scenedesmus* sp. IITRIND2. The microalga was able to tolerate half a gram of As (III) and As (V) forms in synthetic soft water (SSW) triggering lipid production along with efficient removal of the toxic heavy metal from SSW. The bioremediation mechanism was studied by analysing the changes in its biochemical, biophysical and metabolic characteristics. The results suggested that by using a complex interplay of biomolecular, photosynthetic agents and varied metabolites, the microalga tolerated the arsenic stress. The study also revealed that the metabolic changes in the presence of As (III) and As (V) are differential in nature, and were more extensive in the presence of As (V) due to its enhanced toxicity, thus evidencing for variable perturbations in major cellular metabolic pathways.

In summary, the thesis highlighted the unique characteristics of a novel fresh water microalga; *Scenedesmus* sp. IITRIND2 which efficiently adapted to sea water and arsenic contaminated waters along with high biomass and TAG accumulation. Utilization of various biophysical and algal-omics techniques unravelled the physiological and molecular mechanism involved for salt and arsenic tolerance. This comprehensive study will help identifying biomarkers for TAG increment along with salt and metal tolerance that could be potential genetic engineering targets in microalgal strains.

List of Figures

List of Tables

Abbreviations and Acronyms

°C	Degree Celsius
$	Dollar
2D	Two-Dimensional
AB	ArsenoBetaine
AC	ArsenoCholin
ACCase	Acetyl-CoA Carboxylase
ACP	Acyl Carrier Protein
AFDCW	Ash Free Dry Cell Weight
AGP-L	ADP-Glucose Pyrophosphorylase-Large subunit
AMP	Adenosine Monophosphate
AMPK	AMP Kinase
APX	Ascorbate Peroxidase
As	Arsenic
ASTM	American Society for Testing and Materials
ASW	Artificial Sea Water
ATP	Adenosine Triphosphate
BAF	BioAccumulation Factor
BBM	Bold's Basal media
BLAST	Basic Local Alignment Search Tool
CA	Carbonic Anhydrase
Ca^{+2}	Calcium ion
CAT	Catalase
CCM	Carbon concentration mechanism
CE-MS	Capillary Electrophoresis Mass Spectroscopy
CFPP	Cold Filter Plugging Point
cm	Centimetre
CN	Cetane number
CO_2	Carbon dioxide
CPMG	Carr–Purcell–Meiboom–Gill
d	Days
DAG	Diacylglycerol

DCW	Dry Cell Weight
DGAT	Diacylglycerol Acyltransferase
DGDG	DiGalactosylDiacylGlycerol
DIC	Dissolved Inorganic Carbon
DMA	DiMethylArsinate
DOE	U.S. Department of Energy
DU	Degree of Unsaturation
EMS	Ethyl Methane Sulfonate
EN	European Committee for Standardization
ENR	Enoyl ACP Reductase
EPS	Extracellular PolySaccharide
ER	Endoplasmic Reticulum
FAMEs	Fatty Acid Methyl Esters
FAS	Fatty Acid Synthase
Fd	Ferredoxin
FE-SEM	Field Emission Scanning Electron Microscopy
FTIR	Fourier-Transform Infrared spectroscopy
g	Gram
G 3-P	Glycerol 3- Phosphate
GADPH	Glyceraldehyde 3 Phosphate Dehydrogenase
GC-MS	Gas Chromatography- Mass Spectroscopy
GGPP	Geranyl Geranyl Pyrophosphate
GPAT	Glycerol Phosphate Acyl Transferase
GPC	GlyceroPhosphoCholine
GSH	Glutathione
Gt	Gigatonnes
h	Hour
HD	3-Hyroxyacyl ACP Dehydrase
HHV	High Heating Value
HMF	5-HydroxyMethylFurfural
HPLC	High-Performance Liquid Chromatography
ICPMS	Inductive Coupled Plasma Mass Spectroscopy
IEA	International Energy Agency
iTRAQ	Isobaric Tags for Relative and Absolute Quantification

IV	Iodine Value
JME	Jatropha oil Methyl Esters
K^+	Potassium
KAR	3-Ketoacyl ACP Reductase
Kg	Kilograms
KV	Kinematic Viscosity
L	Litre
LC	Liquid Chromatography
LCSF	Long Chain Saturation Factor
LDSP	Lipid Droplet Surface Protein
LPAAT	Lyso-Phosphatidic Acid Acyltransferase
LPAT	Lyso-Phosphatidylcholine Acyltransferase
m	Meters
MALDI	Matrix-Assisted Laser Desorption/Ionization
ME	Malic Enzyme
MGDG	Mono Galactosyl DiacylGlycerol
MGDG	Monogalactosyl Diacylglycerol
min	Minute
MJ	Mega Joules
mL	MilliLiter
MLDP	Major Lipid droplet protein
mm	MilliMetre
MMA	MonoMethylArsonate
mmol	Milli Moles
MS	Mass Spectroscopy
MUFA	MonoUnsaturated Fatty Acids
Na^+	Sodium
NADH	Nicotinamide Adenine Dinucleotide
NADPH	Nicotinamide Adenine Dinucleotide Phosphate
NCBI	National Centre for Biotechnology Information
NMR	Nuclear Magnetic Resonance
NREL	National Renewable Energy Laboratory
OS	Oxidative Stability
P5CR	Pyrroline-5-Carboxylate Reductase

P5CS	D^1- Pyrroline -5- Carboxylate Synthetase
PAD	Pulsed Amperomtric Detector
PBR	PhotoBio Reactor
PBS	Phosphate Buffer Saline
PC	PhosphatidylCholine
PC	PhytoChelatins
PCA	Principal Component Analysis
PDAT	Phospholipid:Diacylglycerol Acyl Transferase
PDC	Pyruvate Dehydrogenase Complex
PE	PhosphatidylEthanolamine
PE	Photosynthetic Efficiency
PG	PhosphatidylGlycerol
PGAM	Phosphoglycerate Mutase
PGK	PhosphoGlycerate Kinase
PK	Pyruvate Kinase
PL	PhosphoLipids
PME	Palm oil Methyl Esters
PMM	PhosphoMannoMutase
PPH	PhosphoPyruvate Hydratase
PPI	PeptidylProlyl Isomerase
PsaC	Photosystem II reaction centre protein subunit C
PUFA	Poly Unsaturated Fatty acid
ROS	Reactive Oxygen Species
rpm	Rotations Per Minute
RT-PCR	Real Time Polymerase Chain Reaction
RuBisCo	Ribulose-1,5-Bisphosphate Carboxylase
SAD	Stearoyl-ACP Desaturase
SERI	Solar Energy Research Institute
SFA	Saturated Fatty Acid
SOD	SuperOxide Dismutase
SQDG	Sulfoquinovosyl Diacylglycerol
SS	Sucrose Synthase
SSW	Synthetic Soft Water
STO	Salt Tolerant Protein

SV	Saponification Value
TAG	Triacylglycerol
TBARS	ThiobarBituric Acid Reacting Substance
TCA	Tri Carboxylic Acid
TEM	Transmission Electron Microscopy
TMAO	Trimethylamine N-oxide
TMP	TetraEthoxyPropane
TOF	Time of Flight
UDP	Uridine Diphosphate
USEPA	US Environmental Protection Agency
ZP	Zeta Potential
μg	Microgram
μL	Microliter
μm	Micro Meter
μM	Micro Molar
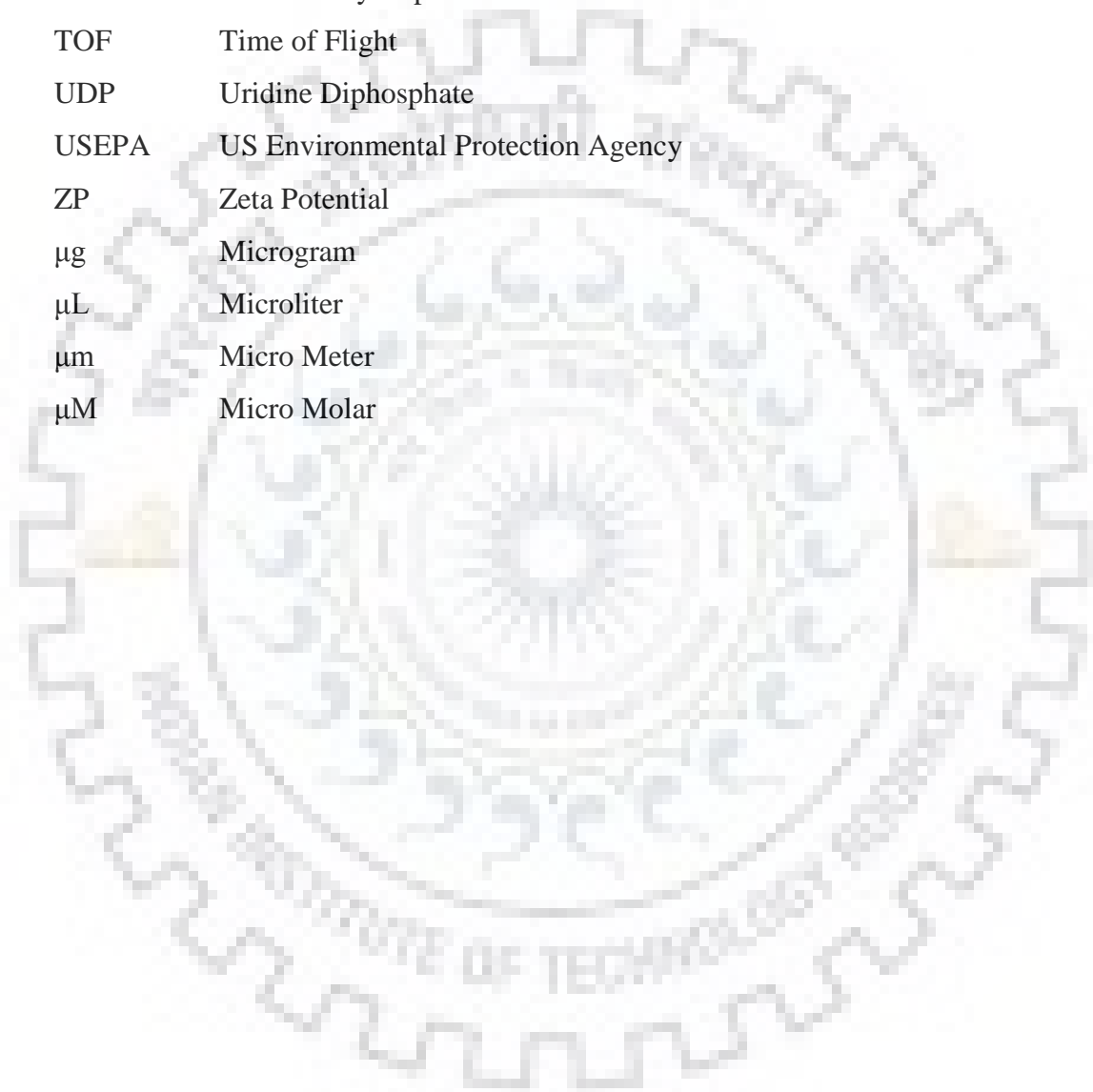
List of Publications

Thesis related articles

1. **N. Arora**, A. Patel, M. Sharma, J. Mehtani, P.A. Pruthi, V. Pruthi, K.M. Poluri, Insights into the Enhanced Lipid Production Characteristics of a Fresh Water Microalga under High Salinity Conditions, Ind. Eng. Chem. Res. 56 (2017) 7413–7421. doi:10.1021/acs.iecr.7b00841.

2. **N. Arora**, K. Gulati, A. Patel, P.A. Pruthi, K.M. Poluri, V. Pruthi, A hybrid approach integrating arsenic detoxi fi cation with biodiesel production using oleaginous microalgae, Algal Res. 24 (2017) 29–39. doi:10.1016/j.algal.2017.03.012.

3. **N. Arora**, A. Patel, P.A. Pruthi, V. Pruthi, Boosting TAG Accumulation with Improved Biodiesel Production from Novel Oleaginous Microalgae *Scenedesmus* sp. IITRIND2 Utilizing Waste Sugarcane Bagasse Aqueous Extract (SBAE), Appl. Biochem. Biotechnol. 180 (2016). doi:10.1007/s12010-016-2086-8.

4. **N. Arora**, A. Patel, P.A. Pruthi, V. Pruthi, Synergistic dynamics of nitrogen and phosphorous influences lipid productivity in *Chlorella minutissima* for biodiesel production, Bioresour. Technol. 213 (2016). doi:10.1016/j.biortech.2016.02.112.

5. **N. Arora**, P.T. Pienkos, K.M. Poluri, V. Pruthi, M.T. Guarnieri, Leveraging algal omics to reveal potential targets for TAG accumulation. Biotech. Advances (In press corrected proof).

6. **N. Arora**, K. Gulati, S. Triptahi, V. Pruthi, K.M. Poluri, **2018**. Algae as a budding tool for mitigation of arsenic from aquatic systems. Mechanisms of arsenic toxicity and tolerance in plants, **Springer Publication. (Accepted)**. Book Chapter

7. **N. Arora**, L.L. Laurens, N. Sweeney, K.M. Poluri, V. Pruthi and P.T. Pienkos. Elucidating the unique physiological responses of halotolerant *Scenedesmus* sp. cultivated in sea water for biofuel production. Algal Res. (Submitted).

8. **N. Arora**, D. Dubey, M. Sharma, A. Patel, A. Guleria, P.A. Pruthi, D. Kumar, V. Pruthi, K.M. Poluri, NMR based metabolomics approach to elucidate the differential cellular responses during mitigation of arsenic (III, V) in a green microalga. Ind. Eng. Chem. Res. (Submitted)

9. **N. Arora**, P. Kumari, A. Kumar, R. Gangwar, K. Gulati, P.A. Pruthi, R. Prasad, D. Kumar, V. Pruthi, K.M. Poluri, Delineating the molecular responses of a halotolerant microalga using integrated omics approach to identify genetic engineering targets for enhanced TAG production. Biotech. for Biofuels. (Submitted).

Other articles

1. A. Patel, **N. Arora**, J. Mehtani, V. Pruthi, P.A. Pruthi, Assessment of fuel properties on the basis of fatty acid profiles of oleaginous yeast for potential biodiesel production, Renew. Sustain. Energy Rev. 77 (2017) 604–616. doi:10.1016/j.rser.2017.04.016.

2. A. Patel, **N. Arora**, K. Sartaj, V. Pruthi, P.A. Pruthi, Sustainable biodiesel production from oleaginous yeasts utilizing hydrolysates of various non-edible lignocellulosic biomasses, Renew. Sustain. Energy Rev. 62 (2016) 836–855.

3. **N. Arora**, S. Triptahi, K.M. Poluri, V. Pruthi, **2018**. Advanced gene technology and synthetic biology approaches to custom design microalgae for biodiesel. Microalgae Biotechnology for Development of Biofuel and Wastewater Treatment. **Springer Publication**. **(Accepted)**. Book Chapter

4. V. Kumar**, N. Arora**, M. Nanda, V. Pruthi, **2018**. Different cell disruption and lipid extraction methods from microalgae for biodiesel production, Microalgae Biotechnology for Development of Biofuel and Wastewater Treatment. **Springer Publication**. **(Accepted)**. Book Chapter

5. **N. Arora**, S. Triptahi, V. Pruthi, K.M. Poluri, **2018**., An integrated approach of wastewater mitigation and biomass production for biodiesel using *Scenedesmus* sp. **Springer Publication**. **(Submitted)**. Book Chapter

6. **N. Arora**, A. Patel, P.A. Pruthi, K.M. Poluri, V. Pruthi, Utilization of stagnant non-potable pond water for cultivating oleaginous microalga *Chlorella minutissima* for biodiesel production, Renew. Energy. 126 (2018) 30–37. doi:10.1016/j.renene.2018.03.033.

7. J. Mehtani[#], **N. Arora**[#], A. Patel, P. Jain, P.A. Pruthi, K.M. Poluri, V. Pruthi, Augmented lipid accumulation in ethyl methyl sulphonate mutants of oleaginous microalga for biodiesel production, Bioresour. Technol. 242 (2017) 121–127. doi:10.1016/j.biortech.2017.03.108. **(# equal contribution)**.

8. **N. Arora**, A. Patel, K. Sartaj, P.A. Pruthi, V. Pruthi, Bioremediation of domestic and industrial wastewaters integrated with enhanced biodiesel production using novel oleaginous microalgae, Environ. Sci. Pollut. Res. (2016) 1–11. doi:10.1007/s11356-016-7320-y.

9. **N. Arora**, A. Patel, P.A. Pruthi, V. Pruthi, Recycled de-Oiled Algal Biomass Extract as a Feedstock for Boosting Biodiesel Production from *Chlorella minutissima*, Appl. Biochem. Biotechnol. 180 (2016). doi:10.1007/s12010-016-2185-6.

10. A. Patel, **N. Arora**, V. Pruthi, P.A. Pruthi, A novel rapid ultrasonication-microwave treatment for total lipid extraction from wet oleaginous yeast biomass for sustainable biodiesel production, Ultrasonics Sonochemistry (2018).

11. F. Deeba, A. Patel, **N. Arora**, V. Pruthi, P.A. Pruthi, Y.S. Negi, Amaranth seeds (*Amaranthus palmeri* L.) as novel feedstock for biodiesel production by oleaginous yeast, Environ. Sci. Pollut. Res. 25 (2018). doi:10.1007/s11356-017-0444-x.

12. P. Kumari, R. Mishra, **N. Arora**, A. Chatrath, R. Gangwar, P. Roy, R. Prasad, Antifungal and anti-biofilm activity of essential oil active components against *Cryptococcus neoformans* and *Cryptococcus laurentii*, Front. Microbiol. 8 (2017) 1–14. doi:10.3389/fmicb.2017.02161.

13. P. Jain, **N. Arora**, J. Mehtani, V. Pruthi, C.B. Majumder, Pretreated algal bloom as a substantial nutrient source for microalgae cultivation for biodiesel production, Bioresour. Technol. 242 (2017) 152–160. doi:10.1016/j.biortech.2017.03.156.

14. A. Patel, K. Sartaj, **N. Arora**, V. Pruthi, P.A. Pruthi, Biodegradation of phenol via meta cleavage pathway triggers de novo TAG biosynthesis pathway in oleaginous yeast, J. Hazard. Mater. 340 (2017). doi:10.1016/j.jhazmat.2017.07.013.

15. A. Patel, **N. Arora**, V. Pruthi, P.A. Pruthi, Biological treatment of pulp and paper industry effluent by oleaginous yeast integrated with production of biodiesel as sustainable transportation fuel, J. Clean. Prod. 142 (2017). doi:10.1016/j.jclepro.2016.10.184.

16. N. Raghuwanshi, A. Patel, **N. Arora**, R. Varshney, A.K. Srivastava, P.R. Partha, V. Pruthi, Antineoplastic and Antimicrobial Potential of Novel Phytofabricated Silver Nanoparticles from *Pterospermum acerifolium* Leaf Extract, Nanoscience & Nanotechnology-Asia (2017). doi:10.2174/2210681207666170607154529.

17. N. Raghuwanshi, **N. Arora**, R. Varshney, P.R. Partha, V. Pruthi, Antineoplastic and antioxidant potential of phycofabricated silver nanoparticles using microalgae *Chlorella minutissima*, IET Nanobiotechnology 11 (2017) 1-23.

18. A. Patel, D.K. Sindhu, **N. Arora**, R.P. Singh, V. Pruthi, P.A. Pruthi, Biodiesel production from non-edible lignocellulosic biomass of *Cassia fistula* L. fruit pulp using oleaginous yeast *Rhodosporidium kratochvilovae* HIMPA1, Bioresour. Technol. 197 (2015) 91–98. doi:10.1016/j.biortech.2015.08.039

List of presentations in conference/Workshops

International

1. **N. Arora**, P. Kumari, K.M. Poluri, V. Pruthi, Delineating the halotolerance mechanism of *Scenedesmus* sp. by integrated omics approach: Potential implications for biofuel production. International conference on 'European biomass conference and exhibition' from 14- 17th May 2018 at Copenhagen, Denmark.

2. Workshop on routine measurement and biochemical analysis of microalgal cultures: March 13-17, 2017, ATP^3, AzCATI, Arizona, USA.

3. **N. Arora**, A. Patel, P.A. Pruthi, V. Pruthi, Lipid accumulation in response to nitrogen starvation and photosynthetic performance by *Chlorella minutissima*. International conference on 'Algal biomass, biofuels and bioproducts' from 7-10th June 2015 at San Diego, USA.

National

1. **N. Arora**, V. Pruthi, K.M. Poluri, Delineating the differential metabolic responses of a green microalga during arsenic (III, V) mitigation. ACS on Campus, on 7th February 2018, IIT Roorkee, India.

2. S. Triptahi, **N. Arora**, V. Pruthi, K.M. Poluri, Phycoremedation of toxic cadmium synchronized with enhanced biodiesel production. Symposium on Advances in Biology of Algae and Cyanobacteria from 8-9 February 2018, Banaras Hindu University, Varanasi, India.

3. **N. Arora**, A. Patel, J. Mehtani, P.A. Pruthi, V. Pruthi, Insights into Lipid accumulation and halotolerance mechanism of novel oleaginous microlaga for enhancing biodiesel production. International conference on current trends in Biotechnology (ICCB) from 8-10th December 2016 at VIT, University, Vellore, India.

4. **N. Arora**, Pruthi, V. Integrating phycoremediation with biodiesel production from novel oleaginous microalgae *Scenedesmus* sp. IITRIND2. National symposium on Biofuel: Indian Scenario on 29th April 2016. (**First runner up in oral presentation**).

5. **N. Arora**, A. Patel, P.A. Pruthi, V. Pruthi, V. Kinetic modeling to optimize synergistic dynamics of nitrogen and phosphorous affected lipid productivity in *Chlorella minutissima* for biodiesel production. International conference on 'New Horizons in Biotechnology' from 22-25th November 2015 at Trivandrum, India.

6. **N. Arora**, R. Katiyar, P.A. Pruthi, V. Pruthi, B. Gujar, Microalage lipid extraction for biodiesel production. International Conference on 'Molecular Signalling: Recent Trends in Biomedical and Translational Research' (ICMS: RTBTR-2014) from December: 17-19; 2014 at Department of Biotechnology Indian Institute of Technology Roorkee, Roorkee 247667, India.

7. R. Katiyar, **N. Arora**, B. Gujar, V. Pruthi, Comparison of two different solvents for lipid extraction from Chlorella sp. to produce biofuel. International Conference on 'Molecular Signalling: Recent Trends in Biomedical and Translational Research' (ICMS: RTBTR-2014) from December: 17-19; 2014 at Department of Biotechnology Indian Institute of Technology Roorkee, Roorkee 247667, India.

Awards

1. Awarded prestigious **Bioenergy Awards for Cutting Edge Research (B-ACER)** funded by Indo-US Science Technology Forum (IUSSTF) and Department of Biotechnology (DBT), Govt. of India (October 2016 to April 2017).

2. **Young Scientist -2017** awarded by Scientific Planet Society (SPS), India.

Introduction and Review of Literature

1.1 Energy crisis

Rapid industrialization and urbanization have led to depletion of fossil fuel reserves, escalation in the levels of greenhouse gas emissions and heavy metals in environment which are consequently posing threat to energy security, environment and well-being of all the life forms. On the energy front, renewable and sustainable energy development is the way forward to avoid further stressing the energy crisis and global climate change thereby restoring energy reserves [1,2]. The International Energy Agency (IEA) reported that the transportation sector alone consumes 63 % of the fossil fuels and is responsible for ~ 22 % of the world's CO_2 emissions [3]. This has led to the increase in the CO_2 global emissions reaching a new high of 37 Gt in 2035 along with a global temperature rise to ~ 0.17 °C per decade [4,5]. Recently, Paris agreement established firmly to limit the earth's temperature increase to 2 °C and this requires 90 % coal reserves, 50 % of gas and 2/3rd fossil fuels reserves to be kept intact [5,6]. Replacing fossil fuels with biofuels can provide a leap towards solving the energy crisis and limiting the deterioration of the environment. Biofuels are liquid fuels that can be derived from biomass obtained from agricultural, forest, industrial wastes or microbial biomass [7]. They can be broadly categorised into seven distinct categories including bioethanol, biomethanol, biogas, biodiesel, Fisher Tropsh diesel, biohydrogen and biomethane respectively [8].

1.2 Biomass based biodiesel production

Biomass is the fourth largest available energy resource in the world and could be utilized for sustainable biofuel generation [9,10]. Among the biofuels, biodiesel can be directly used in diesel engines without any major modifications and the infrastructure for storage and transportation currently existing for petroleum based fuels could be utilized [11]. Biodiesel is derived from lipids, which are fatty acids produced from plants, animals or microorganisms. Compared to conventional diesel, burning of biodiesel reduces the total hydrocarbons, particulates and carbon monoxide by 55 %, 53 %, and 48 % respectively. It is also more readily biodegradable than petroleum diesel [12]. Biodiesel is produced by a mono-alcoholic

transesterification process, in which triglycerides reacts with a mono-alcohol (most commonly methanol or ethanol) with the catalysis of alkali, acids, or enzymes [13–15]. The transesterification process involves reaction of 1 mole of triacylglycerol (TAG) with 3 moles of methanol at moderate temperature catalysed by acid or alkali or enzyme to form 1 mole of glycerol and 3 moles of fatty acid methyl esters (FAMEs) which can be utilized for biodiesel as depicted in **Fig. 1.1** [16].
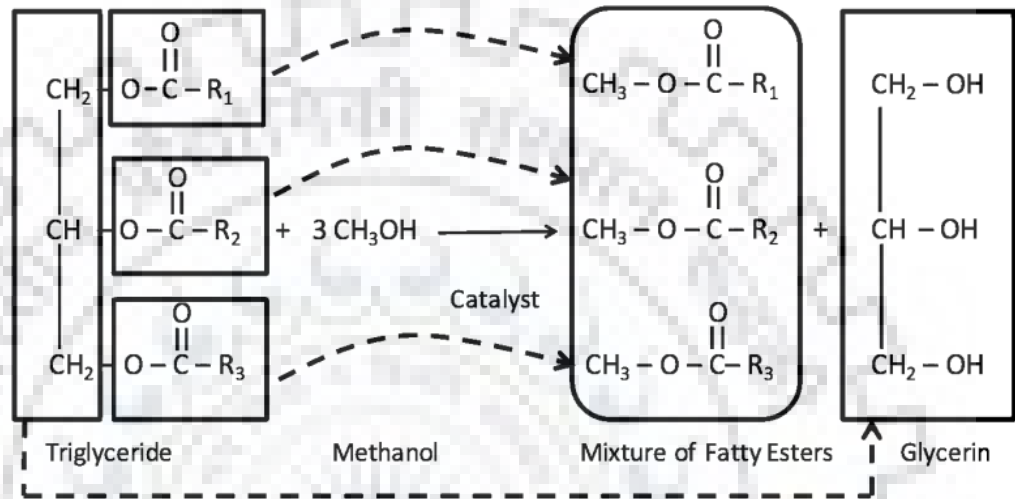
Fig. 1.1: *Transesterification reaction.*

Biodiesel can be classified into four major categories based on the feedstock namely first generation, second generation, third generation and fourth generation (**Fig. 1.2**). First and second generation are conventional biodiesel which are derived from edible and non-edible terrestrial plants including corn, sugarcane bagasse, soyabean, rapeseed, canola, jatropha [4,17,18]. However, the major drawback of these conventional fuels include requirement of large area, water and nutrients supply for cultivation which directly competes with the agriculture food production [17,19,20]. These disadvantages can be overcome by using third generation biofuels, derived from biomass of various microorganism including bacteria, yeast, fungi and microalgae which can be cultivated on smaller land areas along with high areal productivity [21]. On the other hand, fourth generation biofuels include genetically engineered microorganism for augmenting their biodiesel potential [22]. Among these, photosynthetic microalgae offer an edge over their counterparts due to their ability to utilize CO_2 and solar energy for generating biomass thereby eliminating the need for organic carbon which entails hefty cost [20].
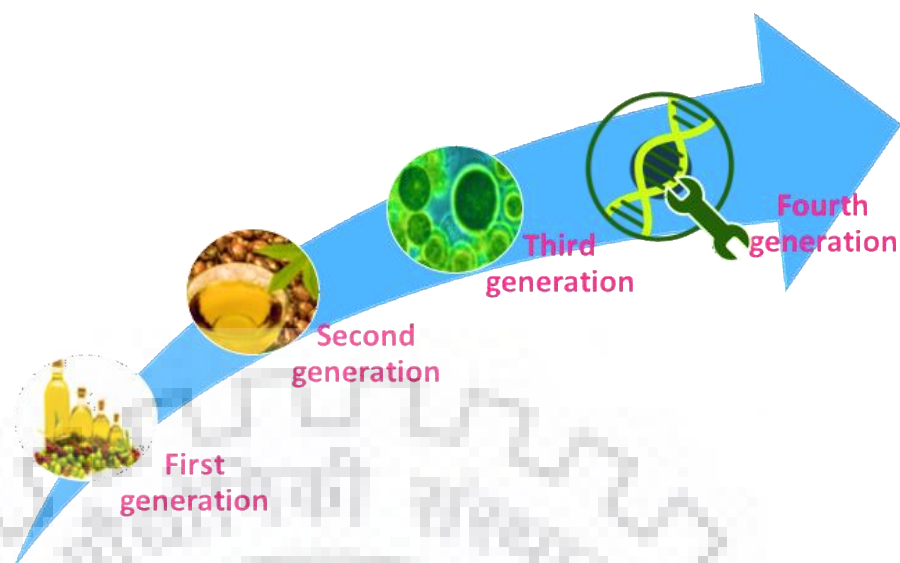
Fig. 1.2: *Different categories of biodiesel generation.*

1.3 Heavy metal pollution

In addition to developing and deploying biofuels, mitigation of heavy metals from the aquatic ecosystems is a significant challenge. Anthropogenic activities and disturbance in the natural biogeochemical cycle due to climate change have led to mobilization of toxic and carcinogenic heavy metals including lead, arsenic, mercury, cadmium, lithium etc. into the environment [23]. Among the heavy metals, US Environmental Protection Agency (USEPA) has listed thirteen heavy metals in which arsenic (As) has been listed as category 1 and class A carcinogen [12]. High levels of arsenic in potable water sources have been reported in various countries including south–west Finland (17–980 mg/L), western United States of America (1–48000 mg/L) and Inner Mongolia China (up to 1354 mg/L) [24]. Further, the arsenic laden discards released from the drinking water treatment plants contain very high concentration of arsenic for example, the arsenic bearing liquid wastes contain ~ 200-500 mg/L, while arsenic bearing solid wastes can have a maximum of ~7500 mg As/Kg waste [25,26]. These arsenic bearing wastes are directly dumped into the nearby ponds or in open fields thereby posing a greater risk for human exposure and recontamination of water sources. Removal of arsenic from the contaminated water bodies has been achieved by various physiochemical techniques [27]. However, these methods require high maintenance and expensive mineral adsorbents making the overall process costly [28]. This necessitates the exploration of innovative, sustainable and eco-friendly means to effectively mitigate arsenic from the aquatic bodies.

1.4 Algae

Algae are recognized as the oldest life forms which are the basis of marine food chain as they produce ~ 50 % of the oxygen we inhale [29,30]. They are classically defined as oxygen evolving thallophytes (plants lacking root, stems and leaves), containing chlorophyll or chlorophyll like pigments as their primary photosynthetic apparatus and lack a sterile covering around the reproductive cells [31,32]. Algae are practically found in every type of environment ranging from fresh water to salt water, hot springs to snowfields and can tolerate wide range of pH, temperature, turbidity, light etc. [31]. They are also extremely diverse in morphology and size ranging from picoplankton (0.2- 2 μm) in diameter to giant kelps (60 m) [30]. Depending on the coloration of their pigments, ecological habitant, structural and reserve polysaccharides including both prokaryotic and eukaryotic, they can be classified into ten distinct groups; Chlorophyceae (green algae), Xanthophyceae (yellow-green algae), Diatomaceae (yellow/golden brown algae), Phaeophyceae (brown algae), Rhodophyceae (red algae), Chrysophyceae (golden-brown algae), Chrysophyceae (diverse pigmentation), Dinophyceae (yellowish green to deep golden algae), Euglenineae (pure green algae) and Chloromonodineae (distinct green colour) respectively [30]. Further, another algal group, Cyanophyceae (blue green algae) have been placed in a distinct bacterial domain, hence are named cyanobacteria [33]. To date, approximately 32,260 species of living algae have been reported in AlgalBase (http://www.algaebase.org). Algae can either be autotrophic (utilize inorganic carbon source such as CO_2 and light), heterotrophic (require organic carbon sources and nutrients) or mixotrophic (can utilize both inorganic and organic carbon sources) to divide and grow [29].

1.4.1 Microalgae derived biodiesel

The concept of cultivating microalgae for biofuel particularly biodiesel was introduced between 1978-1996 by the U.S. Department of Energy (DOE), under the Aquatic Species Program (ASP), funded by Solar Energy Research Institute (SERI), which became National Renewable Energy Laboratory (NREL) in 1991 [34]. ASP focused on production of biodiesel from oleaginous microalgae and documented their finding in "A look back at the U.S. Department of Energy's biodiesel from Algae" [34,35]. Microalgae offer an edge in comparison to other conventional plant based feedstocks owing to their relatively rapid growth rate, higher yields of bioenergy per hectare, and their ability to thrive without a need for arable land along with reduction of freshwater, thus mitigating potential impact on food supplies [36,37]. Furthermore, microalgae can capture CO_2 not only from the environment but also from

4

different industrial waste streams, which might provide a positive sustainability impact [38]. Microalgae (and cyanobacteria) harness sunlight and CO_2 from the environment to synthesize lipids, carbohydrates, proteins and various value-added products (e.g. carotenoids, phycobiliproteins, sterols and vitamins) [39]. The neutral lipids (TAGs) and carbohydrates accumulated inside microalgal cells can serve as efficient raw materials for biodiesel and bioethanol production respectively. TAGs are composed of fatty acids with a glycerol backbone, which can be transesterified to form FAMEs [40,41]. The detailed procedure for biodiesel production from microalgae has been outlined in the flow chart **(Fig. 1.3)**.

Fig. 1.3: *Flow chart of biodiesel production from microalgae.*

Oleaginous microalgae have the inherent capability to accumulate large quantities of TAGs (20-60 % of dry cell weight) under adverse conditions in specialized lipid bodies [42]. The adverse conditions can be categorized as physical (e.g. shifts in temperature, light intensity, wavelength of light) and chemical (e.g. nutrient depletion, salinity, CO_2, heavy metal exposure) [4,43]. TAGs help microalgae to withstand the imposed stress by maintaining intracellular lipid homeostasis, cellular function and energy supply [44]. However, prolonged stress can results in breakdown of the photosynthetic apparatus, resulting in chlorophyll degradation (manifesting as chlorosis), limiting cell division, and reducing the overall TAG

productivity [45]. Additionally, there is an inverse relation between active growth and lipogenesis. Therefore, an optimum balance between growth rate and TAG accumulation is essential for commercial algal biodiesel production which necessitates in depth knowledge of TAG accumulation pathway in microalgae [46].

1.4.2 Overview of TAG accumulation in microalgae

Understanding lipid synthesis mechanism in microalgae is one of the governing criteria for enhancing TAG accumulation [47]. Whole genome sequencing, *de novo* transcriptomics, proteomics and metabolomics of different microalgae have revealed a detailed mechanism of lipid catabolism and anabolism under various growths (autotrophic, heterotrophic, mixotrophic) and stress (physiological, chemical and operational) conditions [44]. Neutral lipid (TAG) synthesis in microalgae can be subdivided into **two steps**: *de-novo* fatty acid synthesis occurring in the plastid and acyl-lipid assembly in endoplasmic reticulum as shown in **Fig 1.4 (A-C)**. The **first step** *de-novo* synthesis of fatty acid begins with the formation of glycerol-3-phosphate via Calvin cycle which is a photosynthetic product (autotrophic mode) and then its subsequent conversion to pyruvate in the plastid of microalgae [47]. Pyruvate is then catalysed by pyruvate dehydrogenase complex (PDC) to acetyl-CoA thereby initiating lipid synthesis **(Fig. 1.4A)**. The formation of acetyl-CoA is dependent on photosynthetic efficiency (PE) as ATP (Adenosine triphosphate), NADPH (Nicotinamide adenine dinucleotide phosphate) and NADH (Nicotinamide adenine dinucleotide, reducing power) which is provided by photosynthesis [44]. Acetyl Co-A then carboxylates to malonyl–CoA catalyzed by plastid acetyl-CoA carboxylase (ACCase) which is the first rate limiting step of lipid synthesis [44].
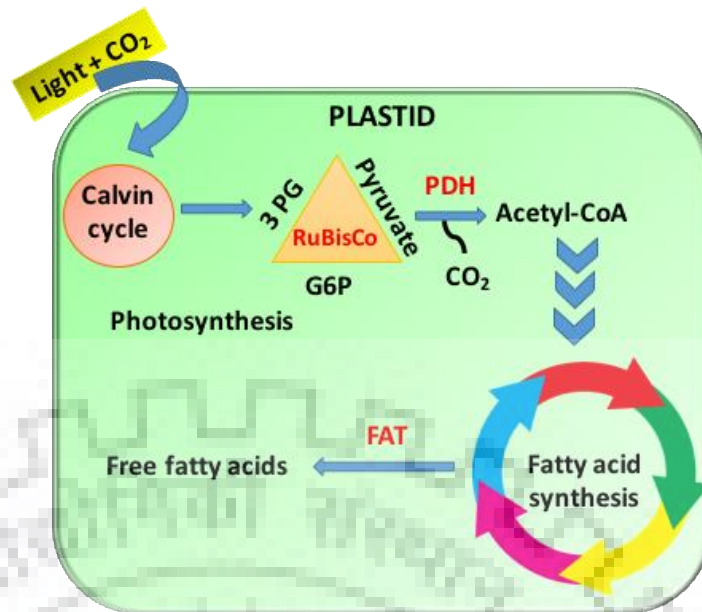
Fig. 1.4A: *Schematic representation of de-novo synthesis of fatty acid in plastid.*

In the stroma malonyl- CoA is then transferred to an acyl carrier protein (ACP) with the help of fatty acid synthase (FAS) complex as depicted in **Fig. 1.4B** [48]. The formation of malonyl-ACP starts a series of fatty acid elongation steps involving various intermediate products such as 3-keto butyrl-ACP, 3-Hydroxy butyrl-ACP, trans Δ^3- butenoyl-ACP, butyrl-ACP and finally 3-keto-acyl-ACP which are catalysed by 3-ketoacyl ACP reductase (KAR), 3-Hyroxyacyl ACP dehydrase (HD) and enoyl ACP reductase (ENR) respectively [49]. This cycle continues till saturated fatty acids (16:0 ACP and 18:0 ACP) are not formed after which the cycle is terminated by either removing the acyl group and then transferring it to glycerol 3-phosphate (G3P) in the cytosol catalysed by acyl-ACP thioesterase or by acyl transferases in the plastid [47]. Further, to generate unsaturated fatty acid chains, double bond is introduced by a soluble enzyme stearoyl-ACP desaturase (SAD). The free fatty acids are transferred to the cytosol and then to endoplasmic reticulum (ER) for further processing and conversion to TAGs [44,50].
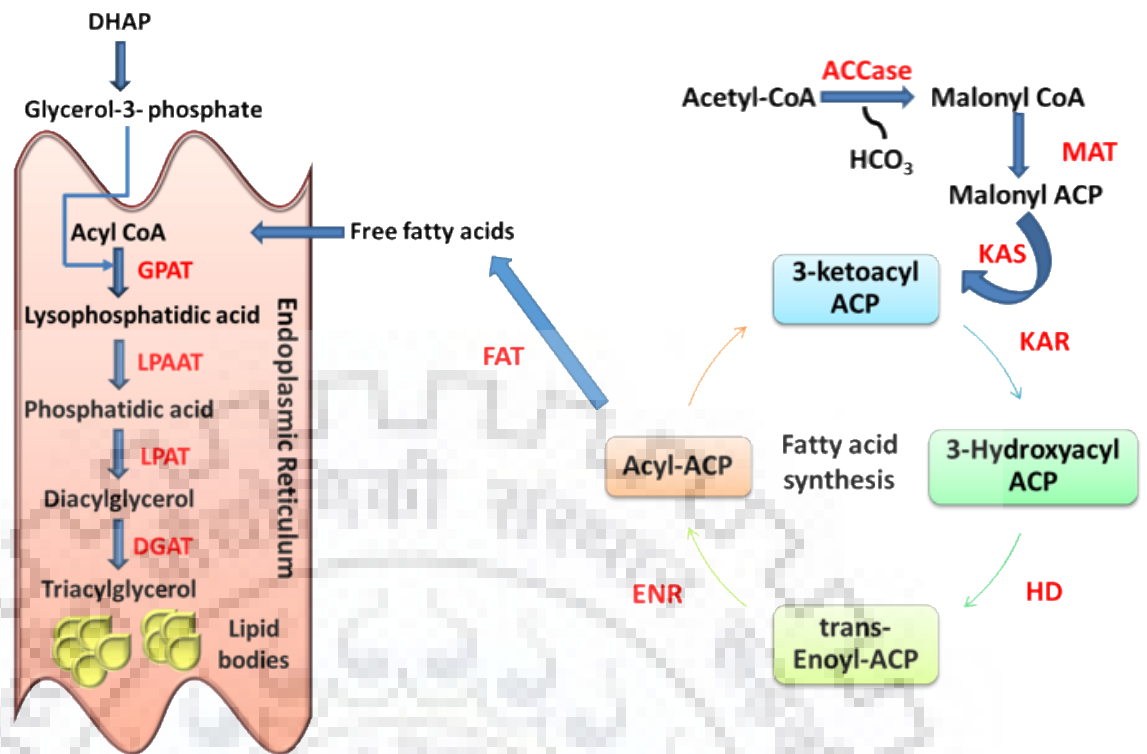
Fig. 1.4B: *Overview of Triacylglycerol synthesis in microalgae.*

Second step of TAG synthesis is the acyl lipid packaging also called the Kennedy pathway occurring in the ER results in formation of three major intermediates: lysophosphatidic acid, phosphatidic acid and diacylglycerol catalysed by glycerol phosphate acyl transferase (GPAT), lyso-phosphatidic acid acyltransferase (LPAAT) and lyso-phosphatidylcholine acyltransferase (LPAT) respectively [44]. Diacylglycerol (DAG) is the precursor of triacylglycerol (TAG) and its conversion is catalysed by diacylglycerol acyltransferase (DGAT) as shown in **Fig. 1.4B**.

Besides this there also exists an alternative to the Kennedy pathway, the acyl-CoA independent pathway for TAG accumulation in microalgae involving phospholipid:diacylglycerol acyl transferase (PDAT). It is postulated that PDATs transfers fatty acyl moiety from phospholipid to DAG. PDAT utilizes the chloroplast membrane lipids including monogalactosyl diacylglycerol (MGDG), sulfoquinovosyl diacylglycerol (SQDG) and phosphatidylglycerol (PG) as substrate for the synthesis of TAGs. Thus, both *de-novo* and acyl-CoA independent pathways contribute to overall TAG accumulation in microalgae (**Fig. 1.4C**).
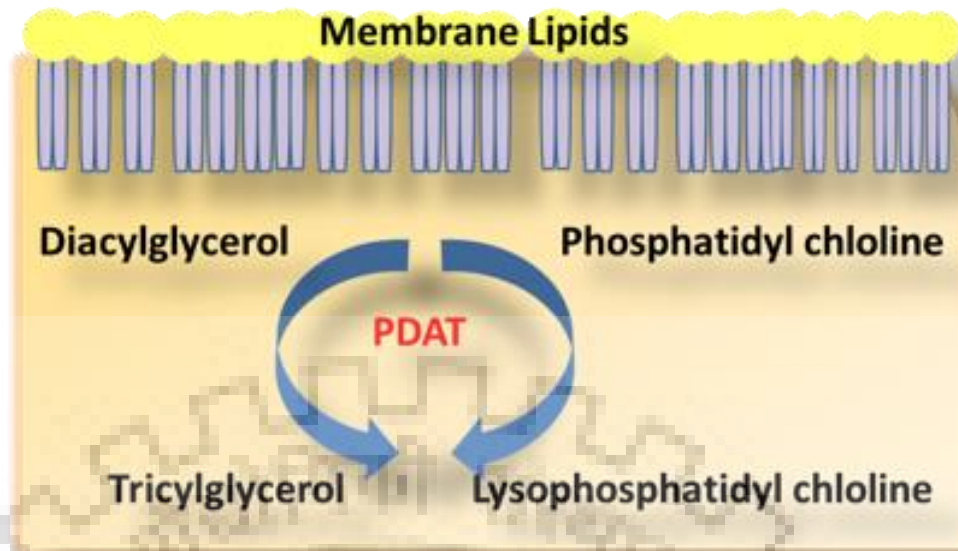
Fig. 1.4C: *Alternate lipid synthesis pathway in microalgae.*

1.4.3 Commercial prospects of microalgal biodiesel production

Considerable effort has been made to cultivate microalgae on large scale in open ponds and closed photobioreactors (PBRs), but there is still a long road ahead for its commercial deployment. Economic evaluation of microalgae derived biodiesel indicated selling price of $ 5-10.31/gallon, which is higher than the petroleum ($ 3.17/gallon) and conventional biodiesel ($ 4.21/gallon) [51]. Two key factors that could expedite the economical production of biodiesel production include increasing the algal biomass with reduced cost of feedstocks and cost effective extraction of lipids along with utilization of residue biomass for high-value products [52]. Keeping this in view, research is now focused on finding feedstocks for cultivation of microalgae such as municipal, industrial wastes, hydrolysates of lignocellulosic biomass (sugarcane bagasse, cassava starch, corn powder) and saline waters (sea water and brackish water)[53–59].

However, the utilization of lignocellulosic biomass hydrolysate as culture medium involves intensive labour and high capital cost for pre-treatment in order to break the lignocellulosic biomass making it economically less feasible. The conversion of any lignocellulosic biomass to hydrolysates requires additional acid hydrolysis and neutralization steps, adding up to the cost of media. Moreover, the hydrolysates contain components such as acetic acid, furfural, 5-hydroxymethylfurfural (HMF) and phenolic compounds which inhibit the growth of microalgae [56]. Further, the major monomeric sugars present in cellulosic

hydrolysates are glucose and xylose, microalgae can readily utilize glucose but till date only one *Chlorella* sp. has been reported that can metabolize xylose [60].

On the other hand, replacement of fresh water with seawater or wastewater, not only relieves a burden on fresh water reserves, but, in the case of wastewater, it may also significantly reduce the cost associated with nutrient consumption [61]. However, wastewater contains high amounts of organic carbon which increases the chances of contamination and cultures crashing in open pond systems. The above listed bottle neck can be resolved by utilization of saline water (sea water or saline groundwater) which is an optimum and sustainable feedstock for large scale cultivation of microalgae either in open ponds or closed photobioreactors as freshwater supply is limited [62,63]. This in turn necessitates bioprospecting or generation of microalgal strains capable of adapting to fluctuating and wide range of salinity along with high biomass and lipid generation. Further, in order to reduce the cost, biorefinery approach which integrates biodiesel production with conversion/extraction of all the available compounds into spectrum of marketable high value compounds (omega 3 fatty acids, bioactive compounds, etc.) without generation of waste needs to be implemented [52].

1.5 Microalgae as budding tool for arsenic mitigation

Microalgae also finds its application in arsenic bioremediation and has an edge over other conventional technologies as it can efficiently accumulate and metabolize all the arsenic species with adequate efficiency, generating biomass in the process that can be used as biofertilizers and biofuels.

1.5.1 Arsenic pollution

Fate of arsenic in environment and its pernicious behaviour made it the most controversial element since its discovery by a German alchemist Albert Magnus in 1250 A.D. [64]. Over past decade, arsenic has been widely used in medicines, agriculture, livestock, electronics and metallurgy which have led to worldwide contamination in aquatic ecosystems [65]. Arsenic is a toxic metalloid having property of both metal and non-metal. On the basis of its occurrence, it has been ranked 20th, 14th and 12th among trace elements in earth's crust, seawater and human body respectively [66]. In nature, arsenic is widely distributed in inorganic forms which are more toxic as compared to their organic counterparts. The major inorganic forms of arsenic include arsenate (As V), arsenic acids (H_3AsO_4, $H_2AsO_4^-$, $HAsO_4^{2}$), arsenite (As III) and arsenious acids (H_3AsO_3, $H_2AsO_3^-$, $HAsO_3^{2-}$) respectively. On the other hand, the

organic forms are resultant of arsenic combining with other carbon or sulfur containing molecules, such as arsenobetaine (AB), arsenocholine (AC), arsenosugars, arsenolipids, dimethylarsinate (DMA), monomethylarsonate (MMA) respectively **(Fig. 1.5)**. Depending on the physiological/biological conditions, arsenic can convert into different forms i.e., inorganic or organic, and this phenomenon is termed as arsenic speciation. The solubility of arsenic in aqueous medium mainly depends on the pH and presence of other ionic species in the environment. Among the above mentioned forms, As (V) is the most thermostable and majorly present in oxic environments, whereas As (III) is prevalent in anoxic ecosystems [67]. Recent studies have suggested the toxicity of arsenic in following order: MMA (III) > As (III)> As (V) > DMA (V) > MMA (V) respectively [68].
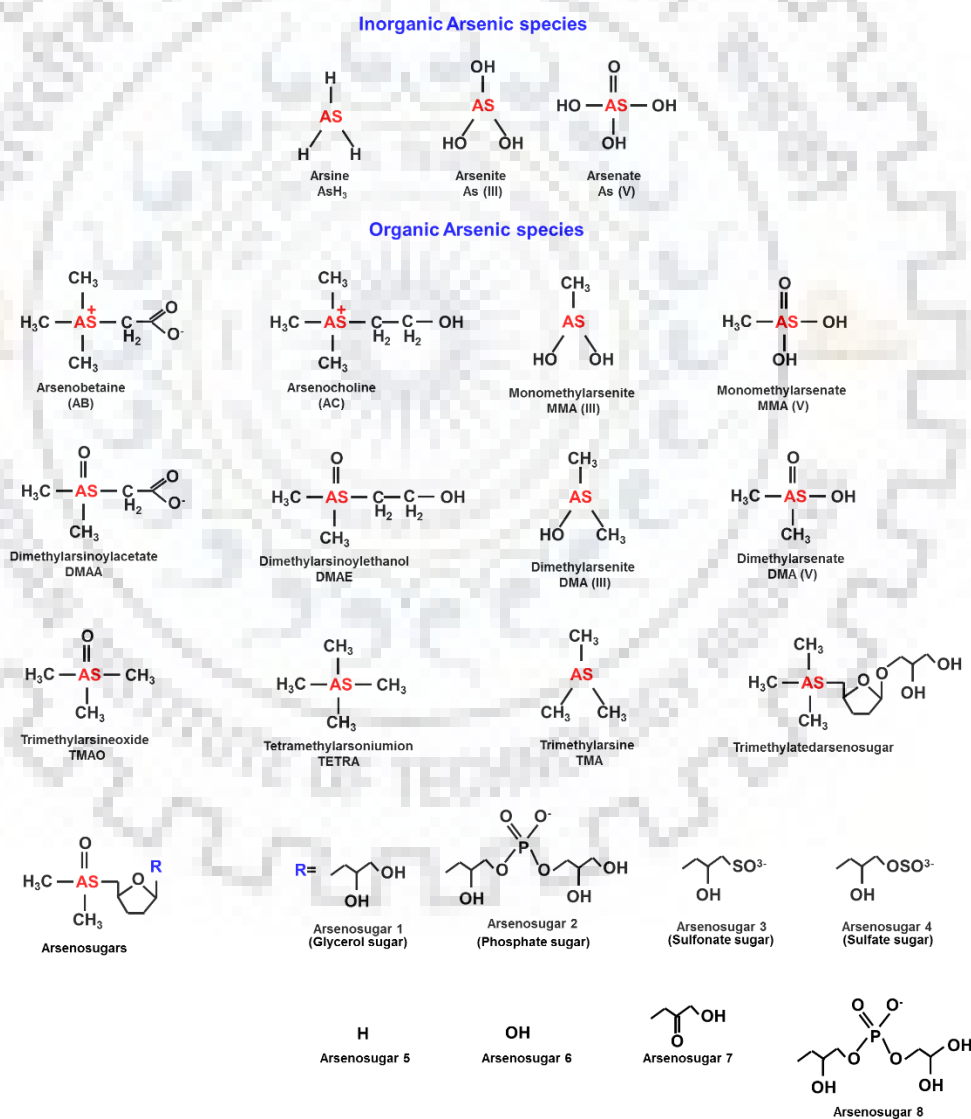
Fig. 1.5: *Chemical structures of various inorganic and organic forms of arsenic.*

In current scenario, arsenic contamination in the ground waters is affecting more than 150 million people all around the world. Particularly countries in South-East Asia namely Bangladesh, Pakistan, Nepal, India, China, Combodia, Taiwan, Myanmar are at a higher risk [64]. Significant amounts of arsenic exposure to human body results in the development of arsenicosis, which is the common term used for the health effects related to arsenic toxicity such as skin pigmentation, skin cancers, internal cancers (bladder, kidney, lungs), diseases related to blood vessels, leg and feet pigmentation, diabetes, high blood pressure, reproductive disorders, and impairment of respiratory system (WHO 2011). Exposure to inorganic arsenic species is associated with numerous disorders including dermatitis, keratosis, melanosis, irritations of the skin mucous membranes, and vascular diseases such as blackfoot disease and hypertension [66]. Therefore, remediation of arsenic in contaminated water and soil is quintessential to reduce the degree of health risk to human kind.

In recent studies it has been reported that arsenite can bind to the sulphydryl groups of enzymes thereby inhibiting more than 200 enzymes in human resulting in functional impairments [69]. On the other hand, arsenate being the structural analogue of phosphate competes with the uptake of phosphate ions by the cells. This in turn causes interference with the normal cellular processes like oxidative phosphorylation by replacing the phosphate group in the nucleic acid, which leads to mutations and cancer [70].

1.5.2 Bioaccumulation of arsenic by microalgae

Several conventional physico-chemical and polymer based techniques such as oxidation, coagulation-flocculation, adsorption, ion exchange, membrane driven technologies are reported for efficient arsenic removal [71,72]. However, the above listed conventional methods suffer from a number of drawbacks considering the economic factors and environment concerns, which has led to a growing interest in the development of cheaper, efficient, environment friendly and pH independent technologies without any production of secondary toxic and arsenic laden discards. In this regard, bioremediation techniques utilizing biological materials (live/dead) can potentially contribute to mitigate arsenic in a sustainable and eco-friendly manner [73]. Bioremediation mainly involves two modes; biosorption and bioaccumulation. Biosorption is a metabolically passive process to remove heavy metals via non-living biomass such as bio-char, fungal biomass, methylated yeast biomass, chicken feathers, algal biomass, alginate and orange waste gel from an aqueous solution [74,75]. The advantages of using biosorption for removal of arsenic includes; reusability of bioadsorbent, low operating cost, specificity for heavy metals, short operational time and no production of

arsenic laden discards or secondary toxic compounds [76]. On the other hand, bioaccumulation is an active mechanism requiring energy from a living organism (bacteria, yeast, fungi, algae and plant) to absorb heavy metal on to its cell surface and its subsequent transport into the cytoplasm, which is then metabolized [73]. This technique has an additional advantage of detoxification of arsenic compounds (arsenite, arsenate, MMA, DMA etc.), thereby reducing the metalloid pollution in the environment.

Considering the green and renewable sources for mitigation of toxic materials, bioremediation of arsenic using plants and algae has gained significant importance. Algae are one of the most promising alternatives due to their high biomass production (compared to plants), cheap availability in both fresh and salt waters, large surface to volume ratio (high arsenic binding), no seasonal limitation, rapid metal uptake capacity, potential for genetic engineering, eco as well as user friendly, suited for both batch and continuous culture with its applicability in both low and high contaminated sites [75]. The biosorption of arsenic by algae have been attributed to the presence of various functional groups present on its cell wall [75]. The carboxylic groups are the most abundant acidic functional group followed by sulfonic, hydroxyl and amino that aids in binding of the arsenic to the cell surface of algae via electrostatic attraction, ion exchange and complexation respectively [74]. After the adsorption, algae uptake the arsenic inside its cellular machinery and metabolizes it. In this context, different domains of algae (macroalgae, cyanobacteria, microalgae and diatoms) have been extensively studied by various researchers throughout the world to remove arsenic. It is noteworthy that various microalgae are capable of tolerating high concentrations of arsenic (up to 2000 mg/L) showing elevated intracellular arsenic accumulation followed by its subsequent metabolism and conversion to less toxic compounds. Studies on removal of arsenic (III, V) by microalgae of genre *Chlorella*, *Scenedesmus* and *Chlamydomonas* have known to show maximum arsenic (III, V) tolerance and accumulation **(Table 1.1)**. Researchers have showed that *Scenedesmus quadricauda*, accumulated more arsenic at pH 8.2 (25.23 µg/g) as compared to pH 9.3 (8.39 µg/g) [77]. Moreover, a difference between As (V) removal in batch and continuous cultures of *Dunaliella tertiolecta* has been reported [78]. Further, in case of batch cultures of *D. tertiolecta*, the arsenic accumulation peaked on the 7 day (11 µg/g) and subsequently decreased on the 42nd day (7 µg/g). This was due to the death of the algal cells as the nutrients got exhausted in the growth media with time. The above hypothesis was proven to be true as the heat treated algal cells also showed similar arsenic accumulation (6 µg/g). On the other hand, higher accumulation (13 µg/g) was observed in the continuous culture of the microalga as it had more live cells [78]. Another crucial factor that affects As (V) bioaccumulation inside live algal cells is the phosphate concentration in the growth media. It is

also crucial to note that the arsenic toxicity, mitigation and its response to above discussed factors can vary with the speciation of alga and its site of isolation.

Microlgae/Diatom	As (III) mg/L	As (V) mg/L	IC_{50} (mg/L)	Arsenic removal (mg/g dry weight)	References
Dunaliella sp.	-	10	-	As (V) – 0.57	[79]
	10	10	-	As (III)- 0.27 As (V)- 0.56	[80]
D. tertiolecta	-	0.002	-	As (V) – 0.013	[78]
D. salina	10	1000	-	As (III) – 0.37 As (V) – 2.74	[81]
	-	1.12	As (V) - 41.5	As (V) – 0.27	[82]
Chlorella sp.	0.75	0.75	As (III) – 93.8 As (V) – 0.57	As (III) – 1.04 As (V) – 1.26	[83]
C. vulgaris	-	1000	-	As (V) – 2.7	[84]
	-	200	-	As (V)- 45.4	[85]
	50	-	-	As (III)- 0.53	[86]
	-	1000	-	3.6	[87]
Scenedesmus obliquus	-	0.75	As (V) – 33.5	As (V)- 6.33	[88]
Chlamydomonas reinhardtii	-	0.75	As (V) – 0.57	As (V) – 10.2	
	-	180	-	As (V)- 1.76	[89]
	-	18	As (V)- 54	-	[90]
Scenedesmus sp.	0.75	0.75	As (III) – 196.5 As (V) – 20.6	As (III) – 0.61 As (V) – 0.76	[91]
S. quadricauda	0.03	-	-	As (III) – 0.03	[77]
	100	-	-	As (III) – 42.3	
Nannochloropsis sp.	12.9	-	-	As (III)- 2.01	[92]

Table 1.1: *Summary of arsenic (III, V) removal (mg/g dry cell weight) and IC_{50} by various microalgae reported in the literature.*

1.6 Mechanistic insights into algal omics and its role in augmenting TAG accumulation

Omics world majorly comprises of four major components: genomics, transcriptomics (mRNA-transcription), proteomics (proteins-translation/ post translation) and metabolomics (metabolites) as depicted in **Fig. 1.6** [93]. Importance of omics technologies have proven their eminent role in biological and biomedical applications by underpinning key regulators in disease progression and tailoring therapies. Recently, these omic technologies have been applied to understand algal biology and genome due to their prominent role as renewable energy sources. Algal system offers an advantage as the existing omics are well-developed for unicellular organisms which can be directly applied to it [94]. Omics studies strive to analyze entire class of molecules which can play a vital role in underpinning key elements (genes/ proteins/metabolites) regulating microalgal growth, lipid accumulation, resistance to predators and settlement traits [94]. Understanding the above mentioned traits can expedite the economic feasibility of algal oils. Gaining in-depth knowledge of either one or all of the components

could accelerate the basic understanding of TAG synthesis in microalgae in response to stress by identifying regulatory pathways and key genes/proteins/metabolites leading to strategic genetic engineering and strain improvement [44,95].
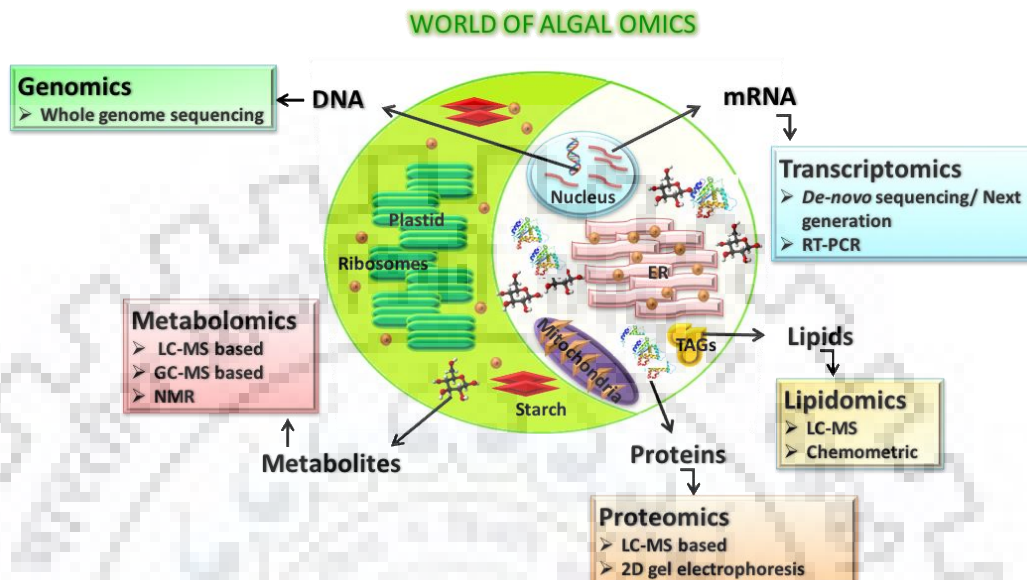
Fig. 1.6: *Omics techniques for increasing TAG accumulation in microalgae.*

In the last decade, utilization of omic technologies to understand algal lipid metabolisms under different stress conditions have revealed potential targets in various microalgae which can pave path for targeted genetic engineering [93]. The detailed literature of omic components: proteomics, metabolomics and lipidomics used in the present study along with related technologies pertaining to algal omics have been discussed below individually.

1.6.1 Proteomics

Transcriptional profiling (mRNA levels) represent only a brief change in the expression of genes but many of the key regulatory pathways differ at the post-transcriptional level. Further, the correlation between transcription and translation is known to be less than 50 % [96]. Expression of a gene can be correlated appropriately by quantifying the level of proteins as they not only provide the fundamental organization and pathways occurring inside a cell but also indicate the cell's state (healthy, stressed or apoptotic) [97]. Thus, in depth understanding of stressed induced TAG accumulation in microalgae requires integration of transcriptomics and proteomics approach. Quantitative algal proteomics identify and quantify the dynamics of

protein abundance and its corresponding function both at translational and post translational level in response to any environmental stress leading to augmentation of TAG. Various techniques used to quantify the proteome including classical two-dimensional (2D/DIGE) gel electrophoresis and liquid chromatography (LC) based methods such as isotopic labelling and label free methods followed by mass spectroscopy (MS) [98]. LC based technologies have an edge over the conventional 2D as they can overcome the shortcomings of throughput and low coverage of extreme pH, hydrophobic, low abundance proteins [98]. With the advent of nano-HPLC (High-performance liquid chromatography) systems combined with improved MS (high accuracy and resolving power), thousands of protein abundances can be identified and quantified [99]. Stable isotope labelling techniques primarily tag the proteins with ^{13}C, ^{15}N, ^{18}O and then analyze using LC-MS or LC-MS/MS thereby increasing the precision and accuracy of quantification [99]. Recently, iTRAQ (isobaric tags for relative and absolute quantification) has been used to quantify proteomic changes in algal systems which are robust and easy to use [98]. Nevertheless, iTRAQ system has disadvantages such as underestimated ratios, expensive labelling and limited dynamic range [98]. Label free techniques, on the other hand are inexpensive, rapid with wider dynamic range and broader proteomic coverage [99]. The two major label free quantification methods are spectral counting (number of MS/MS spectra) and MS ion intensity (peak area). A brief representation of proteomics workflow is depicted in **Fig. 1.7**.
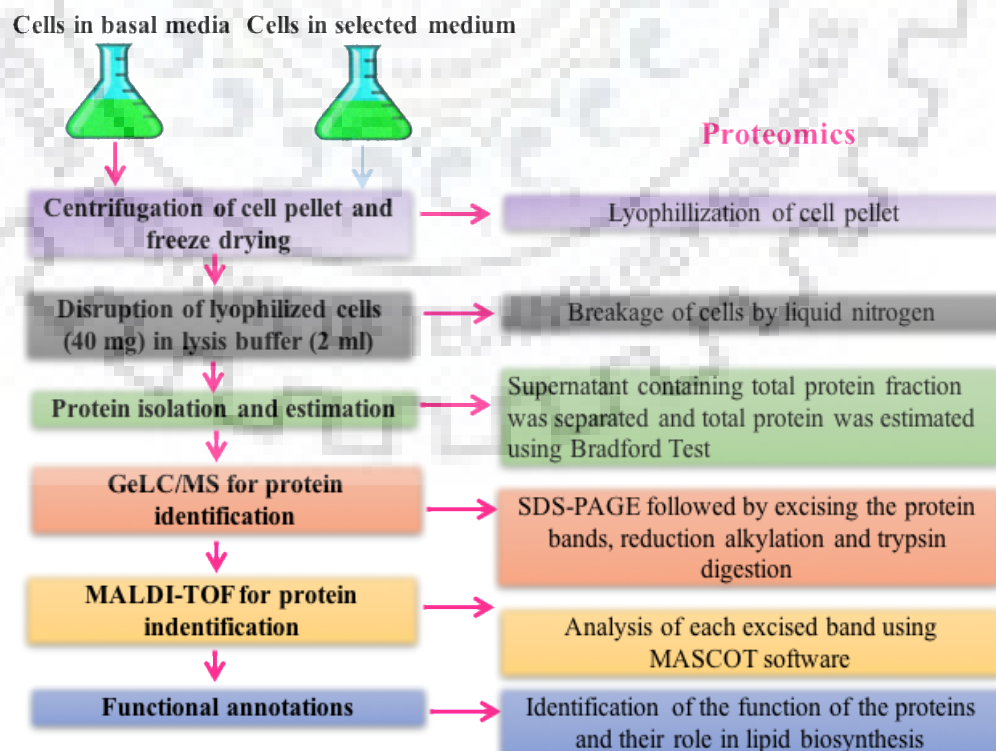
Fig. 1.7: *Workflow of proteomics analysis for microalgal samples.*

The proteomics studies carried out of various microalgae under different stress conditions reported in the literature are listed in **Table 1.2**. The proteome of different microalgal species under nitrogen deprivation showed an upregulation of acyl carrier proteins (ACP), malonyl-CoA:ACP transacyclase, lipid droplet surface protein (LDSP), ACCase, MAT, enoyl-acyl carrier protein reductase (Fab I), trans-2 enoyl CoA reductase, the four condensing enzymes involved during fatty acid synthesis (KAS, HD, ENR) and DGAT. On the other hand, a decline in the levels of AMP activated kinase (AMPK), fatty acid catabolism (acyl CoA dehydrogenase) and stearoyl-ACP desaturase was recorded. AMPK inhibits the ACCase activity by phosphorylating while stearoyl-ACP desaturase catalyzes the formation of oleoyl ACP form stearyl-ACP [95,100–106]. The proteomic studies also revealed decline in the proteins involved in the photosynthesis, chlorophyll and carotenoid synthesis respectively [95,100–104,106,107]. However, an upregulation in the TCA cycle proteins, glycolysis enzymes, ATP synthase and nitrate reductase were observed [101,103,108,109]. The above proteomic results indicated redirection of carbon and energy flux towards the TAG accumulation under nitrogen deplete conditions.

Apart from changes in the proteome of microalga in response to nitrogen stress, other environment stimuli has also been investigated including effect of coper, lipid mutants, light intensity/inoculum size and heterotrophic mode **(Table 1.2)**. Due to the availability of *C. reinhardtii* starchless and lipid mutants, the alga been most exploited for studying changes in expression of proteins [96,107,110,111]. Most of the responses reported in these lipid mutants were similar to the observations obtained under nitrogen starvation such as activation of glycolysis, TCA, heat shock, ATP synthase, fatty acid biosynthesis proteins while decrease in the abundance of ribosomal, photosynthetic, nucleotide synthesis proteins. However, few differences in protein expression were also reported such as increase in thiamine metabolic process in starchless mutant of *C. reinhardtii* (sta 6) as compared to wild type (cw15) [110]. Elevation in the expression of two main proteins involved in thiamin biosynthesis (hyroxylmethyl pyrimidine phosphate synthase and thiazole biosynthetic enzyme) indicated decrease in carbon fixation and sugar synthesis by the mutant strain as thiamine plays a vital role in intermediary carbon metabolism [110]. Further, Choi et al. reported an increase in 3-methyl-2-oxobutanoate hyroxymethyl transferase in ethyl methane sulfonate (EMS) of *Scenedesmus obliquus* indicating an escalation in pantothenate biosynthetic pathway thereby increasing the synthesis of coenzyme-A and metabolism of proteins and fats resulting in accumulation of lipids inside the microalga [112]. The effect of salt stress on the proteomic profile of *Chlorella vulgaris* studied by Li et al. reported an increase in Mao-C like protein (modulates fatty acids), Spp30 like protein (transports lipid to Golgi for packaging), profiling

(maintains cell's structure integrity) and glycine rich like proteins (forms an independent structure within the extracellular matrix to assist in proper cell wall assembly) resulting in overall increase in lipid accumulation [113]. Interestingly, they also reported an increase in 60S ribosomal protein L5 and 40S ribosomal protein S12 which was contradictory to the nitrogen depletion assisted lipid accumulation in microalgae. The possible reason for this could be an increase in these ribosomal proteins promotes the functional restructuring of protein synthesis in *C. vulgaris* under salt stress.

Microalgae	Media	Method used for analysis	References
Nitrogen depletion			
Chlorella vulgaris	BBM	GeLC/MS	[105]
	BBM		[114]
	Watanabe media + NaCl	2DE/MALDI-TOF	[115]
C. protothecoides	Basal medium		[116]
	Watanabe medium		[102]
Chlamydomonas reinhardtii	TAP		[98]
			[117]
			[118]
Chlorella sp. FC2IITG	BG-11	2D and iTRAQ	[119]
Phaeodactylum tricornutum	F/2 + Si medium	LC-MS/MS	[106]
Nannochloropsis oculata	Artificial seawater enriched with f/2 medium		[95]
Nannochloropsis oceanica IMET1	Artificial seawater medium	2DE/MALDI-TOF	[108]
Neochloris oleoabundans	BBM	LC-MS/MS	[120]
Phaeodactylum tricornutum	F/2 + Si medium	NanoLC-MS/MS	[101]
Dunaliella parva	F/2	iTRAQ	[104]
Copper stress			
C. protothecoides	BCM+ 10g/L glucose	2DE/MALDI-TOF	[121]
Salinity			
C. reinhardtii	TAP	GeLC/MSMS	[122]
Dunaliella salina	1M NaCl	LC-MS/MS	[123]
Lipid mutants			
Scenedesmus dimorphus	BBM	2DE/MALDI-TOF	[112]
Tisochrysis lutea	Walne's medium		[107]

Table 1.2: *Proteomics studies on microalgal strains cultivated under stress conditions.*

1.6.2 Metabolomics

Metabolome is the qualitative and quantitative collection of all low molecular weight compounds such as amino acids, carbohydrates, nucleotides, organic acids, energy compounds, fatty acids, lipids, vitamins responsible for maintaining cell's biological processes [124]. These compounds or preferably called metabolites are the products of cellular regulatory processes and their evaluation can shed light into cell's response towards any environment stimuli [125]. Measurement of metabolites does not require organism's genomics information and thus can be an ideal omics tool for depicting cellular response of any non-model organism. However, accurately measuring the metabolites profile of an organism exposed to different environment cues is cumbersome due to wide variation in the chemical properties including polarity, solubility, volatility, ionic charge and molecular weight [125]. To combat this scenario, various techniques to quantify metabolome of an organism have been developed such as capillary electrophoresis mass spectroscopy (CE-MS), gas chromatography- mass spectroscopy (GC-MS), liquid chromatography- mass spectroscopy (LC-MS), nuclear magnetic resonance (NMR), Fourier transform ion cyclotron resonance- mass spectroscopy [124]. Among these, MS combined with chromatography is the most widely used technique in metabolomics as it is rapid, sensitive, selective but it shows laboratory variation, requires expensive reagents and derivatization of samples. On the other hand NMR is less sensitive than MS but at the same time is more robust, non-destructive along with high throughput and reproducibility and minimal sample preparation requirements [124,126]. In the thesis, NMR based metabolomics was done and the overview of the steps involved is depicted in **Fig. 1.8**.

Cultivation of microalgae in controlled growth conditions
Harvesting of microalgal cells   Freeze drying of cells

Metabolite extraction from microalgal cells
Lyophilized cells crushed using liquid nitrogen   Metabolome extraction using cold methanol: chloroform and water

Preparation of metabolites
Hydrophilic phase dried under steam of nitrogen   Addition of Phosphate buffer followed by lyophilisation

^{1}H NMR profiling
Dissolving the metabolites in D_2O ^{1}H NMR data procurement   Processing of NMR data using Top Spin (Bruker)

Statistical analysis of metabolites
Normalization of data and application of appropriate statistical test   PCA, Heat Map and box plot generation

Fig. 1.8: *Steps involved in a NMR based metabolomics study.*

Recently metabolomics has been applied to identify biochemical targets triggering lipid accumulation in various microalgae (including cyanobacteria) and diatoms on exposure to different conditions **(Table 1.3)**. The documented differentially expressed metabolites under various stress conditions (nitrogen, salinity, heavy metal) complemented the existing knowledge of the transcriptomics and proteomics data. In case of nitrogen deprivation, an increase in the levels of citrate, malate, succinate, fructose 1, 6 biphosphate, glucose 6 phosphate, isocitrate, 2-oxoglutarate while decrease in amino acids (phenylalanine, tryptophan, aspartate, arginine, glutamine, proline, ornithine, citrulline and aspargine) indicated activation of glycolysis, depression of protein synthesis and concomitant increase in lipid accumulation inside microalga [118,125,127]. Further, Wase et al., reported an increase in trehalose a non-reducing disaccharide which helps in stabilizing cellular membranes and proteins maintaining cell's integrity [118].

Microalgae	Cultivation media	Limitation/mode	Reference
Chlamydomonas reinhardtii	TAP	Nitrogen depletion	[127]
			[118]
Chlamydomonas sp. JSC4	Modified Bold 3 N medium	Light + nitrogen depletion	[128]
		Salinity + nitrogen depletion	[4]
C. reinhardtii	TAP	Salinity	[122]
Chlorella vulgaris	LC Oligo medium	Nitrogen depletion + cadmium stress	[129]
C. sorokiniana	BG-11	Inoculum size	[130]
Scenedesmus obliquus		-	[131]
Synechocystis sp. PCC6803			
Anabaena sp. PCC7120			
Schizochytrium sp.	-	-	[132]
Pseudochoricystis ellipsoidea	A5	Nitrogen depletion	[125]

Table 1.3: *Details of metabolomics studies carried on different microalgae.*

Interestingly, the metabolic profile of *C. vulgaris* altered under simultaneous nitrogen deprivation and cadmium stress showing an increase in the free amino acids (proline, valine, isoleucine, sarcosine, phenylalanine, methionine) which could be due to microalga's defense mechanism against cadmium [133]. Sarcosine, glycine, valine, thioproline, methionine, phenylalanine, glutamine and ornithine help in the complexation of heavy metal on microalgal cell membrane while glutathione aids in the synthesis of phytochelatins which quench the reactive oxygen species (ROS) generated due to heavy metal stress [134]. Proline is a well-

known osmoregulatory molecule playing a vital role in scavenging free radicals as well as stabilizer and electron sink alleviating side effects caused by heavy metal on microalgae [135]. Likewise, an increase in metabolites playing a crucial role in augmenting TAG accumulation (ethanolamine, glycerol, glycerol 3-phosphate, acetyl Co-A, 3 phosphoglyceric acid, 2-ketoglutaric acid) was reported while studying effect of salinity, light intensity, 6-benzyl amino purine and butylated hyroxyanisole) on different algal species [128,136–138]. The above discussed studies on the metabolic profiles offer a snapshot of various biomarkers for increasing TAG accumulation thus opening potential targets for metabolic engineering and also improving the basic understanding of the systemic response.

1.6.3 Lipidomics

Lipidomics is a branch of metabolomics to identify and differentiate classes of lipids as well as the molecules that interact with these lipids [139]. Both LC-MS and chemometric methods combined with multivariate analysis are the most widely used techniques for carrying out lipidomics [139]. Characterizing the dynamics in the lipidomic in response to different environmental cues can help not only in understanding the lipid metabolism of microalgae but may also inform manipulation of the lipid yield and profile to achieve desirable results for favorable biofuel production metrics [140]. To date, only few studies have characterized changes in the lipidome in response to various stress conditions such as temperature, salt, and nutrient depletion. These studies identified few lipid biomarkers including free fatty acids, hardero porphyrin, phosphatidyl glycerol, 1,2 diacyl glycerol-3-0-4`- (N,N-trimethyl)-homoserine, TAG, cholesterol, sulphoqunovosyl diacylglycerol, lysosulphoqunovosyl diacylglycerol, digalactosyl diacylglycerol and lysodigalactosyl diacylglycerol that increased/decreased in order to adapt to the given environmental stress in various microalgae (*Nitzschia closterium f. minutissima*; *C. reinhardtii*, *N. oceanica* IMET1, *Dunaliella tertiolecta*, *Chloromonas*, *Chlamydomonas nivalis*) respectively [111,116,139,141,142].

Additionally, a few studies have characterized the integral proteins attached with lipid droplets that aid in oil globule formation and interaction with other organelles [143]. Among the integral proteins, the presence of oleosin (structural protein) and caleosin (calcium binding lipid body protein) have been reported in various green algae including *C. reinhardtii*, *D. salina*, *H. pluvialis*, *C. variablis*, *Coccomyxa sp. C-169*, *Chlorella*, *N. oceanica*, *N. gaditana*, *N. granulata*, and *N. salina* [143–151]. Most of these studies have been identified and functionally characterized Major Lipid droplet protein (MLDP) and LDSP. MLDP, a 28 kDa hydrophobic protein was shown to provide integrity to the lipid droplets by interacting with

tubulins while its suppression (~ 60 % reduction in MLDP gene expression) resulted in 40 % increase in lipid droplet size with concurrent reduction in lipolysis [145,151]. Interestingly, increases in lipid droplet size did not increase the overall TAG accumulation inside the microalga. On the other hand, LDSPs are actively involved in formation and stabilization of lipid droplets as their expression was directly proportional to accumulation of TAGs [150], underscoring the potential value in such lipidomic approaches. However, this microalgal field is still in its infancy and further detailed studies are imperative for identifying potential biomarkers that could be exploited for enhancing lipid yield in microalgae for biofuel production.

1.7 Gene technology approaches to increase the TAG accumulation in microalgae

Transgenic microalgae are gaining focus due to their potential to provide researchers with the opportunity to reconstruct and remodel the microalga's lipid biosynthetic pathways to examine and develop high TAG accumulating phenotypes. In recent years, microalgae have been successfully transformed using various genetic tools such as random integrative selection marker and homologous recombination (HR)-mediated DNA incorporation and RNA silencing via electroporation and biolistic transformation [152]. Microalgae can be transformed either in the nuclear, chloroplast or mitochondrial genomes depending on the type of gene/construct to be expressed or deleted [153].

There are four major routes to increase lipid production in microalgae proposed to date: (a) enhancing flux and/or biosynthetic rate of fatty acid metabolism, (b) inhibiting competing carbon pathways (e.g. starch synthesis) (c) improving energy efficiency and carbon uptake and (d) reducing TAG catabolism. To date, most of the recombinant studies for increasing lipid accumulation in microalgae have targeted enhanced flux via overexpression of lipid biosynthetic genes; ACCase was the first gene to be overexpressed (3-4 fold) in diatom *C. cryptica* and then in *Navicula saprophila,* though neither case resulted in an increase in TAG accumulation [154,155]. Similar efforts have been made in other microalgal strains (*C. reinhardtii*, *P. tricornutum*) by overexpression of other lipid accumulating genes such as DGAT isoforms (DGAT2-1, DGAT 5), KAS III, FAS (fatty acid synthase) enzymes, and ME, while RNA silencing of DGAT2-4 resulted in ~ 30-50 % increase in lipid content [153,155,156]. Apart from these lipid genes, thioesterase has been overexpressed in the nuclear genomes of *P. tricornutum,* and *C. reinhardtii,* which did not result in increase in fatty acid synthesis, but significantly increased the C12-C14 fatty acids [153]. However, recently, the overexpression of fatty acid- ACP thioesterase in *C. reinhardtii* resulted in an increase in the

total lipid by 14-15 % [157]. Moreover, overexpression of LPAAT (from *Brassica napus*) and GDPI (*S. cerevisiae*) in *C. reinhardtii* resulted in an increase in total fatty acids by 17.4 % and 23.6 % as compared to non-transformed cells [158]. Further, knockout of a multifunctional lipase gene resulted in 3-fold higher lipid accumulation in *T. pseudonana* [153].

Besides this, an attempt has been made to block the competing starch synthesis pathway. AGPase or isoamaylase deletion in *C. reinhardtii* resulted in higher TAG content compared to wild type strains under nitrogen deplete conditions [155]. However, this increase in lipid accumulation was minor compared to starchless mutants of the respective microalgal strain, indicating alternative pathways may be upregulated in engineered strains, thus requiring a thorough knowledge of the regulatory metabolic pathways for successful metabolic manipulation [159]. Further, disrupting the primary carbon pathways can lead to low biomass generation, thus knockdown rather than knockout of lipid catabolism pathways can be a viable alternative. The above approach has been evaluated in model lipid accumulating diatom (*T. pseudonana*) in which a predicted hydrolase (Thaps3_264297) responsible for breakdown of lipid was knocked down using antisense and RNAi approaches. The deleted mutant showed 2.4-3.3 fold higher lipid accumulation under silicon deficiency as compared to wild type without compromise in growth [160]. In a recent study, overexpression of an E2- conjugating enzyme (Cr UBC2), which has homology to a yeast and Arabidopsis MMS2/UEV) in *C. reinhardtii* increased the lipid content by 20 % as compared to wild type. E2-conjugating enzyme is crucial for transferring ubiquitin and ubiquitin like protein to substrates and actively involved in DNA repair and DNA damage tolerance. These results suggested that a protein substrate of CrUBC13–CrUBC2 polyubiquitination is involved in lipid accumulation [161].

Although the above-mentioned genes boosted the lipid accumulation in respective microalgal strains, the results vary from species to species i.e. one target may be effective in one microalgal strain but fail to increase fatty acid synthesis in another strain. It is also worth pointing out that it is not unusual for researchers to use lipid extraction and gravimetric analysis or lipophilic dyes such as Nile Red or BODIPY (boron-dipyrromethene) along with fluorometry to measure TAG content. Results from this approach do not always correlate well with actual lipid content. This scenario calls for the identifying and exploiting universal lipid triggers that could substantially boost the TAG production without inhibiting cell growth. This can be achieved by integrating the omics data of all the prospective high lipid accumulating strains under various stress conditions.

1.8 Thesis objectives and outline

The main objective of the thesis is to study the stress induced TAG accumulation in a novel halotolerant and heavy metal tolerant oleaginous microalgal strain using various biochemical and biophysical techniques.

Photosynthetic microalgae represent a viable alternative to plant-based fuels due to their high biomass and oil productivity, year round production, marginal use of agricultural land, no requirement of any herbicide/pesticide treatment and biofixation of atmospheric as well as excess CO_2 emissions. However, several techno-economic reports suggest mass scale microalgal cultivation for biofuel production is still at its infancy in comparison to land based energy crops. The commercial scale up barriers towards economical and sustainable operations includes high lipid productivity achievement, fresh water resource and nutrient availability, CO_2 supply, process stability and downstream product development. Bioprospecting of high biomass and lipid accumulating strains capable of growing in low cost feedstocks such as saline waters and waste waters contaminated with heavy metals can provide a gigantic leap towards reduction of both the cost and sustainability challenges for biodiesel production. Algal-omics techniques have the potential to unravel key metabolic engineering targets for enhancing the lipid productivity. Keeping the above prospects in mind, the specific objectives of the thesis are as follows:

1. To bioprospect novel indigenous high biomass and lipid accumulating microalgal strains capable of growing in sea water.
2. To elucidate the molecular halotolerance mechanism of *Scenedesmus* sp. using integrated omics approach.
3. To assess the robust growth and lipid accumulating characteristics of *Scenedesmus* sp. cultivated in natural sea water using small scale custom built photobioreactor.
4. To delineate the differential metabolic responses of *Scenedesmus* sp. during arsenic (III, V) mitigation.

Bioprospecting of novel indigenous high biomass and lipid accumulating microalgal strains capable of growing in sea water

2.1 Introduction

Microorganisms such as algae that can grow in the absence as well in presence of salts are designated as halotolerant. These halotolerants have a great metabolic flexibility to cope and adapt to high saline environments. They do this by accumulating high amounts of organic osmotic solutes to maintain the osmotic balance [162]. On exposure to salinity, microalgal cells restore turgor pressure by eliminating Na^+, accumulating K^+ while maintaining the intracellular level of Ca^{2+} constant. Accumulation of metabolites such as glycerol, fructose, sucrose and trehalose maintains osmolality while charged molecules, including proline and glycine betaine readjust the osmotic equilibrium by preventing water loss [163–166]. These readjustment of metabolites inside microalgae generates stress resulting in the accumulation of large amounts of either carbohydrate or lipid content for its survival. Indeed, the carbohydrate accumulated in the microalgal cells is also an important energy source, and can be potentially used for bioethanol, biohydrogen and bioplastic generation [167,168]. However, the strains with incremented lipid contents that act as an energy reserve material, for cell survival are appropriate and novel candidates for producing algal oils/biodiesel [164,169]. Understanding the mechanism of enhanced lipid accumulation in response to salinity stress would provide useful insights on key regulators of lipid metabolism and halotolerance in microalgae, leading to targeted pathway engineering for reducing biodiesel production costs.

Hence, bioprospecting of indigenous high biomass and lipid accumulating microalgal strains capable of growing in sea water was carried out. A total of four strains (*Scenedesmus* sp. IITRIND2, *Chlamydomonas debarayna* IITRIND3; *Chlorella* sp., and *Tetradesmus obliquus* IITRIND1) were isolated and three acquired strains (*Chlorella minutissima*, *Scenedesmus abundans* and *Chlorella pyrendosia*) were evaluated for their salt tolerance by cultivating in artificial sea water (ASW). Among the microalgae tested, *Scenedesmus* sp. IITRIND2 capable of growing in 100 % ASW was selected for further analysis. The potential of the novel microalga was analysed by estimating its biomass and lipid productivity. The results were

correlated to the alterations observed in the cell size, photosynthetic pigments, lipid, carbohydrate, protein content, stress related enzymes and osmolytes under saline conditions to shed light on the adaptive strategies of microalga. The results unveil that the metabolic alterations occurred in the microalga when exposed to sea water salinity commensurate with enhanced TAG accumulation, with an acceptable fatty acid profile for biodiesel production.

2.2 Materials and Methods

2.2.1 Materials

Chemicals used for the preparation of ASW and modified Bold's Basal media (BBM) were purchased from Himedia, India. All solvents and reagents were HPLC grade. Nile Red stain (9-diethylamino-5H-benzo[α]-phenoxazine-5-one) was procured from Invitrogen (Life Technology, USA).

2.2.2 Algal strains isolation and identification

Microalgae samples were collected from fresh water lake nearby Gas Station, National Highway 73, Bhagwanpur, Uttarakhand, India (30.0694 $^\circ$N, 77.8400 $^\circ$E). Pure culture was isolated by serial dilution and then streaking the samples on to 1 % modified BBM agar plate and incubated for 6 days at 27 °C with illumination of 200 mmol/m/s (Light/Dark cycle of 16 h : 8 h). Modified BBM had the following composition (g/ L): $NaNO_3$, 0.25; KH_2PO_4, 0.175; K_2HPO_4, 0.075; $MgSO_4 \cdot 7H_2O$, 0.075; NaCl, 0.025; $CaCl_2.2H_2O$, 0.025; $FeSO_4.7H_2O$, 0.005; EDTA, 0.005; and 1mL of micronutrient stock including: H_3BO_3, 2.86; $ZnSO_4.7H_2O$, 0.222; $CuSO_4.5H_2O$, 0.079; $MnCl_2.4H_2O$, 1.81; Co $(NO_3)_2.6H_2O$, 0.041 and $Na_2MoO_4.2H_2O$, 0.390 [105]. The initial pH of the medium was adjusted to 7.4. Single colonies were picked and inoculated in 5 mL BBM with illumination of 200 mmol/m/s (Light/Dark cycle of 16 h: 8 h), 130 rpm at 27 °C. The morphology of the isolated microlagal strains were visualized under light microscope *(EVOS-FL, Advance Microscopy Group, AMG, USA, 60X)* and by Field Emission Scanning Electron Microscopy (FE-SEM Quanta 200 FEG). For FE-SEM visualization, the microalgal cells were fixed by incubating them overnight with 2.5 % glutaraldehyde solution at 4 °C in dark. The fixed cells were then dehydrated by sequential treatments with 10-100 % ethanol and then were gold spurted to make them electro conductive for FE-SEM analysis.

For microalgal identification, genomic DNA was isolated, amplified using ITS1F (TCCGTAGGTGAACCTGCGG), ITS4R (TCCTCCGCTTATTGATATGC) primers and sequenced. The sequences obtained were compared with the sequences available at NCBI (National Center for Biotechnology Information) database (http://www.ncbi.nlm. nih.gov), using BLAST (Basic Local Alignment Search Tool) programme. To determine the taxonomic position and relationships of novel microalgae isolates, phylogenetic tree was constructed using MEGA 6 software [170].

2.2.3. Microalgae strains procurement

Chorella minutissima (MCC-27) was obtained from the Centre for the Conservation and Utilization of Blue Green Algae, Indian Agricultural Research Institute, New Delhi. *Chlorella pyrenoidosa* (NCIM 2738) and *Scenedesmus abundans* (NCIM 2897) were procured from National Chemical Laboratory, Pune.

2.2.4. Assessment of salt tolerance by the microalgal strains

Microalgal strains were cultivated in 500 mL shake flasks containing 100 % ASW (35 g/L sea salts) for 10 days at 27 °C, with photoperiod of 16:8 h (light- dark cycle) and irradiated with 6 white light (2000 lux). The modified ASW had the following composition (g/L): 6.29 $MgSO_4 \cdot 7H_2O$, 1.0 $NaNO_3$, 0.07 KH_2PO_4, 0.18 $NaHCO_3$, 0.098 KBr, 0.026 H_3BO_3, 0.003 NaF with 4.66 $MgCl_2 \cdot 6H_2O$, 1.02 $CaCl_2 \cdot 2H_2O$, 28.65 NaCl, 0.67 KCl as sea salts respectively. The DCW (g/L) was estimated by drying the wet biomass at 80 °C for 12 h in hot air oven. The microalga that adapted to 100 % ASW with maximum biomass was selected for further analysis.

2.2.5. Effect of salinity on microalgal growth and lipid accumulation

To understand the salinity stress resistance and to evaluate the maximum lipid productivity of microalga in brackish water and sea water, cells were grown in four different salinity percentages of ASW (0, 30, 50, 80 and 100 %) corresponding to 0, 10.5, 17.5, 28 and 35 g/L of sea salts respectively. The rest of the nutrients concentrations were kept constant and pH was set at 7.2-7.4. Modified BBM was used as control. The detailed recipe of the different ASW (%) is listed in **Table 2.1**. The cultures were grown in 1 L shake flasks in triplicates with

initial inoculum of 0.02 g/L (fresh weight) for 7 days. All flasks were shaken periodically after every 6 h on a magnetic stirrer.

Sea salts concentration (g/L)	Artificial sea water				
	0 %	30 %	50 %	80 %	100 %
$MgCl_2.2H_2O$	0	1.39	2.33	3.73	4.66
$CaCl_2.2H_2O$	0	0.32	0.51	0.82	1.02
NaCl	0	8.59	14.33	22.9	28.65
KCl	0	0.2	0.34	0.54	0.67

Table 2.1: *Sea salt concentrations for different % of Artificial sea water.*

Microalga growth phases were monitored after every 24 h by measuring the absorbance at 750 nm. The dry cell weight (DCW; g/L) was calculated by harvesting the cells and washing the pellet thrice with distilled water to remove any medium components. The pellet was then dried at 80 °C for 24 h and gravimetrically measured to obtain the DCW. Biomass productivity (mg/L/d) was calculated by the following equation:

$$\text{Biomass productivity} = \frac{\text{Final DCW} - \text{Initial DCW}}{\text{Cultivation time}}$$

Lipid accumulation in the microalga cells was estimated by Nile red staining. Briefly, microalga cells suspension (200 μL) was incubated with 10 μl of Nile red (0.1 mg/mL in Dimethyl sulfoxide) for 15 min in dark. The cell suspension was then centrifuged; the pellet obtained was washed thrice with 0.9 % saline solution and visualized under a fluorescent microscope (EVOS-FL, Advance Microscopy Group, AMG, USA) equipped with the RFP light cube. The total lipid was extracted using modified protocol of Bligh and Dyer [171]. Briefly, the biomass was harvested by centrifugation at 6500 g for 5 min and then air dried. Dried biomass was treated with liquid nitrogen, and then suspended in chloroform: methanol (1:2; v/v) for 3 h with continuous stirring. The cell suspension was then centrifuged at 6500 g for 5 min and the supernatant was aspirated into a new screw cap glass tube. Sequential treatment with 0.034 % $MgCl_2$, 0.2 N KCl and artificial layer (chloroform: methanol: water; 3:47:48; v/v/v) each followed by centrifugation and then aspirating out of lower layer. The

lower layer was then vacuum dried and total lipid was gravimetrically weighed. Lipid productivity (mg/L/d) was calculated using the following equation:

$$\text{Lipid productivity} = \frac{(\text{Final total lipid concentration} - \text{Initial total lipid concentration})}{\text{Biomass productivity}}$$

2.2.6 Estimation of fatty acid profile and biodiesel properties

Total extracted lipids were transesterified using 6 % methanolic H_2SO_4. Briefly, total lipids (5 mg) were mixed with 4 mL methanolic H_2SO_4 and incubated in water bath for 2 h at 80 °C. The transesterified product was cooled to room temperature. FAMEs were recovered by mixing with hexane and then washed with distilled water (2:1; v/v). The mixture was centrifuged at 6500 g for 5 min and FAME phase was aspirated in screw cap glass tube for FAME analyses by GC-MS (Agilent technologies, USA) equipped with DB-5 capillary column (30 mm, 0.25 mm, 1μm) and FID detector. Helium (1mL/min) was used as carrier gas. 1μL of FAMEs sample was injected at 250 °C in split less mode. Temperature profile was programmed by adjusting initial temperature of column oven at 50 °C for 1.5 min then ramped to180 °C (25 °C/min) for 1 min followed by 220 °C (10 °C/min) for 1 min and finally to 250 °C (15 °C/min), held for 3 min [172].

Biodiesel physical properties such as saponification value (SV; mg KOH), iodine value (IV; gI_2/100 g), cetane number (CN), degree of unsaturation (DU; % wt), long chain saturation factor (LCSF; % wt), cold filter plugging point (CFPP; °C), high heating value (HHV; MJ Kg^{-1}), kinematic viscosity (KV (v_i); 40 °C in mm^2 s^{-1}), density (ρ; 20 °C in g cm^{-3}) and oxidative stability (OS; h) were estimated according to the empirical formulas listed below [41].

$SV = \sum 560 \ (\% \ FC) / M$

$IV = \sum 254 \ DB * \% \ FC / M$

$CN = 46.3 + 5458 / SV - (0.255 * IV)$

$DU \ (\%) = MUFA + (2 * PUFA)$

$LCSF = (0.1 * C16) + (0.5 * C18)$

$CFPP = (3.417 * LCSF) - 16.477$

$HHV = 49.43 - 0.041 \ (SV) - 0.015 \ (IV)$

$\ln (KV) = -12.503 + 2.496 * \ln (\sum M) - 0.178 * \sum DB$

$Density = 0.8463 + 4.9 / \sum M + 0.0118 * \sum DB$

OS = 117.9295 / (wt % C18:2 + wt % C 18:3) + 2.5905

Where M = molecular mass of each fatty acid component, DB = number of double bonds, FC = % of each fatty acid component, MUFA = weight % of monounsaturated fatty acids, PUFA = weight % of poly unsaturated fatty acid.

2.2.7 Cell size and biochemical composition estimation

Cell diameters of approximately 100 microalga cells were measured using 'Image J 1.49a' software. Nitrogen content was estimated using an CHNS elemental analyser (Thermo Fischer, USA) and the crude protein was estimated using the following equation:

$$\text{Crude protein (\%)} = 6.25 \times \text{Total Nitrogen (\%)}$$

Total carbohydrate in the lipid extracted microalga sample was estimated using phenol sulphuric acid method [173]. Briefly, 100 mg of de-oiled biomass was treated with 2 % H_2SO_4 and autoclaved at 120 ℃ for 30 min. The cell suspension was then centrifuged and the supernatant obtained was used for estimation of sugar using glucose as standard. Pigments (chlorophyll a, chlorophyll b and carotenoids) in microalgae cultivated in ASW after 7 days (early stationary phase) were estimated using the protocol of Lichtenthaler, 1987 [174]. Briefly, 2 mL of cell suspension was harvested and then the pellet was suspended in 2 mL methanol (99 %) and incubated for 24 h at 45 °C. The supernatant obtained was used for estimation of pigments (μmol) using the following equations:

$$\text{Chlorophyll a} \left(\text{Chla;} \frac{\mu g}{mL}\right) = 16.72 A_{665.2} - 9.16 A_{652.4}$$

$$\text{Chlorophyll b} \left(\text{Chlb;} \frac{\mu g}{mL}\right) = 34.09 A_{652.4} - 15.28 A_{665.2}$$

$$\text{Caratenoids} \left(\frac{\mu g}{mL}\right) = (1000 A_{470} - 1.63\,\text{Chla} - 104.9\,\text{Chl b})/221$$

$$\text{Pigments in extract (μmol)} = \frac{\text{Pigments in the extract (μg)}}{\text{Molecular weight of the pigment}}$$

where standard molecular weight of chlorophyll a, chlorophyll b and carotenoids were 894, 908 and 570 respectively.

2.2.8 Stress metabolites estimation

Reactive oxygen species (ROS): To estimate the ROS content in microalgae after 7 days grown in ASW, changes in H_2O_2 and lipid peroxidation were recorded. For H_2O_2 estimation, the cell suspension was centrifuged at 6500 g for 10 min. Cells pellet (0.5 g) was homogenised with 0.1 % trichloroacetic acid (TCA; w/v) and centrifuged at 10,000 rpm for 10 min. Supernatant (0.5 mL) obtained was mixed with 0.5 mL phosphate buffer saline (PBS), (10 mM, pH 7.0) and 1 M potassium iodide (KI; 1mL). Absorbance at 390 nm was recorded and H_2O_2 content was expressed as l mol H_2O_2 g/ fresh weight (FW) [175]. The calibration curve was obtained with H_2O_2 (0 nmol to 14 nmol) standard solutions prepared in 0.1 % TCA. Lipid peroxidation was determined in terms of thiobarbituric acid reacting substance (TBARS) as per the protocol described by Tian and Yu [176]. The standard curve for TBARS estimation was generated by using 1,1,3,3 tetraethoxypropane (TMP) in 0.2-20 μM concentration range. TBARS content was measured by using the following formula:

$$\text{TBARS content} = (A532 - A600) \times EC$$

where A is the absorbance in nm and EC is the extinction coefficient (155 X 10^5 M/cm).

Osmolytes: Total proline in microalgal cells grown in ASW was extracted using 3 % sulphosalicyclic acid and estimated using L-proline as standard. The optical density was measured at 520 nm for determining total proline content in cells [177]. Glycine betaine content in microalga was estimated by taking 0.5 g cells and homogenizing it in equal volumes (200 μL) of deionised water, 2N H_2SO_4 and incubating in ice bath for 2 h. After incubation, 200 μL of cold KI-I_2 reagent (1.75 g I_2 and 2 g KI in 10 mL deionized water) was added and kept at 4 ℃ overnight. The cell suspension was then centrifuged at 10,000 g for 10 min and the supernatant was removed. Betaine periodic complexes formed were extracted by 1-2 dichloro-ethane and incubated in dark for 2 h. Absorbance at 365 nm was measured using glycine betaine as standard [178].

Antioxidant enzymes: To estimate the antioxidant potential of microalga grown in ASW, enzymatic extract was prepared and activities of catalase (CAT) and ascorbate peroxidase (APX) were recorded [179]. CAT activity was determined by mixing 0.1 mL enzymatic extract with 3 % H_2O_2 and phosphate buffer (pH 7.0) and measuring the change in the initial rate of disappearance of H_2O_2 at 240 nm for 150 s using an extinction coefficient of 0.0436 mM/cm.

APX activity was estimated by monitoring changes in absorbance at 290 nm and using an extinction coefficient of 2.8 mM/cm [179]. One unit of the enzyme activity was defined as the enzyme amount that transforms 1μmol of the substrate per minute. H_2O_2 and ascorbate were used as substrate for measuring CAT and APX activities. The enzyme specific activity(U/mg protein) was calculated using the following equation:

$$\text{Specific activity} = \frac{\{(\text{change in O. D. per min}) \times 1000 \times \text{reaction volume}\}}{\text{EC} \times \text{Volume enzyme in sample}} \times \text{Protein Conc.}$$

Where reaction volume was 3 mL, volume of enzyme in sample was 0.1mL respectively.

2.2.9 Statistical analysis

The experiments were carried out in triplicates (n=3) and all the data values are expressed as mean ± standard deviation.

2.3. Results

2.3.1 Microalgae isolation and identification

Microalgal strains were isolated from extreme environments such as wastewaters, heavy metal contaminated sites etc. and from sites faced with variable ecological conditions have highly adaptive capacity. These microlagal strains have also enhanced lipid accumulation which is a survival strategy. In light of these insights, the isolation of microalgae was carried out from a fresh water lake that receives discharges from local sewage treatment facilities along with presence of faeces and urine from domesticated animals and is expected to face variable ecology. A total of four species were isolated and were initially characterized based on morphology using light and FE-SEM microscopy **(Fig. 2.1)**. The phylogenetic relationship was constructed on the basis of the 18s rRNA gene and designated as strains of *Scenedesmus* sp. IITRIND2 (GeneBank Accession no: KT932960), *Tetradesmus obliquus* IITRIND1 (GeneBank Accession no: MH058029) *Chlamydomonas debarayana* IITRIND3 (GeneBank Accession no: KT932961) and *Chlorella* sp. (Submitted) respectively.
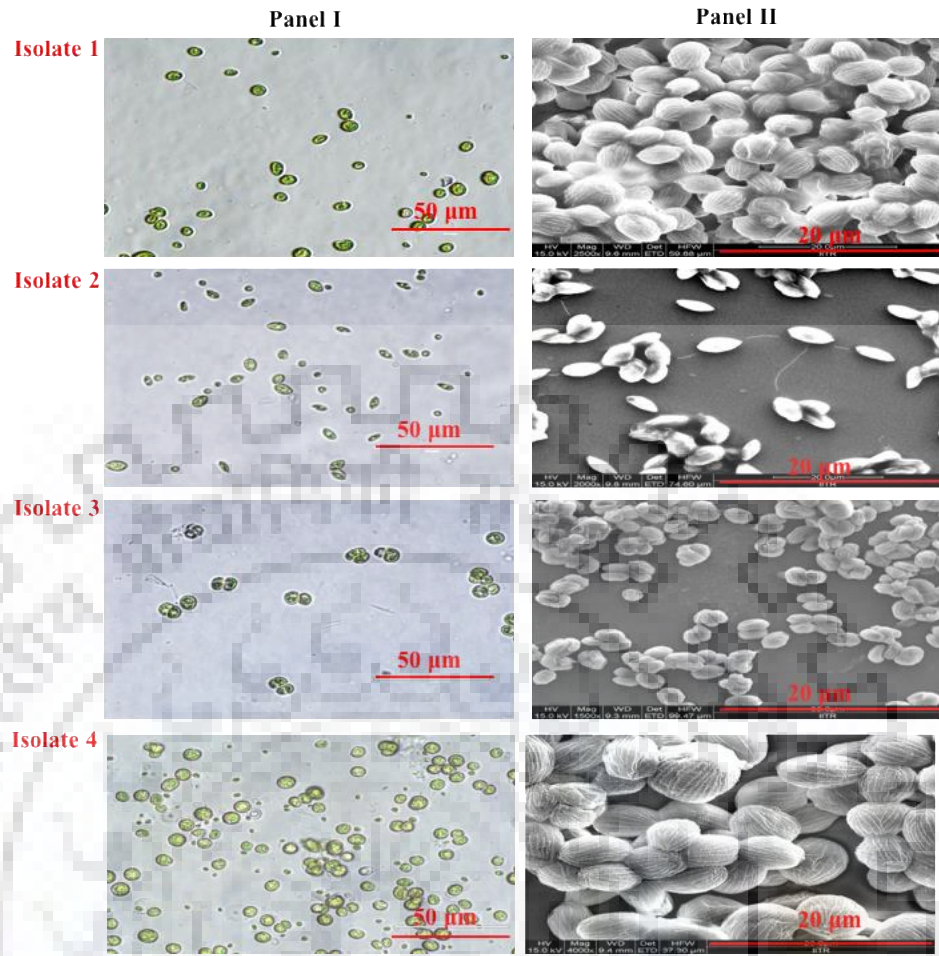
Fig. 2.1: *Light microscopic (Panel I) and FE-SEM images (Panel II) of isolated microalgal strains.*

2.3.2 Selection of salt tolerant microalgal strain

The isolated microalgal strains and three other reference strains (*C. minutissima*, *C. pyrendiosia* and *S. abundans*) were cultivated in ASW for a period of 10 days. Among the tested microalgal strains, *Scenedesmus* sp. IITRIND2 efficiently adapted to 100 % ASW along with maximum DCW (1.12 ± 0.04 g/L) and thus was selected as prospective microalgal strain for further analysis **(Table 2.2)**.

Microalgae	DCW (g/L) in ASW
Scenedesmus sp. IITRIND2	1.12 ± 0.04
Tetradesmus obliquus IITRIND1	0.12 ± 0.01
Chlamydomonas debarayana IITRIND3	0.54± 0.02
Chlorella sp.	No growth
Chlorella minutissima	0.36 ± 0.01
Chlorella pyrendiosia	No growth
Scenedesmus abundans	No growth

Table 2.2: *Dry cell weight (g/L) of microalgae cultivated in ASW.*

BLAST analysis of the isolate 1 sequence showed 99 % similarity and 91 % query cover to *Scenedesmus* sp. PSV1 (Genebank Accession no. JX519261). The isolate was identified as *Scenedesmus* sp. and the phylogenetic tree was drawn **(Fig. 2.2)**. The evolutionary history was inferred using the Neighbour-Joining method. The optimal tree with the sum of branch length = 0.57388747 is shown in **Fig. 2.2**. The evolutionary distances were computed using the Tamura 3-parameter method. Evolutionary analyses were conducted in MEGA6. The genus *Scenedesmus* comes under the family *Scenedesmaceae*.

Fig. 2.2: The phylogenetic tree of *Scenedesmus* sp. IITRIND2.

2.3.3 Estimation of dry cell weight, biomass productivity and lipid productivity

The adaptability of *Scenedesmus* IITRIND2 grown in ASW with different salt concentrations (0, 30, 50, 80 and 100 %) was tested by evaluating dry cell weight (DCW), biomass productivity, lipid productivity and compared with BBM grown microlagal cells. An increase in optical density (O.D.) was recorded in microalgal cells grown in ASW as compared to BBM with distinct growth phases, as shown in **Fig. 2.3A**.
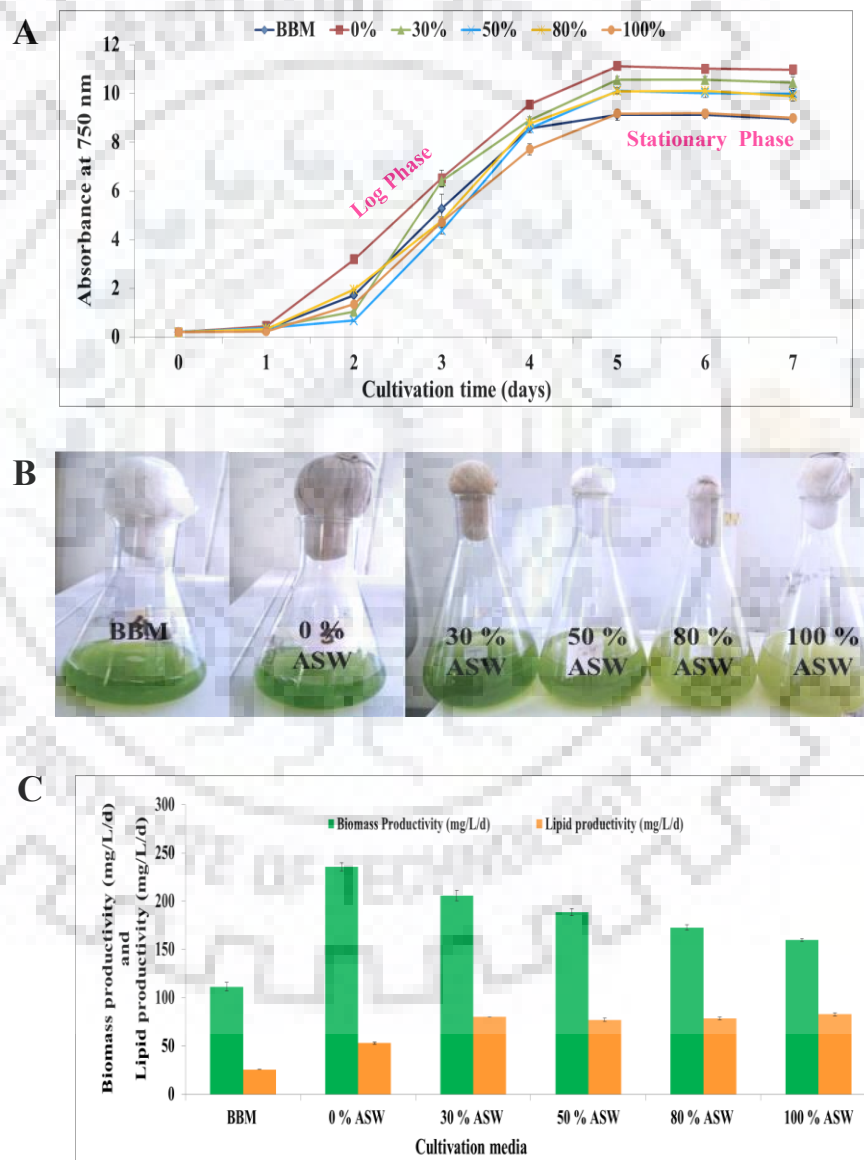
Fig. 2.3: (*A*) *Growth curve* (*B*) *Flask cultures* (*C*) *Biomass productivity (mg/L/d) and lipid productivity (mg/L/d) of Scenedesmus sp. IITRIND2 grown in different percentages of artificial sea water (ASW) and BBM for a period of 7 days*.

35

Comparison of *Scenedesmus sp. IITRIND2* with other reported freshwater microalgae grown in different salinities showed an increase in lipid content (%) and lipid productivity (mg/L/d) as to *Dunaliella* sp., *Nannochloris oleobundans, Scenedesmus sp.* CCNM 1077*, C. sorokiniana* HS1 and *Chlorococcum* sp. RAP 13 (**Table 2.3**).

Microalgae	Growth media	Salt (g/L)	DCW (g/L)	Lipid content (%)	Biomass productivity (mg/L/d)	Lipid productivity (mg/L/d)	Reference
Nannochloris oleobundans	Enriched natural sea water	0.2	1.5	14.8	123.3	56.4	[163]
Scenedesmus sp. CCNM 1077	BG-11 (two stage culture)	23.4	0.4	33.1	19	6.3	[180]
Chlorella sorokiniana CYI	Deep sea water (20%)	-	2.40	51.7	176.6	140.8	[181]
C. sorokiniana HS1	BG-11	30	1.0	35.6	101	36	[182]
Desmodesmus abundans	BG-11	20	1.8	40.4	200.2	67.1	[165]
Chlorococcum sp. RAP 13	Natural sea water (50 %)	-	2.3	20.8	152.5	31	[183]
Scenedesmus sp. IITRIND2	**Artificial sea water**	0	1.35	27.4	235.7	52.9	**This study**
		10.5	1.44	38.9	205.7	80	
		17.5	1.32	40.9	188.6	77.1	
		28	1.21	45.5	172.9	78.6	
		35	1.12	51.8	160	82.8	

Table 2.3: *Comparison of DCW (g/L), lipid content (%), biomass productivity (mg/L/d) and lipid productivity (mg/L/d) obtained from different fresh water microalgae species grown in salt media.*

2.3.4 Fatty acid profile and biodiesel properties

The GC-MS profile of *Scenedesmus* sp. IITRIND2 cultivated in different percentages of ASW revealed the presence of myristic acid (C14:0), palmitic acid (C16:0), 7, 10-hexadecadienoic acid methyl ester (C16:2), 7, 10, 13-hexadecatrienoic acid methyl ester (C16:3), stearic acid (C18:0), oleic acid (C18:1) and linoleic acid (C18:2) as major fatty acids **(Fig. 2.4)**. Data showed that linolenic acid (C18:3) was present only in 0 % and 30 % ASW grown cells while no traces of arachidic acid (C20:0) was in 100 % ASW. Increasing salinity

from 0- 35 g/L resulted in an increase in the proportion of oleic acid from ~ 29 % to 54 % **(Fig. 2.4)**.
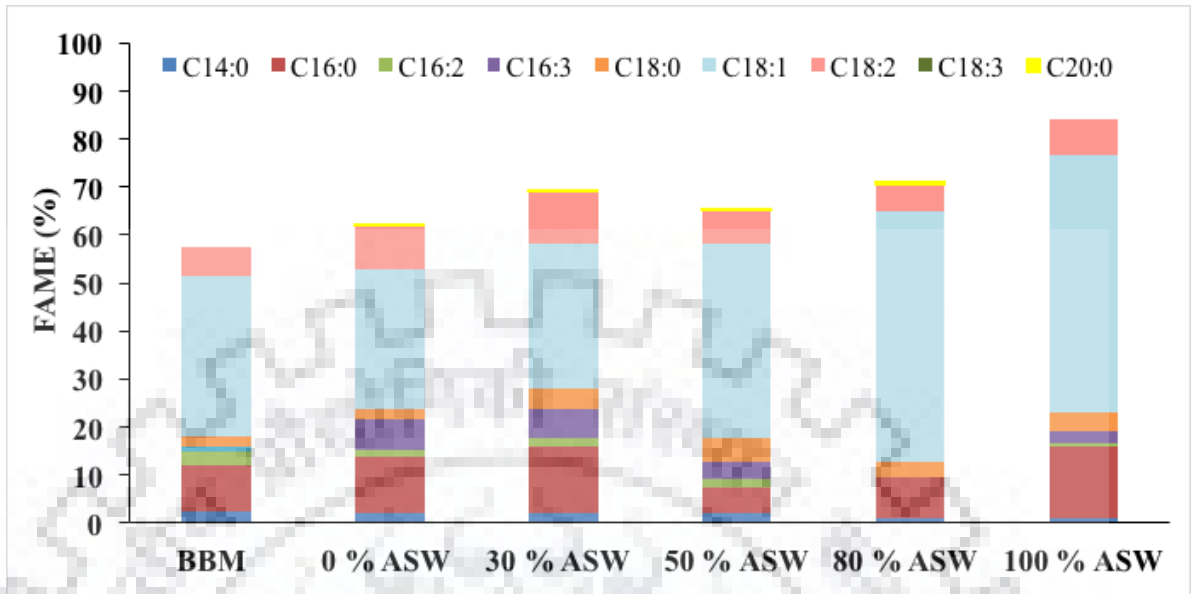
Fig. 2.4: *FAME profile (%) of Scenedesmus sp. IITRIND2.*

Physical properties of biodiesel derived from of *Scenedesmus* sp. IITRIND2 cultivated in ASW and BBM were shown to be in compliance with ASTM D6751-02 (American Society for Testing and Materials) and EN 14214 (European Committee for Standardization) biodiesel standards **(Table 2.4)**. The microalga irrespective of the % ASW showed better physical properties as compared to Jatropha oil methyl ester (JME) and Palm oil methyl esters (PME) **(Table 2.4)**. Iodine value (67 g I_2/100g) with cetane number of 62 was recorded in biodiesel derived from cells cultivated in 100 % ASW. The biodiesel derived from these cells showed the high heating value of 42 MJ/Kg, cold filter plugging property of -4 ℃, kinematic viscosity of 3.7 mm^2/s and oxidative stability of 19 h. The density of the derived biodiesel ranged between 0.87-0.88 g/cm^3.

Physical properties	Standard fuel parameters		Control	Artificial sea water					Plant oil methyl esters	
	ASTM D6751-02	EN 14214	BBM	0 %	30 %	50 %	80 %	100 %	JME	PME
Saponification value (mg KOH)	-	-	110	123	137	127	137	163	96.55	49.56
Iodine value (g I_2/100g)	-	120 (max)	44	61	65.68	60.25	54.67	67	-	-
Cetane number	47 min	51 (min)	85	75	70	74	72	62	54	61
Degree of unsaturation (% wt)	-	-	51	62	68	65	64	75	-	-
Long chain saturation factor (% wt)	-	-	2	2.4	3.7	3.3	3.1	3.6	-	-
High heating value (MJ/kg)	-	-	44	44	42.84	42	43	41.73	-	-
Cold flow plugging property (^{o} C)	-	≤ 5/≤ -20	-9.5	-8.2	-3.8	-5.1	-6.1	-4.2	-2	13
Kinematic viscosity (mm^2/s)	1.9-6.0	3.5-5.0	3.99	3.99	3.99	4.02	4.65	3.72	4.33	4.43
Density (g/cm^3)	-	0.86-0.90	0.87	0.88	0.88	0.87	0.87	0.88	0.88	0.87
Oxidative stability (h)	-	≥6	22	16	13	20	23	19	3.86	16.5

Table 2.4: *Comparison of biodiesel physical properties of Scenedesmus sp. IITRIND2 cultivated in different percentages of ASW and BBM with ASTM D6751, EN 14214 fuel standards and plant oil methyl esters (Jatropha and Palm).*

2.3.5 Changes in cell size and biochemical composition

The holistic effects of ASW (%) on *Scenedesmus sp. IITRIND2* were analysed by estimating changes in cell size, carbohydrate, protein, lipid content and photosynthetic pigments. Data showed positive correlation between cell size and different percentages of ASW **(Fig. 2.5 and Fig. 2.6)**.
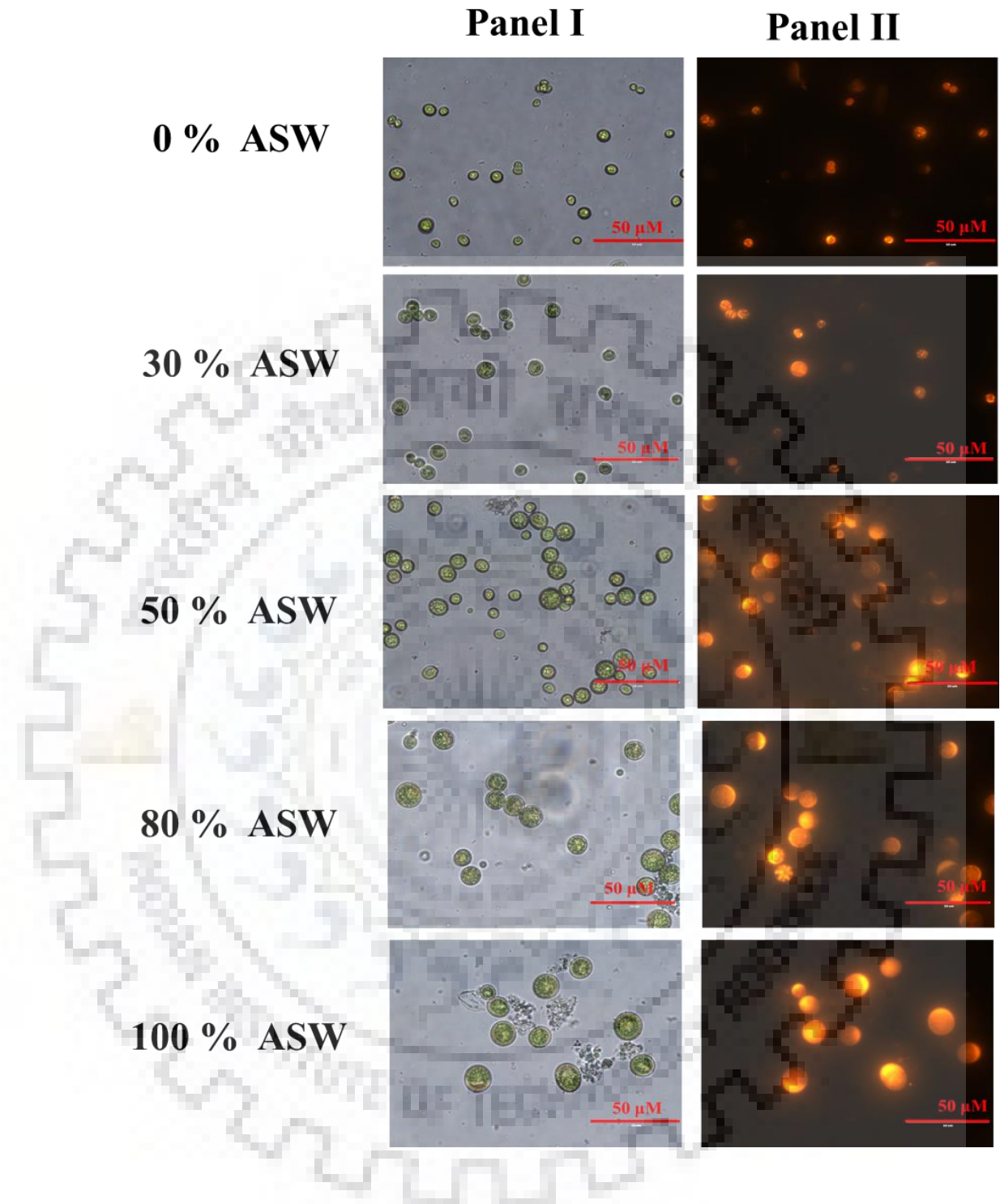
Fig. 2.5: *Scenedesmus sp. IITRIND2 viewed under a light microscope (Panel I) and epifluorescent microscope with 450-500 nm excitations (Panel II) -cell's stained with Nile red cultivated in different percentages of ASW on the 7th day. Scale 50 μm bars.*

A
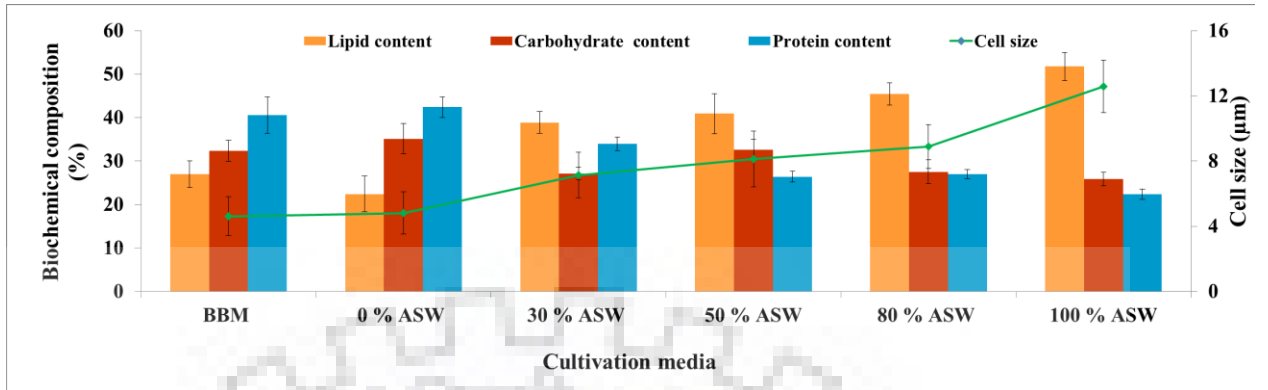
B
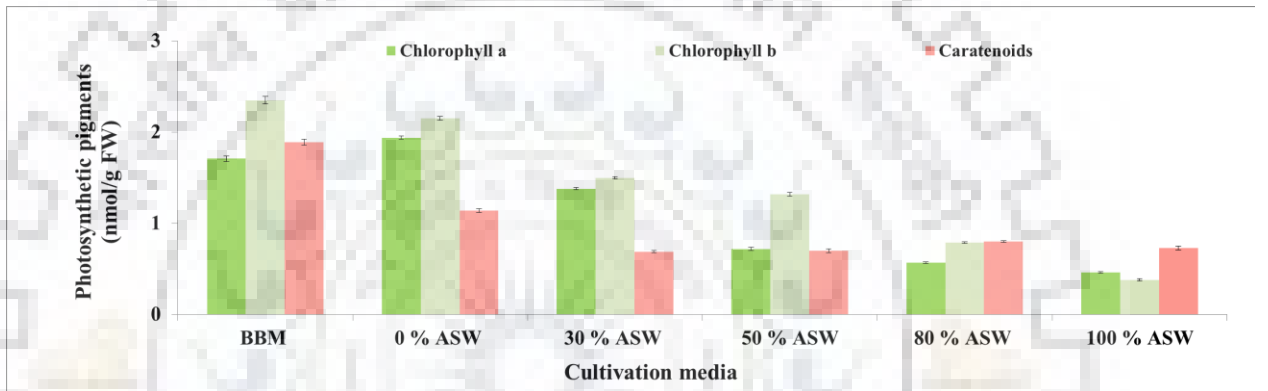
Fig. 2.6: *Changes in the* **(A)** *cell size (μm), total protein (%), total carbohydrates (%) and total lipid content (%)* **(B)** *chlorophyll a, chlorophyll b and carotenoids.*

The maximum cell size (12.58 ± 1.62 μm) was obtained in 100 % ASW which was 2.7 fold higher than BBM (4.62 ± 1.2 μm) as shown in **Fig. 2.6A**. Nile red staining of algal cells grown in different percentages of ASW showed bright yellow lipid droplets encompassing three fourth of the cell **(Fig. 2.5)**. A gradual increase in lipid content (%) was observed with an increase in ASW (%) attaining maximum (51.78 ± 3.23 %) lipid content in 100 % ASW followed by 80 % > 50 % > 30 % > 0 % > BBM respectively **(Fig. 2.6A)**. Escalation in lipid content (%) was accompanied by a decrease in protein content with maximum protein content in BBM (40.62 ± 4.2 %) while the carbohydrate content ranged between ~ 26 to 33 % respectively.

The changes in photosynthetic pigments (chlorophyll a, chlorophyll b and carotenoids) in *Scenedesmus* IITRIND2 cultivated in different percentages of ASW are shown in **Fig. 2.6B**. Data revealed an apparent decline in chlorophyll a, chlorophyll b and carotenoids with an increase in percentage of ASW, demonstrating inhibition of its photosynthetic apparatus.

40

Chlorophyll a and chlorophyll b contents were majorly affected as reduction of ~ 4 fold and ~ 6 fold was recorded, while ~2.5 fold decrease in carotenoids was recorded in cells cultivated 100 % ASW.

2.3.6 Changes in stress metabolites

The effects of ASW with different concentrations of sea salts on intracellular ROS (H_2O_2, lipid peroxidation), osmolytes (proline, glycine betaine) and antioxidant enzymes (CAT, APX) of *Scenedesmus* sp. IITRIND2 are illustrated in **Fig. 2.7**. The levels of H_2O_2 and TBARS progressively increased with the concentration of sea salts in ASW, subsequently reaching 38.75 ± 4.5 µM/gFW and 0.18 ± 0.03 µM/gFW which was 10.33 and 4.74 fold higher than BBM (p < 0.05). The content of proline (177.52 ± 7.09 µM/gFW) and glycine betaine (4.54 ± 0.05 µM/gFW) were also enhanced with sea salts in ASW. These cells also showed an elevation in antioxidant enzymes (CAT and APX) activities (**Fig. 2.7**). CAT activity ranged from 8.19* 10^3 ± 0.12 to 47.7 * 10^3 ± 1.78 U/mg protein while the activity of APX ranged from 0.43 ± 0.02 to 2.54 ± 0.04 U/mg protein when the concentration of sea salts was increased from 0-35 g/L respectively (p<0.05).
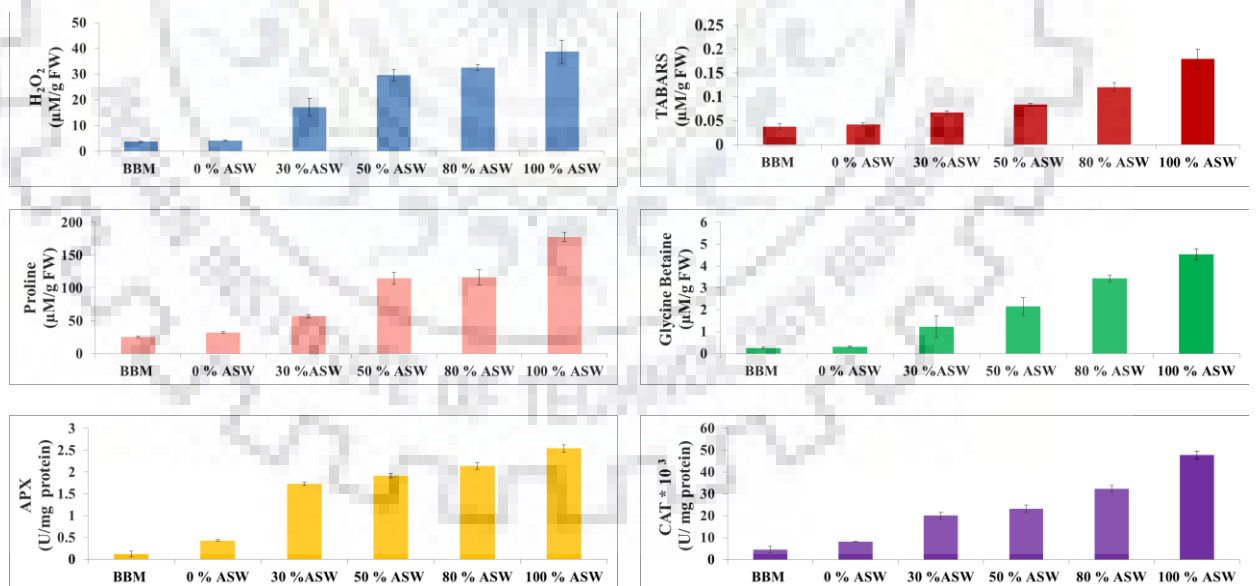
Fig. 2.7: *Changes in H₂O₂, lipid peroxidation (TBARS), osmolytes (proline and glycine betaine) contents and antioxidant enzymes (CAT and APX) activity in Scenedesmus sp. IITRIND2.*

2.4   Discussion

Microalgae can alter their metabolic infrastructure in order to acclimatize to various adverse environments ranging from physiological to operational. Most of the stress conditions lead to increase in lipid accumulation in the form of TAGs which serve as feedstocks for biodiesel production. However, large scale production of microalgal derived biodiesel requires a copious, low cost natural growth medium and high lipid accumulating strain. Bioprospecting of novel microalgal strains capable of growing in waste/sea water along with enhanced lipid accumulation can fulfil the above two criteria paving a path for commercialization of algal oils. *Scenedesmus* sp. IITRIND2 had both these economically viable properties and is therefore an ideal candidate for biodiesel production. Gaining insights on the lipid accumulation and the halotolerance mechanism of this microalga on cultivation in ASW with different concentration of sea salts (0-35 g/L) is imperative to advance in both applied and basic research of algal biodiesel.

Given this interest, changes in DCW, lipid content, cell size, biochemical composition, photosynthetic components and stress metabolites of *Scenedesmus* sp. IITRIND2 were evaluated at high concentrations of sea salts using ASW and compared to BBM. Data showed higher DCW and biomass productivity in ASW cultivated cells compared to BBM, which could be due to the presence of sodium bicarbonate (0.18g/L) and high sodium nitrate (1 g/L) in the ASW medium as compared to BBM **(Fig. 2.2A-C)**. It is well documented that nitrogen is essential for microalgae growth and its scarcity reduces its cell division, leading to low biomass [184]. Further, the addition of sodium bicarbonate in the medium enhances the cell division and metabolic rate of microalgae along with efficient uptake of nitrogen and phosphorous from the medium [185]. However, an increase in the concentration of sea salts in ASW from 0-35 g/L led to decrease in the DCW and biomass productivity, which suggests that high salinity inhibited the growth of microalgae **(Fig 2.2C)**. Similar observations have been reported in various freshwater microalgae such as *Nannochloropsis* sp., *Desmodesmus abundance* and *Scenedesmus* sp. CCNM 1077 when the concentration of NaCl was increased periodically [165,180,186]. A profound increase in lipid content and lipid productivity were observed in ASW cultivated cells, which could be due to salinity (alkaline pH stress) and sodium bicarbonate (dissolved inorganic carbon), triggering the accumulation of neutral lipids preferably as TAGs inside cells **(Fig. 2.5)**. Elevation of dissolved inorganic carbon (DIC) in the medium results in an increase in RuBisCO enzyme which converts 3-phosphoglycerate, a substrate for the biosynthesis of carbohydrate and fatty acid in plants and microalgae [185].

Fatty acid composition and biodiesel physical properties of *Scenedesmus* sp. IITRIND2 cultivated in ASW with different sea salt concentrations were evaluated to enumerate the

vehicular quality of biodiesel. Microalgae contain both saturated (SFAs) and unsaturated fatty acids (MUFAs, PUFAs) which get altered by both biotic and abiotic factors. Investigation showed that salinity stress caused by cultivating microalgae in ASW led to 1.72 fold increase in oleic acid (C18:1) which requires large amounts of NAD(P)H and oxygen. This eases the effect of reactive oxygen species (accumulated due to salinity stress), aiding in cell survival. Increase in MUFA's content was recorded in ASW cells as compared to BBM cells **(Fig. 2.4)**. This increase in MUFA's content in microalgae cultivated in ASW maintains fluidity of cell membrane [187]. Similar results have been reported in different microalgae grown under salinity [164,165]. The biodiesel obtained from *Scenedesmus* sp. IITRIND2 grown in ASW abided by ASTM D6751-02 and EN 14214 standards **(Table 2.4)**. The iodine value (67.17g I_2/100g) obtained in cells cultivated in 100 % ASW was lower than 120 g I_2/100g making the biodiesel less susceptible to gum formation. High cetane number in ASW cultivated microalgal cells as compared to BBM will ensure less ignition delay, smooth engine run, better cold start properties with reduced gaseous and particulate emissions from the obtained biodiesel [188]. Cold filter plugging point (CFPP) of the biodiesel derived from microalgae grown in ASW was lower as compared to plant oil methyl esters (Jatropha and Palm oil) suggesting its usage at low temperatures. CFPP is directly dependent on the content of SFA's mainly C16:0 and C18:0 as these two fatty acids precipitate faster under low temperatures [189]. The cultivation condition (BBM or ASW) did not affect the kinematic viscosity and density as both were within the set range of acceptable standards for biodiesel **(Table 2.4)**. The oxidative stability of microalgae cultivated in 100 % ASW was higher than plant oil methyl esters indicating a long shelf life of the obtained biodiesel. The results obtained corroborated that *Scenedesmus* sp. IITRIND2 can accumulate high lipid content (%) with vehicular quality under varying saline conditions which makes this microalga versatile and promising feedstock for biodiesel production.

The effect of ASW on morphology and biochemical composition of *Scenedesmus sp. IITRIND2* was analysed by estimating changes in cell diameter, lipid content, carbohydrate content and protein content **(Fig. 2.6A)**. Increase in cell size could be due to arrest in cell division which also increased the cell weight leading to an overall increase in biomass productivity. The results were in line work done on a halotolerant strain, *C. sorokiniana* HS1 cultivated in BG-11 media supplemented with 30 g/L NaCl [182]. On exposure to salinity, movement of water occurs inside the microalgae cells which maintain its osmotic turgor by inflow of K^+, outflow of Na^+ and Cl^- ions, thereby regulating cells osmotic potential as shown in **Fig. 2.8** [178,190].
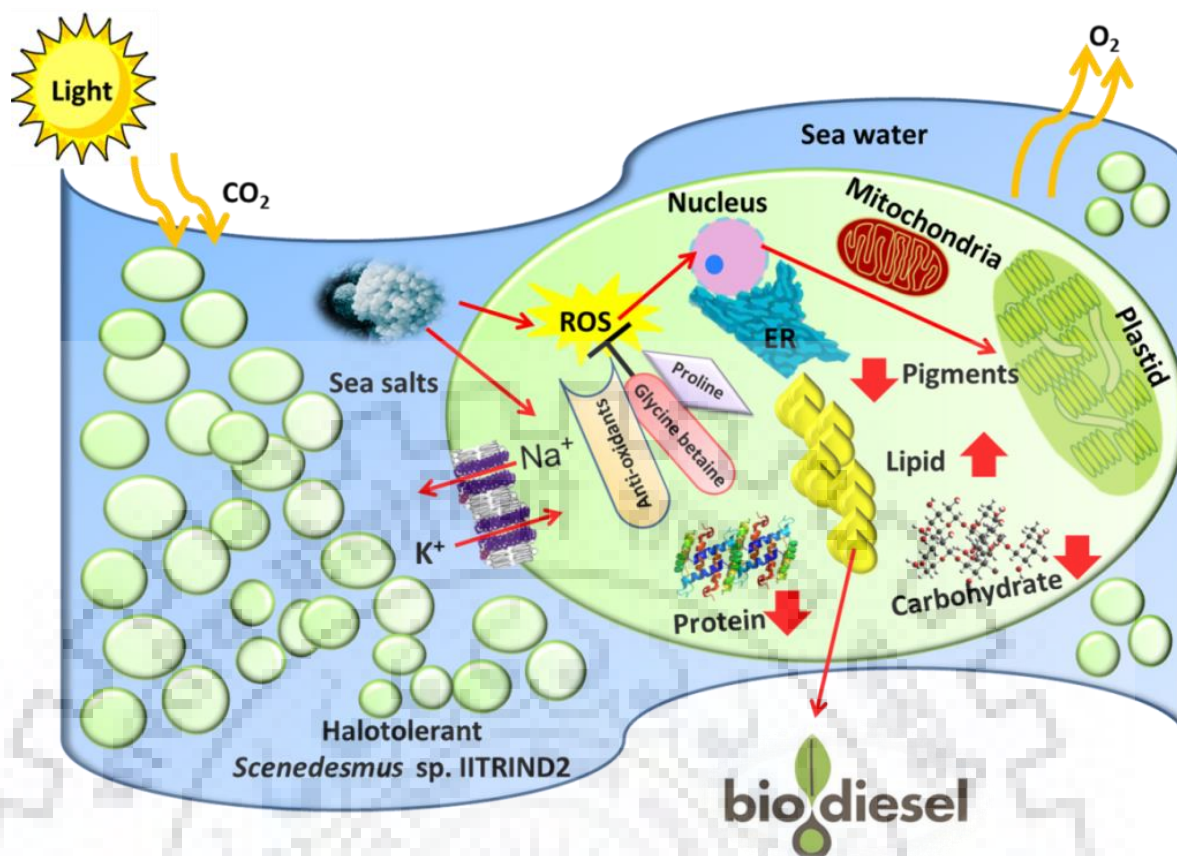
Fig. 2.8: *Schematic representation of physiological and metabolic changes occurring in Scenedesmus sp. IITRIND2 when grown in ASW.*

Increase in concentration of sea salts from 0-35 g/L in ASW significantly enhanced the lipid content (27 % to 51.78 %) as shown in **Fig. 2.6A**. Microalgae grown in salinity stress up regulates Glycerol-3-phosphate synthesis causing accumulation of glycerol, which is a precursor for TAGs [4]. This increase in lipid content (%) was accompanied by loss of protein content due to degradation of proteins **(Fig. 2.6A)**. Under salinity stress, microalgae down regulate genes involved in the primary metabolism and protein synthesis while up regulate autophagy genes [191].

Decrease in photosynthetic pigments (chlorophyll a, chlorophyll b and carotenoids) of *Scenedesmus* sp. IITRIND2 cultivated in ASW with different concentrations of sea salts was recorded as compared to BBM, which was also evident from the colour of cultures showing yellowish green colour in ASW as compared green colour in BBM **(Fig 2.2B)**. This investigation for the first time delineated a comparison among the stress metabolites (ROS), osmolytes (proline and glycine betaine) and antioxidant enzymes (CAT and APX) in *Scenedesmus* sp. IITRIND2 cultivated under ASW with different sea salt concentrations and BBM **(Fig. 2.6)**. The results displayed an increase in H_2O_2 and TBARS content in cells with increase in sea salts from 0-35 g/L in ASW. This increase in ROS was positively correlated

with the increase in osomolytes and antioxidant enzyme activity **(Fig. 2.7)**. Microalgae when cultivated under environmental stress conditions produce various reactive oxygen species (ROS) such as H_2O_2, superoxide (O_2^-) and hydroxyl (OH^-) that causes oxidative damage to the cells. ROS target lipids, carbohydrates, proteins and DNA, which leads to the cell's demise [179]. TBARS is the product of lipid peroxidation and indicates presence of free radicals [192]. In order to mitigate the oxidative stress, microalgae had developed efficient intrinsic antioxidant systems involving enzymes such as superoxide dismutase (SOD), catalase (CAT) and ascorbate peroxidase (APX) [176]. SOD is responsible for scavenging ROS enzymatically by converting O_2^- to H_2O_2. CAT then decomposes H_2O_2 to O_2 and H_2O while APX degrades H_2O_2 with ascorbate oxidation to dehydroascorbate and water [176]. Along with the generation of antioxidant enzymes, microalgae also starts accumulating osmolytes mainly proline and glycine betaine, which maintains the osmoregulation by scavenging excess ROS and re-establish cellular redox balance, cytosolic pH buffer and stabilize subcellular structures as depicted in **Fig. 2.8** [179].

However, before deploying sea water for commercial cultivation of salt tolerant microalgae, high quality geological assessment of saline waters needs to be investigated to understand the strengths and limitations of this source. Moreover, in order to grow microalgae on commercial scale, large amounts of sea water is essential which requires establishment of proper water pumping systems which can pump the on-shore sea water continuously to the cultivation facility [193]. One major issue with pumping systems is biofouling of the sea water that can increase the contamination risk of microalgal cultures. Thus, the collected sea water has to be processed to remove any sediments/microorganisms before using it for algal cultivation.

2.5 Concluding remarks

In conclusion, a novel halotolerant microalga *Scenedesmus* sp. IITRIND2 was isolated from a fresh water lake. This microalga efficiently acclimatized to 35 g/L sea salts by enhancing its lipid content in order to counter salinity stress. The fatty acid profiles and biodiesel physical properties analysed of the microalga were found to abide with ASTM D6751 and EN 14214 biodiesel standards, signifying its applicability in diesel engines. The utilization of such halotolerant strains cultivated in saline/sea water can reduce the fresh water footprint and nutrient consumption leading to suitable biodiesel production. Thus, the mechanistic insights gained on *Scenedesmus* sp. IITRIND2 halotolerance by systematic monitoring of the changes in ROS, osmolytes and antioxidant enzymes can open new avenues to identify hyper

salt responsive gene(s), which can be optimized for further lipid enhancement and biodiesel production via metabolic engineering concepts.

Elucidation of molecular halotolerance mechanism of Secendesmus sp. using integrated omics approach

3.1 Introduction

Halotolerant microalgae have the inherent ability to adapt and thrive in high saline conditions. Salt tolerance by microalgae is a complex phenomenon involving a plethora of morphological, biochemical and molecular changes that aid its survival. These microalgae can regulate their ion transport, modulate membrane permeability, synthesise osmolytes and other stress related molecules that restore the turgor pressure and protect the cell from salinity generated ROS thereby adjusting to the new environment [194,195]. Understanding the halotolerance mechanism of high lipid accumulating microalgal strains could be helpful in gaining insights into the key regulatory pathways that could facilitate future metabolic engineering strategies to leverage successful manipulation of non-halotolerance oleaginous microalgae into high lipid accumulating halotolerant strains. In **chapter 2**, the halotolerance characteristics and high lipid accumulation capability of a novel fresh water microalga *Scenedesmus* sp. IITRIND2 when cultivated in ASW was established. However, to gain mechanistic insights into the halotolerant nature of the microalga, integrated omics studies are imperative. Recent advances in "algal-omics" approaches such as transcriptomics, proteomics, metabolomics and lipidomics on various microalgal strains under different conditions have strengthened our understanding of microalgal's response and adaptation towards both biotic and abiotic stress [93].

The current chapter aims to delineate the metabolic pathway interactions and regulatory genes involved in adaptation of *Scenedesmus* sp. IITRIND2 in response to full strength sea water as compared to fresh water. The physiological changes in the microalga in response to salinity has been studied using electron microscopy, zeta potential and extracellular polysaccharide (EPS) formation. The study also sheds light into the changes in the membrane permeability by analysing key intracellular ions (Na^+, Mg^{+2}, Ca^{+2} and K^+). Furthermore, differential protein, metabolite and lipid expression profiles were obtained using metabolomics, proteomics and lipidomics approaches.

3.2 Materials and Methods

3.2.1 Microalga cultivation

The microalga was adapted to ASW (35 g/L) and no salt water (0 g/L, control) as described in Chapter 2, section 2.2.4. These adapted cultures were then used for further studies by cultivating them in 250 mL Erlenmeyer flasks for a period of 7 days.

3.2.2 Analysis of intracellular metal ions and zeta potential of microalga

The intracellular ions (Na^+, K^+, Mg^{+2}, Ca^{+2}) of the cultivated cells in ASW and control medium were extracted using the standard protocol by Wiley et al. and estimated using Inductive coupled plasma mass spectroscopy (ICP-MS; Perkin Elmer, ELAN DRC-e) [196]. The zeta potential (ZP) of the microalgal cells were obtained at 25 °C and in suspension under an applied electric field of 80 mV using a Zeta sizer (Nano-Z590, Malvern) and measured using Malvern software (v 7.03).

3.2.3 Electron microscopy of microalgal cells

To analyse the size and surface of microalgal cells, FE-SEM was used as detailed in Chapter 2 (section 2.2.2). Transmission electron microscopy (TEM) was performed to visualize the ultrastructure of microalgal cells. Briefly, microalgal cells grown in control and ASW were harvested on the 7th day and then fixed overnight with 2.5 % glutaraldehyde and 2 % paraformaldehyde in 0.1 M phosphate buffer (pH 7.4) at 4 °C. The cell pellets were then washed thrice with 0.1 M phosphate buffer and post fixed with osmonium tetraoxide (OsO_4) in Soresen phosphate buffer (0.05 M buffer, 1 % OsO_4 and 0.25 M glucose) for 1 h and again washed twice with distilled water. The cells were double stained with uranyl acetate and lead citrate solution for 12 h and then visualized under TECNAI 200 KV TEM (Fei, Electron Optics).

3.2.4 Proton NMR based metabolomics and lipidomic analysis

The metabolites from the microalgal cells cultivated in ASW and control were extracted using the protocol of Zhang et al. [197]. In detail, the cultures were harvested on the 7th day, washed thrice with double distilled water and lyophilized. These lyophilized cells (40 mg) were then grounded using liquid nitrogen using 1 mL of 20 % methanol. The process was repeated twice and the supernatant was pooled and lyophilized. Phosphate buffer (0.1M, pH 7.4) was then added to the supernatant and again lyophilized. To these samples 550 μL of D_2O

containing a chemical shift indicator (4,4-dimethyl- 4-silapentane- 1- sulfonic acid (DSS), 0.5 mM) was added and the proton (^{1}H) CPMG (Carr–Purcell–Meiboom–Gill) NMR spectra were then acquired on a 800 MHz NMR spectrometer (Bruker Avance III) equipped with Cryoprobe. The NMR spectral data were processed using standard Fourier Transformation (FT) procedure in Bruker software Topspin-v2.1 (Bruker-BioSpin GmbH, Silberstreifen 4 76287 Rheinstetten, Germany). Prior to FT, each free induction decay (FID) was zero-filled to 64 k data points, multiplied by an exponential window function and a line broadening function of 0.3 Hz was applied. Chemical shifts in the spectra were identified and assigned for various metabolites using commercial software Chenomx NMR Suite (form Chenomx Inc., Edmonton, AB, Canada containing 800 MHz chemical shift database).

The multivariate data analysis was performed by integrating the NMR spectra of 6 biological replicates of each culture and normalized against the internal standard (DSS) at 0 ppm to obtain NMR based metabolite profiling. Prior to multivariate data analysis, all the 1D ^{1}H CPMG NMR spectra were manually phased, baseline corrected and referenced internally to the methyl resonance of lactate at δ 1.3102. The data was then reduced into spectral bins (0.03 ppm width) using Pathomx [198]. The spectral bins were then imported into Metaboanalyst (v3.0) software and scaled to Pareto variance for multivariate analysis [199,200]. Principal component analysis (PCA) was performed and metabolites of discriminatory significance were identified in the 2D loading plot based on their coefficient score $> \pm 0.1$. The discriminatory metabolites were further tested for statistical significance using student T-test in Metaboanalyst. The relative metabolic changes were assessed using univariate (or box-plot) analysis and unsupervised hierarchical clustering using Ward linkage was further employed to create the heat map consisting of 25 metabolite entities (with $p < 0.001$) that had the highest impact on separation of the different treatment groups.

For lipidomic analysis, the total lipid was extracted using modified Bligh and Dyer method as detailed in chapter 2 (section 2.2.5). The total extracted lipids (10 mg) were mixed with 550 μL deuterated chloroform ($CdCl_3$) and ^{1}H NMR spectra was recorded using a 500 MHz NMR spectrometer. The chemical shifts in the spectra were identified and assigned using earlier published studies [201]. The intensity/fold change in their respective peaks was obtained using Burked Topspin 3.5.

3.2.5   Proteomic analysis using mass spectrometry

For protein extraction, ASW and control grown cultures were harvested on the 7th day by centrifuging at 4000 g for 10 min at 4 °C. The fresh cell pellets (1g) were washed thrice

with chilled double distilled water and then frozen at - 80°C. The total protein was extracted using the protocol of Guarneiri et al. with minor modifications [105]. In detail, the cell pellets were grounded in liquid nitrogen and then solubilized on ice in 1 mL lysis buffer [50 mM Tris; pH 8.0; 150 mM NaCl, 1mM DTT, 10 % glycerol supplemented with 1X complete protease inhibitor cocktail (Roche Diagnostics Corporation, Indianapolis, IN)]. The process was repeated twice and then the supernatant was collected for proteomic analysis. Total soluble protein content was quantified using Bradford assay, and 20 µg of soluble protein was resolved using 12 % SDS-PAGE. Three biological replicates were used for protein isolation and all subsequent analysis. The selected protein bands were then manually excised, washed with 25 mM ammonium bicarbonate in 40 % acetonitrile, followed by reduction with 10 mM DTT in 20 % acetonitrile for 20 min at room temperature. The gel bands were then alkalyated with 40 mM iodoacetamide in 20 % acetonitrile for 15 min at room temperature. Gel bands were further washed as described above followed by incubation in 100 % acetonitrile on ice for 10 min. The proteins were then digested overnight at 37 °C by adding 25 µg/mL trypsin (Gold trypsin, Promega, Madison, WI) in 30 mM acetonitrile. The resulting peptide mixture was acidified by addition of 0.1 % formic acid for 20 min and then dried in vacuum concentrator, and stored at -20 °C for further processing.

Protein identification was performed on MALDI (Matrix-assisted laser desorption/ionization)-TOF (Time of Flight) -MS/MS (Autoflex, speedTM, Bruker Dalton, Bremen, Germany). Equal volumes of trypsinised protein fragments and matrix solution containing 5 mg/mL of α-cyano-4 hydroxycinnamic acid (Sigma Aldrich Fluka, St. Louis, MO) were prepared in trifluroacetic acid 40 (600 µL MS grade water, 400 µL acetonitrile, 0.6 µL trifluroacetic acid). The mixture was spotted on a 96 well MALDI-TOF-MS target plate with peptide mix (Brukers Dalton, Bremen, Germany) as calibrant. The spectra were collected from 300 shots per spectrum over m/z range of 700-3000 and the peak list was generated using Flex analysis 3.0. All the MS/MS spectra were searched against Chlorophyta protein database from the Uniprot website (http://www.uniprot.org/taxonomy/3041) using the MASCOT search engine version 2.2 (Matrix Science) with MW, pI, modifications including carboamidomethyl (C) and variable modifications such as Acetyl (N term), Oxidation (Met) and a mass tolerance of ± 0.1 Da. Mascot score greater than 55 was considered significant. The functional annotation and grouping of the identified proteins was done using QuickGo, EMBL-EBI (https://www.ebi.ac.uk/QuickGO/) using Explore biology tool. The up/down regulation of proteins were estimated using Image J 1.4a software.

3.2.6 RNA extraction and Quantitative qRT-PCR analysis

Total RNA was extracted from the harvested microalgal biomass using RNeasy plant mini kit (Qiagen) according to the manufacturer's instructions. The yield of the total RNA extraction was measured by NanoDrop spectrophotometer (Biorad). For Real time polymerase chain reaction (RT-PCR) analysis, first strand cDNA synthesis was carried out from 1 µg of total RNA using Verso cDNA synthesis kit (Thermo Scientific) according to manufacturer's instructions. Gene-specific primers were designed to amplify fragments of 100-150 bp in length (**Table 3.1**). *Scenedesmus* sp. α-actin primers were used to demonstrate equal amounts of templates and loading. RT-PCR was carried out on Eppendorf RT-PCR. Gene expression was calculated using $2^{-\Delta\Delta Ct}$ method [ΔCt= Ct (target gene)- Ct (house-keeping gene)] where Ct is the cycle number at which the fluorescent signal rises statistically above the background [202].

Gene	Forward	Reverse	Tm	GC	Reference
Beta Actin	ACATCAAGGAGAAGCTGGCCTA	ATGTCGACGTCGCACTTCATGA	F 54.8	50	-
			R 54.8	50	
DGAT-3280	GGCACAAAGAGTTCACCGT	ACAAACTTGAGGTGGGTG	F 51.1	53	[203]
			R 48	50	
ME-3137	CCCTCTCGTTCCCCTTTTATT	AAATGCTGACGCAAGTGTGA	F 52.4	48	
			R 49.7	45	
P5CS	GTGCCCATCGGCGTGCTTCT	CGTGTTGCGCTTGATGTGGC	F 57.9	65	[204]
			R 55.9	60	
BC	TGCGATTGGGTATGTGGGGGT	ACCAGGACCAGGGCGGAAAT	F 56.3	57	[205]
			R 55.9	60	
SAD	TCCAGGAACGTGCCACCAAG	GCGCCCTGTCTTGCCCTCAT	F 55.9	60	
			R 57.9	65	
PGAT	GGATAAGAGCGGCACAAGGA	GAAGGGCGAGATTGGAATGA	F 53.8	55	[206]
			R 51.8	50	
LIP	GGCCTCAAAGCCACCAGTAC	GGCAGTGCACATGTTGCAG	F 55.9	60	
			R 53.2	58	
SS	CAGGCAAGGATACATCTACTG	TACTGCCCAACCATCTCATC	F 55.5	47.6	-
			R 56.9	50	
AGP-L	CCATGAGCAACTGCATCAAC	GGTTGAGCGAGGTGGAGTT	F 51.8	50	[113]
			R 53.2	58	
Psac	GAACATCACCACCACCAGGA	CGGTGCTTGGCTTTTAGTTTG	F 53.8	55	[207]
			R 52.4	48	
CA	TGAAGGAGGGCTCTGATGAT	GTTTGCGAATGAGATGGTGT	F 51.8	50	[208]
			R 49.7	45	

Table 3.1: *List of RT-PCR primers used in the expression analysis.*

3.2.7 Compositional analysis of extracellular polysaccharide (EPS)

The EPS was extracted by harvesting the ASW and control cultures at 15000 g for 20 min, the supernatant was filtered (Whatmann, UK) twice and then concentrated to one forth

volume on magnetic stirrer at 60 °C for 12 h [178]. The EPS was precipitated by gradually mixing equal volume of cold methanol to the supernatant and then kept at 4 °C overnight. The supernatant was then centrifuged at 15000 g for 30 min at 4 °C to remove methanol, washed with absolute ethanol and then dissolved in Milli-Q water (Millipore, USA). The EPS was then dialysed against distilled water for 24 h using 1 kD membrane to remove ions and salts. The EPS was lyophilized and stored at -20 °C till further processing.

Total carbohydrates and proteins in the lyophilized EPS were estimated using phenol-sulphuric method and Bradford assay respectively. Fourier-Transform Infrared spectroscopy (FT-IR) spectra of EPS was recorded in the region of 4000-400 cm^{-1} on a GX FT-IR spectrometer (Perkin-Elmer, USA).

3.2.8 Statistical analysis

All the experiments were performed in triplicates (except for metabolomics which had 6 replicates) and the results have been presented as mean ± S.D. One-way ANOVA followed by T-test was done for statistically significant results with $p < 0.05$.

3.3 Results

In the face of high salinity, halotolerant microalgae undergo a series of adaptive changes both at physiological and molecular level. Deciphering the salinity response at both levels is crucial not only to understand the algal physiology but also to unveil potential genome editing targets for tailor made high lipid accumulating halotolerant microalgal strains. In this investigation, we evaluated various physiological (ion transport, membrane potential, ultrastructure, EPS) and molecular (metabolomics, proteomics and lipid composition) adaptation aspects of *Scenedesmus* sp. IITRIND2; a prospective high lipid and halotolerant strain for biodiesel production.

3.3.1 Salinity induced changes in intracellular ion composition and membrane potential of *Scenedesmus* sp. IITRIND2

The first line of defence deployed by the microalga to adapt and thrive in high saline environments is selective retention or exclusion of ions. Monovalent ions such as Na$^+$, K$^+$ and divalent ions including Mg^{+2}, Ca^{+2} are crucial for maintaining the turgor pressure and osmotic balance inside the cells [209]. Analysis of the intracellular ions of *Scenedesmus* sp. IITRIND2

cultivated in ASW showed maximum concentration (44.7 ± 0.6 mg/L) of K$^+$ which was ~ 100 fold higher as compared to control **(Fig. 3.1)**. Interestingly, despite, high Na$^+$ concentration in the ASW (23 g/L), its intracellular concentration was 2.8 ± 0.1 mg/L, being ~ 40 fold higher than control which suggests active extrusion of Na$^+$ from the cells against the concentration gradient **(Fig. 3.1)**. Earlier, salinity tolerance in *D. salina*, has been reported to be mediated by up regulation of two distinct Na$^+$ extrusion systems in the plasma membrane including a Na$^+$ ATPase and NADH-driven electron transport Na$^+$ pump (H$^+$ ATPase pump) [210]. On the other hand, intracellular concentration of Ca^{+2} in ASW grown cells were only ~ 2.6 fold higher than control cultures while no statistical difference was recorded in Mg^{+2} concentration **(Fig. 3.1)**. The data suggested that K$^+$ is the major osmolyte that competed and regulated the accumulation of toxic Na$^+$ inside the microalgal cells. Similar results have also been reported in *C. pyrenoidosa* and *Prasiola crispa* when cultivated in high saline medium [211,212]. Further a high K$^+$/Na$^+$ ratio inside the cells have been reported to increase the salinity tolerance in plants and could be the same for salt tolerant microalgae [213].
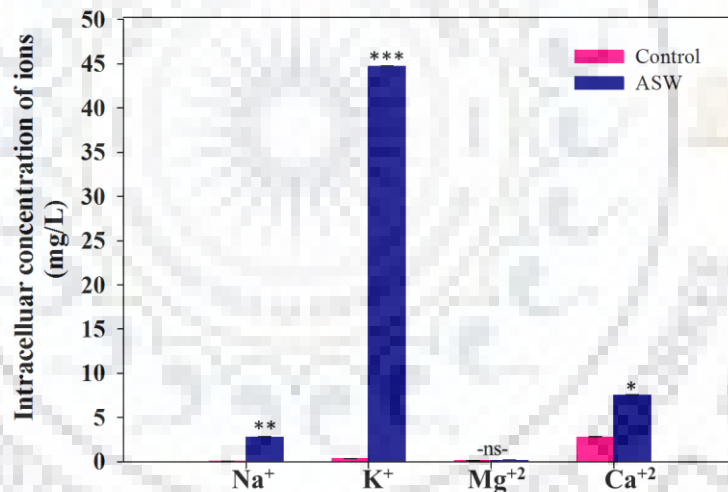
Fig. 3.1: *Intracellular concentration of ions in control and ASW cultures of Scenedesmus sp. IITRIND2 analysed on the 7th day.*

Selective K$^+$ retention in the ASW cultivated cells can alter the membrane potential for maintaining the turgor pressure. Hence, we measured the surface zeta potential of the cells under halotolerant conditions. The observed zeta potential of *Scenedesmus* sp. IITRIND2 grown in control medium was -6 mV which decreased to -12 mV in ASW cultivated cells. A similar decrease in zeta potential has also been observed for *C. pyrendosia* when grown in NaCl medium [209].

3.3.2 Morphology and ultrastructure changes in *Scenedesmus* sp. IITRIND2 under halotolerant conditions

Electron microscopy was used to visualize microalgal cells grown in ASW and compared to control. The FE-SEM images of the ASW cultivated microalga cells showed an increase in cell size (~12 μm) as compared to control treated cells (~ 4 μm) as depicted in **Fig. 3.2A and B**. Further, the TEM micrographs of control cell showed well organised organelles with discernible chloroplast (Ch), nucleus (N), mitochondria (M), starch granules (S) and lipid bodies (L) **(Fig. 3.2C)**. On exposure to salinity, the TEM images showed disorganization in the cellular structure with large accumulation of several lipid droplets with few starch granules and the chloroplast was collapsed with no distinct demarcation of the thylakoids or stroma **(Fig. 3.2D)**. The cell wall (CW) of the ASW cultivated cells was thicker (0.20 ± 0.01 uM) as compared to the control (0.12 ± 0.02 uM) **(Fig. 3.2C and D)**.
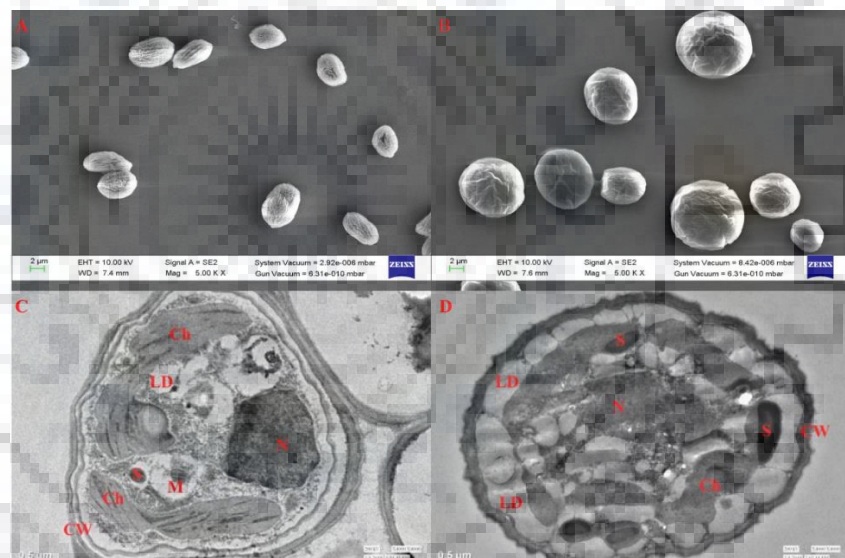
Fig. 3.2: Electron micrographs of *Scenedesmus* sp. IITRIND2 **(A)** FE-SEM of control **(B)** FE-SEM of ASW **(C)** TEM of control **(D)** TEM of ASW cells on the 7th day.

3.3.3 Effect of salinity on lipids composition and EPS formation

The rearrangement of lipids particularly in membranes is crucial to protect the cells from high salt environments. The changes in the total lipid composition under halotolerance conditions was estimated using ^{1}H NMR **(Fig. 3.3A)**.
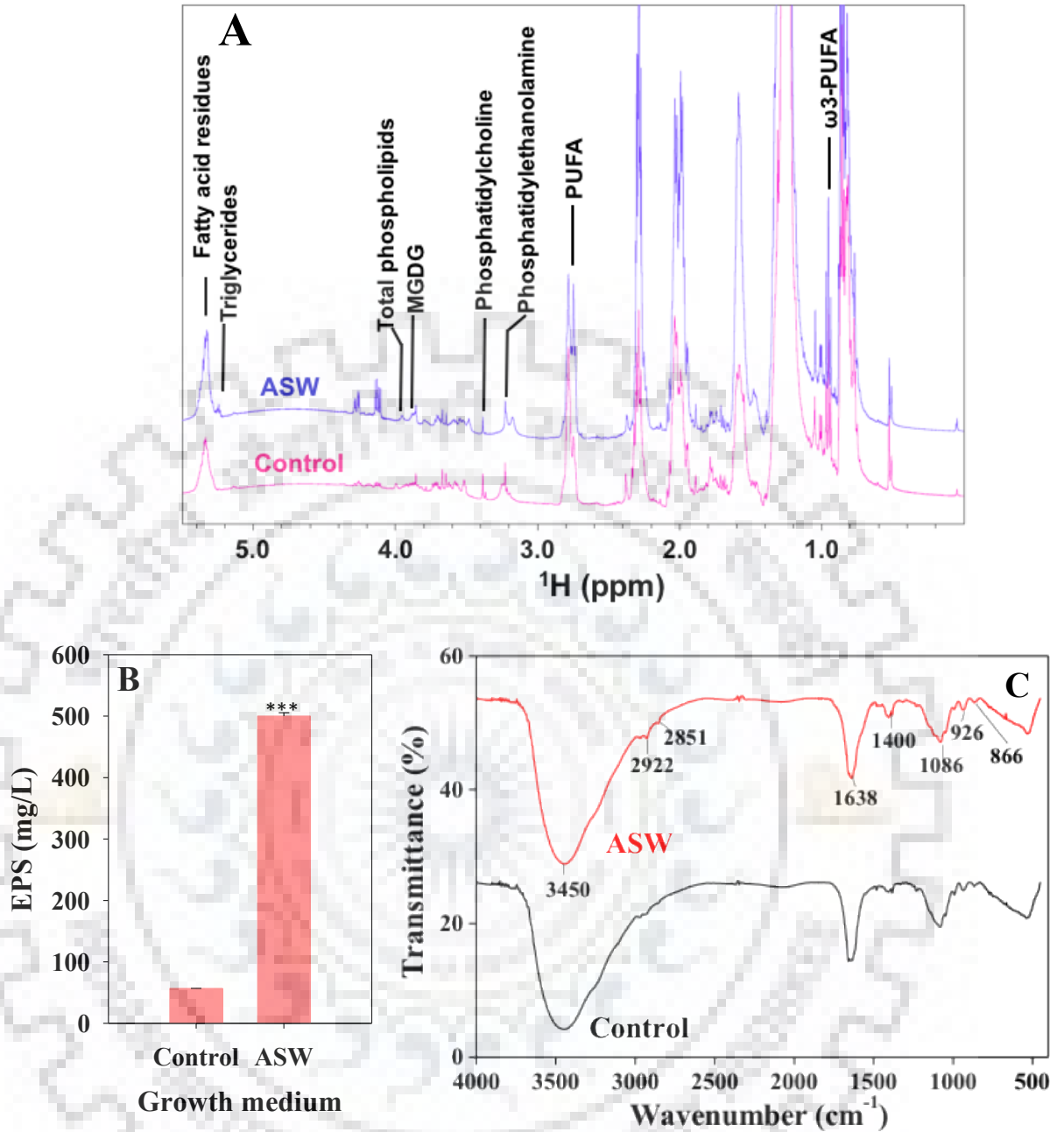
Fig. 3.3: (A) *The cumulative 1D ^1H NMR spectra (n=3) of total lipid extracted from control (Red) and ASW cultivated cells (Blue)* (B) *Changes in the EPS production* (C) *FTIR of EPS extracted from control and ASW cultures of Scenedesmus sp. IITRIND2 on 7th day.*

The ^1H NMR showed distinct peaks for different classes of lipids including PUFA, phosphatidylcholine (PC), phosphatidylethanolamine (PE), total phospholipids (PL), TAGs, fatty acid residues, mono galactosyl diacylglycerol (MGDG) and ω^3 PUFA respectively (**Fig. 3.3A, Table 3.2**). Interestingly, all the classes of lipids showed an increase in total lipids extracted from ASW cultivated cells as compared control (**Fig. 3.3A**). The maximum increase in TAGs (~17 fold) followed by fatty acid residues (~ 10 fold) > PUFA (~8 fold) > PL (~8

fold) > ω^3 PUFA (~ 6 fold) > PE (~4 fold) > PC (~ 3 fold) > MGDG (~1.9 fold) and ω^3 PUFA (1.2 fold) respectively. These NMR observations corroborate well with the changes in the ultrastructure of *Scenedesmus* sp. IITRIND2.

S.No.	Lipids	Chemical shift (ppm)	Fold change
1	PUFA	2.76 (d)	8.7
2	Phosphatidylcholine	3.38 (s)	3.05
3	Phosphatidylethanolamine	3.22 (s)	4.09
4	Total phospholipids	3.95 (s)	8.13
5	Triglycerides	4.12 (q)*, 4.27 (q), 5.25 (s)	17.2
6	Fatty acid residues	5.32 (m)	10.05
7	MGDG	3.88 (s)	1.9
8	Omega3 PUFA	0.85 (t)*, 0.95 (t)	6.03

Table 3.2: *List of lipids along with their respective chemical shifts and fold change as evaluated using Bruker Top spin 3.5 (* indicates the chemical shift taken for fold change estimation).*

Parallel to perturbations in the lipid composition, the presence of EPS layer around the microalgal cell, reduces the penetration of toxic Na$^+$ and Cl$^-$ ions through the cell membrane which in turn aids its survival under salt stress [214]. *Scenedesmus* sp. IITRIND2 cultivated in ASW showed a 30-fold increase in EPS production as compared to control cells **(Fig. 3.3B)**. Compositional analysis of the EPS from ASW cultivated cells showed ~ 4-fold increase in total carbohydrates (20 ± 0.25 mg/mL) as compared to control cells (5.2 ± 0.03 mg/mL) while negligible amount of protein was detected in both the samples. Further, to obtain structural information, we analysed the EPS using FTIR spectroscopy **(Fig. 3.3C)**. The spectra showed clear transmittance at 3500-3300 cm^{-1} indicating O-H stretching, 2915-2935 cm^{-1} of asymmetric C-H stretching which is common to all the polysaccharides while peak from 1000-1200 cm^{-1} corresponds to presence of carbohydrates [215,216]. The peak around 1640 cm^{-1} indicated presence of mannose/galactose and peak at ~ 1400 cm^{-1} corresponded to galacturonic acid [214,216,217]. The characteristics peak at ~860 cm^{-1} showed presence of α-configuration glucose and peak at ~ 890-900 cm^{-1} indicated presence of β-D- glucans [214]. Further, less pronounced peaks ~ 1536 cm^{-1} indicated absence of proteins from the EPS samples.

The compositional and structural analysis presented in the above sections point towards the fact that *Scenedesmus* sp. IITRIND2 has most probably rewired its metabolic pathways in order to tolerate the salinity stress and hence forth to accumulate high lipid content. Thus, to

unravel its molecular responses we have adapted an integrated omics approach comprising of metabolomics, proteomics and RT-PCR analysis as discussed in the sections below.

3.3.4 Changes in the metabolite composition of *Scenedesmus* sp. IITRIND2 in response to salinity stress

In addition to the changes in the membrane permeability, halotolerant microalgae accumulate low molecular weight compatible solutes termed as metabolites which aid in osmoregulation, homeostatic balance and in maintaining the membrane and protein integrity etc. [218]. The metabolite profile of *Scenedesmus* sp. IITRIND2 cultivated in ASW as compared to control was analysed using ^{1}H NMR spectroscopy (**Fig. 3.4A- C**). The cumulative ^{1}H NMR spectra of ASW cultivated microalgal cells identified a total of 44 metabolites including amino acids (15), organic acids (09), sugars (05), phosphagen (02), osmolytes (03), nucleotides (03) and others (07) respectively (**Table 3.3**). The intensity profiles of ^{1}H NMR resonances showed a clear metabolite difference between control and ASW cultured cells (**Fig. 3.4A**). To statistically validate these differences across the two groups, multivariate analysis was performed first using PCA (**Fig. 3.4B**). The PCA analysis showed clear clustering of the six biological replicates and distinct difference between the control and ASW grown cultures (**Fig. 3.4A**). The PCA loading plot also revealed the metabolites responsible for the observed discrimination pattern (**Fig. 3.4C**). Data obtained from the univariate analysis was represented using box-cumulative whisker plots along with hierarchically clustered heat maps which showed quantitative data of significantly altered metabolites between the two experimental groups (**Fig. 3.5A and B**).
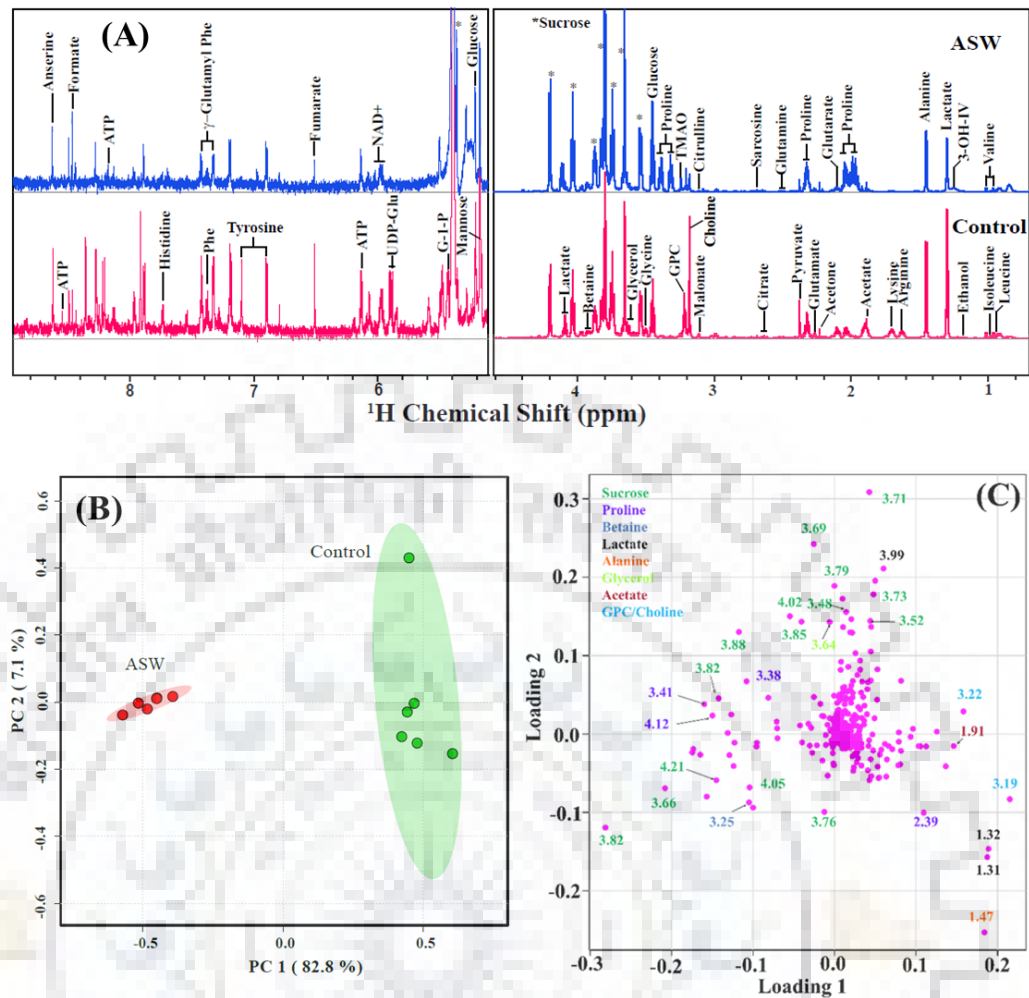
Fig. 3.4: (A) *The cumulative 1D ^{1}H NMR spectra (n=6) of Scenedesmus sp. IITRIND2 Control polar extracts (**pink**) stacked up with that of ASW cultures (**blue**). The spectral peaks were assigned for particular small-molecule metabolites. The water region at δ 4.6–4.9 was removed for clarity. **(B)** The combined PCA 2D score plot resulted from the analysis of 1D ^{1}H CPMG spectra of Scenedesmus sp. IITRIND2 cultivated in control and ASW medium (**green** = Control; **red** = salt). The semi-transparent red and green ovals represent the 95% confidence interval. **(C)** PCA loadings plot revealing the metabolites of responsible for the discrimination pattern, the more the metabolite is away from the origin (0,0) more it contributes in the group discrimination.*

Metabolite Name	Assignment	Chemical shifts (δ) in ppm	Relative Change in Treated cells
Amino acids			
Leucine	δ-CH3 δ-CH3	0.95 (d) 0.96 (d) [ε]	↓
Isoleucine	γ-CH3 δ-CH3	0.93 (t) [ε] 1.00 (d)	↓
Valine	γ-CH3 γ-CH3	0.98 (d) 1.03 (d) [ε]	↓
Arginine	γ-CH2	1.68 (m) [ε]	↓↓
Lysine	δ-CH2	1.69 (m) [ε]	↓↓
Alanine	β-CH$_3$ α-CH	1.47 (d) [ε] 3.79 (q)	↓
Proline	γ-CH2 γ-CH2 ½ β-CH2 ½ β-CH2 ½ β-CH2	1.99 (m) 2.00 (m) 2.06 (m) 3.32 (m) [ε] 3.41 (dt)	↑↑↑
Histidine	C4H-ring	7.71 (d)	↓
Glutamate	β-CH$_2$ γ-CH$_2$	2.11 (m) [ε] 2.34 (m)	↓
Glutamine	β-CH$_2$ γ-CH$_2$	2.12 (q) 2.44 (m) [ε]	↓
Sacrosine	N-CH$_3$	2.71 (s)	↑
Glycine	α-CH$_2$	3.56 (s)	-
Tyrosine	C2H & C6H C3H & C5H	6.88 (d) [ε] 7.18 (d)	-
Phenylalanine	C2H & C6H C4H C3H & C5H	7.31 (m) 7.37 (m) 7.43 (m) [ε]	↓
γ -glutamyl-phenylalanine	C2H, C6H & C4H C3H & C5H	7.3 (m) [ε] 7.4 (m)	-
Organic acids			
Lactate	*β*-CH$_3$ *α*-CH	1.32 (d) [ε] 4.10 (m)	↓
Acetate	CH$_3$	1.91 (s)	↓
Aspartate	C6H, C6H	2.8 (m) [ε], 2.66 (q)	↓
Pyruvate	γ -CH 3	2.4 (s)	↑
Glutarate	β, δ- CH2	2.16 (t)	↓
Succinate	α, β-CH2	2.39 (s)	↓
Citrate	½ γ-CH2 ½ γ-CH2	2.52 (d) [ε] 2.69 (d)	-
Fumarate	CH	6.51 (s)	↓
Formate	CH	8.44 (s)	-

Metabolite Name	Assignment	Chemical shifts (δ) in ppm	Relative Change in Treated cells
Carbohydrates/sugar			
Sucrose	C10H	3.46 (t) [€]	↑↑↑
	C12H	3.55 (dd)	
	C13H	3.66 (s)	
	C11H	3.75 (m)	
	C17H & C19H	3.77 (m)	
	C5H & C9H	3.81 (dd)	
	C4H	4.04 (t)	
	C3H	4.21(d)	
	C7H	5.40(d)	
α-Glucose	C4H	3.39 (m)	↑↑
β-Glucose	C5H	3.45 (m)	↑↑
	C3H	3.47 (m) [€]	
	C1H	5.22 (d)	
Mannose/Trehalose	C1H	5.19 (d)	↑↑
Glucose-1-phosphate	C1H	5.55 (d,d)	-
Phosphagen			
Choline/PC	N–(CH$_3$)$_3$	3.20 (s)	↓
GPC	N–(CH$_3$)$_3$	3.22 (s)	↓
Osmolytes			
Glycerol	½ γ-CH2	3.63 (d) [€]	
	½ γ-CH2	3.65 (d)	-
Betaine	N–(CH$_3$)$_3$	3.26(s) [€]	↓
	β-CH$_2$	3.91 (s)	
TMAO	N–(CH$_3$)$_3$	3.27(s) [€]	↑
Nucleotides			
Adenine	C2H	8.19 (s)	↓
	C6H		
ATP	C7H	8.61 (s) [€]	↓
	C12H	8.25 (s)	
	C2H	6.13 (d)	
NAD+	C28H	6.08 (m)	↓
Others			
Ethanol	CH3	1.17 (t)	-
Acetyl choline	S-(CH$_2$)$_2$	3.2 (s)	↑
3-hydroxy-isovalerate	γ-CH3	1.24 (s)	-
Acetone	CH$_3$	2.22 (s)	-
UDP-Glucose	C22H	6 (m)	↓
Ethanolamine	N-CH$_2$	3.13(m)	↑
Methanol	CH$_3$	3.34 (s)	-

Table 3.3: *List of metabolites along with their respective chemical shifts and metabolic change patterns as a consequence salt stress. Two-way ANOVA followed by post-hoc Tukey's HSD was conducted to determine significant (p < 0.001) metabolic changes. The up (↑) and down (↓) arrows represent, respectively, increased and decreased metabolite levels.*

Note: All the values of the metabolites were statistically significant with p value 0.001 respectively. For visualization interpretation, single (↑,↓) and double (↑↑,↓↓) and multiple arrows are used to represent relative change in the mean value of metabolite concentration (as evaluated from their respective box-plots). "€" represents he metabolite peak used for evaluating the quantitative difference as represented here using up (↑) and down (↓) arrows in the case of multiple signals/chemical shift values.
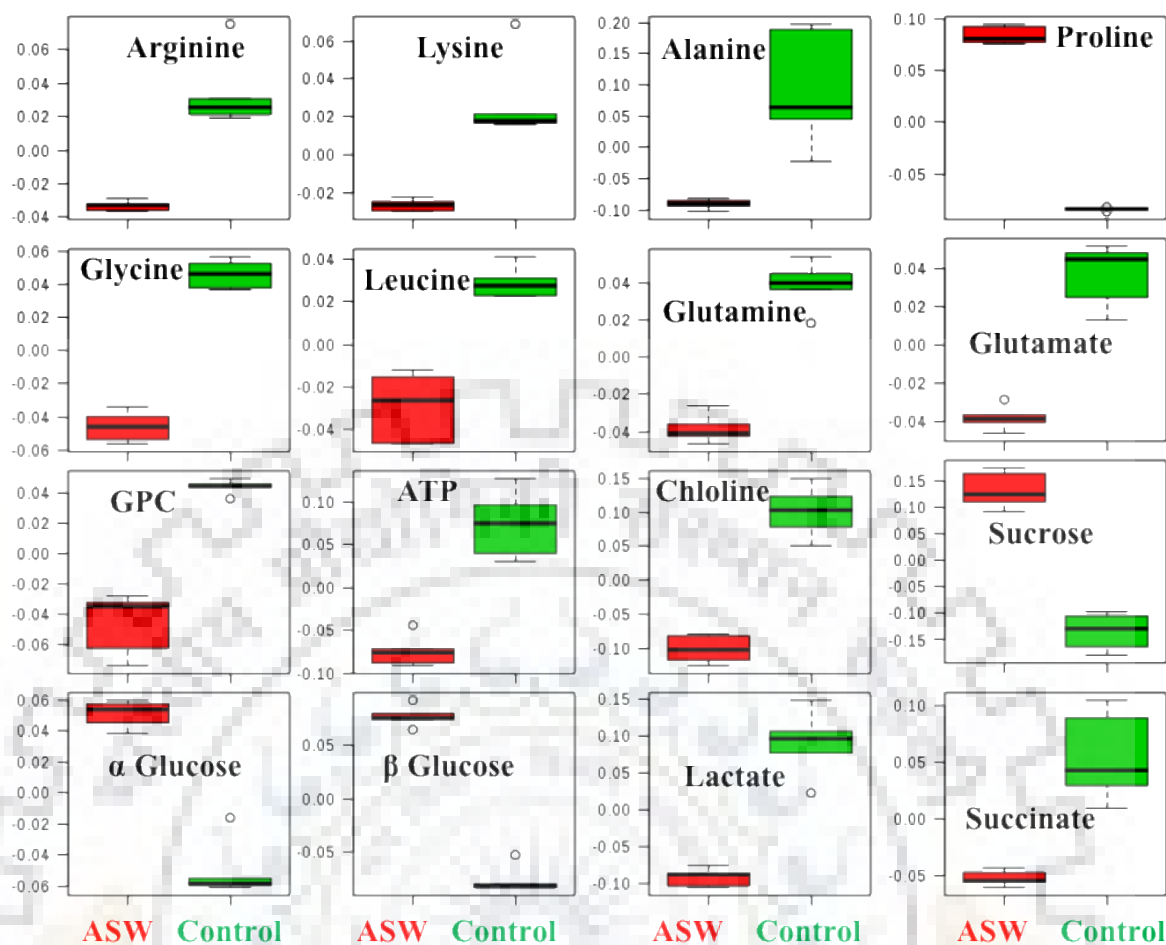
Fig. 3.5A: *The box plots showing relative abundance of some of the metabolites showing significant variation in ASW cultures compared to control cells. In the box plots, the boxes denote interquartile ranges, horizontal line inside the box denote the median, and bottom and top boundaries of boxes are 25th and 75th percentiles, respectively. Lower and upper whiskers are 5th and 95th percentiles, respectively.*
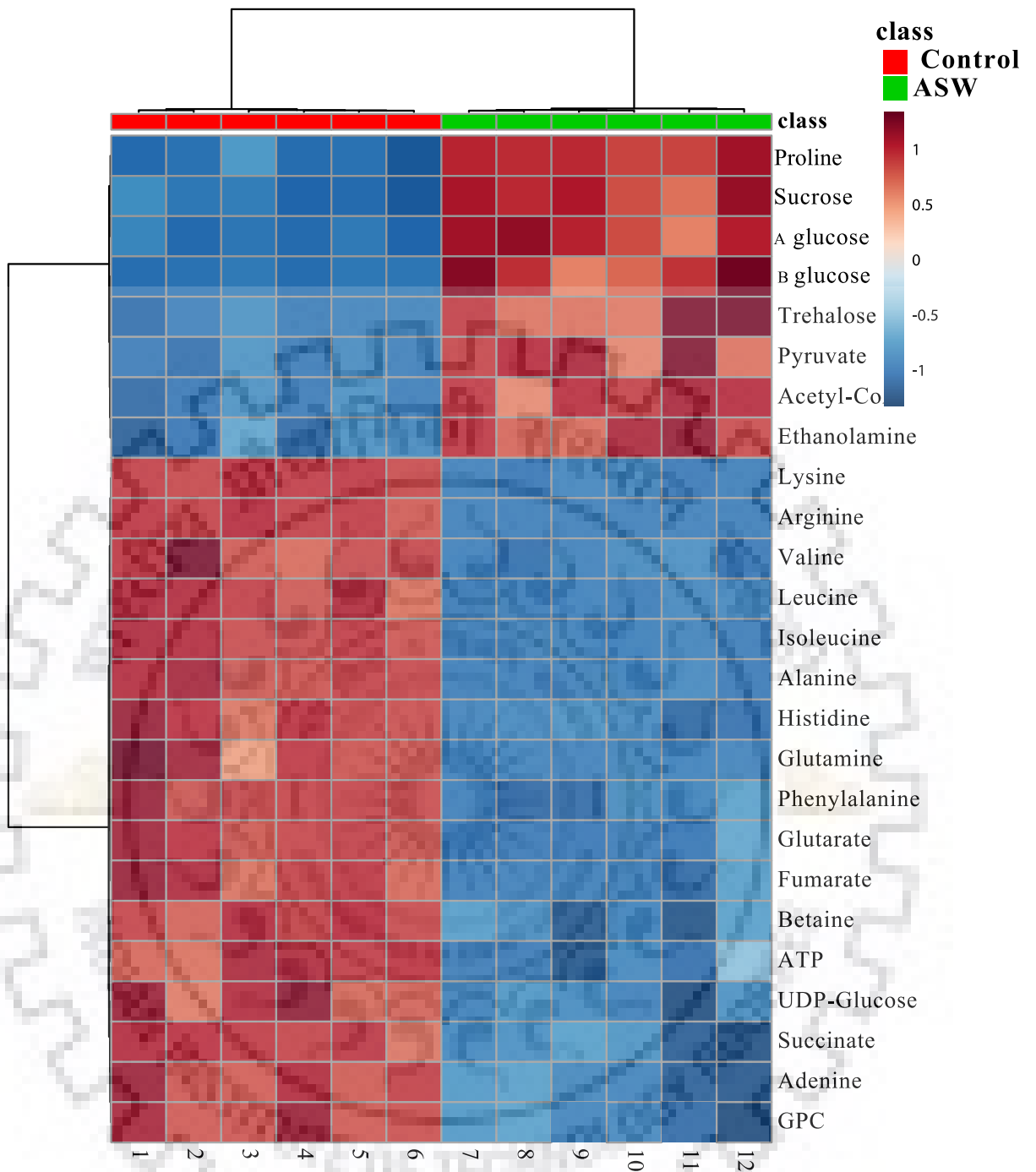
Fig. 3.5B: *Heat maps showing z-scores of discriminatory metabolite entities in ASW cells compared to control culture. X-axis represents the replicates of the culture (A); (Control – lane (1-6) - red bar (B); ASW – lane (7-12)-green bar. The colour scheme through signifies the elevation and reduction in metabolite concentration in ASW compared to control: dark blue: lowest; dark red: highest.*

Among the identified amino acids, proline contributed maximum to the pool with a 10 fold increase in its concentration in ASW algal extracts as compared to control **(Table 3.3)**. An increase in sarcosine was recorded in ASW grown cells while the concentration of the rest of the amino acids (leucine, isoleucine, valine, arginine, lysine, alanine, histidine, glutamate, glutamine and phenylalanine) dropped by ~ 1.2 fold **(Table 3.3)**. Similarly, the levels of the organic acids (lactate, acetate, glutatrate, succinate, fumarate, aspartate) significantly decreased in ASW algal extracts as compared to control cells **(Table 3.3)**. However, an increase in the levels of pyruvate (~ 1.5 fold) was observed in ASW cultures as compared to control. Interestingly, the amount of sugars particularly sucrose peaked to 6 fold followed by α glucose (~ 4 fold) and β glucose (~ 3 fold) in ASW cultivated cells as compared to control cultures **(Table 3.3)**. A 2.5 fold increase in trehalose/mannose was also recorded while no change in glucose-1-phosphate (G-1-P) was recorded in ASW cultures **(Table 3.3)**. Further, a significant decrease in the levels of chloline, GPC (glycerophosphocholine) adenine, ATP, NAD^+ and UDP-Glucose (Uridine Diphosphate) were recorded in ASW cultures while no change was observed in the amounts of glycerol and betaine. However, the ASW cultures showed an increase in the levels of TMAO (Trimethylamine N-oxide) (~ 1.5 fold) and ethanolamine (~ 1.2 fold) as compared to control algal extracts **(Table 3.3)**.

Synthesis of osmolytes is one of the criteria for differentiating different halotolerant microalgal species [219]. Based on the accumulation of proline, four distinct groups have been categorised which include: (1) microalgae accumulating high proline as the major osmolyte e.g. marine microalga, *Chlorella autotrophica*; (2) microalgae accumulating high proline along with large quantity of other osmotic solutes such as sorbitol (e.g. *Stichococcus bacillaris*) or aspargine (e.g. *Agrostis stolonifera*); (3) microalgae synthesising low proline but accumulate other organic solutes in high amounts such as glycerol (e.g. *Dunaliella* sp.) and (4) microalgae accumulating low proline along with low capacity to synthesize other osmolytes respectively [219,220]. Based on the metabolomics results, *Scenedesmus* sp. IITRIND2 can be categorised under group 2 as along with high accumulation of proline it also increased sucrose biosynthesis. Such high accumulation of proline and sucrose have also been reported in various algae including *Synechocystis*, *Microcoleus vaginatus Gom.*, *C. autotrophica*, *S. bacillaris*, *Picochlorum* and *N. oleoabundans* [59,218,219,221].

3.3.5 Assessing the differential proteome response of *Scenedesmus* sp. IITRIND2 using MALDI–TOF-MS/MS

Parallel to the perturbations in the metabolite levels, reorganization of gene expression (reflected in the proteome) of the halotolerant microalga is essential for adaptation to the altered physiological state in response to salinity stress. To this end, proteomics was applied at early stationary phase (7th Day), to reveal the differential expression of proteins in response to salinity stress. One dimensional (1D) SDS PAGE was sufficient to separate the differential proteins and 24 unique protein bands based on their presence/absence, up regulation/down regulation were excised and subsequently identified using MALDI–TOF-MS/MS against the Uniprot Chlorophyta database **(Fig. 3.6A)**. Among the excised bands, only 17 bands showed mascot score above 55 and thus only these were included in the results and discussion of the present study **(Table 3.4)**.
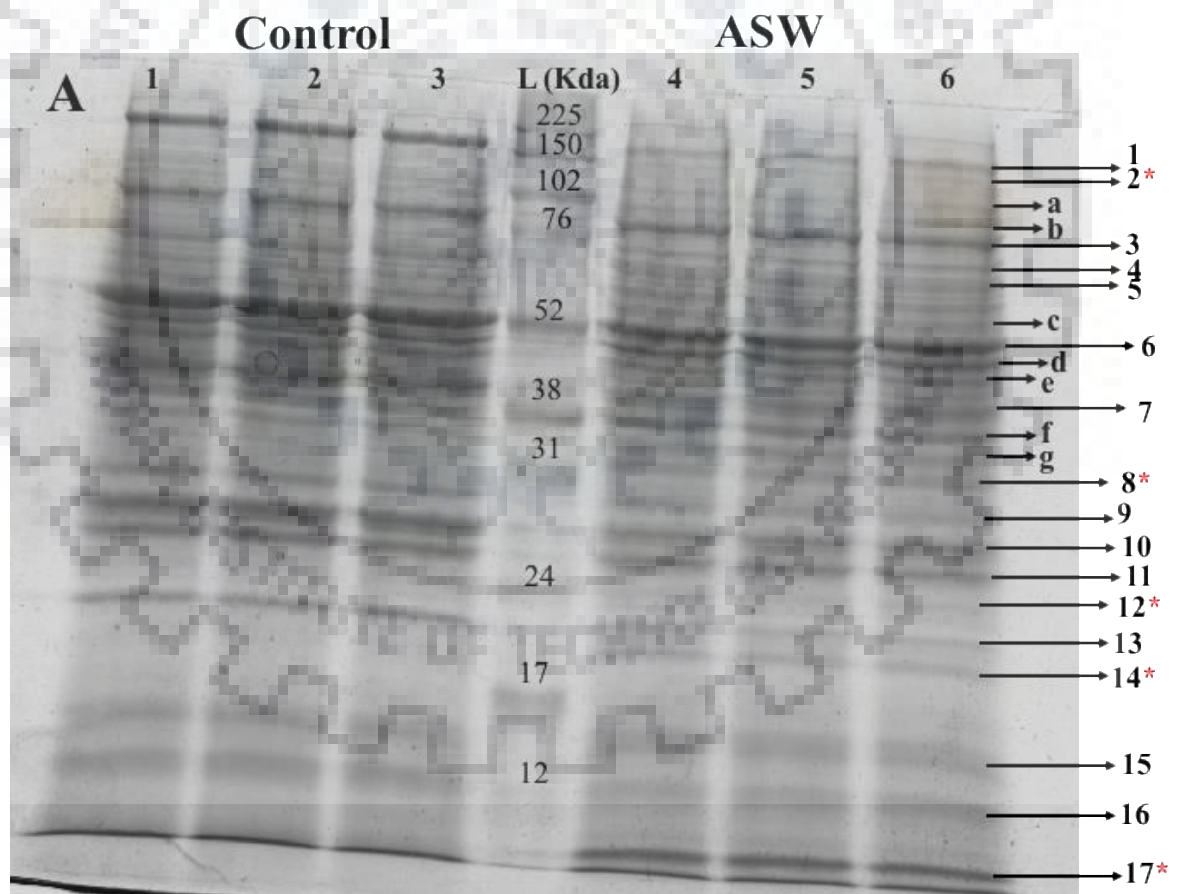
Fig. 3.6: (**A**) *1D SDS PAGE gel showing differential expressed proteins and the bands excised (1-17, Mascot score > 55; a-g (Mascot score <55, *differentially expressed proteins).*

Band ID	Identification in	Protein name	Function categories	Theoretical /Actual MW (KD)	Mascot score	Coverage (%)	Subcellular location	Fold change
1	A0A1D1ZZ74_AUXPR	Uncharacterized protein	unknown	200/207.9	57	14	unknown	3.5 (↓)
2	C1E424_MICC	Uncharacterized protein (Fragment)	Helicase activity (predicted)	150/111.5	88	14	unknown	-
3	K8F2R1_9CHLO	Malic enzyme	Lipid biosynthesis	76/78	69	15	Mitochondria	1.4 (↑)
	A0A087SEW0_AUXPR	Alpha-1,4 glucan phosphorylase	Starch synthesis	76/100.2	77	19	Chloroplast	
4	C1DY39_MICCC	Peptidylprolyl isomerase	Protein degradation	70/63.3	76	13	Cytoplasm	4.3 (↑)
	A0A0D2LKL19_CHLO	Glucose-6-phosphate isomerase	Glycolysis	70/64.59	144	27	Cytoplasm	
5	Q6PYY4_OSTTA	Starch synthase	Starch synthesis	60/58.7	74	16	Chloroplast	1.78 (↓)
	E1ZTI5_CHLVA	Glucose-1-phosphate adenylyltransferase	Starch synthesis	60/55.6	75	19	Chloroplast	
6	A0A172C330_9CHLO	Ribulose bisphosphate carboxylase large chain (Fragment)	Calvin cycle	52/36.59	69	30	Chloroplast	1.34 (↓)
7	C0SKA4_9CHLO	Tubulin beta chain (Fragment)	Flagellar motion/Cytoskeleton microtubule	40/41.6	87	22	Cytoplasm	1.42 (↓)
8	A8JHU0_CHLRE	Malate dehydrogenase	TCA cycle	31/38.8	59	16	Mitochondria	-
	A0A059LS29_9CHLO	Catalase	Antioxidant	31/57.37	96	13	Cytoplasm	
	A0A0D2M0Q2_9CHLO	3-ketoacyl-CoA synthase	Lipid biosynthesis	31/33.9	71	21	Chloroplast	
9	A0A097KLR8_9CHLO	Mg-protoporphyrin IX chelatase	Chlorophyll synthesis	27/39.6	77	36	Chloroplast	1.5 (↓)
10	A0A150H154_GONPE	Uncharacterized protein	Unknown	26/31.4	71	21	Unknown	1.2 (↓)
11	A0A1D1ZTJ7_AUXPR	Uncharacterized protein	Unknown	25/20.87	68	20	Unknown	1.1 (↓)
Band	Identification in	Protein name	Function categories	Theoretical	Mascot	Coverage	Subcellular	Fold

ID				/Actual MW (KD)	score	(%)	location	change
12	D8TLP0_VOLCA	Glutathione peroxidase	Detoxification of H_2O_2	24/22.27	67	11	Cytoplasm	-
13	A0A061S0Z1_9CHLO	Phosphodiesterase	Hydrolase activity	20/48.2	52	14	Cytoplasm	2.3 ($\downarrow$)
14	A8J7H6_CHLRE	Thioredoxin-like protein	Antioxidant	19/27.6	67	29	Cytoplasm	-
	A0A06IRYCR_9CHLO	Pyrroline-5-carboxylate reductase	Proline synthesis	19/28.3	78	29	Cytoplasm	
	A0A1C9ZQC69_CHLO	Alfin-like protein	Salt tolerance	19/20.1	52	17	Cytoplasm	
15	C1KR5_MICCC	50S ribosomal protein L14	Protein synthesis	15/13.40	87	40	Chloroplast	1.1 ($\uparrow$)
	Q946N2_9CHLO	Ribulose 1,5-bisphosphate carboxylase/oxygenase large subunit (Fragment)	Calvin cycle	15/21.8	71	45	Chloroplast	
16	A0A06IQQ83_9CHLO	Nadh:ubiquinone oxidoreductase 13 kDa subunit	Oxidative phosphorylation	12/16.3	52	20	Chloroplast	1.50 ($\downarrow$)
17	A0A061QN19_9CHLO	Putative salt tolerance-like protein (Fragment)	Salt tolerance	10/7.9	54	48	Unknown	-

Table 3.4: *List of identified 1D-resolved protein spots from control and ASW of Scenedesmus sp. IITRIND2.* (**Note:** *For visualization interpretation, single ($\uparrow$,$\downarrow$) arrows are used to represent relative change in the value of protein expression (as evaluated from their intensities using Image J software.*

The identified proteins were functionally grouped into 09 different biosynthesis categories including lipid biosynthesis (02), starch metabolism (02), photosynthesis (03), glycolysis and TCA cycle (03), detoxification and antioxidants (04), salt tolerance (02), protein metabolism (03), cellular structure (01) and unknown (04) respectively using QuickGO which is a gene annotation and ontology tool **(Table 3.4)**. The characteristics details of identified proteins including the accession no (Uniprot database), protein name, functional category, theoretical molecular weight, Mascot score, coverage and subcellular location has been summarized in **Table 3.4**. Based on annotation, proteomics analysis suggested that the identified proteins belonged to 15 different algae which comprises of both fresh water and marine species. For fresh water species, the maximum hits were related to *Desmodesmus communis* (12 %), followed by *C. reinhardtii* (11 %) and *Ettlia pseyudoalveolaris* (10 %) respectively **(Fig. 3.6B)**. On the other hand, for marine algae, maximum similarity was recorded with *Ostreococcus tauri* (8.33 %) respectively **(Fig. 3.6B)**.
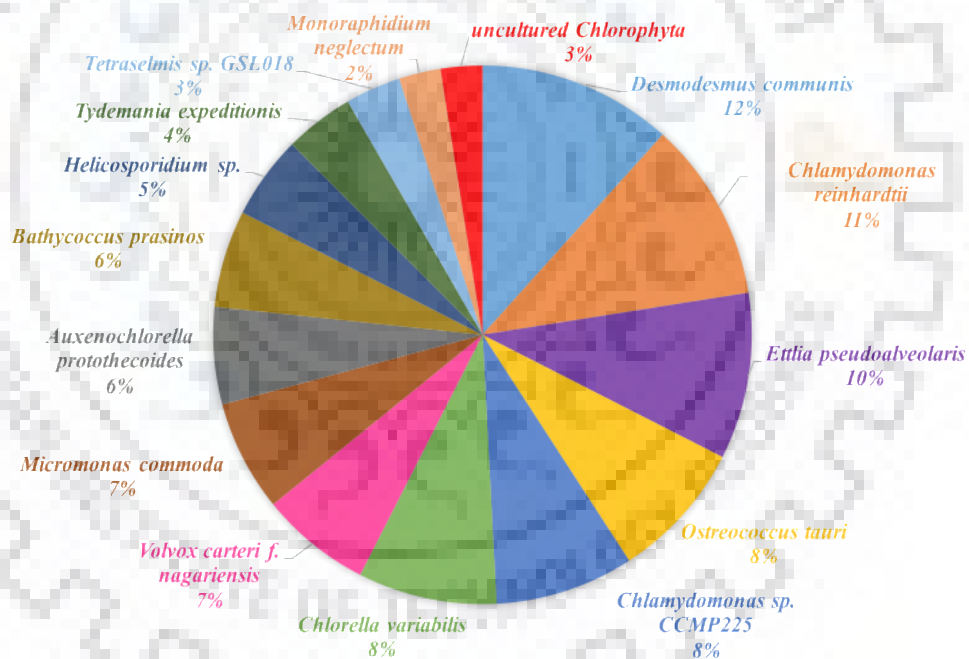
Fig. 3.6: (**B**) *Identification in different algae obtained by QuickGo.*

Interestingly five unique protein bands (2, 8, 12, 14 and 17) as shown in **Fig. 3.6A, Table 3.4** were identified in only ASW cultures. The identified proteins majorly belong to three unique functional categories. They include: (a) antioxidant and detoxifying proteins (catalase, glutathione peroxidase, thioredoxin like protein and pyrroline-5-carboxylate), (b) salt-tolerant proteins (Alfin-like-protein and putative salt like protein) and (c) lipid augmenting proteins (malate dehydrogenease and 3-ketoacyl CoA synthetase) respectively **(Table 3.4 and**

Fig. 3.6A). The expression of proteins such as starch synthase (band 5), ribulose bisphoshate carboxylase large chain fragment (band 6), tubulin β chain (band 7), Mg-protoporphyrin IX chelatase (band 9), phosphodiesterase (band 13) and NADH:ubiquinone oxidoreductase 13 kDa subunit (band 16) were down regulated (2-3 fold) while proteins including peptidylprolyl isomerase (band 4), glucose-6-phosphate isomerase (band 4), 50 S ribosomal protein L14 (band 15) were up regulated (2-4 fold) **(Table 3.4 and Fig. 3.6A)**. Further, four uncharacterized proteins (band 1, 2, 10 and 11) were also identified, however QuickGo was able to predict functional category to only band 2 for helicase activity.

3.3.6 Gene expression analysis of major metabolic pathways using RT-PCR

Substantiation of differential protein expression profiles using gene expression analysis delineated the metabolic pathways that are crucial for halotolerance behaviour of *Scenedesmus* sp. IITRIND2. In order to analyse the relative gene expression patterns, six lipid biosynthesis [malic enzyme (ME), diacylglycerol acyl transferase (DGAT), steroyl-ACP-desaturase (SAD), lipase, Phospholipid:diacylglycerol acyltransferase (PDAT) and biotin carboxylase (BC)], two carbohydrate synthesis genes [sucrose synthase (SS) and ADP-glucose pyrophosphorylase-large subunit (AGP-L)], carbon concentration mechanism (CCM) [carbonic anhydrase (CA)], proline biosynthesis [Δ^{1}- pyrroline -5- carboxylate synthetase (P5CS)] and photosynthesis [Photosystem II reaction center protein subunit C (PsaC)] were studied. Compared to the control, all the lipid biosynthetic genes showed an increase in ASW except lipase (LIP). Among the elevated genes, lipid biosynthesis showed maximum expression (BC > SAD > ME > DGAT > PDAT) **(Fig. 3.7)**. On the other hand, both carbohydrate synthesis genes expression decreased by 2-3 fold in ASW as compared to control cells. Further, a 5-7 fold increase in proline and CCM genes expression was recorded in ASW cultivated cells with down regulation of photosynthesis gene as compared to control cells **(Fig. 3.7)**.
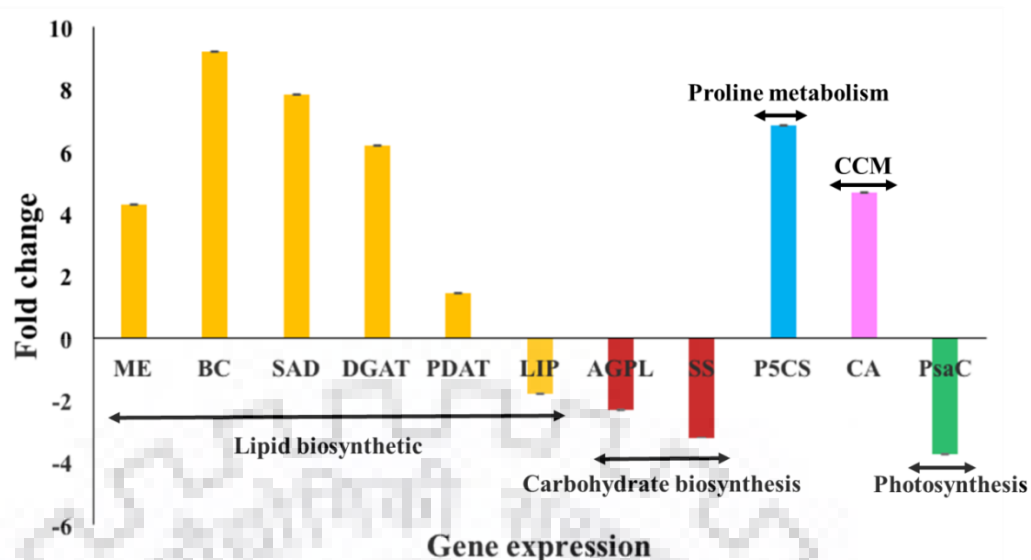
Fig. 3.7: *Gene expression of metabolic pathways analysed by RT-PCR.*

3.4 Discussion

Integrated omics approach studies are helpful in facilitating the correlation of metabolic pathways by linking gene, proteins and metabolites of any organism. In the last decade, researchers have made a progress in unravelling the microalgae complex biosynthetic pathways by utilizing various omics techniques [93]. These algal-omics studies have led to well established metabolic maps which aided identification of targets for genetic engineering for high lipid accumulating microalgal strains [153,222]. Keeping this view in mind, the present study utilized an integrated omics approach to unfold the halotolerance mechanism of a novel high lipid accumulating microalgal isolate *Scenedesmus* sp. IITRIND2, and also identified potential genome editing targets.

The results obtained aided in postulating that in order to survive the salinity stress, *Scenedesmus* sp. IITRIND2 essentially needs to maintain the osmotic equilibrium across the membrane and cytoplasm which can be achieved via alterations to membrane permeability, cell surface charge and lipid composition along with perturbations in the gene, protein and metabolites biosynthesis. Based on the results obtained from biochemical, structural and integrated omics studies, a salinity driven metabolic pathway of the microalga, which enabled it to tolerate the salt stress along with high lipid accumulation is proposed **(Fig. 3.8)**.
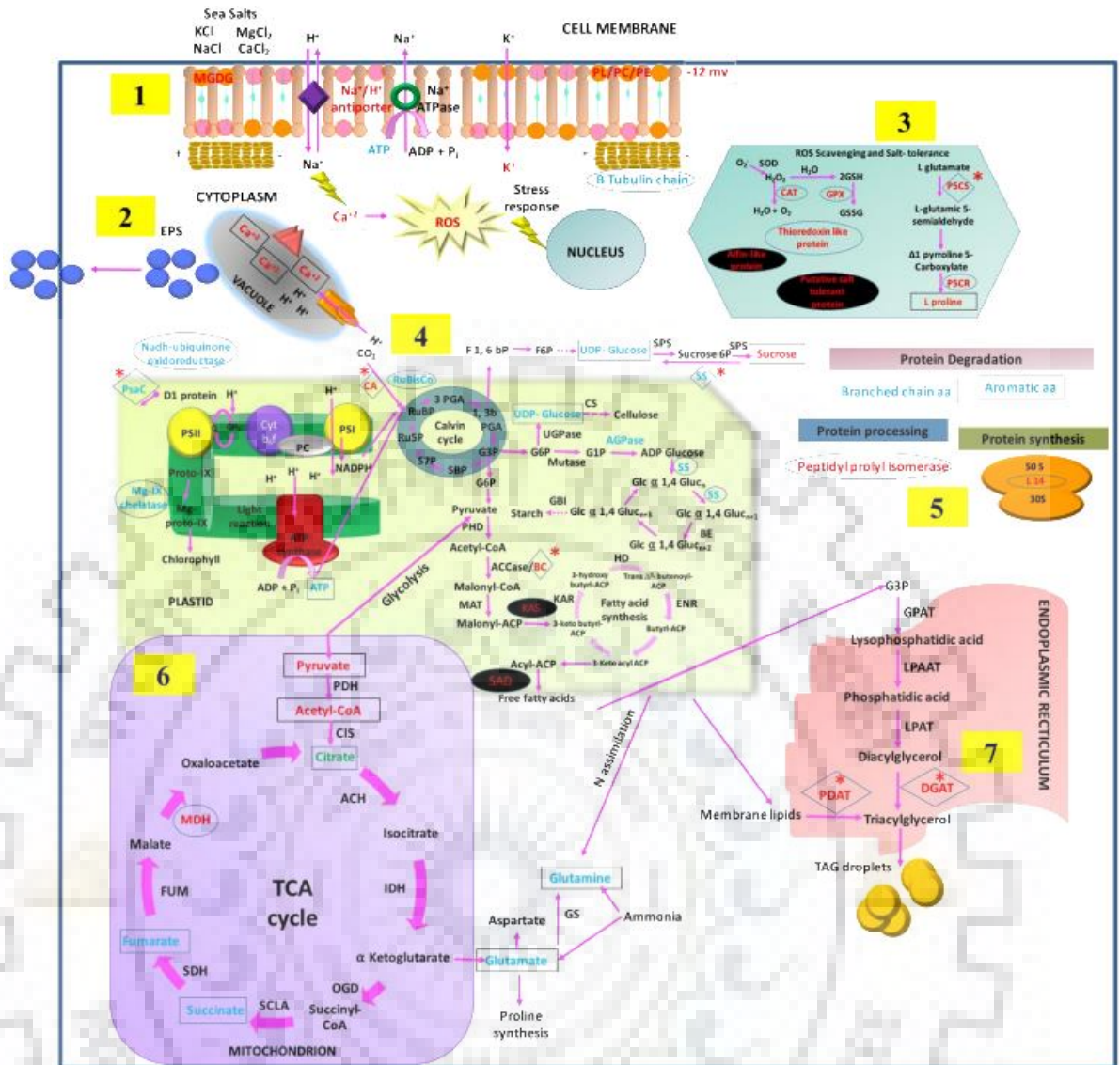
Fig. 3.8: *Schematic representation of salt-tolerant mechanism deployed by Scenedesmus sp. IITRIND2 by alteration in various cell organelles/pathways (**1**) ion channels and cell membrane (**2**) production of EPS (**3**) ROS scavenging and salt-tolerance (**4**) Lipid and carbohydrate metabolism and photosynthesis (**5**) Protein metabolism (**6**) TCA cycle (**7**) TAG synthesis. The genes are presented in diamond shape, proteins in circular and metabolites/ions in square. The up regulated genes/proteins/metabolites are shown in red while in blue for down regulation. The four potential biomarkers for genetic engineering are represented in Black.*

The first adaption step by the microalga towards salinity stress is the change in the membrane potential and permeability, as an increase of the K^+ ions inside the microalga indicated it to be an important coping mechanism which helps to reduce the toxic effects of enhanced Na^+ ions **(Fig 3.8: Panel 1)** [223]. An increase in uptake of Ca^{+2} also helps the microalgae to counteract the toxic effects of Na^+ ions, and thus reduces the permeability of the

plasma membrane [224]. Parallel to the ions balance, fluctuations in the lipid composition particularly the membrane lipids was also an essential acclimatisation mechanism deployed by *Scenedesmus* sp. IITRIND2. The ^{1}H NMR showed increase in the negatively charged lipids including PE, PC and PL which contributed towards the negative charge of the cell membrane under halotolerant conditions as substantiated by the decrease in its surface zeta potential **(Fig. 3.3A and Fig 3.8: Panel 1)**. Such an increase in the negatively charged lipids indicate to shield the microalgal cell membrane from the Na^+ ions and avoid membrane destabilization [225]. Similar results have also been reported in various microalgae including *D. salina* and *C. nivalis* [226,227].

An increase in the SFAs in the algal plasma membrane is crucial to decrease its permeability towards the small ions (Na^+, Cl^-) but at the same time keep it fluid and flexible enough to carry out normal cellular processes [187,213]. Earlier a two-fold increase in the content of C18:1 followed by a 1.5 fold increase in C16:0 in the fatty acid composition under salinity stress has been reported indicating that the microalga maintained an optimum balance of cell permeability and potential (In chapter 2, section 3.4) [228]. Further, a two fold increase was observed in the MGDG levels **(Fig. 3.3A)**, a non-bilayer forming lipid that balances the membrane fluidity, and is also crucial for photosynthetic processes involving lateral, rotational and transmembrane diffusion during electron transfer from photosystem II (PSII) and phostosytem1 (PSI) [229]. The cells cultivated in ASW also showed an increase in EPS formation which can further enhance its salinity tolerance characteristics **(Fig. 3.3B, Fig. 3.8: Panel 2)**.

Apart from the modulation of the membrane permeability, increase in the accumulation of osmolytes was observed to be an important phenomenon for restoring the osmotic equilibrium **(Table 3.3 and Fig. 3.8: Panel 3)**. High concentrations of proline and sucrose in ASW cultivated *Scenedesmus* cells suggested them to be the major osmolytes engaged in regulating the internal osmotic balance **(Table 3.3 and Fig. 3.8: Panel 3, 4)**. Proline is actively involved in the restoration of turgor pressure, regulation of cellular water structure, ROS, inhibition of lipid peroxidation and as an antioxidant [135]. On analysis of the proteomics of the ASW grown cells, unique band was observed of pyrroline-5-carboxylate reductase (P5CR) **(Table 3.4)**. The L-proline is synthesized from L-glutamate via two successive reactions catalysed by the P5CS and P5CR (pyrroline -5-carboxylate reductase), with consumption of 1 molecule of ATP and 2 molecules of NADPH [204]. Indeed, RT-PCR analysis showed the overexpression of P5CS, thus substantiating the metabolic and proteomic results related to L-proline increase in ASW cells **(Fig. 3.7)**. A significant reduction in the levels of glutamate and ATP also indicated their flux towards proline synthesis **(Table 3.3)**. Apart from proline

accumulation, sugar accumulation also contributes towards the maintenance of osmotic strength the microalgal cells under salt stress. Such an accumulation of sugars not only prevents cellular degradation but also provides a source of energy under saline conditions [230]. Among the sugars, the omics data indicated that sucrose was synthesized prior to other sugars as an apparent decline in the level of UDP-glucose and down regulation of sucrose synthase (catalyses the breakdown of sucrose) was recorded **(Table 3.3, Fig. 3.6 and Fig. 3.8: Panel 4)**. Sucrose plays a vital role in decreasing the toxicity of Na^+ ions by aiding its active extrusion, inhibition of membrane vesicles and improving the H^+-ATPase activity [221]. The metabolomics analysis also showed a rise in the levels of glucose and mannose/trehalose in the ASW cultivated cells. Trehalose has an established role in stabilization of proteins under salt stress by acting as an antioxidant and osmoregulatory molecule [231]. Another important adaptive mechanism involves the quenching of the ROS generated due to salt stress. *Scenedesmus* sp. IITRIND2 efficiently grew in ASW due to differential expression of three antioxidant proteins including thioredoxin like protein, glutathione peroxidase and catalase **(Table 3.4 and Fig. 3.8: Panel 3)**. Interestingly, *Scenedesmus* sp. IITRIND2 exhibited distinct salt tolerant response as two unique proteins: (a) putative salt-tolerant protein and (b) Alfin-like protein were identified **(Table 3.4 and Fig. 3.8: Panel 3)**.

Excessive intrusion of Na^+ ions into the cells due to salt stress can inhibit the amino acid /protein biosynthesis. A decrease in the levels of all the aromatic and branched chain amino acids under salt stress was observed **(Table 3.3)**. The salt induced stress on protein folding machinery was also evident as the halotolerant cells showed for up regulation of Peptidylprolyl isomerase (PPI), a potential molecular chaperon and ROS scavenger **(Table 3.3 and Fig. 3.8: Panel 5)** [232]. As chloroplast is one of the major sources of ROS production, suppression of photosynthesis combats for oxidative damage under salt stress. In line with this, a reduced expression of Mg-protoporphyrin IX chelatase, Ribulose bisphosphate carboxylase large chain (Fragment) and PsaC in ASW cells were noted **(Table 3.4, Fig. 3.6 and Fig. 3.7: Panel 4)**. Further, as salinity decreases the solubility of the CO_2 in water thereby decreasing its availability to the microalgal cells, an increase in the gene expression levels of carbonic anhydrase (CA) was recorded **(Fig. 3.6 and Fig. 3.8: Panel 4)**. It has been reported that under stress conditions, the levels of CA increases which facilitates CO_2 acquisition along with activation of C4 CCM [233].

A subsequent up regulation of malate dehydrogenase (catalyses the conversion of malate to oxaloacetate in TCA cycle) in ASW grown cultures indicated accumulation of acetyl-CoA; precursor for fatty acid synthesis **(Table 3.3, 3.4 and Fig. 3.8; Panel 6)**. Further, an up regulation in the levels of malate dehydrogenase has been related to salt adaptation in

Arabidopsis [234]. A decline in the starch metabolism was recorded as proteomics/RT-PCR analysis of ASW cultures showed down regulation of starch synthase and Glucose-1-phosphate adenylyltransferase (AGPase) **(Table 3.4, Fig. 3.6 and Fig. 3.8: Panel 4)**. Additionally, an up regulation in the glycolysis (Glucose-6-phosphate isomerase and glucose) and down regulation of TCA cycle (succinate and fumarate) indicated redirection of cell's carbon flux towards lipid body formation **(Table 3.3 and 3.4)**. Such a rewiring of metabolic pathway towards synthesis of TAGs can be a unique survival trait adopted by the microalga to survive under stress conditions.

In Chapter 2, section 2.3.3, an increase in TAG accumulation (52 % of dry cell weight) in microalgal cells cultivated in ASW as compared to control cells was observed which is well corroborated with the TEM micrographs showing deposition of large number of intracellular lipid droplets **(Fig. 3.2C and D)** [228]. These results were complimented by the proteomics and gene expression analysis as lipid biosynthesis genes (ME, BC, KCS, SAD, DGAT, and PDAT) which were up regulated in ASW grown cultures **(Fig. 3.8: Panel 2, 6)**. An apparent up-regulation in the levels of ME at both transcriptional (RNA) and translational (protein) levels indicates the elevated conversion of malate to pyruvate, thus leading to generation of more NADPH and the direction of its flux towards lipid synthesis **(Fig. 3.8: Panel 3)**. Increase in ME has been reported under nitrogen depletion, CO_2 deprivation and salinity stress respectively [59,105].

The first committed step towards the fatty acid synthesis is the conversion of acetyl-CoA to malonyl-CoA catalysed by ACCase [235]. Biotin carboxylase is the part of ACCase that catalyses the carboxylation of ACP and transfer of carboxyl group thereby generating malonyl- CoA [120]. On the other hand, KCS catalyses the conversion of malonyl-coA to acyl-coA, the first rate limiting step in fatty acid elongation while SAD is responsible for the conversion of stearoyl-ACP to oleoyl-ACP and is crucial for maintaining the ratio of saturated fatty acids and unsaturated fatty acids [236,237]. Augmentation in the levels of DGAT that catalyse the conversion of DAG to TAG was also observed. Additionally, PDAT which is responsible for the conversion of chloroplastic membrane lipids to TAGs was also enhanced. These observations established that both *de-novo* and lipid recycling pathways are essential and responsible for the overall increase in TAG content under salinity stress conditions **(Fig. 3.8: Panel 7)**.

In a nutshell, integrated omics results on *Scenedesmus* sp. IITRIND2 have unravelled four unique genetic targets, whose overexpression could potentially convert fresh water microalgae to halotolerant species. These four targets include: (a) Alfin-like protein, (b) putative salt-tolerant protein (c) KCS and (d) SAD. Alfin-like protein family was discovered in

alfalfa (*Medicago sativa*) and its overexpression in parent plant and *Brassica napa* resulted in increasing the salt tolerance [236,238]. This is the first report showing the differential expression of alfin-like protein in an algal strain, and could be a potential genetic engineering target in microalgae also for increasing the halotolerance and warrants further investigation. On the other hand, putative salt tolerance protein could be a possible homolog of salt tolerant protein (STO) identified in *Arabidopsis thaliana* which is an Na^+/H^+ antiporter, whose overexpression has resulted in increased salt tolerance [239,240]. KCS and SAD which are involved in the lipid biosynthesis pathway are the two other important genetic targets revealed from the current study. They together are responsible for MUFAs formation, and also helps to acclimatize the algal intracellular membrane compartment to function in high internal osmolytes concentration [237].

3.5 Concluding remarks

A novel halotolerant microalga isolate *Scenedesmus* sp. IITRIND2 was shown to modulate its cellular machinery by adapting in high saline environments which was reflected in changes to the ion channels, membrane permeability, ultrastructure, metabolites and proteome. The observed metabolic rewiring of the microalgae is unique and different from common halotolerant microalga; *D. salina*. The investigation identified four biomarkers including KCS, SAD, Alfin-like protein and putative salt tolerant protein that could be the potential genetic engineering targets for non-halotolerant strains.

The present study also pointed out the ease of harvesting the microalgal biomass cultivated in ASW as the cells showed an increase in cell size, EPS formation and loss of β tubulin chain expression which is crucial for motility thereby enhancing the auto sedimentation property, thus reducing the cost of downstream processing. Another interesting aspect for reducing the cost of algal production is biorefinery approach which integrates biodiesel production with conversion/extraction of all the available compounds into spectrum of marketable high value compounds (omega 3 fatty acids, bioactive compounds, etc.) without generation of waste [52,241,242]. *Scenedesmus* sp. IITRIND2, along with augmented lipid accumulation showed high amounts of proline and sucrose which are industrially relevant products. In summary, the outcomes of this study has not only enhanced our existing molecular level knowledge of halotolerance and lipid accumulation in response to salt stress but also yielded genetic targets for generating novel halotolerant algal strains.

Assessing the robust growth and lipid accumulating characteristics of Scenedesmus sp. cultivated in natural sea water using small scale custom built photobioreactor

4.1 Introduction

In the past decade, extensive studies have been carried out to study the effects of sodium chloride (NaCl) on various genera of microalgae such as *Desmodesmus* sp, *Chlamydomonas* sp., *Chlorella* sp., *Acutodesmus* sp., *Scenedesmus* sp. and *Dunaliella* sp. etc. [165,230,243–245]. However, to mimic natural sea water salinity variation, cultivation of microalgal strains in sea water (using representative sea salt composition) is absolutely essential. To this end, recently various microalgae such as *Chlorococcum* sp. RAP13, *Tetraselmis* sp. CTP4, *Picochlorum* SENEW3, *Marinichlorella kaistiae* KAS603 and *Scenedesmus* sp. IITRIND2 have been identified as halotolerant and grown in sea water/sea salts for biofuel generation [59,183,228,246,247]. The major difference between sea water and NaCl lies in the presence of essential elements such as the calcium, magnesium and potassium salts of sulfate and carbonate in a complex buffer system that aid in microalgal growth.

The halotolerant microalga *Scenedesmus* sp. IITRIND2 was cultivated in different sea water salinities (0-100 %) in a small-scale custom built photobioreactor, to evaluate its potential for carbohydrate and lipid accumulation. The main objective of the study was to delineate the temporal changes in the bioenergy stored in the algae cells, as fatty acids and carbohydrate content and respective composition. This will shed light on the physiological energetic responses of microalgae as an adaptation response to high salinity, when nutrients in the culture are not limited. Furthermore, the growth performance of the microalga was compared with NaCl supplemented medium to examine the efficiency for biomass generation and distinguish the observed response in sea water from the salt induced salinity. Our study showed evidence of rapid modulation in the cell's carbohydrate content, which may aid the microalga to maintain cell's osmotic balance and subsequent adaptation to high salinity conditions, thereby making it less permeable to sodium and maintaining osmotic balance. The insights obtained from this study will helps in unravelling physiological changes occurring in a halotolerant microalga in response to salinity.

4.2 Materials and Methods

4.2.1 Microalgal strain and cultivation conditions

To test the adaptability of *Scenedesmus* sp. IITRIND2 in sea water and exclusive NaCl supplemented media, the cells were cultivated in 250 mL Erlenmeyer flasks containing sea water/ NaCl based growth media having four different salinities- no salt, quarter strength (8.75 g/L), half strength % (17.5 g/l) and full strength % (35 g/L). The sea water media obtained from Bigelow laboratory for Ocean Sciences (60 Bigelow Drive, East Boothbay, ME, USA) had the following composition, 0.39 g/L NH_4HCO_3, 1 mL 0.313 M $NaH_2PO_4.2H_2O$, 1 mL F/2 trace element stock, 1 mL F/2 vitamin stock in 1 L filtered sea water. In case of NaCl supplemented media, the sea water was replaced by distilled water and appropriate amount of NaCl was dissolved to obtain equivalent salinities **(Table 4.1)**. The media used was vacuum filtered (Thermo Scientific Nalgene Filtration unit). The cultures were incubated at 25 ℃ with continuously illuminated at 70 µmol photons m^{-2} s^{-1} by white fluorescent lamps and air containing CO_2 (2 %; v/v).

Media components	Sea water medium (g/L)				NaCl medium (g/L)		
	0	8.75	17.5	35	8.75	17.5	35
Sea water (mL)	0	250	500	1000	0	0	0
Distilled water (mL)	1000	750	500	0	1000	1000	1000
NaCl (g/L)	-	-	-	-	8.75	17.5	35
NH_4HCO_3 (g/L)	0.39	0.39	0.39	0.39	0.39	0.39	0.39
0.313 M $NaH_2PO_4.2H_2O$ (mL)	1	1	1	1	1	1	1
F/2 trace element stock (mL)	1	1	1	1	1	1	1
F/2 vitamin stock (mL)	0.5	0.5	0.5	0.5	0.5	0.5	0.5

Table 4.1: *Details of sea water and NaCl supplement media components.*

4.2.2 Inoculum preparation and photobioreactor cultivation

A photobioreactor (PBR) with programmable high Bay LED lights (Grainger) plugged into a control device (National Control Device) that mimics the outdoor light (photosynthetically active radiation) conditions was used to run the experiments. The LEDs provided a maximum light intensity of 900 µmol photons m^{-2} measured in the culture tubes

(150 mL; 20 cm X 3.5 cm). The system utilized a water bath for temperature control with a programmable water circulator providing controlled temperatures based on a two week average measured in open ponds operated in the summer in Mesa, AZ (warmest temperature during the day was 32 °C for almost one hour starting at 14:00 and the coldest temperature drops to 21°C at 5:00) respectively **(Fig. 4.1)**. The culture tubes had gas tight stoppers with three inlet/outlet tubes. These were used to deliver 2% CO_2 enriched air to the bottom of the tube for mixing, provide a gas out line, and a liquid sampling line that was used to monitor cell density of the cultures every day. The culture tubes were held in place by a rigid bracket that keeps all 36 tubes in two parallel rows where the light intensity is the same for each position. Four different seawater and NaCl salinities (0, 8.75, 17.5 and 35 g/L) with culture volume of 100 mL and initial O.D. at 750 nm of 0.1 for 120 h in the same conditions as detailed above were used.
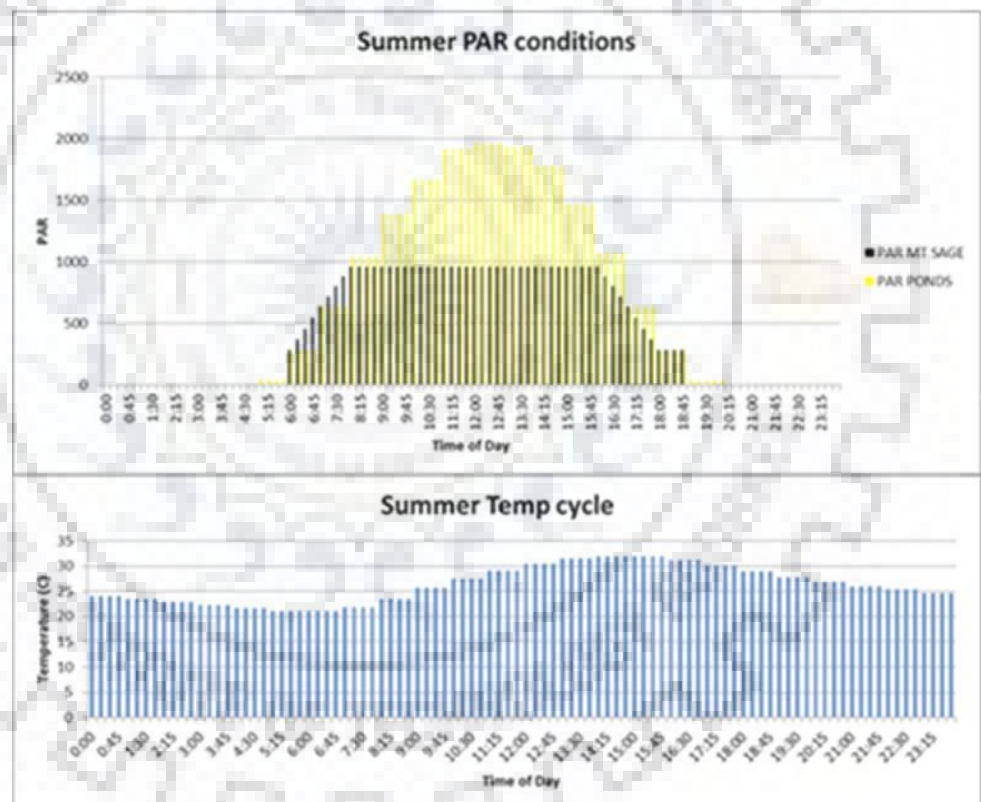
Fig. 4.1: *Photobioreactor temperature and light intensity cycle.*

4.2.3 Microalgal growth estimation

The microalgal growth rate was monitored daily by spectrophotometry (Beckman Coulter DU 800 Spectrophotometer) at 750 nm. Ash free dry cell weight (AFDCW) determination was carried out as described by Wychen et al. [248]. In brief, the crucibles were

preconditioned in the 575 °C muffle furnace overnight to remove any combustible contaminants and then their weights were recorded at room temperature. In each crucible 100 ± 5 mg of freeze-dried algae was added and the weight of each sample was recorded. Samples were then placed in a 40 °C vacuum oven overnight and gravimetrically the weight was recorded, after which the samples were placed in the ramping 575 °C oven overnight. The biomass productivity (mg/L/d) was then calculated according to the following equation:

$$\text{Biomass productivity} = \frac{\text{Final AFDCW} - \text{ Initial AFDCW}}{\text{Cultivation time}}$$

4.2.4 Nitrogen, phosphate and pH estimation

The inorganic nitrogen was measured as total ammonium ions present in the form of NH_4HCO_3. Residual ammonium was measured in pre-filtered (0.45 μm membrane filter, Millipore Corporation, Billerica, MA, USA) cell free supernatant every 24 h using commercially available Nitrogen, Ammonia Test kit (Model no: NI-SA, Hach Company, Loveland, CO, USA). The residual phosphate was determined in pre-filtered (0.45 μm membrane filter, Millipore Corporation, Billerica, MA, USA) cell free supernatant every 24 h using commercially available phosphate assay kit (MAK 30-KT, Sigma, USA). Cell free supernatant pH was measured on samples using a standard bench top pH meter (Beckman 40 pH Meter) after every 24 h time interval.

4.2.5 Compositional analysis

The total carbohydrate content was determined in duplicate for each of the samples [249]. The lyophilized biomass (25 mg) and 250 μL of 72% (w/w) sulfuric acid were added into a 10 mL glass vial. The first step hydrolysis was performed in a 30 °C water bath for 1 h followed by addition of 7 mL of 18.2 MΩ into the vial which was then sealed and autoclaved for 1 h at 121 °C. Hydrolyzed samples were then run on a high pressure ion chromatography (ICS-5000+, Thermofisher Scientific) using a Carbopac PA20 column/guard column and pulsed amperomtric detector (PAD). Monomeric sugars and uronic acids were eluted at 0.45 mL/min using an isocratic eluent concentration of 27 mM NaOH for the first 10 min, followed by the ramping of a 1M NaOAc/100mM NaOH eluent from 2 − 19% (the remainder as water − 98 − 81%). This was followed by a linear increase from 10 minutes upto 30 minutes, then turning off ramp and running the 100 mM NaOH for 5 minutes. This was then re-equilibrated

for 10 minutes at the initial NaOH concentration (27mM) with a total run time of 45 minutes respectively. The column and compartment/detector temperatures were set to 35°C. For detection, the gold standard PAD waveform (carboquad, waveform A): E1: +0.1V for 400 ms, E2: -2.0V for 1 ms, E3: +0.6V for 1 ms, E4: -0.1V for 6 ms was used.

Lipids were measured as fatty acid methyl esters (FAMEs) in biomass, through an *in situ* FAME preparation method [250]. Approximately, 4-7 mg of lyophilized microalgae biomass was added to a pre-weighted GC vial. An internal standard tridecanoic acid methyl ester, chloroform/methanol (2:1) and HCl methanol solution (5%, v/v) were added and the solution was heated at 85 °C for 1 h, extracted with 1 mL of hexane and analyzed by GC-FID equipped with a DB-WAX column (Agilent, USA), 30 m 0.25 mm and 0.25 μm, temperature program 100 °C for 1 min, then to 25 °C min^{-1} to 200 °C, hold for 1 min, then 5 °C to 250 °C and hold for 7 min, at a helium as carrier gas (1 mL/min). The individual FAME concentrations was quantified and normalized against the internal standard [250].

4.2.6 Statistical analysis

The PBR experiments were run twice (*n*=2) with two replicates each time and the results have been presented as mean ± S.D. of all four replicates respectively. Statistical analysis was done using one-way ANOVA followed by post hoc Tukey's test (Graph pad V7) and $p<0.05$ was taken as significant.

4.3 Results

4.3.1 Photobioreactor design and adaptation of microalga under high saline conditions

To enhance the economic feasibility of microalgal biofuel production, a halotolerant microalga *Scenedesmus* sp. IITRIND2 was cultivated in different salinities by diluting sea water into the medium base and compared to equivalent NaCl based media using the custom-built moderate throughput PBR. The microalgae showed broad halotolerance ability as the seed cultures grown in the respective sea water or NaCl salinities media adapted well under incubator conditions (25 ºC, 70 μmol photons m^{-2} s^{-1}). However, when the seed cultures were cultivated under programmed fluctuating temperatures and higher light regimes in the PBR, the microalga failed to grow in culture media that contained 35 g/L NaCl, and growth was equally inhibited when NaCl concentration were 8.75 and 17.5 g/L respectively **(Fig. 4.2)**.
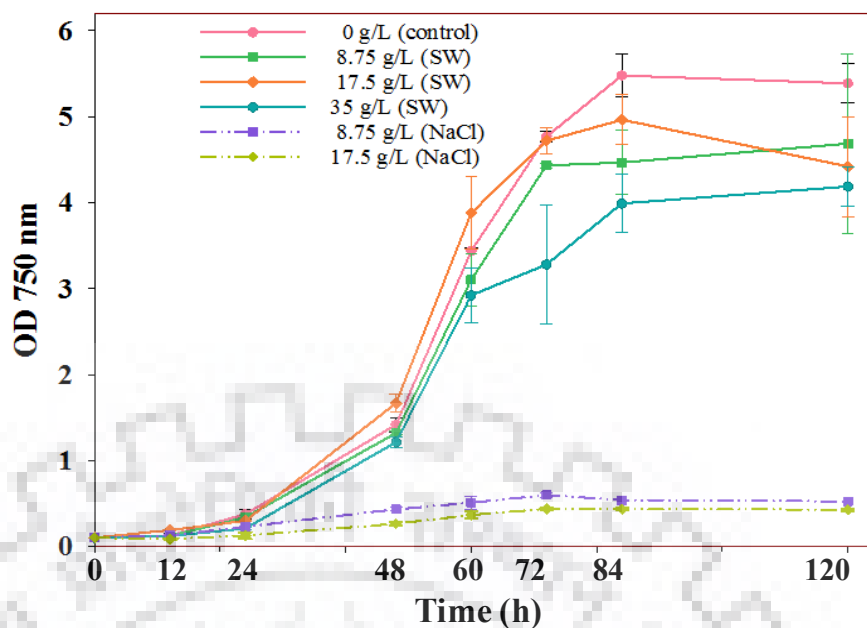
Fig. 4.2: *Effect of sea water salinity and exclusive NaCl on cell growth* of *Scenedesmus* sp. IITRIND2.

This suggests that presence of pure NaCl in the basal media is more inhibitory to the microalga as compared to equal amounts of sea salts under these growth conditions. Indeed, cultures adapted well in NaCl medium under constant low light intensity suggesting that the physiological effects of NaCl are synergistic with lighting conditions meant to mimic outdoor growth. Also, the inhibitory effects of NaCl can be alleviated by changing the physical conditions such as constant light intensity, temperature and CO_2 of microalgal growth. Similar results have been reported in blue green algae (*Agmenellum quadruplicatum*) when it was cultivated in high NaCl concentrations (70-90 g/L) [251].

4.3.2 Salinity effect on algal growth

The microalga growth was assessed through optical density (O.D.$_{750\ nm}$), AFDW and biomass productivity. Among the four initial concentrations of sea water applied, the 8.75 g/L culture showed a limited response as compared to no salt cultures, along with discrepancy between O.D.$_{750\ nm}$ and AFDW values. This could be due to increase in the cell size or shape of the algal cells when exposed to high saline environments as reported earlier [7]. Half strength seawater (17.5 g/L) cells showed higher O.D.$_{750\ nm}$ than full strength sea water, reaching its maximum AFDW of 2.58 ± 0.04 g/L at 84 h after which the biomass significantly decreased

(Fig. 4.3). Overall the microalgal AFDW (g/L) and biomass productivity (mg/L/d), after a cultivation period of 120 h in sea water-based media was found to decrease with increase in sea salt concentration with maximum (3.18 ± 0.18 g/L; 696 ± 4 mg/L/d) in no salt while minimum (1.91 ± 0.04 g/L; 362 ± 2 mg/L/d) in 35 g/L **(Fig. 4.3)**. However, the cultures with exclusive NaCl supplemented media, grew with a slow and linear manner over 72 hours with approximately 4 -5 fold lower AFDW than sea water salinity in 8.75 g/L (0.61 ± 0.02) and 17.6 g/L (0.67 ± 0.02 g/L) as shown in **Fig. 4.3**. These results indicate that microalga benefitted with mixture of salts present in sea water as compared to exclusive NaCl.
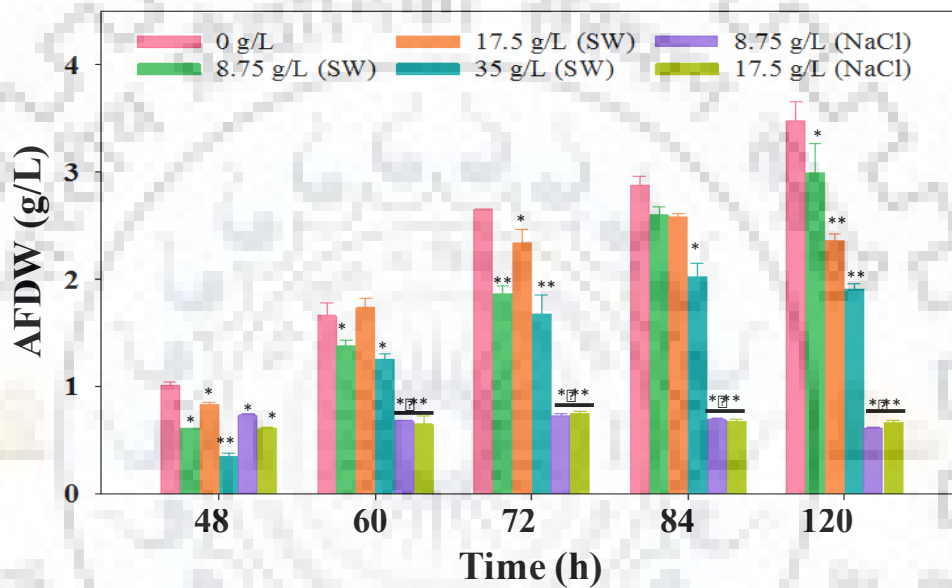
Fig. 4.3: *Effect of sea water salinity and exclusive NaCl on Scenedesmus sp. IITRIND2 on AFDW cultivated in photobioreactor. Error bars indicate standard deviation for four biological replicates (* p <0.05, ** p < 0.01, *** p <0.001).*

4.3.3 Changes in pH and uptake of nutrients

In order to determine the effect of salinity on pH and nutrient uptake from the media during the microalgal growth, changes in the pH, ammonium and phosphate concentrations in the medium were measured. A rapid decline from pH 8.0 (initial) to pH 6.2-6.8 was recorded in half and full-strength sea water cultivated media within 48 h while in case of cultures supplemented with exclusive NaCl, the pH only dropped to 7.1 **(Fig. 4.4A)**. After 48 h time interval, equalization of pH (no significant decrease) took place in quarter, half and full-strength sea water media and NaCl (8.75 g/L and 17.5 g/L), while for culture with no sea water

(0 g/L) the pH further dropped to 6.02 (**Fig 4.4A**). Indeed, the drop in pH could be attributed to the uptake of ammonia by the microalgal cells which causes production of H^+, particularly under unbuffered mediums used in the present study.

The uptake of ammonium and phosphate in each of the cultures is shown in **Fig. 4.4B and C**. Data showed an initial rapid uptake in all the sea water cultures lasted for 60 h for both ammonium and phosphate. Subsequent to afore stated process, a gradual decline in the uptake of ammonium was recorded for all the cultures up to 72 h, and then by 84 h the ammonium was depleted beyond the limit of detection from all the sea water cultures. However, phosphate concentrations dropped to a non-zero minimum (ranging from 0.054 mM to 0.027 mM) after 60 h, and remained constant for up to 120 h in all the sea water cultures. NaCl cultures showed reduced ammonium and phosphate uptake as compared to sea water cultures which reflects the reduced growth of those cultures. Similar to sea water cultures, a rapid decline in ammonium content was recorded in all the NaCl cultures till 60 h, after which the uptake reached a minimum (1.3-0.9 mM), at which point growth had ceased. On the other hand, the phosphate uptake was observed only till 48 h, after which no significant change in the phosphate concentration was recorded in the growth media (**Fig. 4.4C**). Moreover, faster uptake at the beginning of the culture period (60 h) corresponded to the accumulation of nitrogen and phosphorous after the microalgae cell density reached a maximum level, the nutrient uptake from the media (72 -120 h) slowed down as shown in **Fig. 4.4B and C**.
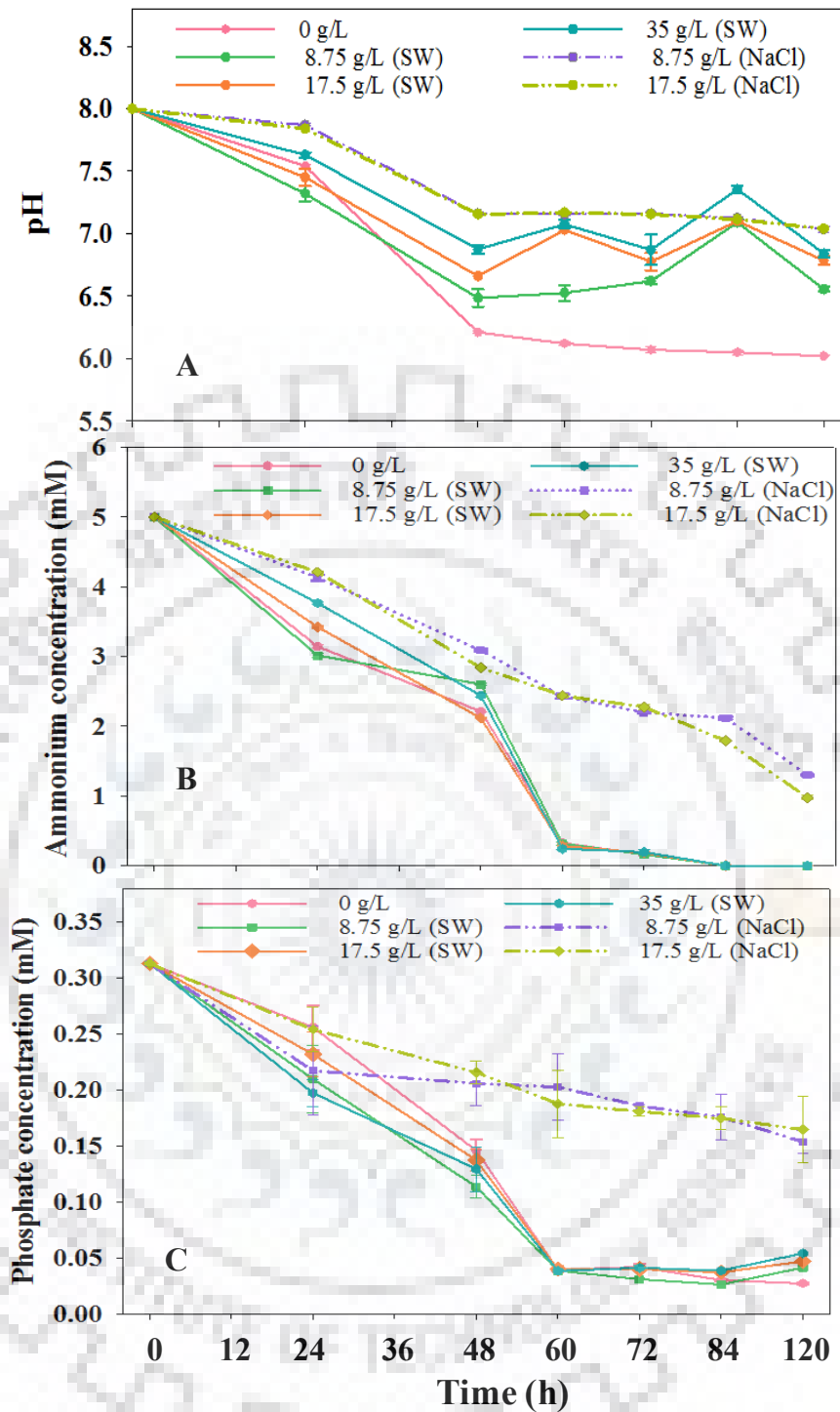
Fig. 4.4: *Temporal changes in (A) pH (B) Total ammonium concentration (C) Total phosphate concentration in the culture media of Scendesmus sp. IITRIND2 grown in media supplemented with sea water and NaCl. Error bars indicate standard deviation for four biological replicates (* p <0.05, ** p < 0.01, *** p <0.001).*

4.3.4 Effect of salinity on carbohydrate composition of the microalga

The analysis of carbohydrate profiles can provide insights into the adaptation of the microalga to high salinity environments. To this end, the time course profile of carbohydrate accumulation for all culture media is illustrated in **Fig. 4.5**. The carbohydrate concentration examined in different seawater salinity media (0-35 g/L) reached maximum values of 67.11 ± 0.24 %, 62. 59 ± 0.35 %, 69.33 ± 0.34 % and 51.9 ± 5.99 % between 60-72 h in the seawater and no salt cultures respectively (**Fig. 4.5**). However, after 72 h, the carbohydrate content decreased by a factor of ~ 1 to 1.5 in all the sea water cultures with a concomitant increase in the FAME content in the cells. On the other hand, in case of NaCl supplemented cultures, maximum carbohydrate (49.71 % and 36.86 %) was attained within 72 h in 8.75 g/L and 17.5 g/L salinity respectively (**Fig. 4.5**).
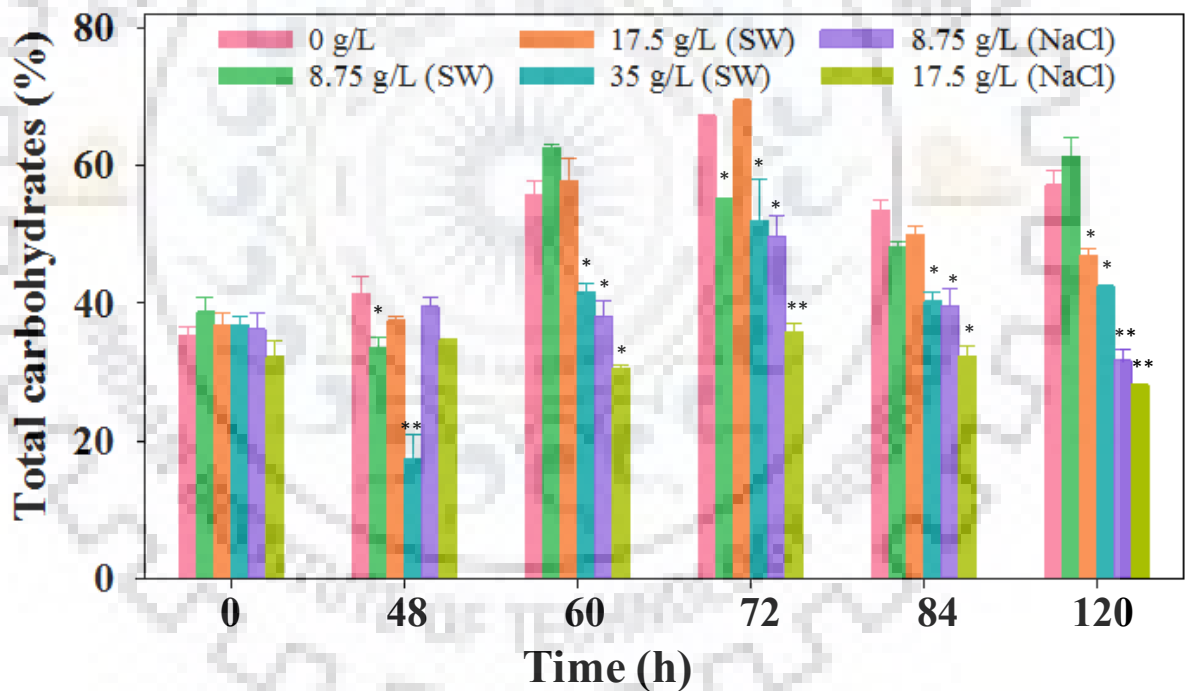
Fig. 4.5: *Changes in the total carbohydrates of Scenedesmus sp. IITRIND2 grown in sea water and exclusive NaCl. Error bars indicate standard deviation for four biological replicates (* p <0.05, ** p< 0.01, *** p<0.001).*

Interestingly, with increase in the salinity of the media, the carbohydrate constituents showed more variation compared to the control, the change in glucose (~ 150 – 600 mg/g AFDW) was most pronounced, followed by mannose (~ 22- 100 mg/g AFDW) and galactose

(~ 5 – 15 mg/g AFDW). In addition, for 8.75 g/L, 17.5 g/L and 35 g/L, small amounts of fucose (~ 0.12 – 5 mg/g AFDW) and ribose (0.3 – 10 mg/g AFDW) were detected **(Fig. 4.6)**. The primary response of glucose accumulation, and the observation that other monosaccharides do not exhibit a similar response profile, indicates the synthesis of a storage glucan as the initial rapid physiological response to salt stress. On a general trend, irrespective of the salinity, the level of galactose decreased with time (48 – 120 h), while the mannose content of the microalga increased with cultivation time up to 84 h and then showed slight decline at 120 h time point **(Fig. 4.6)**. On the other hand, glucose followed a bell shape curve, characterized by maxima between 60 - 72 h and then starts decreasing beyond the specified time intervals. This is consistent with the distinct maximum of storage carbohydrate accumulation in other species, such as *C. vulgaris* and *Scenedesmus acutus*, while the rest of the sugars (fucose and ribose) showed no particular trend [241]. Further, with the presence of high levels of fermentable sugars (glucose and mannose) the microalga can be explored for potential bioethanol (or other fermentation pathway) production, which can be easily metabolized by yeasts such as *Saccharomyces cerevisiae* [242] .
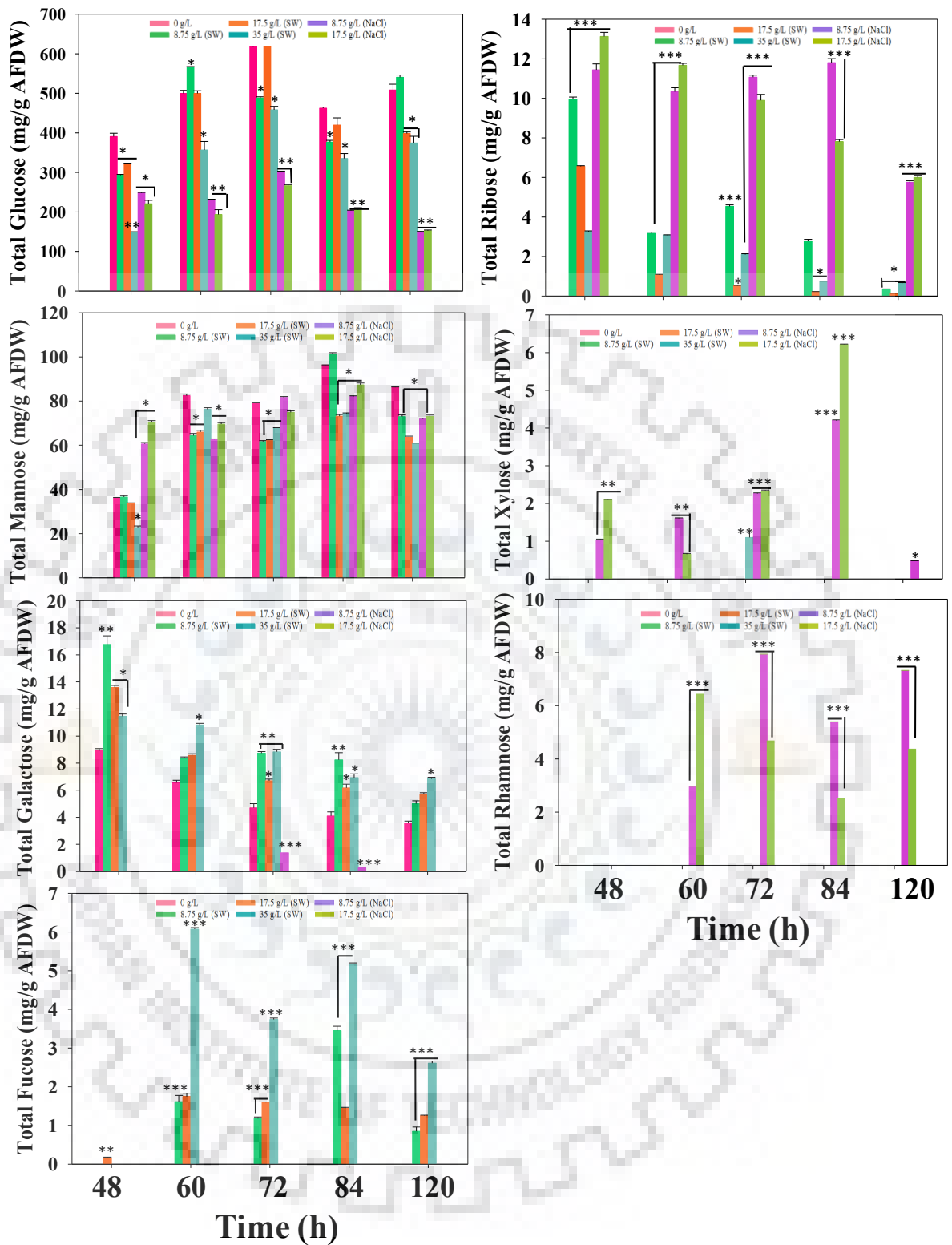
Fig. 4.6: *Changes in the neutral sugar composition of Scenedesmus sp. IITRIND2 grown in sea water and exclusive NaCl medium. Error bars indicate standard deviation for four biological replicates (* p <0.05, ** p< 0.01, *** p<0.001).*

4.3.5 Effect of salinity on FAME composition of the microalga

Exposing microalgae to different salinity environments typically leads to increase in accumulation of neutral lipids (TAGs) that aids in the cell's survival. Thus, we quantified changes in both the content and the composition of FAMEs in response to different salinity levels **(Fig. 4.7)**. Data revealed that FAME content increases with cultivation time in all the sea water supplemented cultures, attaining maximum of 34.38 ± 1.20 % in 17.5 g/L followed by 35 > 0 > 8.75 at 84 h time point, after which the FAMEs content slightly reduced **(Fig. 4.7)**.
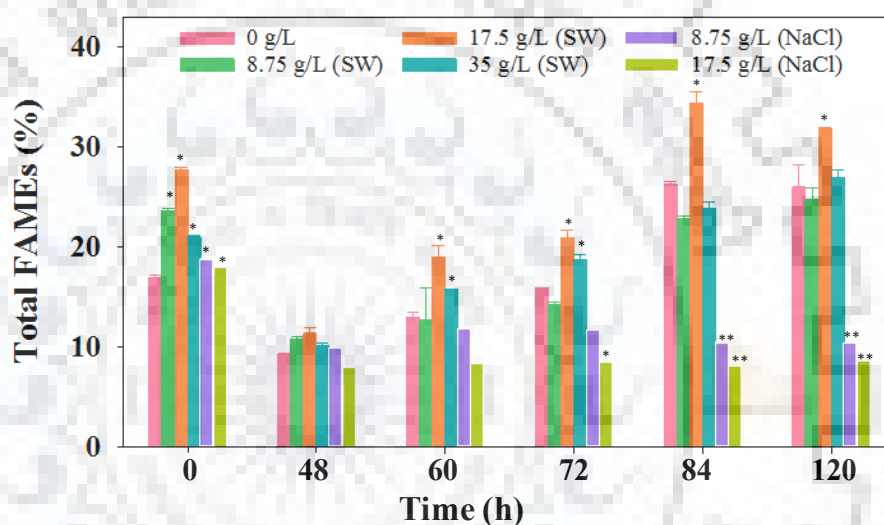
Fig. 4.7: *Relative changes in total FAME of Scendesmus sp. IITRIND2 grown in sea water and exclusive NaCl supplemented medium. Error bars are standard deviation for four biological replicates.*

On the other hand, the NaCl supplemented cultures showed a low FAME content (~8-10 %) in both 8.75 and 17.5 g/L salinity. The major fatty acids in the microalga irrespective of the salinity comprised of C16:0 (~ 25 %), C18:1n9 (~ 35 %), C18:2n6 (~10 %) and C18:3n3 (~15 %) indicating its great potential to be converted into biodiesel as depicted in **Table 4.4 and 4.5**. Furthermore, the content of SFAs and MUFAs increased with cultivation time while the PUFAs amount decreased with time (48-120 h) in all the sea water salinity cultures **(Table 4.6)**. However, for the NaCl cultures, no significant changes in the SFA, MUFA or PUFA content were observed **(Table 4.6)**.

FAME (%)	Sea salt concentration (g/L)																			
	0					8.75					17.5					35				
	48h	60h	72h	84h	120h	48h	60h	72h	84h	120h	48h	60h	72h	84h	120h	48h	60h	72h	84h	120h
C12:0	0	0	0	0.005	0.008	0.04	0	0.036	0.051	0.040	0.04	0.05	0.06	0.03	0.04	0.14	0.06	0.06	0.06	0.04
C14:0	0.28	0.24	0.18	0.18	0.17	0.45	0.39	0.429	0.328	0.231	0.40	0.32	0.26	0.21	0.21	0.44	0.36	0.30	0.28	0.25
C16:0	23.98	24.24	24.12	24.82	25.06	22.05	23.44	22.42	20.98	22.69	22.12	25.98	23.86	25.10	23.74	20.96	23.76	23.76	25.19	24.83
C16:1n9	0.58	1.16	1.09	1.22	1.15	0.58	1.42	1.81	2.03	1.41	0.60	1.08	1.04	1.21	1.25	1.19	1.96	1.37	1.50	1.66
C16 unknown1	1.28	0.41	0.22	0.10	0.11	1.98	0.75	0.70	0.27	0.20	1.70	0.42	0.34	0.19	0.23	1.26	0.38	0.37	0.21	0.27
C16:2	1.74	3.50	4.11	5.60	5.80	1.43	2.36	2.43	3.49	5.28	1.62	3.16	3.77	4.52	4.44	2.66	3.84	4.56	4.86	4.58
C16:3	4.45	4.11	3.96	3.19	3.15	3.32	4.55	4.72	5.35	4.28	4.38	3.66	4.20	3.59	4.43	3.85	3.49	4.04	2.97	3.85
C16:4	6.76	3.09	1.67	0.90	0.74	9.07	4.82	4.32	2.63	1.21	8.03	2.72	1.61	1.09	1.11	6.37	3.34	1.90	1.19	1.25
C18	1.82	2.29	4.01	4.82	4.89	1.27	1.89	1.68	1.66	3.33	1.48	3.32	4.12	5.32	5.87	1.93	2.60	3.23	4.63	3.56
C18:1n9	16.96	25.38	29.57	31.01	31.05	12.94	23.77	27.09	31.16	31.93	14.33	26.32	30.99	31.01	30.11	18.77	24.48	28.65	30.93	30.86
C18:2n6	8.81	10.68	10.80	10.99	11.00	8.04	8.00	6.77	8.09	9.62	7.85	10.47	9.79	10.62	10.08	9.83	11.18	9.75	11.10	10.38
C18:3n3	30.45	21.33	17.10	14.46	14.12	34.50	24.53	23.45	20.09	15.93	33.30	18.41	15.96	13.72	15.04	28.84	20.82	18.28	13.46	14.93
C18:4n3	1.76	1.89	1.18	0.77	0.66	2.28	2.30	1.76	1.28	0.93	2.26	1.68	1.24	0.90	0.82	1.28	1.37	1.16	0.82	0.91
C20:0	0	0	0.39	0.50	0.55	0	0	0	0	0.44	0	0.39	0.46	0.57	0.61	0	0	0.19	0.51	0.40
C20:1	0	0.51	0.73	0.65	0.75	0	0	0.27	0.62	1.06	0	0.59	0.75	0.64	0.69	0	0.54	0.61	0.57	0.57
C22:0	0	0	0	0	0	0	0	0	0.14	0.30	0	0	0.30	0.32	0.33	0	0	0.17	0.35	0.32

Table 4.2: *FAME composition of Scenedesmus sp. IITRIND2 grown in sea water.*

FAME (%)	NaCl concentration (g/L)														
	0					8.75					17.5				
	48h	60h	72h	84h	120h	48h	60h	72h	84h	120h	48h	60h	72h	84h	120h
C14:0	0.28	0.24	0.18	0.18	0.17	0.49	0.49	0.51	0.57	0.58	0.487314	0.49	0.48	0.52	0.50
C16:0	23.98	24.24	24.12	24.82	25.06	19.21	20.60	20.26	18.96	18.29	19.51	18.40	18.68	16.97	16.15
C16:1n9	0.58	1.16	1.09	1.22	1.15	1.50	1.80	1.74	1.73	1.75	1.16	1.33	1.39	1.38	1.43
C16 unknown1	1.28	0.41	0.22	0.10	0.11	1.96	1.54	1.74	1.74	1.61	1.51	1.40	1.49	1.50	1.43
C16:2	1.74	3.50	4.11	5.60	5.80	2.82	3.19	2.94	2.86	2.74	2.92	3.23	3.53	3.29	3.27
C16:3	4.45	4.11	3.96	3.19	3.15	4.18	3.87	3.87	3.79	3.81	3.80	3.86	3.98	3.95	4.06
C16:4	6.76	3.09	1.67	0.90	0.74	6.31	5.55	5.66	6.00	5.68	6.59	5.74	5.32	5.11	4.51
C18	1.82	2.29	4.01	4.82	4.89	1.20	1.40	1.33	1.24	1.25	1.33	1.28	1.26	1.20	1.13
C18:1n9	16.96	25.38	29.57	31.01	31.05	18.79	18.67	18.18	16.87	16.43	16.87	17.02	17.49	17.33	17.89
C18:1n7	0	0.52	0.42	0.41	0.43	0.60	0.59	0.55	0.60	0.59	0.69	0.83	0.90	1.04	1.25
C18:2n6	8.81	10.68	10.80	10.99	11.00	10.63	11.92	11.54	11.83	12.29	10.97	12.50	12.82	13.03	13.58
C18:3n3	30.45	21.33	17.10	14.46	14.12	28.78	26.79	27.37	29.31	30.28	30.35	30.06	29.30	30.36	30.62
C18:4n3	1.76	1.89	1.18	0.77	0.66	1.77	1.66	1.60	1.75	1.78	1.83	1.60	1.49	1.40	1.23
C20:0	0	0	0.39	0.50	0.55	0	0	0	0	0	0	0	0	0	0
C20:1	0	0.51	0.73	0.65	0.75	0	0	0.43	0	0	0	0	0	0	0
C22:0	0	0	0	0	0	0	0	0.39	0.49	0.57	0	0	0	0.68	0.69

Table 4.3: *FAME composition of Scenedesmus sp. IITRIND2 grown in exclusive NaCl supplemented media.*

Salinity (g/L)	FAME (%)														
	Sea water medium														
	SFA					MUFA					PUFA				
	48h	60 h	72h	84h	120h	48h	60 h	72h	84h	120h	48h	60 h	72h	84h	120h
0	26.08 ±0.03	27.77 ±0.05	28.70 ±0.03	30.32 ±0.04	30.67 ±0.01	17.55 ±0.12	27.05 ±0.08	31.40 ±0.18	32.88 ±0.04	32.95 ±0.19	53.97 ±0.04	44.61 ±0.12	38.82 ±0.01	35.91 ±0.39	35.47 ±0.05
8.75	23.78 ±0.05	25.71 ±0.01	24.53 ±0.04	23.11 ±0.02	26.99 ±0.05	13.52 ±0.01	25.19 ±0.03	29.17 ±0.15	33.81 ±0.13	34.40 ±0.07	58.64 ±0.03	46.56 ±0.01	43.46 ±0.02	40.93 ±0.04	37.25 ±0.02
17.5	24.01 ± 0.02	30.01 ±0.04	28.99 ±0.01	31.53 ±0.12	30.77 ±0.09	14.93 ±0.18	27.99 ±0.04	32.78 ±0.27	32.85 ±0.24	32.05 ±0.13	57.44 ±0.06	40.09 ±0.06	36.58 ±0.06	34.43 ±0.22	35.9 3±0.04
35	23.32 ±0.04	26.72 ±0.04	27.64 ±0.02	30.96 ±0.05	29.36 ±0.07	19.95 ±0.08	26.98 ±0.13	30.63 ±0.06	33.01 ±0.05	33.09 ±0.17	52.83 ±0.07	44.05 ±0.02	39.67 ±0.12	34.41 ±0.02	35.91 ±0.09
	NaCl medium														
	SFA					MUFA					PUFA				
	48h	60 h	72h	84h	120h	48h	60 h	72h	84h	120h	48h	60 h	72h	84h	120h
8.75	20.90 ±0.02	22.48 ±0.01	22.49 ±0.12	21.26 ±0.08	20.70 ±0.03	20.28 ±0.18	22.06 ±0.02	20.47 ±0.01	18.59 ±0.01	8.19 ±0.04	54.50 ±0.02	52.97 ±0.01	52.99 ±0.02	55.54 ±0.02	56.59 ±0.02
17.5	21.33 ±0.01	20.18 ±0.02	20.42 ±0.01	19.37 ±0.01	18.47 ±0.02	8.72 ±0.02	19.18 ±0.02	19.77 ±0.02	19.75 ±0.02	20.58 ±0.02	56.46 ±0.03	56.99 ±0.03	56.43 ±0.04	57.14 ±0.04	57.27 ±0.05

Table 4.4: *Temporal changes in SFA, MUFA and PUFA in response to salinity.*

The FAME content increased after the ammonium depletion (72 h) along with a decrease in carbohydrates content in the microalga **(Fig. 4.7)**. These results suggest that the major driving force for FAME content accumulation in this microalga was nutrient depletion, which has been extensively reported for various microalgae [252]. Furthermore, the decrease in carbohydrates during the time period of 72 - 84h after initial increase indicated that the immediate response to salinity stress in the microalga was accumulation of carbohydrates (primarily a storage glucan), which later on converted to FAMEs. These results were in line with the study carried out by Laurens et al. which suggested degradation of starch or other storage polysaccharides providing metabolites for fatty acid synthesis in *Scenedesmus* sp. [241].

4.4 Discussion

In recent years, the fresh water scarcity has increased from 69 % to 77 % along with tripling of the water withdrawals [253]. Therefore, utilization of fresh water for cultivating microalgae for biofuel production is unlikely without causing sustainability crises at the large farm deployment envisioned; urging the use of saline waters for large scale deployment. This necessitates the understanding of halotolerance molecular mechanisms in microalgae for the development of genetic engineered halotolerant strains. Salinity stress generates ROS such as H_2O_2, superoxide (O_2^-) and hydroxyl (OH^-) that cause oxidative damage to the cells. However, in order to deploy this strain for large scale cultivation in open raceway ponds, examining this strain under appropriate environmental conditions for monitoring alleviations in carbohydrate and lipid profiles that alter the cell composition and in turn permeability is crucial to understand detailed mechanism of the adaptation in saline environments. Further, the biorefinery concept integrating multiple products has become one of the crucial aspects to produce sustainable and economically viable algal biofuels.

Hence, the microalgal strain; *Scenedesmus* sp. IITRIND2 was cultivated in seawater using a customized photobioreactor to evaluate its potential for integrated bioethanol and biodiesel production. The microalga adapted efficiently to 100 % sea water salinity but when cultivated under exclusive NaCl (35 g/L), the microalga did not survive. Such cell toxicity can be attributed to the high Na^+ ions which alters the K^+ selective ion channels on the algal cell's surface reducing the uptake of essential nutrients including phosphorous, iron and zinc thereby inhibiting the growth [254]. Further, a high Na^+/K^+ ratio disrupts various enzymatic processes in microalgae as K^+ is actively involved in protein synthesis. By consuming the inorganic salts

microalgae regulates its biochemical composition for adaptation and more precisely for modulation of its cell components. The major players that aid the microalgae to adjust to such high levels of salts are carbohydrates and lipids. The carbohydrates accumulated in the microalga serve as major organic osmotic solutes comprised of simple sugars (fructose, glucose, mannose), sugar alcohols (glycerol and methylated inositols) and complex sugars (trehalose, raffinose and fructans) [254]. In the present study, we examined the temporal profile of monomeric sugars, solubilized after acid hydrolysis of polysaccharides in the biomass. The microalga showed increased carbohydrate accumulation in all the sea water cultures and control (no salt). These accumulated carbohydrates and especially simple sugars such as glucose can be used for bioethanol production. Further, these sugars mitigate these effects by metabolism and protection of both ROS producing and ROS scavenging pathways including mitochondrial respiration, photosynthesis and oxidative pentose phosphate pathway [255]. Such high accumulation of carbohydrates in response to salinity stress have been reported in various microalgae including *Chlamydomonas* sp., *Chlorella emersonii*, *Dunaliella* sp., *Desmodesmus armatus*, *Mesotaenium* sp., *Scenedesmus quadricauda* and *Tetraedron* sp. [256,257]. The principal sugar was glucose irrespective of the culture medium, followed by mannose and galactose. Presence of glucose in all the cultures indicated synthesis of glucose polysaccharides like starch by the microalga, while mannose could have been synthesized to form structural mannans (or gluco-mannans) in the cell wall or associated with glycoproteins in the cell matrix [258,259]. The occurrence of galactose could have been derived from galactolipids such as MGDG and digalactosyldiacylglycerol (DGDG) present in the chloroplastic membranes or from β(1-6) galactans present in the cell wall glycoproteins [258–260]. Interestingly, presence of trace amounts of fucose and ribose in all the sea water medium and detection of rhamnose and xylose exclusively in NaCl cultures suggested re-modulation of microalgal cell wall or membrane composition in response to salinity as well difference between the two (**Fig. 4.3B**). Since the cell membrane is a semipermeable barrier between cytoplasm and external medium it undergoes adaptive changes in the face of altered salinity particularly in terms of carbohydrates/lipids. It has been reported that fucose is present primarily as sulfated polysaccharides such as fucoidan and carrageenan in various marine green, red and brown algae. These complex polysaccharides play a vital role in maintaining selective cationic transfer in saline media thereby maintaining low Na^+ concentration in the cytoplasm [261]. The presence of rhamnose and xylose in trace amounts has also been observed in marine microalgae such as *D. tertiolecta* and *Nannochloris atomus* [262]. Thus, the hierarchy of the sugar profile indicates that rhamnose and xylose may be synthesized under extreme stress conditions which could be a survival strategy of microalga. Another counterpart

apart from sugar is lipid, which can help microalgae to acclimate to high saline conditions [164,165]. However, no significant change was observed in the FAME profile (reflecting overall lipid composition) with respect to changes in the salinity (sea water or NaCl), indicating that this microalga primarily modulates its carbohydrate response as opposed to lipid molecular rearrangements in its initial stress response. Further, we observed an underlying lipid quantitative response that can be attributed to the initial phase of nutrient stress (72-120 h), the cultures experienced.

4.5 Concluding remarks

The present investigation sheds light on an aspect of adaptive mechanism of a halotolerant microalgae cultivated in sea water with fluctuating light and temperature conditions. The obtained results indicate significant changes in the carbohydrates which can be attributed to the plasticity and survival mechanism of the microalgal cells under high saline conditions. Further, the data provides a proof-of-concept for utilizing sea water instead of exclusive NaCl as the latter was found to toxic to algal cells. These observations can serve as a starting material for cultivating halotolerant strains in outdoor systems utilizing sea water or brackish water obtained from coastal regions.

Delineating the differential metabolic responses of Scenedesmus sp. during arsenic (III, V) mitigation

5.1 Introduction

Environmental metabolomics is an effective tool for analysing the changes in complex biochemical mechanisms/pathways against the stress generating agents such as toxic chemicals, heavy metals, extreme pH/temperature conditions [263,264]. Although couple of research groups have attempted to unravel the metal induced proteomics changes on algal species, [265,266] comprehensive metabolic studies delineating the metal induced stress response in oleaginous and hyper-tolerant microalgae is still infancy.

In the investigation, a novel hybrid approach of arsenic (As) removal coupled with biodiesel production potential using *Scenedesmus* sp. IITRIND2 cultivated in synthetic soft water (SSW) was carried out. The tolerance of the microalga towards As (III) and As (V) stress was compared to a control strain *Scenedesmus abundans*. NMR based metabolomics approach coupled with various biophysical techniques were used to unravel the differential metabolic profiles of a novel fresh water microalga (*Scenedesmus* sp. IITRIND2), when cultivated in the presence of As (III) and As (V). Between the two microalgal species tested, *Scenedesmus* sp. IITRIND2 was able to tolerate half-a-gram of both the forms of As (III) and As (V) with a high metal bioaccumulation factor (BAF) and can be categorized as hyperaccumulator of arsenic. Variations in cell size, biochemical composition (proteins, lipids and carbohydrates) and photosynthetic pigments indicated reduction in all the components while an apparent increase in the lipid content on exposure to arsenic. Higher lipid productivity was obtained in As stressed microalgal cells along with the fatty acid profile and biodiesel properties complying with vehicular quality biodiesel. The results showed the metabolic responses it exhibited to cope with the stress mechanism were significantly different between As (III) and As (V), and are more pronounced with As (V). These results unveiled differential metabolomic changes that are characteristic of hyper-tolerance, mitigation and alteration of hosts signalling pathways upon uptake of As (III) and As (V).

5.2 Materials and Methods

5.2.1 Microalgae cultivation

Scenedesmus species IITRIND2 and the control species was *Scendesmus abundans* (NCIM 2897) maintained in modified Bold's Basal medium (BBM) as described in Chapter 2, section 2.2.2. To perform the experiments both the microalgal strains were adapted and cultivated in SSW. SSW had the following composition (g L^{-1}): $NaNO_3$ (0.25); KH_2PO_4 (0.25); $MgCl_2 . 6H_2O$ (12.16); $CaCl_2.6H_2O$ (17.5); $Ca(NO_3)_2.4H_2O$ (3.54); $CaCO_3$ (0.093); Na_2SO_4 (16.33); $KHCO_3$ (2.5); $NaHCO_3$ (1.678) [267]. Arsenic stock solutions (10 g L^{-1}) were prepared by dissolving salts of $NaAsO_2$ (As-III) and $Na_2HAsO_4.7H_2O$ (As-V) in sterilized distilled water.

5.2.2 Experimental Design

Arsenic tolerance was estimated by cultivating both the microalgae separately in SSW with different As (III) and As (V) concentrations ranging from 10-1000 mg/L. The inoculum was prepared by cultivating the microalgal strains in 250 mL Erlenmeyer flasks containing 75 mL of culture for 96 h (log phase) in SSW at 27 °C, with a photoperiod of 16: 8 h light- dark cycle irradiated with 6 white fluorescent lights (300 μmol m^{-2} s^{-1}) was centrifuged at 6000 x g for 10 min. The cell pellet (1 X 10^5 cells/ml) was washed thrice with autoclaved distilled water and then re-suspended for inoculation. All the experiments were performed in triplicates and the sample analysis apart from the arsenic removal DCW were calculated on the 10th day. Statistical analysis was done using two-way ANOVA (Graph pad V7) and $p < 0.05$ was taken as significant. For the biochemical, biophysical and NMR analysis, 500 mg/L As (III) and As (V) concentrations have been taken for evaluating the respective characteristics of the microalga.

5.2.3 Arsenic speciation analysis

The visual MINTEQ computer program was used for analysing As (III) and As (V) speciation. As pH controls the oxidation states of arsenic speciation, a range of 7 to 8.8 pH was taken to evaluate their distribution as the experimentally observed pH values for the culture media were in the range of 7.2-8.2 (https://vminteq.lwr.kth.se).

5.3.4 Estimation of arsenic toxicity and tolerance by microalgal species

The toxicity of As (III) and As (V) to both the microalgal strains was determined using a 96 h growth inhibition bioassay [83]. After 96 h, the growth of algal cells was measured by counting cell number using Neubauer chamber. The 50 % inhibitory concentration (IC_{50}) was then calculated using a non-linear regression equation [83]. The microalgal biomass was harvested after every 48 h and the cell pellet was vacuum dried at 80 ºC for 2 h. The dried biomass obtained was then gravimetrically weighed and dry cell weight (DCW) was calculated.

ICP-MS was used to estimate the amount of arsenic (III, V) left in the SSW after 10 days of algal growth. The concentration of arsenic was calculated by plotting a standard curve from different concentrations (0, 10, 20, 50, 100, 250, 500 mg/L) of As (III) and As (V) using a mixture of Rh, Ge, Ir (100 mg/L) as internal standard. The metal uptake capacity was evaluated using the following equation:

$$\text{Metak uptake capacity (\%)} = \frac{\text{Initial metal conc. in medium} - \text{Final metal conc. in medium}}{\text{Intial metal conc. in the medium}} * 100$$

$$\text{Metal removal} \left(\frac{\mu g}{g}\right) = \frac{(\text{Initial metal conc. in medium} - \text{Final metal conc. in medium})}{\text{DCW}} * \text{Volume of sample}$$

$$\text{Bioaccumulation factor (BAF)} = \frac{\text{Arsenic conc. in the algal DCW}}{\text{Intial metal conc. in medium}}$$

5.2.5 Estimation of changes in biochemical composition of *Scenedesmus* sp. IITRIND2

The biochemical composition of untreated and treated microalgal cells was analyzed using elemental CHNS analyzer (Thermo Fisher, USA). Total carbohydrate content was calculated using phenol sulfuric method [173], total proteins by multiplying the total nitrogen concentration by 6.25 (nitrogen to protein conversion ratio) and total lipids content were estimated using modified Bligh and Dyer method [171]. The photosynthetic pigment estimation was done as described in Chapter 2, section 2.2.7.

5.2.6 Transesterification, fatty acid profile and biodiesel properties determination

Transesterification was carried out using 6 % methanolic H_2SO_4, fatty acid profile estimated using GC-MS and the biodiesel physical properties were calculated as per the protocol detailed in Chapter 2, section 2.2.6.

5.2.7 Characterization of arsenic interaction and morphological changes in *Scenedesmus* sp. IITRIND2

The adsorption of arsenic on to the microalga was analyzed by FT-IR spectroscopy (Thermo Nicolet NEXUS, Maryland, USA) at 400–4000 cm^{-1} wavenumber range and FE-SEM with EDX (FE-SEM Quanta 200 FEG) as described in Chapter 2, section 2.2.2. AFM analysis (NT-MDT-INTEGRA) was performed to visualize the changes in the surface morphology of arsenic spiked microalgal cells. Briefly, the microalgal cells (2×10^6) were fixed on poly-L-lysine coated glass slides using 2.5 % glutaraldehyde (24 h in dark at 4°C) followed by dehydration (100-10 % ethanol).

5.2.8 NMR based metabolomics and multivariate analysis

The metabolites corresponding to the control, As (III) and As (V) cultures were extracted according to protocol reported by Zhang et al. [199] with few modifications. In detail, 40 mg of lyophilized microalgal biomass (harvested on 10th day) was grounded with liquid N_2 using 1 ml of 20 % methanol. The process was repeated twice; supernatant was pooled together and lyophilized for overnight. Lyophilized samples were reconstituted in phosphate buffer (0.1 M, pH 7.4) and the samples were re-lyophilized again for further processing. The lyophilized samples were dissolved in 550 μL of D_2O containing a chemical shift indicator (4,4-dimethyl-4-silapentane- 1- sulfonic acid (DSS), 0.5 mM). All proton NMR spectra were acquired on an 800 MHz NMR spectrometer equipped with cryoprobe. Chemical shifts in the ^{1}H NMR spectra were identified and assigned using the 800 MHz chemical shift database in Chenomx Profiler and were further confirmed by comparing it with the other databases and literature report [200,268].

For multivariate data analysis, the NMR spectra were integrated, normalized against internal standard area of DSS, and the data were reduced into spectral bins (0.03 ppm width) using Pathomx [198]. The resultant data was imported into Metaboanalyst (v3.0) software for multivariate data analysis [270]. Principal component analysis (PCA) and statistical

significance was determined by two-way analysis of variance (ANOVA) followed by post hoc Tukey's test in Metaboanalyst [270]. Additional information regarding the NMR spectral parameters, box plots and hierarchical cluster analysis as per the procedure detailed in chapter 3, section 3.2.4.

5.3 Results

5.3.1 Quantifying the arsenic removal and biochemical composition changes in arsenic (III, V) spiked *Scenedesmus sp*. IITRIND2

To investigate the maximum arsenic tolerance in *Scenedesmus sp*. IITRIND2 as compared to control species (*Scenedesmus abundans*), the green microalga strains were cultivated at different concentrations of As (III, V) ranging from 10-1000 mg/L separately **(Fig. 5.1)**.
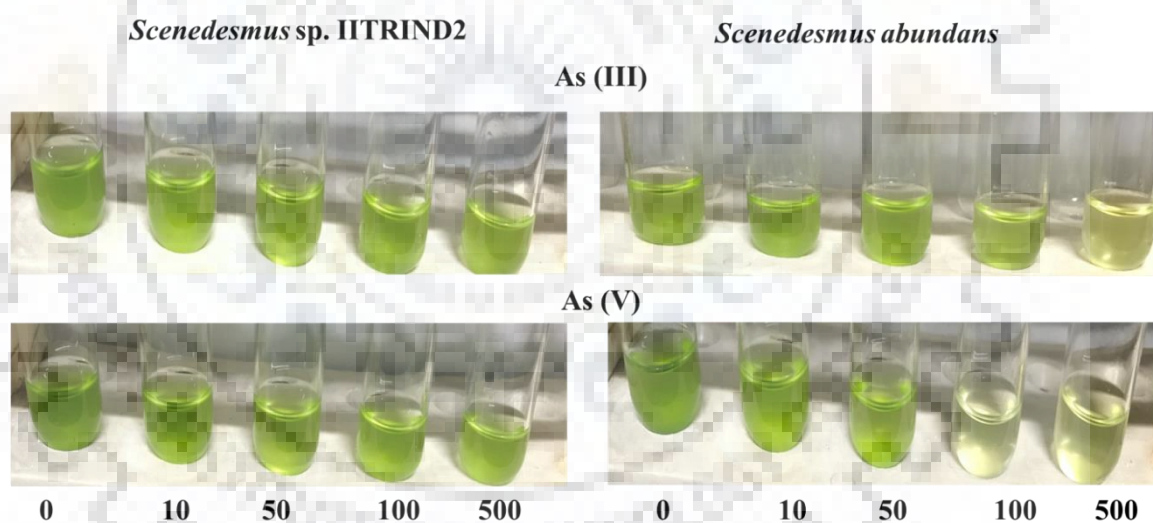
Fig. 5.1: *Scenedesmus sp. IITRIND2 and S. abundans grown in SSW supplemented with different concentrations (0-500 mg/L) of As (III) and As (V).*

Between the two strains, *Scenedesmus sp*. IITRIND2 was able to tolerate up to 500 mg/L of both As (III) and As (V) with an IC_{50} value of ~ 779 and 622 mg/L, while *S. abundans* growth gradually decreased with increase in arsenic concentration and ceased at 100 mg/L by exhibiting an IC_{50} value of 40 and 31 mg/L for As(III) and As (V) respectively **(Fig. 5.2A-B)**. The above results also indicated the higher toxicity of As (V) to As (III) in the microalga. Further, the As (III, V) uptake efficiency and bioaccumulation factor reduced ~ 10-20 % for

Scenedesmus sp. IITRIND2 upon increasing their concentration from 10-500 mg/L in the growth media **(Fig. 5.2C)**. Based on all of the above results, *Scenedesmus* sp. IITRIND2 was used to evaluate the effects of As (III, V) on its physiology, biochemical properties and metabolic activity.
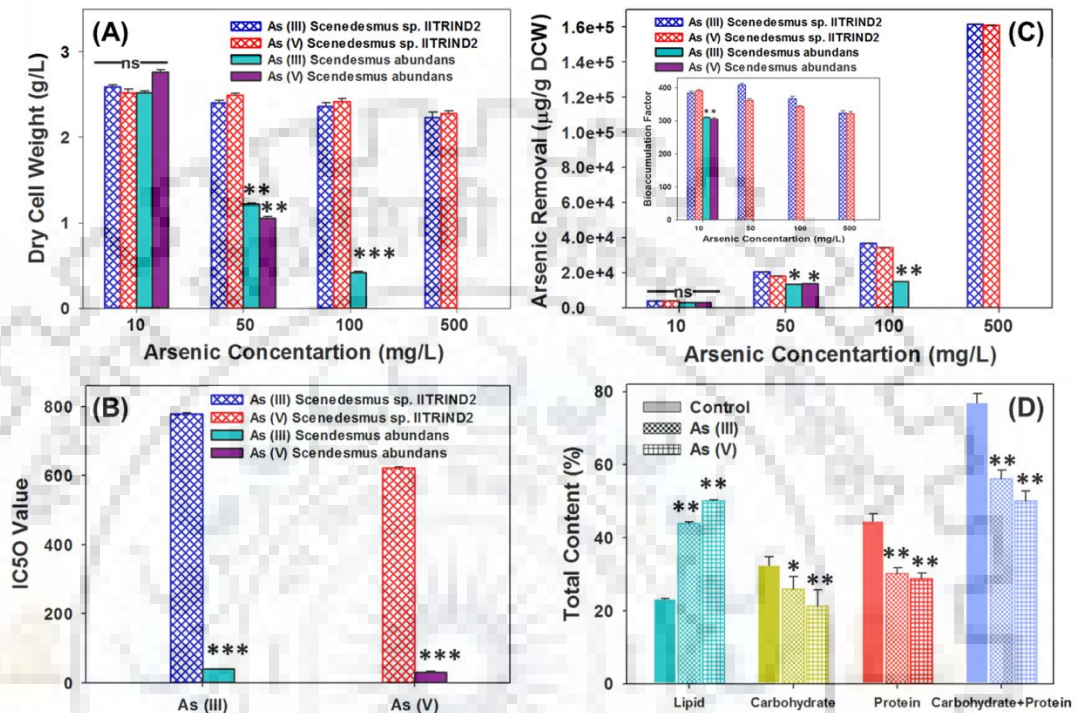
Fig 5.2: *(A) Dry cell weight (B) IC₅₀ value of Scenedesmus sp. IITRIND2 and S. abundans in the presence of 10- 500 mg/L of As (III) and As (V). (C) Arsenic removal and bioaccumulation factor (D) Changes in total lipid, carbohydrates and protein content after 10 days. (* p <0.05, ** p <0.01, *** p <0.001, ns- not significant).*

As arsenic (III, V) is a toxic heavy metalloid, its uptake by the microalga will induce stress and thus influence most of its physico-chemical, biochemical and morphological characteristics. Interestingly, cell size, specific growth rate and doubling time were almost unaffected in arsenic spiked cultures **(Fig. 5.3)**. However, As (III) spiked cultures showed ~ 15 % increase in its doubling time compared to control, which is an offshoot of its slightly lower growth rate as compared to control **(Fig. 5.3)**. Arsenic (III, V) spiked microalgal cells showed decline in protein and carbohydrate and an increase in total lipid content indicating that the alga has tolerated the arsenic induced stress conditions by altering its biochemical compositions. Further, the stress levels are higher for As (V) in comparison to As (III), when viewed as a combination of both protein and carbohydrate content against the total accumulated lipid **(Fig.**

5.3). The total protein and carbohydrate content was reduced from 72 % in control to 56 % in As (III) and 49 % in As (V) spiked species **(Fig. 5.3)**. These results also represent the higher toxicity of As (V) compared to As (III). The analysis of the photosynthetic pigments indicated approximately 1.2 fold decrease in chlorophyll a and chlorophyll b and unaltered levels of carotenoids in the arsenic spiked microalgal cultures, signifying that arsenic hampered the photosystem to a certain extent but did not cause chlorosis **(Fig. 5.3)**.
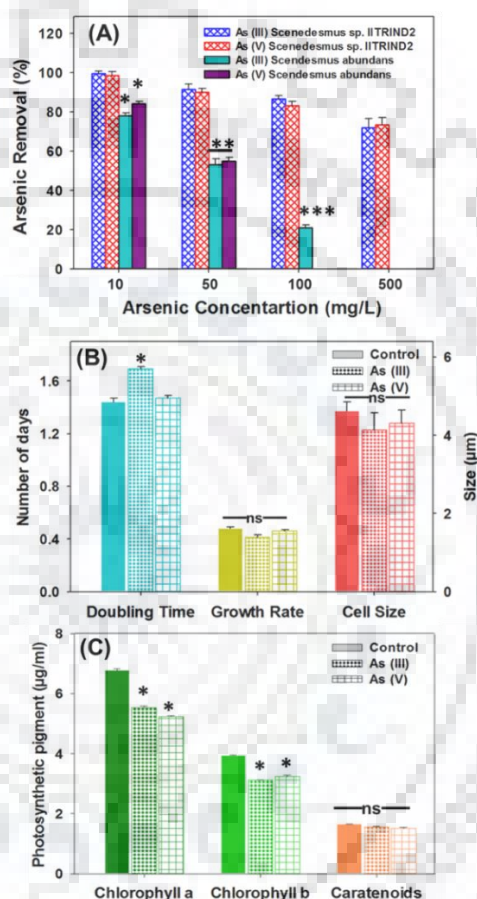
Fig. 5.3: (**A**) *Percentage removal of As (III) and As (V) by Scenedesmus sp. IITRIND2 and S. abundans cultivated in SSW at the end of tenth day. Effect of arsenic (III, V) on (**B**) Growth rate, doubling time and cell size; (**C**) Photosynthetic pigments content of Scenedesmus sp. IITRIND2 after a growth period of 10 days (* p<0.05, ** p<0.01, *** p<0.001).*

5.3.2 Arsenic speciation in water with respect to changes in pH

As ~70-73 % arsenic removal in *Scenedesmus* sp. IITRIND2 was recorded, the distribution of arsenic species with pH was studied as the nature of arsenic species strongly influences its removal profile [271]. Arsenite or As (III) can be present as H_3AsO_3 (neutral),

protonated forms ($H_4AsO_3^+$) and deprotonated forms ($H_2AsO_3^-$, $HAsO_3^{-2}$, AsO_3^{-3}) while arsenate or As (V) is present as H_3AsO_4 and deprotonated forms ($H_2AsO_4^-$, $HAsO_4^{-2}$, AsO_4^{-3}) in ground waters respectively [271]. The distribution of both As (III) and As (V) species within pH range of 7 to 8.8 as the observed pH values for the culture medium initially on the 1st day was 7.2, and the final pH of the culture medium on 10th day was around 8-8.2 respectively. According to the speciation diagram for As (III), ~99-90 % were present in H_3AsO_3 in the pH range 7 to 8.2 as As (III) has a pKa 9.2 (dissociation constant) **(Fig. 5.4A and Table 5.1)**. As (V) primarily present in its deprotonated forms $H_2AsO_4^-$ and $HAsO_4^{-2}$ in the chosen pH range 7 to 8.2. At pH 7, both these species exist almost at the same concentration. An increase of pH sharply shifts the population of $H_2AsO_4^-$ to $HAsO_4^{-2}$ (~ 53 to 95 %, pH 7.0 - 8.2) at the end of the experiment **(Fig. 5.4B and Table 5.1)**. Thus, the speciation analysis suggested that both the As (III) and As (V) exists in multiple protonated/deprotonated forms under the culturing conditions, and the inter-conversion of the As (V) species is more pronounced due its inherent pKa values.

pH	As (III)		As (V)		
	H_3AsO_3	$H_2AsO_3^-$	$HAsO_4^{-2}$	$H_2AsO_4^-$	AsO_4^{-3}
6	99.93	0.068	11.27	88.71	0
6.2	99.89	0.107	16.92	83.06	0
6.4	99.83	0.17	24.69	75.29	0
6.6	99.731	0.269	34.61	65.39	0
6.8	99.57	0.427	46.08	53.92	0
7	99.304	0.696	53.248	46.75	0
7.2	98.901	1.099	64.35	35.648	0
7.4	98.27	1.73	74.097	25.899	0
7.6	97.286	2.714	81.926	18.068	0
7.8	95.765	4.235	87.776	12.214	0.01
8	93.451	6.549	91.913	8.07	0.017
8.2	90.003	9.997	94.724	5.247	0.028
8.4	85.031	14.969	96.578	3.376	0.046
8.6	78.186	21.814	97.77	2.156	0.074
8.8	69.339	30.661	98.511	1.371	0.118

Table 5.1: *Distribution of Arsenic (III, V) species in water with respect to pH.*
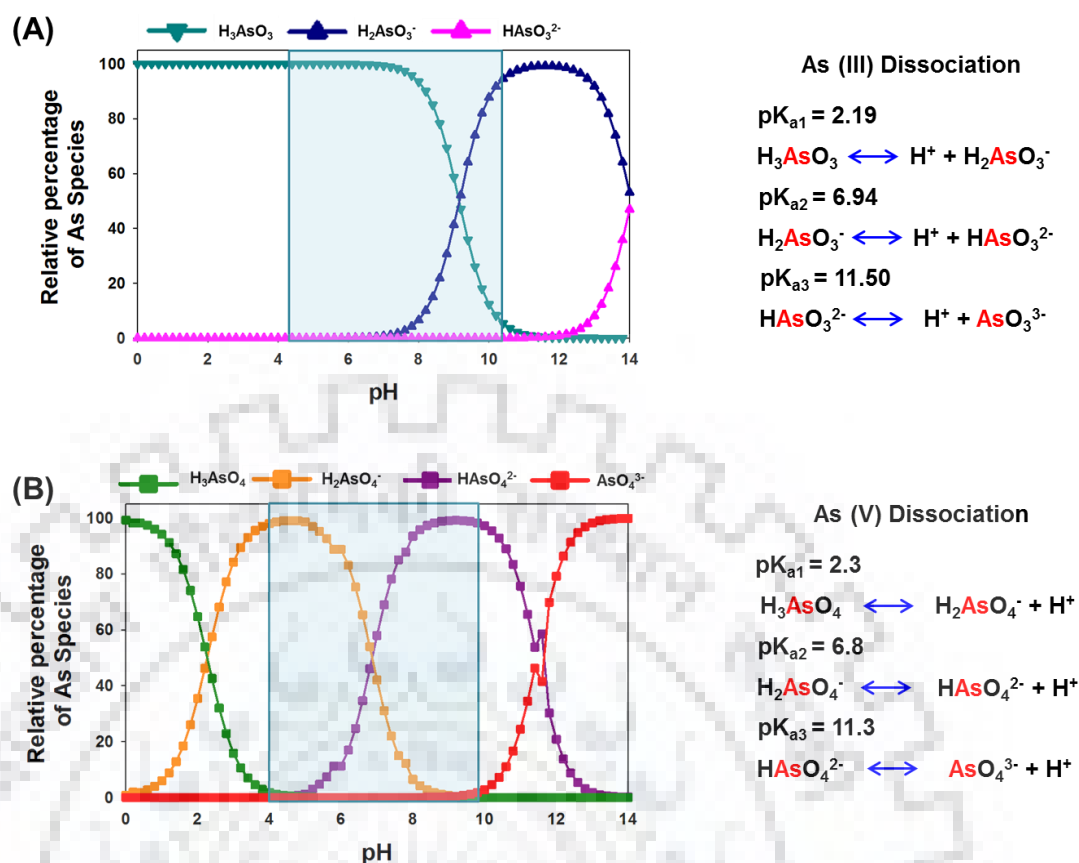
Fig. 5.4: *Arsenic speciation analysed by MINTEQ program with respect to changes in pH (A) As (III) (B) As (V).*

5.3.3 Effect of arsenic stress on fatty acid profiles and biodiesel properties

To analyse the vehicular quality of biodiesel, fatty acid profile and biodiesel physical properties were estimated. The major fatty acids present in *Scenedesmus* sp. IITRIND2 ranged from C16-C18 with palmitic acid (C16:0), stearic acid (C18:0); oleic acid (C18:1) and linoleic acid (C18:2) as major constituents **(Fig. 5.5)**. Interestingly, oleic acid was present in maximum proportions in the selected microalgal strain cultivated in arsenic accounting for approximately 55-65 % of total FAMEs. FAMEs data showed that cultivation of arsenic increased the SFA, MUFA and PUFA content in both the microalgae as compared to control. The biodiesel derived from the microalgae cultivated in As (III) and As (V) had a low cetane number with high cold flow, plugging properties, cloud point and pour point as compared to control **(Table 5.2)**. All the biodiesel properties were in compliance with the biodiesel standards (ASTM D6751-52 and EN14214) and comparable to plant oil methyl esters (JME and PME) signifying its potential

use in diesel engines **(Table 5.2)**. Further, the higher oxidative stability of the obtained biodiesel from microalgae cultivated in arsenic indicated longer shelf life.
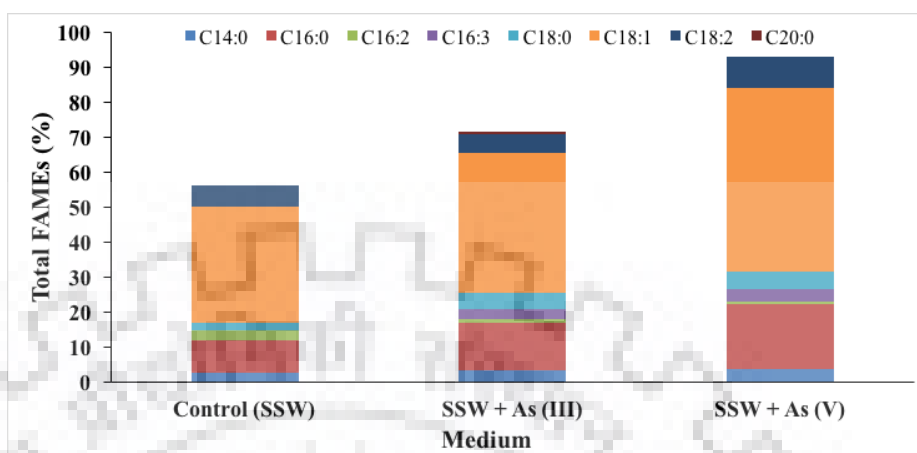
Fig. 5.5: *FAME profile Scenedesmus sp. IITRIND2.*

Physical properties	Standard fuel parameters		*Scenedesmus* sp. IITRIND2		Plant oil methyl esters	
	ASTM D6751-52	EN 14214	As (III)	As (V)	JME	PME
Saponification value (mg KOH)	-	-	174	139	96	49
Iodine value (g I$_2$/100g)	-	120 (max)	82	54	-	-
Cetane number	47 min	51 (min)	57	72	57	42
Degree of unsaturation (% wt)	-	-	95	59	-	-
Long chain saturation factor (% wt)	-	-	6	4	-	-
High heating value (MJ/kg)	-	-	41	42	-	-
Cold flow plugging property (^{0} C)	-	≤ 5/≤ -20	-5	-3	-2	13
Cloud point (^{0} C)	-3 to 12	-	2	5	4	31
Pour point (^{0} C)	-15 to16	-	-5	-2	-3	23-40
Kinematic viscosity (mm^2/s)	1.9 to 6.0	3.5 to 5.0	4.3	4	4.3	4.5
Density (g/cm^3)	-	0.86 to 0.90	0.87	0.87	0.88	0.92
Oxidative stability (h)	-	≥6	9	24	4	16

Table 5.2: *Summary of the biodiesel physical properties of Scenedesmus sp. IITRIND2 obtained in the current study.*

5.3.4 Effect of arsenic on morphology and cell surface of *Scenedesmus* sp. IITRIND2

The FE-SEM micrographs of As (III) and As (V) spiked *Scenedesmus* sp. IITRIND2 suggested that the microalgal cells maintained their ellipsoidal shape **(Fig. 5.6A-C)**. However, the surface of the cells appeared more ruptured, rough with ridged textures as compared to control cells which were smooth **(Fig. 5.6A-C)**. The resultant rigid texture of algal cell spiked with arsenic can be attributed to the adsorption of arsenic on to the cell surface, which has been confirmed by EDX spectrum **(Fig. 5.6D-F)**.

AFM imaging was also performed to visualize changes in the cell surface exposed to arsenic. As shown in **Fig. 5.6G-I**, the AFM image (3D) of cell surface of control was smooth without drops, while on treatment with arsenic (III, V), the surface of the cell became rough, irregular with frequent drops throughout. Thus AFM analysis further validated the aberrations caused by As (III) and As (V) to the surface of microalgal cells.
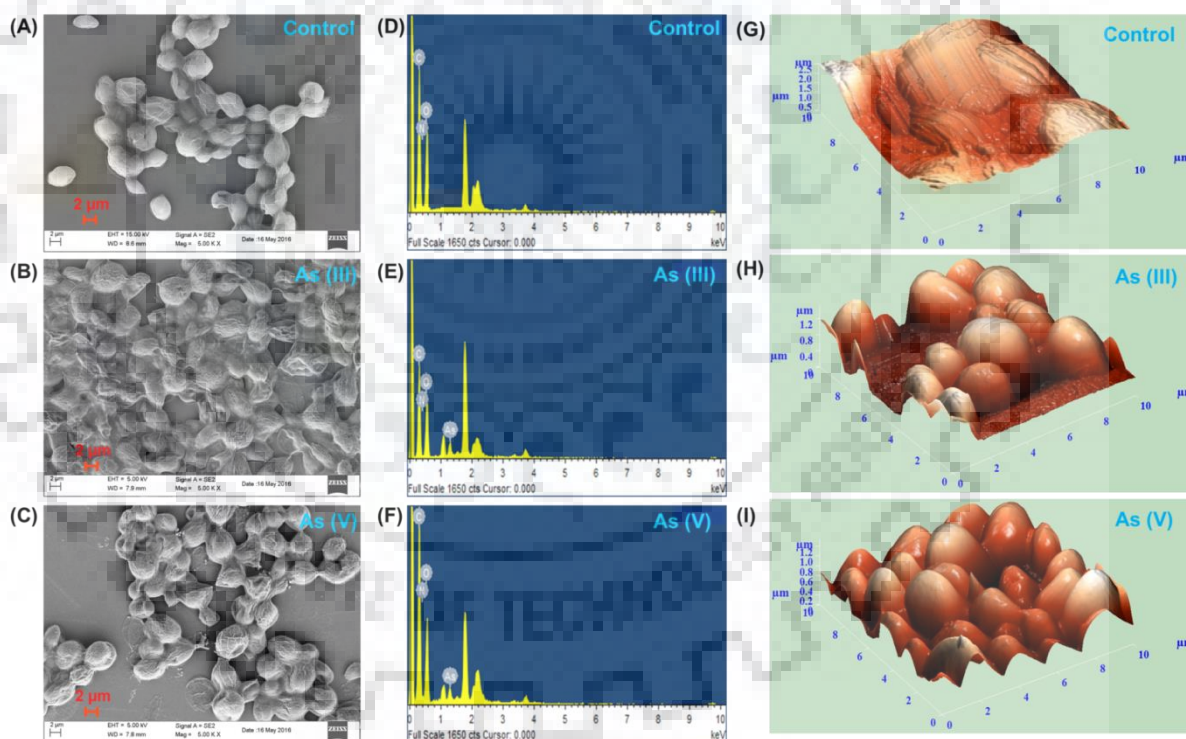
**Fig. 5.6:** *FE-SEM (A-C) EDX (D-F) analysis and (G-I) AFM of Scenedesmus sp. IITRIND2. Control - (A,D,G); As (III) - (B,E,H); and As (V) - (C,F,I). The images were collected at a concentration of 500 mg/L of As (III, V).*

5.3.5 Interaction between arsenic and microalgal cell surface

The green microalgae cell wall possesses distinct functional groups (O-, N-, S- and P-) that helps in binding of heavy metals onto its cell surface [272]. Heavy metals also bind to microalgal cell wall via phytochealtins, which aids in detoxification of heavy metal [273]. FT-IR spectroscopy was performed to identify the functional groups involved in the biosorption of arsenic onto the microalgal cell surface (**Fig. 5.7**). The FT-IR spectra of *Scenedesmus* sp. IITRIND2 unloaded and loaded with arsenic indicated shifting of various peaks. A shift in 3307 cm^{-1} in control to 3428 cm^{-1} in As (III) and 3419 cm^{-1} As (V) microalgal biomass indicated complexation of arsenic with O-H and N-H stretching of algal biomass. The presence of peaks at 2921 cm^{-1} in arsenic loaded samples designated interaction of arsenic with aliphatic C-H and aldehyde C-H stretching. The absorption peak at 1660 cm^{-1} in unloaded arsenic microalgal biomass shifted to 1641 cm^{-1} in As (III) and to 1651 cm^{-1} in As (V) loaded biomass suggesting complexation of amide group (N-H and C=O stretching) with arsenic. Shift in peak from 1058 cm^{-1} in non-spiked biomass to 1039 cm^{-1} in arsenic spiked biomass attributing to the C–N stretching vibrations of amino groups indicating interaction between nitrogen of amino group with arsenic (**Fig. 5.7**). Such a differential characteristic peak(s) shifting of hydroxyl, carboxyl and amide groups observed in As (III) and As (V) spiked microalgal biomass with respect to control indicate an distinct ion-exchange interaction between the algal surface with As (III, V) [75,76,274].
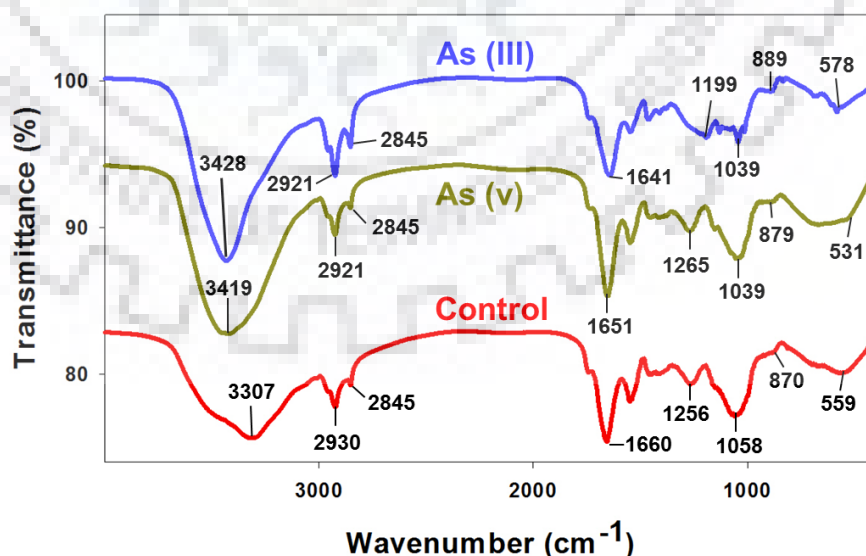

Fig 5.7: *FTIR profiles of Scenedesmus sp. IITRIND2 cultivated in the control and presence of 500 mg/L As (III) and As (V).*

5.3.6 Metabolic changes observed in *Scenedesmus* sp. IITRIND2 upon exposure of As (III) and As (V)

The biophysical and biochemical characteristics clearly indicated that As (III) and As (V) produces differential cellular responses in algal cells. In order to gain in depth insights on the variable effects of As (III) and As (V) on *Scenedesmus* sp. IITRIND2, the metabolites obtained from aqueous methanolic extract of microalgal were analyzed using proton (^{1}H) NMR spectroscopy. The cumulative ^{1}H-NMR spectra (n=6 replicates) of *Scenedesmus* sp. IITRIND2 control polar extracts stacked up with that of cultures spiked with As (III) and As (V) metal systems is shown in **Fig. 5.8A** respectively. A total of 45 metabolites were identified which composed of carbohydrates/sugar (5), amino acids (17), organic acids (7), phosphagen (2), nucleotides (2), osmolytes (3) and others (9) respectively **(Table 5.3)**. Further, the assignment of ^{1}H NMR data showed clear differences in the peaks of carbohydrates (sucrose, glucose, mannose), amino acids (leucine, alanine, valine, serine, cysteine), ATP, organic acids (fumarate, succinate, citrate, acetate) and nucleotides in control as compared to As (III) and As (V) algal extracts, and also between the two arsenic species **(Fig. 5.8A)**. To validate these variabilities across the three treatments, multivariate analysis was performed using PCA **(Fig. 5.8B)**. The PCA analysis showed statistically significant clustering of the six biological replicates and distinct differences between the control and arsenic treated algal samples, as well as between As (III) and As (V), assuring a differential metabolic profiling in all the three cases **(Fig. 5.8B)**. The PCA loadings plot revealing metabolites responsible for the discrimination pattern was provided in **Fig. 5.8C** along with the assignment of few relevant metabolites. Univariate analysis was further performed to identify the relative change in the metabolite levels. Representative box-cum-whisker plots derived from the univariate analysis are shown in **Fig. 5.9**, which clearly revealed the quantitative variations of relative signal integrals for algal metabolites in response As (III) and As (V) treatment.
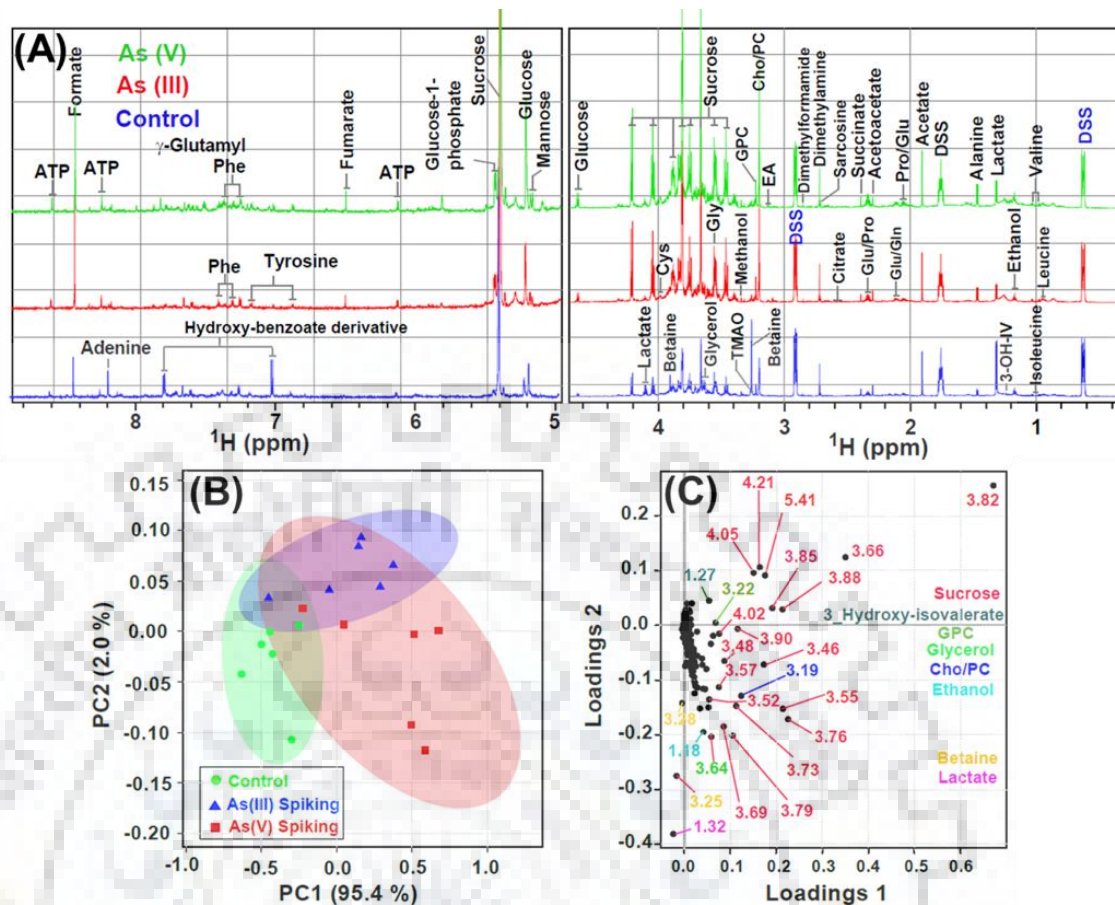
Fig. 5.8: (*A*) *The cumulative 1D ^1H NMR spectra (n=6) of Scenedesmus sp. IITRIND2 control polar extracts (**blue**) stacked up with that of cultures spiked with As (III) (**red**) and As (V) (**green**) metal systems. The spectral peaks were assigned for particular small-molecule metabolites. The water region at δ 4.6–4.9 was removed for clarity. (**B**) The combined PCA 2D score plot resulted from the analysis of 1D ^1H CPMG spectra of Scenedesmus sp. IITRIND2 exposed to different metal treatments over a period of 10 days (**green** = Control; **blue** = As (III) spiking; **red** = As (V) spiking. The semi-transparent red and blue ovals represent the 95% confidence interval. (**C**) PCA loadings plot revealing the metabolites of responsible for the discrimination pattern, the more the metabolite is away from the origin (0,0) more it contributes in the group discrimination.*

Metabolite Name	Assignment	Chemical shifts (δ) in ppm	Relative Change*	
			As (III) Spiking vs Control	As (V) Spiking vs Control
Amino acids				
Leucine	δ-CH3 δ-CH3	0.95 (d) 0.96 (d) $^\epsilon$	↑	↑↑
Isoleucine	γ-CH3 δ-CH3	0.93 (t) $^\epsilon$ 1.00 (d)	↑	↑↑
Valine	γ-CH3 γ-CH3	0.98 (d) 1.03 (d) $^\epsilon$	--	↑↑
Threonine	γ-CH$_3$	1.29 (d) $^\epsilon$	--	↑
Alanine	β-CH$_3$ α-CH	1.47 (d) $^\epsilon$ 3.79 (q)	↑	↑↑
Proline	γ-CH2 ½ β-CH2 ½ β-CH2	2.00 (m) $^\epsilon$ 2.06 (m) 2.34 (m)	↑	↑↑
Glutamate	β-CH$_2$ γ-CH$_2$	2.11 (m) $^\epsilon$ 2.34 (m)	↑	↑↑
Glutamine	β-CH$_2$ γ-CH$_2$	2.12 (m) 2.44 (m) $^\epsilon$	--	↑
N,N-Dimethylamine (DMA)	N-CH$_3$	2.71 (s)	--	↑
Sacrosine	N-CH$_3$	2.72 (s)	↑	↑↑
N,NN,-Trimethylamine (TMA)	N-CH$_3$	2.86 (s)	↑	↑
Glycine	α-CH$_2$	3.56 (s)	↑	↑↑
Cysteine	□-CH2 □-CH	3.07 (m) 3.97 (dd) $^\epsilon$	↑	↑↑
N,N-dimethylglycine	N-CH3	3.71 (s)	↑	↑↑
Tyrosine	C2H & C6H C3H & C5H	6.88 (d) $^\epsilon$ 7.18 (d)	↑↑	↑
Phenylalanine	C2H & C6H C4H C3H & C5H	7.31 (m) 7.37 (m) 7.43 (m) $^\epsilon$	↑	↑
γ -glutamyl-phenylalanine	C2H, C6H & C4H C3H & C5H	7.3 (m) $^\epsilon$ 7.4 (m)	↑	↑↑
Organic acids				
Lactate	β-CH$_3$ α-CH	1.32 (d) 4.10 (q) $^\epsilon$	↑↑	↑
Acetate	CH$_3$	1.91 (s)	--	↑
Glutarate	β, δ- CH2	2.16 (t)	--	↑
Succinate	α, β-CH$_2$	2.39 (s)	--	↑
Citrate	½ γ-CH2 ½ γ-CH2	2.52 (d) $^\epsilon$ 2.69 (d)	--	↑
Fumarate	CH	6.51 (s)	↑	↑
Formate	CH	8.44 (s)	↑↑	↑↑

Metabolite Name	Assignment	Chemical shifts (δ) in ppm	Relative Change*	
			As (III) Spiking vs Control	As (V) Spiking vs Control
Carbohydrates/sugar				
Sucrose	C10H	3.46 (t)		
	C12H	3.55 (dd)	↑	↑↑
	C13H	3.66 (s)		
	C11H	3.75 (m)		
	C17H & C19H	3.77 (m)		
	C5H & C9H	3.81 (dd)		
	C4H	4.04 (t)		
	C3H	4.21(d) $^\epsilon$		
	C7H	5.40(d)		
α-Glucose	C1H	4.63 (d)	↑	↑↑
β-Glucose	C1H	5.22 (d)	↑	↑↑
Mannose/Trehalose	C1H	5.19 (d)	↑	↑
Glucose-1-phosphate	C1H	5.55 (d,d)	↑↑	↑
Phosphagen				
Choline/PC	N–(CH$_3$)$_3$	3.20 (s)	↑	↑↑
GPC	N–(CH$_3$)$_3$	3.22 (s)	↑	↑
Osmolytes				
Glycerol	½ γ-CH2	3.63 (d) $^\epsilon$	↑	↑↑
	½ γ-CH2	3.65 (d)		
Betaine	N–(CH$_3$)$_3$	3.26(s)	↓↓	↓
	β-CH$_2$	3.91 (s)		
TMAO	N–(CH$_3$)$_3$	3.27(s) $^\epsilon$	↓↓	↓
Nucleotides				
Adenine	C2H	8.19 (s) $^\epsilon$	--	↓
	C6H	8.19 (s)		
ATP	C7H	8.61 (s) $^\epsilon$	↑↑	↑↑
	C12H	8.25 (s)		
	C2H	6.13 (d)		
Others				
Isopropanol	β-CH$_3$	1.16 (d)	--	--
Ethanol	CH3	1.17 (t)	--	↑↑
3-hydroxy-isovalerate	γ-CH3	1.24 (s)	↑	↑↑
Acetone	CH$_3$	2.22 (s)	--	↑
Aceto-acetate	δ-CH3	2.3 (s)	--	↑
N,N-Dimethyl-formamide (DMF)	N-CH$_3$	2.85 (s)	--	↑
Ethanolamine	N-CH$_2$	3.13(m)	↑	↑↑
Methanol	CH$_3$	3.34 (s)	↑	↑↑
Hydroxy-benzoate derivative	C2H & C6H	7.02 (d) $^\epsilon$	↓	↓↓
	C3H & C5H	7.79 (d,d)		

Table 5.3: *List of metabolites along with their respective chemical shifts and their respective metabolic change patterns as a consequence of uptake of Arsenic III and V. Two-way ANOVA followed by post-hoc Tukey's HSD was conducted to determine significant (p < 0.001) metabolic changes. The up (↑) and down (↓) arrows represent, respectively, increased and decreased metabolite levels. "Є" represents the metabolite peak used for evaluating the quantitative difference as represented.*
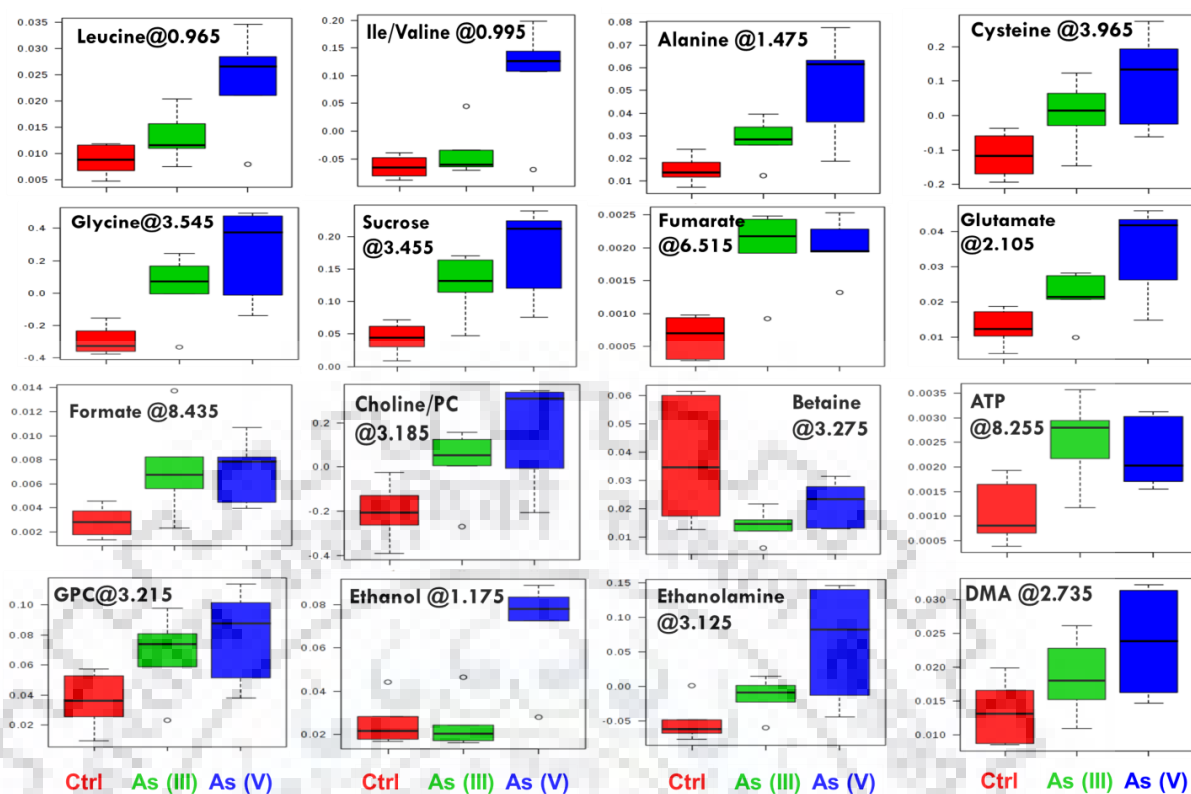
Fig. 5.9: *The box plots showing relative abundance of some of the metabolites showing significant variation after As (III) and As (V) spiking compared to normal algal culture. In the box plots, the boxes denote interquartile ranges, horizontal line inside the box denote the median, and bottom and top boundaries of boxes are 25th and 75th percentiles, respectively. Lower and upper whiskers are 5th and 95th percentiles, respectively.*

The quantitative data of significantly altered algal metabolites were visualized using quantitative NMR analysis and hierarchically clustered heat maps to discern the dissimilarity between the three experimental groups **(Table 5.2, Fig. 5.10)**. The results clearly established that the As (V) treated group is remarkably different in terms of the expression levels of metabolites compared to control and As (III) treated groups **(Fig. 5.10, Table 5.3)**. Based on the NMR metabolic data, it is evident that the levels of the metabolites including amino acids, organic acids, sugars and osmolytes are distinct between As (III) and As (V) species. A two fold increase in the levels of free amino acids such as leucine, isoleucine, valine, alanine, sarcosine, glutamate, glutamine, proline and cysteine was recorded in As (V) treated microalgal cells in comparison to As (III) treatment **(Table 5.3)**. The levels of the remaining amino acids were same while tyrosine levels were lower in As (V) as compared to As (III) spiked microalgal cells. Analogous to the results of the free amino acids, the levels of organic acids

(acetate, succinate, citrate and formate) and carbohydrates (sucrose, glycerol, glucose) were higher in As (V) spiked cells as compared to As (III).
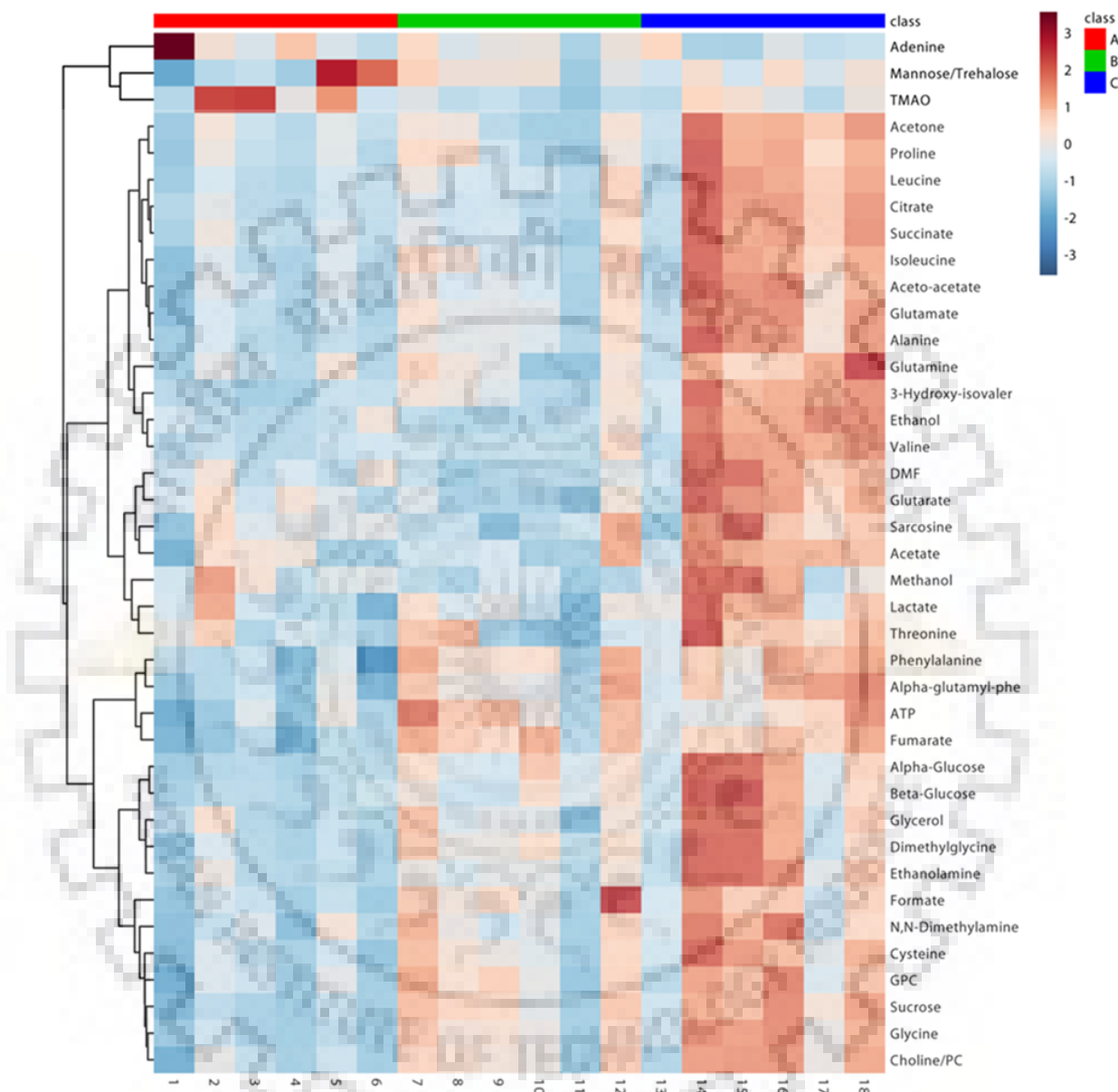
Fig. 5.10: *Heat maps showing z-scores of discriminatory metabolite entities altered in either As (III) or As (V) spiking compared to control algal culture. X-axis represents the replicates of the culture (Control – lane (1-6) - red bar (A); As (III) – lane (7-12) - green bar (B) As (V) – lane (13-18) - blue bar (C). The colour scheme through signifies the elevation and reduction in metabolite concentration in As (III) or As (V) spiking compared to normal algal culture: dark blue: lowest; dark red: highest.*

Interestingly, the arsenic treated cells showed decline in betaine and TMAO content, with As (III) showing more decrease than As (V). Thus, the above metabolic responses established that As (V) is more toxic to the microalgal cells as compared to As (III). Furthermore, these metabolic levels were incoherence with the biochemical analysis results which showed a drastic increase in lipid content in arsenic treated cells as escalation in the levels of ethanolamine, glycerol and citrate were recorded in As (III) and As (V) spiked cells with two fold higher expression in the latter (**Table 5.3**). Ethanolamine has been recently reported to act as a trigger for lipid accumulation in microalgal cells while glycerol forms backbone of fatty acids [131]. Citrate on the other hand is a substrate for acetyl CoA which is a precursor for fatty acid synthesis [109]. In line with the observed metabolite as a lipid accumulation trigger, the lipid yields reported under As (III, V) stress conditions clearly showed an increase in the total lipid content (**Fig. 5.2**). Increase lipid accumulation has also been observed in various microalgal species such as *C. minutissima*, *C. protothecoides*, *S. obliquus* when exposed to other heavy metal stress [129,138,275,276].

5.4 Discussion

Arsenic is a natural metalloid that has been recognized as a major carcinogen. Its exposure even in small quantity can lead to cancers and adverse health effects [25]. In the past decade, there has been a considerable increase in arsenic levels in the aquatic ecosystems. Unfortunately, the physico-chemical methods deployed for arsenic removal are costly, result in large arsenic laden discards and are specific to arsenic speciation as As (III, V) are present in various anionic and neutral forms (**Fig. 5.4, Table 5.1**) [277]. pH is one of the major constraint for such an interconversion among the arsenic species, in comparison to conversion between As (V) and As (III) in a growth media/natural habitant conditions. In this regard, microalgae can serve as propitious renewable "green alternative" for bioremediation of arsenic from water sources as it can efficiently remove both As (V) to As (III) irrespective of its inter and intra speciation events.

Although microalgae bioremediates all the arsenic species, the mechanism by which it mitigates the two different arsenic forms is different. Indeed, previously it has been reported that As (III) gets converted to DMA and MMA, whereas As (V) reduces to As (III), DMA and MMA respectively (**Fig. 5.11**). The reduction of As (V) to As (III) reduces the cellular toxicity levels and also decreases As (V) interference as a phosphate epitope [278,279].
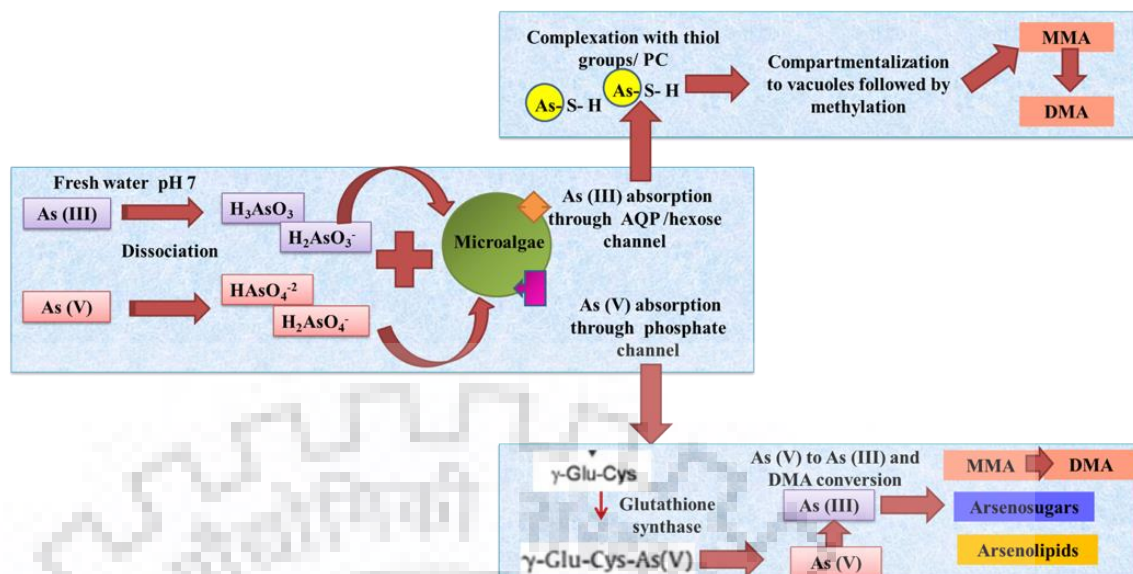
Fig. 5.11: *Schematic of arsenic adsorption and metabolism by fresh water microalgae*

The current study is an attempt to delineate the differential biochemical and metabolic responses of microalgae that are capable of tolerating and mitigating high quantities of both As (III) and As (V) forms. The *Scenedesmus* sp. IITRIND2 turned out be hyper-tolerant and effective remediator of arsenic in both forms as compared to control species (*S. abundans*). *Scenedesmus* sp. IITRIND2 was comparable to the hyper-accumulator ferns such as *Pteris vittata* L., *Pteris cretica* (*albo-lineata*, *mayii* and *parkeri*) which can uptake ~1114 to 4360 µg/g DCW arsenic in their fronds [280]. The biochemical analysis of algal cells evidenced that the loss of protein and carbohydrate content under As (V) stress is much higher than of As (III), indicating the toxic nature of the As (V). Further, the unaltered levels of carotenoids in arsenic spiked microalgal cells as compared to control indicated healthy state of photosynthetic apparatus and in turn algal tolerance to the metalloid. Carotenoids play a crucial role in deactivating excited triplet chlorophyll, quenching the ROS species generated within the cell during stress thereby protecting the photosynthetic apparatus and aiding cell survival [281]. It is well documented that exposure of heavy metal to microalgae causes cellular oxidation stress due to formation of ROS such as H_2O_2, OH^-, O_2 [273,282].

The comprehensive NMR based metabolic profile supported the gross features obtained from physico-chemical analysis which provided deep insights into the cellular signaling events in order to formulate a mechanism for algal based arsenic bioremediation. An apparent increase in all the three branched chain amino acids (leucine, isoleucine and valine) was observed which could be due to suppressed protein biosynthesis/catabolism in arsenic treated algal cells. An increase in these amino acids indicated perturbation in acetyl-CoA biosynthesis or glycolysis

due to arsenic stress. Escalation in differential levels of glucogenic amino acids (isoleucine, phenylalanine, tyrosine, glutamine, valine, and proline) were evident in arsenic spiked cultures, and were more prominent on As (V) spiking. Moreover, a distinct peak of choline/Phytochelatins and GPC was observed in the ^{1}H NMR spectra of arsenic spiked microalgal cells. Phytochelatins (PC) plays all three essential roles in metal bioremediation; (a) helps in metal binding, (b) act as antioxidant and (c) assist in signaling thereby protecting the algal cell from deleterious effect of heavy metal [273]. Differential shifting of functional groups in FT-IR spectra between As (III) and As (V) combined with distinct levels of choline/PC observed through NMR evidences the distinct binding mitigation pathways of these two arsenic species by microalgae.

Additionally, the elevated levels of sarcosine, glycine, valine, glutamine under arsenic stress may contribute towards the complexation of arsenic to the algal biomass [129]. Proline content was drastically increased in As (V) spiked algal cultures followed by As (III) as compared to control, thereby supporting the fact that As (V) to be more toxic than As (III). Proline has diverse roles during stress such as it acts as a metal chelator, osmoprotectant, inhibitor of lipid peroxidation, ROS scavenger and has antioxidant properties [135]. The excess levels of proline in As (V) cultures depict the intraconversion of arsenic As (V) to As (III), which is essential to counteract on ROS mediated oxidative damage [266]. Under oxidative stress, the microalgal cell starts generating components such as ascorbate, glutathione (GSH or GSSG) and pyridine nucleotides (NAD$^+$/ NADP$^+$) to combat this stress [273]. These components also protect the cell by scavenging ROS species thereby aiding in cell survival. The metabolomics profile showed an increase in the levels of cysteine, glutamine and glutamate in arsenic spiked cultures as compared to control, with more elevation in the As (V) cultures [279]. These results also point out that the algal cells have a great metabolic flexibility to adjust and to acclimatize towards stress conditions. Earlier, studies on the changes in the proteome of microalga in response to arsenic stress also reported an increase in the expression of glutamine synthetase which catalyzes the conversion of glutamate to glutamine [265,266,283].

Parallel to changes in the amino acids, *Scenedesmus* sp. IITRIND2 showed attenuations in various sugars and organic acids in response to arsenic (III, V) **(Table 5.3)**. An increase in soluble sugars was recorded in arsenic spiked microalgal cells due to perturbations in the carbohydrate metabolism. High levels of sucrose, α/β-glucose were observed in As (V) cultures as compared to As (III). Similar increase was also observed for glycerol (osmolytic polyol), which maintains a carbon pool during stress conditions to protect the photosystem [283]. Carbohydrates and polyols also act as osmo-protectants and helps to stabilize the cell

membrane [284]. Interestingly, the organic acids showed significant differences in their level of increase in As (III) and As (V) spiked cultres as compared to control. Levels of several of the organic acids such as succinate, citrate, acetate, and glutarate levels are unchanged upon As (III) spiking and enhanced substantially upon As (V) spiking. Organic acids such as citrate and fumarate plays an essential role in Krebs cycle with citrate acting as a detoxifying molecule by quenching the metal ions while fumarate on the other hand limits the deleterious effects of the heavy metal [135]. The increase of fumarate in both As (III, V) spiked cultures, and the selective enhancement of organic acids in As (V) spiked cultures showed that algal cells used additional mechanisms to cope of with its toxicity, and for its efficient bioremediation by protecting its cellular mechanisms and powerhouses.

The levels of ATP were also heightened in arsenic spiked cultures, which could be due to increase in the respiration rates during stress and decrease in the photosynthetic activity [266,285]. Interestingly, the arsenic toxicity and the levels of betaine and TMAO showed negative correlation, which could be due to increase in free amino acids and other osmolytes (glycerol, sucrose, and proline) that act as compensatory osmolytes [286].

All the above results concisely deduce the hierarchy of arsenic tolerance/ bioremediation (Fig. 5.12). Firstly, arsenic gets adsorbed on microalgal by complexation with various functional groups present on its cell wall followed by slow intracellular metabolism. As (III) gets transported across plasma membrane via aquaglyceroporine (AQP) and hexose permeases, while As (V) competes with the phosphate transporters [263]. Post internalization, As (V) to a certain extent can be reduced to As (III) by GSH while PC and its derivatives inside cell shield As (III) with S-H groups (increase in levels of cysteine, PC, glutamine, glutamate). Furthermore, both As (III, V) also get converted to their methylated compounds (DMA, MMA) inside the algal cells. Inhibition of the oxidative phosphorylation and its methylation by arsenic species results in buildup of oxidative stress inside microalgal cells causing perturbations in TCA cycle [263]. To combat this oxidative stress, microalga starts accumulating proline, fumarate and trehalose which act as antioxidant molecules scavenging ROS. This can be synchronized with protein catabolism (increase in levels of free amino acids), carbohydrate and lipid biosynthesis (Fig. 5.12). The methylated compounds (DMA, MMA) are then converted to arsenosugars and arsenolipids. An increase in the levels of glycerol and sucrose indicated the formation of arsenosugars.
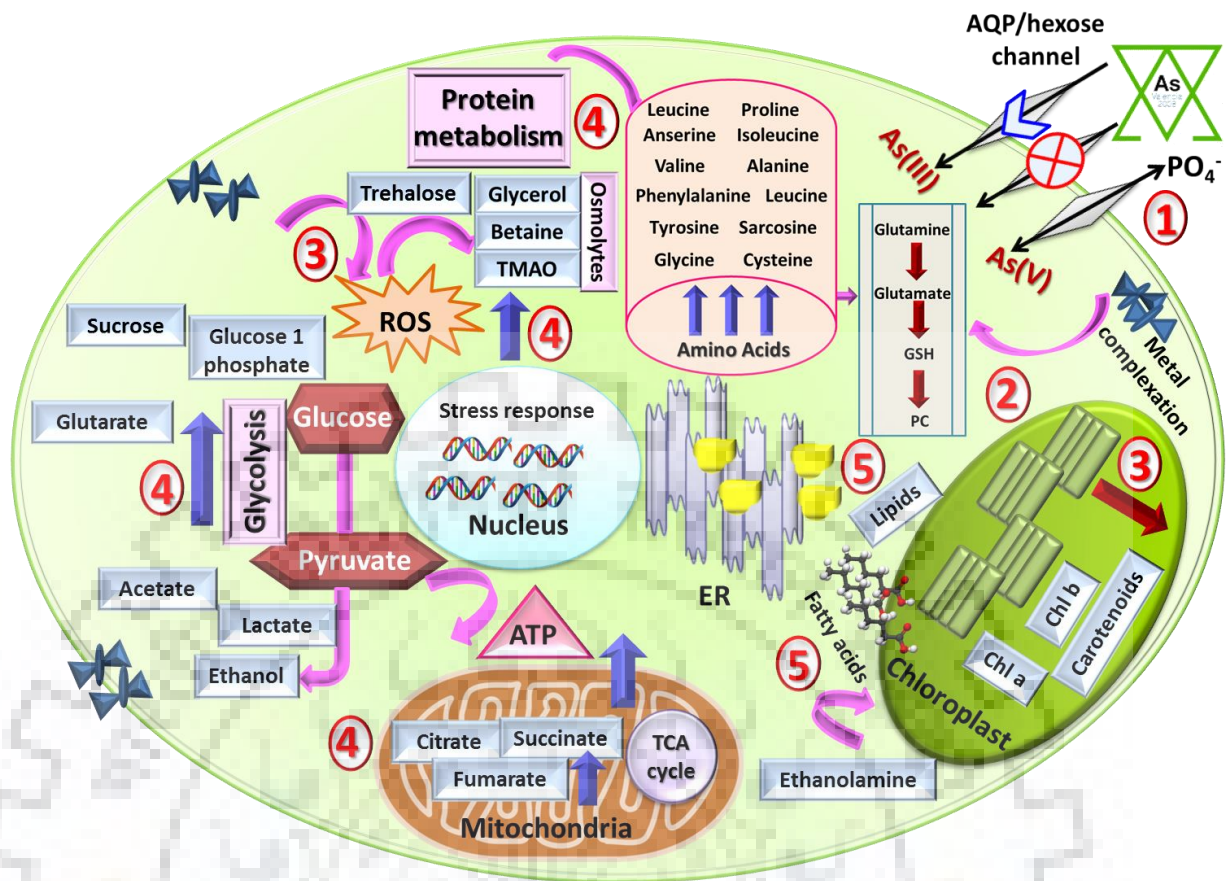
Fig. 5.12: *Schematic showing the hierarchy of arsenic (III, V) induced metabolic changes in the microalgal cells: (**1**): Arsenic intake via AQP/hexose channels, (**2**) metal complexation by PC, (**3**) ROS generation in response to arsenic stress, (**4**) mitigating ROS stress by modulating protein metabolism, photosynthesis, glycolysis and TCA (**5**) ER stress resulting in increase in lipid content.*

5.5 Concluding remarks

The above proposed synergistic modus operandi to remediate arsenic from contaminated water sources by microalgae strategy congregated with biodiesel production could become one of the most propitious treatment solutions with two-fold benefit (a) the treated water could be used for irrigation and recreational purposes and (b) the dry de-oiled algal biomass can act as a feedstock for biofertilizers or bioethanol/biogas. *Scenedesmus* sp. IITRIND2 mitigated both the arsenic species (III, V) irrespective of the speciation were efficiently removed by the selected microalgal strains from the SSW. Further, this study demonstrated the effectiveness of using a metabolomics approach in answering environmental and in particular arsenic tolerance mechanism by microalgae which could lead to successful

deployment of microalgae via genetic engineering for bioremediation of arsenic from contaminated water sources.

Conclusion and Future perspectives

6.1 Concluding remarks

In the present study, a novel microalga, *Scenedesmus* sp. IITRIND2 was isolated from a fresh water lake which efficiently adapted to different sea water salinities (0-35 g/L sea salts). The microalga when cultivated in 100 % ASW, showed higher lipid productivity as compared to control (no salt). Such an increase in lipid content was accompanied by a decrease in total protein and carbohydrate content. The adaptability of the microalga to such high salinity was attributed to decrease photosynthetic pigments, accumulation of osmolytes, antioxidant enzymes which efficiently quenched the ROS generated due to oxidative stress. The FAME profile analysis and biodiesel physical properties under saline conditions were in compliance with ASTM D6751-52 and EN 14214 fuel standards which established the microalga to be a prospective strain for biodiesel production.

The microalga when cultivated in 100 % ASW, remodelled its membrane permeability by restricting ions channels, decreasing the surface potential and excretion of EPS as compared to control. Interestingly, an increase in cell size along with disorganization of cellular structure with large lipid accumulation and few starch granules in 100 % ASW culture were visualized in electron micrographs of the microalga as compared to the control cells. Based on an "integrated omics approach" comprising of proteomics, metabolomics and lipidomics a salinity driven metabolic pathway was hypothesized starting with an increase in lipids, up regulation of proline and sugar biosynthesis followed by an apparent decline in amino acids biosynthesis, TCA cycle precursors, photosynthesis and starch metabolism. Further, four potential genetic engineering targets (SAD, KAS, STO and Alfin like protein) were identified whose overexpression might increase the halotolerance of any microalga along with augmentation in TAG content.

After delineating the halotolerance mechanism of *Scenedesmus* sp. IITRIND2, its adaptability in natural sea water cultivated in custom built photobioreactor mimicking outdoor PAR and temperature cycles was tested. The microalga showed a remarkable ability to thrive in natural sea water along with high carbohydrate and lipid accumulation. Such an adaptation was attributed to increase in neutral sugars which aided the microalga to adjust its osmotic equilibrium thereby limiting the detrimental effect of salinity. These results obtained provided a base line for future outdoor cultivation of *Scenedesmus* sp. IITRIND2 in sea water which can

substantially reduce the cost of algal biodiesel production.

The ability of *Scenedesmus* sp. IITRIND2 to remediate heavy metal arsenic (III, V) coupled with biodiesel production was also investigated. Interestingly, the microalga was able to tolerated 500 mg/L of As (III, V) from SSW along with ~ 70 % removal without inhibiting its growth. The analysis of biochemical composition of the microalga showed a substantial increase in total lipid content while a decrease in protein and carbohydrate content as compared to control (SSW). The study also revealed perturbations in the levels of metabolites with an apparent increase in branched chain amino acids, organic acids and carbohydrates in arsenic spiked cultures as compared to the control. The FAME profile and biodiesel properties also compiled with the international biodiesel standards, thereby indicating the feasibility of such a hybrid approach.

5.2 Future perspectives

Taking into account the above potential of *Scenedesmus* sp. IITRIND2 to grow in sea water for biodiesel production, it will prove beneficial to cultivate the microalga outdoors on large scale. However, due to low nitrogen and phosphorous in the sea water, addition of wastewater could potentially provide for the limiting nutrients. This will require the optimization of wastewater source, its concentration and location of the algal cultivation side (ideally should be near to sea shore and waste water plant) to maximize the algal biomass and lipid accumulation. To further, reduce the microalgal biodiesel cost, the cultivation system can be equipped with media recycling after biomass harvest. Indeed, a biorefinery approach is quintessential involving extraction of all the high/low value added products from the lipid extracted biomass which makes the process even more sustainable. In case of *Scenedesmus* sp. IITRIND2, proline and sucrose could be extracted which are marketable products. Additionally, for the large scale cultivation of the microalga in sea water, the genetic engineering targets identified could be verified in non-halotolerant strains.

Ultimately, in order to bring to bear the full promise of microalgae, improvements must be realized across the entire value chain. This will undoubtedly require continued efforts in bioprospecting and advances in algal genetic tool development in order to identify and develop novel strains with robust deployment characteristics. To achieve maximum productivity, strain-engineering pursuits in non-model algae will need to focus on enhancing multiple traits beyond TAG accumulation, including enhanced photosynthetic efficiency, CO_2 utilization, and predator and pest tolerance mechanisms, among others. Concurrently, continued efforts targeting outdoor deployment and conversion optimization will also be requisite, encompassing cultivation, harvesting, extraction, and upgrading.

References

[1] H.S. Oberoi, N. Babbar, S.K. Sandhu, S.S. Dhaliwal, U. Kaur, B.S. Chadha, V.K. Bhargav, Ethanol production from alkali-treated rice straw via simultaneous saccharification and fermentation using newly isolated thermotolerant *Pichia kudriavzevii* HOP-1, J. Ind. Microbiol. Biotechnol. 39 (2012) 557–566. doi:10.1007/s10295-011-1060-2.

[2] B. Kiran, K. Pathak, R. Kumar, D. Deshmukh, Cultivation of *Chlorella* sp. IM-01 in municipal wastewater for simultaneous nutrient removal and energy feedstock production, Ecol. Eng. 73 (2014) 326–330. doi:10.1016/j.ecoleng.2014.09.094.

[3] E.G. Arenas, M.C. Rodriguez Palacio, A.U. Juantorena, S.E.L. Fernando, P.J. Sebastian, Microalgae as a potential source for biodiesel production: techniques, methods, and other challenges, Int. J. Energy Res. 41 (2017) 761–789. doi:10.1002/er.3663.

[4] S.-H. Ho, A. Nakanishi, X. Ye, J.-S. Chang, K. Hara, T. Hasunuma, A. Kondo, Optimizing biodiesel production in marine *Chlamydomonas* sp. JSC4 through metabolic profiling and an innovative salinity-gradient strategy., Biotechnol. Biofuels. 7 (2014) 97. doi:10.1186/1754-6834-7-97.

[5] Y. Shinde, D. Dwivedi, P. Khatri, J.S. Sangwai, Biomass and solar: Emerging energy resources for India, In Green Energy and Technology. Springer Verlag. (2018) 297–334. doi:10.1007/978-981-10-8393-8_13.

[6] S. Dhar, M. Pathak, P.R. Shukla, Transformation of India's transport sector under global warming of 2 °C and 1.5 °C scenario, J. Clean. Prod. 172 (2018) 417–427. doi:10.1016/j.jclepro.2017.10.076.

[7] S. Khan, R. Siddique, W. Sajjad, G. Nabi, K.M. Hayat, P. Duan, L. Yao, Biodiesel production from algae to overcome the energy crisis, HAYATI J. Biosci. 24 (2017) 163–167. doi:10.1016/j.hjb.2017.10.003.

[8] G. Joshi, J.K. Pandey, S. Rana, D.S. Rawat, Challenges and opportunities for the application of biofuel, Renew. Sustain. Energy Rev. 79 (2017) 850–866. doi:10.1016/j.rser.2017.05.185.

[9] N. Gaurav, S. Sivasankari, G.S. Kiran, A. Ninawe, J. Selvin, Utilization of bioresources for sustainable biofuels: A Review, Renew. Sustain. Energy Rev. 73 (2017) 205–214. doi:10.1016/j.rser.2017.01.070.

[10] V.P. Zambare, A. Bhalla, K. Muthukumarappan, R.K. Sani, L.P. Christopher, Bioprocessing of agricultural residues to ethanol utilizing a cellulolytic extremophile, Extremophiles. 15 (2011) 611–618. doi:10.1007/s00792-011-0391-2.

[11] J.E. Chen, A.G. Smith, A look at diacylglycerol acyltransferases (DGATs) in algae, J. Biotechnol. 162 (2012) 28–39. doi:10.1016/j.jbiotec.2012.05.009.

[12] M.S. Podder, C.B. Majumder, Phycoremediation of arsenic from wastewaters by Chlorella pyrenoidosa, Groundw. Sustain. Dev. 1 (2015) 78–91. doi:10.1016/j.gsd.2015.12.003.

[13] D.Y.C. Leung, X. Wu, M.K.H. Leung, A review on biodiesel production using catalyzed transesterification, Appl. Energy. 87 (2010) 1083–1095. doi:10.1016/j.apenergy.2009.10.006.

[14] S. Bandhu, D. Dasgupta, J. Akhter, P. Kanaujia, S.K. Suman, D. Agrawal, S. Kaul, D.K. Adhikari, D. Ghosh, Statistical design and optimization of single cell oil production from sugarcane bagasse hydrolysate by an oleaginous yeast *Rhodotorula* sp . IIP-33 using response surface methodology, SpringerPlus. 3(2014) 1–11. doi:10.1186/2193-1801-3-691.

[15] Y.C. Sharma, B. Singh, S.N. Upadhyay, Advancements in development and characterization of biodiesel: A review, Fuel. 87 (2008) 2355–2373. doi:10.1016/j.fuel.2008.01.014.

[16] Y.C. Sharma, B. Singh, Development of biodiesel: Current scenario, Renew. Sustain. Energy Rev. 13 (2009) 1646–1651. doi:10.1016/j.rser.2008.08.009.

[17] A. Doshi, S. Pascoe, L. Coglan, T.J. Rainey, Economic and policy issues in the production of algae-based biofuels: A review, Renew. Sustain. Energy Rev. 64 (2016) 329–337. doi:10.1016/j.rser.2016.06.027.

[18] A. Bhalla, N. Bansal, S. Kumar, K.M. Bischoff, R.K. Sani, Improved lignocellulose conversion to biofuels with thermophilic bacteria and thermostable enzymes, Bioresour. Technol. 128 (2013) 751–759. doi:10.1016/j.biortech.2012.10.145.

[19] J.P. Maity, J. Bundschuh, C.Y. Chen, P. Bhattacharya, Microalgae for third generation biofuel production, mitigation ofgreenhouse gas emissions and wastewater treatment: Present andfuture perspectives - A mini review, Energy. 78 (2014) 104–113. doi:10.1016/j.energy.2014.04.003.

[20] A.K. Bajhaiya, J. Ziehe Moreira, J.K. Pittman, Transcriptional engineering of microalgae: prospects for high-value chemicals, Trends Biotechnol. 35 (2017) 95–99. doi:10.1016/j.tibtech.2016.06.001.

[21] K.K. Brar, A.K. Sarma, M. Aslam, I. Polikarpov, B.S. Chadha, Potential of oleaginous yeast Trichosporon sp., for conversion of sugarcane bagasse hydrolysate into biodiesel, Bioresour. Technol. 242 (2017) 161–168. doi:10.1016/j.biortech.2017.03.155.

[22] J. Lü, C. Sheahan, P. Fu, Metabolic engineering of algae for fourth generation biofuels

production, Energy Environ. Sci. 4 (2011) 2451. doi:10.1039/c0ee00593b.

[23] C.K. Jain, I. Ali, Arsenic : occurrence , toxicity and speciation techniques, Water Res. 34 (2000) 4304–4312.

[24] S. Wang, D. Zhang, X. Pan, Effects of arsenic on growth and photosystem II (PSII) activity of *Microcystis aeruginosa*, Ecotoxicol. Environ. Saf. 84 (2012) 104–111. doi:10.1016/j.ecoenv.2012.06.028.

[25] S. Zhang, C. Rensing, Y.G. Zhu, Cyanobacteria-mediated arsenic redox dynamics is regulated by phosphate in aquatic environments, Environ. Sci. Technol. 48 (2014) 994–1000. doi:10.1021/es403836g.

[26] T.M. Clancy, K.F. Hayes, L. Raskin, Arsenic waste management: A critical review of testing and disposal of arsenic-bearing solid wastes generated during arsenic removal from drinking water, Environ. Sci. Technol. 47 (2013) 10799–10812. doi:10.1021/es401749b.

[27] Z. Veličković, G.D. Vuković, A.D. Marinković, M.S. Moldovan, A.A. Perić-Grujić, P.S. Uskoković, M.D. Ristić, Adsorption of arsenate on iron(III) oxide coated ethylenediamine functionalized multiwall carbon nanotubes, Chem. Eng. J. 181–182 (2012) 174–181. doi:10.1016/j.cej.2011.11.052.

[28] A.C. Samal, G. Bhar, S.C. Santra, Biological process of arsenic removal using selected micro algae, Indian Journal of Experimental Biology. 42 (2004) 522–528.

[29] L. Brennan, P. Owende, Biofuels from microalgae — A review of technologies for production, processing, and extractions of biofuels and co-products, Renew. Sustain. Energy Rev.14 (2010) 557–577. doi:10.1016/j.rser.2009.10.009.

[30] A.M. Frassanito, L. Barsanti, V. Passarelli, V. Evangelista, P. Gualtieri, A second rhodopsin-like protein in *Cyanophora paradoxa*: Gene sequence and protein expression in a cell-free system, J. Photochem. Photobiol. B Biol. 125 (2013) 188–193. doi:10.1016/j.jphotobiol.2013.06.010.

[31] J. Acreman, Algae and cyanobacteria: isolation, culture and long-term maintenance, J. Ind. Microbiol. 13 (1994) 193–194. doi:10.1007/BF01584008.

[32] R.A. Andersen, Diversity of eukaryotic algae, Biodivers. Conserv. 1 (1992) 267–292. doi:10.1007/BF00693765.

[33] P.J. le B. Williams, L.M.L. Laurens, Microalgae as biodiesel & biomass feedstocks: Review & analysis of the biochemistry, energetics & economics, Energy Environ. Sci. 3 (2010) 554. doi:10.1039/b924978h.

[34] R.H. Wijffels, M.J. Barbosa, An outlook on microalgal biofuels, Science (80-.). 329 (2010) 796–799. doi:10.1126/science.1189003.

[35] Y.C. Sharma, B. Singh, J. Korstad, A critical review on recent methods used for economically viable and eco-friendly development of microalgae as a potential feedstock for synthesis of biodiesel, Green Chem. 13 (2011) 2993. doi:10.1039/c1gc15535k.

[36] M.C. Posewitz, Algal oil productivity gets a fat bonus, Nat. Biotechnol. 35 (2017) 636–638. doi:10.1038/nbt.3920.

[37] M.K. Lam, K.T. Lee, Microalgae biofuels : A critical review of issues , problems and the way forward, Biotechnol. Adv. 30 (2012) 673–690. doi:10.1016/j.biotechadv.2011.11.008.

[38] T. Hasunuma, M. Matsuda, A. Kondo, Improved sugar-free succinate production by *Synechocystis* sp. PCC 6803 following identification of the limiting steps in glycogen catabolism, Metab. Eng. Commun. 3 (2016) 130–141. doi:10.1016/j.meteno.2016.04.003.

[39] P. Vazquez-Villegas, M.A. Torres-Acosta, S.A. Garcia-Echauri, J.M. Aguilar-Yanez, M. Rito-Palomares, F. Ruiz-Ruiz, Genetic manipulation of microalgae for the production of bioproducts., Front. Biosci. (Elite Ed). 10 (2018) 254–275. http://www.ncbi.nlm.nih.gov/pubmed/28930617.

[40] E.J. Lohman, R.D. Gardner, T. Pedersen, B.M. Peyton, K.E. Cooksey, R. Gerlach, Optimized inorganic carbon regime for enhanced growth and lipid accumulation in *Chlorella vulgaris*, Biotechnol. Biofuels. (2015) 1–13. doi:10.1186/s13068-015-0265-4.

[41] M.J. Ramos, C.M. Fernandez, A. Casas, L. Rodaguez, Angel Perez, Influence of fatty acid composition of raw materials on biodiesel properties, Bioresour. Technol. 100 (2009) 261–268. doi:10.1016/j.biortech.2008.06.039.

[42] A.J. Klok, P.P. Lamers, D.E. Martens, R.B. Draaisma, R.H. Wijffels, Edible oils from microalgae : insights in TAG accumulation, Trends Biotechnol. 32 (2014) 521–528. doi:10.1016/j.tibtech.2014.07.004.

[43] P. Singh, S. Kumari, A. Guldhe, R. Misra, I. Rawat, F. Bux, Trends and novel strategies for enhancing lipid accumulation and quality in microalgae, Renew. Sustain. Energy Rev. 55 (2016) 1–16. doi:10.1016/j.rser.2015.11.001.

[44] S.K. Lenka, N. Carbonaro, R. Park, S.M. Miller, I. Thorpe, Y. Li, Current advances in molecular, biochemical, and computational modeling analysis of microalgal triacylglycerol biosynthesis, Biotechnol. Adv. 34 (2016) 1046–1063. doi:10.1016/j.biotechadv.2016.06.004.

[45] S. Vonlanthen, D. Dauvillée, S. Purton, Evaluation of novel starch-deficient mutants of *Chlorella sorokiniana* for hyper-accumulation of lipids, Algal Res. 12 (2015) 109–118.

doi:10.1016/j.algal.2015.08.008.

[46] R. Davis, A. Aden, P.T. Pienkos, Techno-economic analysis of autotrophic microalgae for fuel production, Appl. Energy. 88 (2011) 3524–3531. doi:10.1016/j.apenergy.2011.04.018.

[47] R. Radakovits, R.E. Jinkerson, A. Darzins, M.C. Posewitz, Genetic engineering of algae for enhanced biofuel production, Eukaryot. Cell. 9 (2010) 486–501. doi:10.1128/EC.00364-09.

[48] N. Shtaida, I. Khozin-Goldberg, S. Boussiba, The role of pyruvate hub enzymes in supplying carbon precursors for fatty acid synthesis in photosynthetic microalgae, Photosynth. Res. 125 (2015) 407–422. doi:10.1007/s11120-015-0136-7.

[49] Q. Hu, M. Sommerfeld, E. Jarvis, M. Ghirardi, M. Posewitz, M. Seibert, A. Darzins, Microalgal triacylglycerols as feedstocks for biofuel production: Perspectives and advances, Plant J. 54 (2008) 621–639. doi:10.1111/j.1365-313X.2008.03492.x.

[50] S. Bellou, M.N. Baeshen, A.M. Elazzazy, D. Aggeli, F. Sayegh, G. Aggelis, Microalgal lipids biochemistry and biotechnological perspectives, Biotechnol. Adv. 32 (2014) 1476–1493. doi:10.1016/j.biotechadv.2014.10.003.

[51] Y. Zhang, X. Liu, M.A. White, L.M. Colosi, Economic evaluation of algae biodiesel based on meta-analyses, Int. J. Sustain. Energy. 36 (2017) 682–694. doi:10.1080/14786451.2015.1086766.

[52] M. Luisa, N.M. Carneiro, F. Pradelle, S.L. Braga, M. Sebastião, P. Gomes, A. Rosa, F.A. Martins, F. Turkovics, R.N.C. Pradelle, Potential of biofuels from algae : Comparison with fossil fuels , ethanol and biodiesel in Europe and Brazil through life cycle assessment (LCA), Renew. Sustain. Energy Rev. 73 (2017) 632–653. doi:10.1016/j.rser.2017.01.152.

[53] H. Xu, X. Miao, Q. Wu, High quality biodiesel production from a microalga Chlorella prototothecoides by heterotrophic growth in fermenters, J. Biotechnol. 126 (2006) 499–507. doi:10.1016/j.jbiotec.2006.05.002.

[54] A. Bhatnagar, S. Chinnasamy, M. Singh, K.C. Das, Renewable biomass production by mixotrophic algae in the presence of various carbon sources and wastewaters, Appl. Energy. 88 (2011) 3425–3431. doi:10.1016/j.apenergy.2010.12.064.

[55] C. Gao, Y. Zhai, Y. Ding, Q. Wu, Application of sweet sorghum for biodiesel production by heterotrophic microalga *Chlorella protothecoides*, Appl. Energy. 87 (2010) 756–761. doi:10.1016/j.apenergy.2009.09.006.

[56] A. Limayem, S.C. Ricke, Lignocellulosic biomass for bioethanol production: Current perspectives, potential issues and future prospects, Prog. Energy Combust. Sci. 38

(2012) 449–467. doi:10.1016/j.pecs.2012.03.002.

[57]   M.C. Cerón-García, M.D. Macías-Sánchez, A. Sánchez-Mirón, F. García-Camacho, E. Molina-Grima, A process for biodiesel production involving the heterotrophic fermentation of *Chlorella protothecoides* with glycerol as the carbon source, Appl. Energy. 103 (2013) 341–349. doi:10.1016/j.apenergy.2012.09.054.

[58]   J. Mu, S. Li, D. Chen, H. Xu, F. Han, B. Feng, Y. Li, Enhanced biomass and oil production from sugarcane bagasse hydrolysate (SBH) by heterotrophic oleaginous microalga *Chlorella protothecoides*, Bioresour. Technol. 185 (2015) 99–105. doi:10.1016/j.biortech.2015.02.082.

[59]   F. Foflonker, G. Ananyev, H. Qiu, A. Morrison, B. Palenik, G.C. Dismukes, D. Bhattacharya, The unexpected extremophile: Tolerance to fluctuating salinity in the green alga *Picochlorum*, Algal Res. 16 (2016) 465–472. doi:10.1016/j.algal.2016.04.003.

[60]   Y. Liang, Producing liquid transportation fuels from heterotrophic microalgae, Appl. Energy. 104 (2013) 860–868. doi:10.1016/j.apenergy.2012.10.067.

[61]   J. Yang, M. Xu, X. Zhang, Q. Hu, M. Sommerfeld, Y. Chen, Life-cycle analysis on biodiesel production from microalgae: Water footprint and nutrients balance, Bioresour. Technol. 102 (2011) 159–165. doi:10.1016/j.biortech.2010.07.017.

[62]   M.A. Borowitzka, N.R. Moheimani, Sustainable biofuels from algae, Mitig. Adapt. Strateg. Glob. Chang. 18 (2013) 13–25. doi:10.1007/s11027-010-9271-9.

[63]   R. Slade, A. Bauen, Micro-algae cultivation for biofuels : Cost , energy balance , environmental impacts and future prospects, Biomass and Bioenergy. 53 (2013) 29–38. doi:10.1016/j.biombioe.2012.12.019.

[64]   R. Singh, S. Singh, P. Parihar, V.P. Singh, S.M. Prasad, Arsenic contamination, consequences and remediation techniques: A review, Ecotoxicol. Environ. Saf. 112 (2015) 247–270. doi:10.1016/j.ecoenv.2014.10.009.

[65]   V.L. Mitchell, Health Risks Associated with Chronic Exposures to Arsenic in the Environment, Rev. Mineral. Geochemistry. 79 (2014) 435–449. doi:10.2138/rmg.2014.79.8.

[66]   B.K. Mandal, K.T. Suzuki, Arsenic round the world : a review, Talanta. 58 (2002) 201–235.

[67]   P. Zhao, X. Yu, J. Li, X. Tang, Z. Huang, Enhancing lipid productivity by co-cultivation of *Chlorella* sp. U4341 and *Monoraphidium* sp. FXY-10, J. Biosci. Bioeng. 118 (2014) 72–77. doi:10.1016/j.jbiosc.2013.12.014.

[68]   W. Wen, J. Wen, L. Lu, H. Liu, J. Yang, H. Cheng, W. Che, L. Li, G. Zhang,

Metabolites of arsenic and increased DNA damage of p53 gene in arsenic plant workers, Toxicol. Appl. Pharmacol. 254 (2011) 41–47. doi:10.1016/j.taap.2011.04.013.

[69] R.N. Ratnaike, Acute and chronic arsenic toxicity, Postgr. Med J. 79 (2003) 391–396. doi:10.1136/pmj.79.933.391.

[70] S. Tamaki, W. Frankenberger Jr, Environmental biochemistry of arsenic, Rev. Environ. Contam. Toxicol. States. 124 (1992) 79-104. doi:10.1007/978-1-4612-2864-6.

[71] S. V. Jadhav, E. Bringas, G.D. Yadav, V.K. Rathod, I. Ortiz, K. V. Marathe, Arsenic and fluoride contaminated groundwaters: A review of current technologies for contaminants removal, J. Environ. Manage. 162 (2015) 306–325. doi:10.1016/j.jenvman.2015.07.020.

[72] P. Mondal, S. Bhowmick, D. Chatterjee, A. Figoli, B. Van der Bruggen, Remediation of inorganic arsenic in groundwater for safe water supply: A critical assessment of technological solutions, Chemosphere. 92 (2013) 157–170. doi:10.1016/j.chemosphere.2013.01.097.

[73] K. Suresh Kumar, H.U. Dahms, E.J. Won, J.S. Lee, K.H. Shin, Microalgae - A promising tool for heavy metal remediation, Ecotoxicol. Environ. Saf. 113 (2015) 329–352. doi:10.1016/j.ecoenv.2014.12.019.

[74] T.A. Davis, B. Volesky, A. Mucci, A review of the biochemistry of heavy metal biosorption by brown algae, Water Res. 37 (2003) 4311–4330. doi:10.1016/S0043-1354(03)00293-8.

[75] M. Tuzen, A. Sari, D. Mendil, O.D. Uluozlu, M. Soylak, M. Dogan, Characterization of biosorption process of As(III) on green algae *Ulothrix cylindricum*, J. Hazard. Mater. 165 (2009) 566–572. doi:10.1016/j.jhazmat.2008.10.020.

[76] A. Sari, Ö.D. Uluozlü, M. Tüzen, Equilibrium, thermodynamic and kinetic investigations on biosorption of arsenic from aqueous solution by algae (*Maugeotia genuflexa*) biomass, Chem. Eng. J. 167 (2011) 155–161. doi:10.1016/j.cej.2010.12.014.

[77] J. Zhang, T. Ding, C. Zhang, Biosorption and toxicity responses to arsenite (As[III]) in *Scenedesmus quadricauda*, Chemosphere. 92 (2013) 1077–1084. doi:10.1016/j.chemosphere.2013.01.002.

[78] S. Foster, D. Thomson, W. Maher, Uptake and metabolism of arsenate by anexic cultures of the microalgae *Dunaliella tertiolecta* and *Phaeodactylum tricornutum*, Mar. Chem. 108 (2008) 172–183. doi:10.1016/j.marchem.2007.11.005.

[79] O. Takimura, H. Fuse, Y. Yamaoka, Effect of metal ions on accumulation of arsenic in marine green algae, *Dunaliella* sp., Appl. Organomet. Chem. 4 (1990) 265–268. doi:10.1002/aoc.590040315.

[80] O. Takimura, H. Fuse, K. Murakami, K. Kamimura, Y. Yamaoka, Uptake and reduction

of arsenate by *Dunaliella* sp., Appl. Organomet. Chem. 10 (1996) 753–756. doi:10.1002/(SICI)1099-0739(199611)10:9<753::AID-AOC573>3.0.CO;2-V.

[81] Y. Yukiho, T. Osamu, F. Hiroyuki, M. Kastuji, Effect of glutathione on arsenic accumulation by *Dunaliella salina*, Appl. Organomet. Chem. 13 (1999) 89–94. doi:10.1002/(sici)1099-0739(199902)13:2<89::aid-aoc803>3.0.co;2-l.

[82] Y. Wang, C. Zhang, Y. Zheng, Y. Ge, Phytochelatin synthesis in *Dunaliella salina* induced by arsenite and arsenate under various phosphate regimes, Ecotoxicol. Environ. Saf. 136 (2017) 150–160. doi:10.1016/j.ecoenv.2016.11.002.

[83] M.M. Bahar, M. Megharaj, R. Naidu, Influence of phosphate on toxicity and bioaccumulation of arsenic in a soil isolate of microalga *Chlorella* sp., Environ. Sci. Pollut. Res. 23 (2016) 2663–2668. doi:10.1007/s11356-015-5510-7.

[84] L.A. Murray, A. Raab, I.L. Marr, J. Feldmann, Biotransformation of arsenate to arsenosugars by *Chlorella vulgaris*, Appl. Organomet. Chem. 17 (2003) 669–674. doi:10.1002/aoc.498.

[85] Y. Jiang, D. Purchase, H. Jones, H. Garelick, Technical note: Effects of arsenate (As^{5+}) on growth and production of glutathione (GSH) and phytochelatins (PCS) in *Chlorella vulgaris*, Int. J. Phytoremediation. 13 (2011) 834–844. doi:10.1080/15226514.2010.525560.

[86] Suhendrayatna, A. Ohki, S. Maeda, Biotransformation of arsenite in freshwater food-chain models, Appl. Organomet. Chem. 15 (2001) 277–284. doi:10.1002/aoc.139.

[87] S. Maeda, S. Nakashima, T. Takeshita, S. Higashi, Bioaccumulation of arsenic by freshwater algae and the application to the removal of inorganic arsenic from an aqueous phase. Part II. by *Chlorella vulgaris* Isolated from arsenic-polluted environment, Sep. Sci. Technol. 20 (1985) 153–161. doi:10.1080/01496398508058356.

[88] N.X. Wang, Y. Li, X.H. Deng, A.J. Miao, R. Ji, L.Y. Yang, Toxicity and bioaccumulation kinetics of arsenate in two freshwater green algae under different phosphate regimes, Water Res. 47 (2013) 2497–2506. doi:10.1016/j.watres.2013.02.034.

[89] S. Fujiwara, I. Kobayashi, S. Hoshino, T. Kaise, K. Shimogawara, H. Usuda, M. Tsuzuki, Isolation and characterization of arsenate-sensitive and resistant mutants of *Chlamydomonas reinhardtii*., Plant Cell Physiol. 41 (2000) 77–83. http://www.ncbi.nlm.nih.gov/pubmed/10750711.

[90] S. Miyashita, S. Fujiwara, M. Tsuzuki, T. Kaise, Rapid Biotransformation of arsenate into oxo-arsenosugars by a freshwater unicellular green alga, *Chlamydomonas reinhardtii*, Biosci. Biotechnol. Biochem. 75 (2011) 522–530. doi:10.1271/bbb.100751.

[91] M.M. Bahar, M. Megharaj, R. Naidu, Bioremediation of arsenic-contaminated water:

Recent advances and future prospects, Water. Air. Soil Pollut. 224 (2013) 1–20. doi:10.1007/s11270-013-1722-y.

[92]   A.K. Upadhyay, S.K. Mandotra, N. Kumar, N.K. Singh, L. Singh, U.N. Rai, Augmentation of arsenic enhances lipid yield and defense responses in alga *Nannochloropsis* sp., Bioresour. Technol. 221 (2016) 430–437. doi:10.1016/j.biortech.2016.09.061.

[93]   M.T. Guarnieri, P.T. Pienkos, Algal omics: unlocking bioproduct diversity in algae cell factories, Photosynth. Res. 123 (2015) 255–263. doi:10.1007/s11120-014-9989-4.

[94]   M. Hannon, J. Gimpel, M. Tran, B. Rasala, S. Mayfield, Biofuels from algae: challenges and potential, Biofuels. 1 (2010) 763–784. doi:10.4155/bfs.10.44.

[95]   N.A.T. Tran, M.P. Padula, C.R. Evenhuis, A.S. Commault, P.J. Ralph, B. Tamburic, Proteomic and biophysical analyses reveal a metabolic shift in nitrogen deprived *Nannochloropsis oculata*, Algal Res. 19 (2016) 1–11. doi:10.1016/j.algal.2016.07.009.

[96]   Y.E. Choi, H. Hwang, H.S. Kim, J.W. Ahn, W.J. Jeong, J.W. Yang, Comparative proteomics using lipid over-producing or less-producing mutants unravels lipid metabolisms in *Chlamydomonas reinhardtii*, Bioresour. Technol. 145 (2013) 108–115. doi:10.1016/j.biortech.2013.03.142.

[97]   T.I. Mclean, " Eco-omics ": A review of the application of genomics , transcriptomics , and proteomics for the study of the ecology of harmful algae, Microb. Ecol. 65 (2013) 901–915. doi:10.1007/s00248-013-0220-5.

[98]   S.T. Wang, Y.Y. Pan, C.C. Liu, L. Te Chuang, C.N.N. Chen, Characterization of a green microalga UTEX 2219-4: Effects of photosynthesis and osmotic stress on oil body formation, Bot. Stud. 52 (2011) 305–312.

[99]   F. Xie, T. Liu, W.J. Qian, V.A. Petyuk, R.D. Smith, Liquid chromatography-mass spectrometry-based quantitative proteomics, J. Biol. Chem. 286 (2011) 25443–25449. doi:10.1074/jbc.R110.199703.

[100] X. Deng, J. Cai, X. Fei, Involvement of phosphatidate phosphatase in the biosynthesis of triacylglycerols in *Chlamydomonas reinhardtii*., J. Zhejiang Univ. Sci. B. 14 (2013) 1121–31. doi:10.1631/jzus.B1300180.

[101] Z.K. Yang, Y.H. Ma, J.W. Zheng, W.D. Yang, J.S. Liu, H.Y. Li, Proteomics to reveal metabolic network shifts towards lipid accumulation following nitrogen deprivation in the diatom *Phaeodactylum tricornutum*, J. Appl. Phycol. 26 (2014) 73–82. doi:10.1007/s10811-013-0050-3.

[102] Y. Li, Z. Yuan, J. Mu, D. Chen, B. Feng, Proteomic analysis of lipid accumulation in *Chlorella protothecoides* cells by heterotrophic N deprivation coupling cultivation,

Energy and Fuels. 27 (2013) 4031–4040. doi:10.1021/ef4000177.

[103] P. Song, L. Li, J. Liu, Proteomic analysis in nitrogen-deprived *Isochrysis galbana* during lipid accumulation, PLoS One. 8 (2013) 1–13. doi:10.1371/journal.pone.0082188.

[104] C. Shang, S. Zhu, Z. Wang, L. Qin, M.A. Alam, J. Xie, Z. Yuan, Proteome response of *Dunaliella parva* induced by nitrogen limitation, Algal Res. 23 (2017) 196–202. doi:10.1016/j.algal.2017.01.016.

[105] M.T. Guarnieri, A. Nag, S. Yang, P.T. Pienkos, Proteomic analysis of *Chlorella vulgaris*: Potential targets for enhanced lipid accumulation, J. Proteomics. 93 (2013) 245–253. doi:10.1016/j.jprot.2013.05.025.

[106] J. Longworth, D. Wu, M. Huete-Ortega, P.C. Wright, S. Vaidyanathan, Proteome response of *Phaeodactylum tricornutum*, during lipid accumulation induced by nitrogen depletion, Algal Res. 18 (2016) 213–224. doi:10.1016/j.algal.2016.06.015.

[107] M. Garnier, G. Carrier, H. Rogniaux, E. Nicolau, G. Bougaran, B. Saint-Jean, J.P. Cadoret, Comparative proteomics reveals proteins impacted by nitrogen deprivation in wild-type and high lipid-accumulating mutant strains of *Tisochrysis lutea*, J. Proteomics. 105 (2014) 107–120. doi:10.1016/j.jprot.2014.02.022.

[108] H.-P. Dong, E. Williams, D. Wang, Z.-X. Xie, R. Hsia, A. Jenck, R. Halden, J. Li, F. Chen, A.R. Place, Responses of *Nannochloropsis oceanica* IMET1 to long-term nitrogen starvation and recovery, Plant Physiol. 162 (2013) 1110–1126. doi:10.1104/pp.113.214320.

[109] N. Wase, P.N. Black, B.A. Stanley, C.C. Dirusso, Integrated quantitative analysis of nitrogen stress response in *Chlamydomonas reinhardtii* using metabolite and protein profiling, J. Proteome Res. 13 (2014) 1373–1396. doi:10.1021/pr400952z.

[110] D.Z. Wang, C. Li, Y. Zhang, Y.Y. Wang, Z.P. He, L. Lin, H.S. Hong, Quantitative proteomic analysis of differentially expressed proteins in the toxicity-lost mutant of *Alexandrium catenella* (Dinophyceae) in the exponential phase, J. Proteomics. 75 (2012) 5564–5577. doi:10.1016/j.jprot.2012.08.001.

[111] S.Y. Lee, S.H. Kim, S.H. Hyun, H.W. Suh, S.J. Hong, B.K. Cho, C.G. Lee, H. Lee, H.K. Choi, Fatty acids and global metabolites profiling of *Dunaliella tertiolecta* by shifting culture conditions to nitrate deficiency and high light at different growth phases, Process Biochem. 49 (2014) 996–1004. doi:10.1016/j.procbio.2014.02.022.

[112] J. Il Choi, M. Yoon, M. Joe, H. Park, S.G. Lee, S.J. Han, P.C. Lee, Development of microalga *Scenedesmus dimorphus* mutant with higher lipid content by radiation breeding, Bioprocess Biosyst. Eng. 37 (2014) 2437–2444. doi:10.1007/s00449-014-1220-7.

130

[113] T. Li, M. Gargouri, J. Feng, J.J. Park, D. Gao, C. Miao, T. Dong, D.R. Gang, S. Chen, Regulation of starch and lipid accumulation in a microalga *Chlorella sorokiniana*, Bioresour. Technol. 180 (2015) 250–257. doi:10.1016/j.biortech.2015.01.005.

[114] M.T. Guarnieri, A. Nag, S.L. Smolinski, A. Darzins, M. Seibert, P.T. Pienkos, Examination of triacylglycerol biosynthetic pathways via de novo transcriptomic and proteomic analyses in an unsequenced microalga, PLoS One. 6 (2011). doi:10.1371/journal.pone.0025851.

[115] Y. Li, J. Mu, D. Chen, H. Xu, F. Han, B. Feng, H. Zeng, Proteomics analysis for enhanced lipid accumulation in oleaginous *Chlorella vulgaris* under a heterotrophic-Na+ induction two-step regime, Biotechnol. Lett. 37 (2015) 1021–1030. doi:10.1007/s10529-014-1758-0.

[116] Y. Li, H. Xu, F. Han, J. Mu, D. Chen, B. Feng, H. Zeng, Regulation of lipid metabolism in the green microalga *Chlorella protothecoides* by heterotrophy-photoinduction cultivation regime, Bioresour. Technol. 192 (2014) 781–791. doi:10.1016/j.biortech.2014.07.028.

[117] J. Longworth, J. Noirel, J. Pandhal, P.C. Wright, S. Vaidyanathan, HILIC- and SCX-based quantitative proteomics of *Chlamydomonas reinhardtii* during nitrogen starvation induced lipid and carbohydrate accumulation, J. Proteome Res. 11 (2012) 5959–5971. doi:10.1021/pr300692t.

[118] N. Wase, P.N. Black, B.A. Stanley, C.C. Dirusso, Integrated quantitative analysis of nitrogen stress response in *Chlamydomonas reinhardtii* using metabolite and protein profiling, J. Proteome Res. 13 (2014) 1373–1396. doi:10.1021/pr400952z.

[119] V. Rai, M. Muthuraj, M.N. Gandhi, D. Das, S. Srivastava, Real-time iTRAQ-based proteome profiling revealed the central metabolism involved in nitrogen starvation induced lipid accumulation in microalgae, Sci. Rep. 7 (2017) 1–16. doi:10.1038/srep45732.

[120] D. Morales-Sánchez, J. Kyndt, K. Ogden, A. Martinez, Toward an understanding of lipid and starch accumulation in microalgae: A proteomic study of *Neochloris oleoabundans* cultivated under N-limited heterotrophic conditions, Algal Res. 20 (2016) 22–34. doi:10.1016/j.algal.2016.09.006.

[121] Y. Li, J. Mu, D. Chen, F. Han, H. Xu, F. Kong, F. Xie, B. Feng, Production of biomass and lipid by the microalgae *Chlorella protothecoides* with heterotrophic-Cu(II) stressed (HCuS) coupling cultivation, Bioresour. Technol. 148 (2013) 283–292. doi:10.1016/j.biortech.2013.08.153.

[122] G. Mastrobuoni, S. Irgang, M. Pietzke, H.E. Aßmus, M. Wenzel, W.X. Schulze, S.

Kempa, Proteome dynamics and early salt stress response of the photosynthetic organism *Chlamydomonas reinhardtii*, BMC Genomics. 13 (2012) 1–13. doi:10.1186/1471-2164-13-215.

[123] K.W.M. Tan, Y.K. Lee, Expression of the heterologous *Dunaliella tertiolecta* fatty acyl-ACP thioesterase leads to increased lipid production in *Chlamydomonas reinhardtii*, J. Biotechnol. 247 (2017) 60–67. doi:10.1016/j.jbiotec.2017.03.004.

[124] W.B. Dunn, D.I. Ellis, Metabolomics: Current analytical platforms and methodologies, TrAC - Trends Anal. Chem. 24 (2005) 285–294. doi:10.1016/j.trac.2004.11.021.

[125] T. Ito, M. Tanaka, H. Shinkawa, T. Nakada, Y. Ano, N. Kurano, T. Soga, M. Tomita, Metabolic and morphological changes of an oil accumulating trebouxiophycean alga in nitrogen-deficient conditions, Metabolomics. 9 (2013) 178–187. doi:10.1007/s11306-012-0463-z.

[126] V. Gupta, R.S. Thakur, C.R.K. Reddy, B. Jha, Central metabolic processes of marine macrophytic algae revealed from NMR based metabolome analysis, RSC Adv. 3 (2013) 7037. doi:10.1039/c3ra23017a.

[127] I.K. Blaby, A.G. Glaesener, T. Mettler, S.T. Fitz-Gibbon, S.D. Gallaher, B. Liu, N.R. Boyle, J. Kropat, M. Stitt, S. Johnson, C. Benning, M. Pellegrini, D. Casero, S.S. Merchant, Systems-Level Analysis of Nitrogen Starvation-Induced Modifications of Carbon Metabolism in a *Chlamydomonas reinhardtii* Starchless Mutant, Plant Cell. 25 (2013) 4305–4323. doi:10.1105/tpc.113.117580.

[128] S.H. Ho, A. Nakanishi, X. Ye, J.S. Chang, C.Y. Chen, T. Hasunuma, A. Kondo, Dynamic metabolic profiling of the marine microalga *Chlamydomonas* sp. JSC4 and enhancing its oil production by optimizing light intensity Luisa Gouveia, Biotechnol. Biofuels. 8 (2015) 1–17. doi:10.1186/s13068-015-0226-y.

[129] M.A. Chia, A.T. Lombardi, M. da Graça Gama Melão, C.C. Parrish, Combined nitrogen limitation and cadmium stress stimulate total carbohydrates, lipids, protein and amino acid accumulation in *Chlorella vulgaris* (Trebouxiophyceae), Aquat. Toxicol. 160 (2015) 87–95. doi:10.1016/j.aquatox.2015.01.002.

[130] S. Lu, J. Wang, Y. Niu, J. Yang, J. Zhou, Y. Yuan, Metabolic profiling reveals growth related FAME productivity and quality of *Chlorella sorokiniana* with different inoculum sizes, Biotechnol. Bioeng. 109 (2012) 1651–1662. doi:10.1002/bit.24447.

[131] J.S. Cheng, Y.H. Niu, S.H. Lu, Y.J. Yuan, Metabolome analysis reveals ethanolamine as potential marker for improving lipid accumulation of model photosynthetic organisms, J. Chem. Technol. Biotechnol. 87 (2012) 1409–1418. doi:10.1002/jctb.3759.

[132] R. Mioso, F.J.T. Marante, J.E.G. Gonzalez, J.J.S. Rodraguez, I.H.B. de Laguna,

Metabolite profiling of *Schizochytrium* sp. by GC-MS, an oleaginous microbial source of biodiesel, Brazilian J. Microbiol. 45 (2014) 403–409. doi:10.1590/S1517-83822014000200006.

[133] M.A. Chia, A.T. Lombardi, M. da Graça Gama Melão, C.C. Parrish, Combined nitrogen limitation and cadmium stress stimulate total carbohydrates, lipids, protein and amino acid accumulation in *Chlorella vulgaris* (Trebouxiophyceae), Aquat. Toxicol. 160 (2015) 87–95. doi:10.1016/j.aquatox.2015.01.002.

[134] A.A. Meharg, Arsenic uptake and metabolism in arsenic resistant and nonresistant plant species, New Phytologist. (2002) 29–43.

[135] L. Zoghlami, W. Djebali, Z. Abbes, H. Hediji, M. Maucourt, A. Moing, R. Brouquisse, W. Chaïbi, Metabolite modifications in *Solanum lycopersicum* roots and leaves under cadmium stress, African J. Biotechnol. 10 (2013) 567–579. doi:10.4314/ajb.v10i4.

[136] S.H. Ho, X. Ye, T. Hasunuma, J.S. Chang, A. Kondo, Perspectives on engineering strategies for improving biofuel production from microalgae - A critical review, Biotechnol. Adv. 32 (2014) 1448–1459. doi:10.1016/j.biotechadv.2014.09.002.

[137] X. Sui, X. Niu, M. Shi, G. Pei, J. Li, L. Chen, J. Wang, W. Zhang, Metabolomic analysis reveals mechanism of antioxidant butylated hydroxyanisole on lipid accumulation in *Crypthecodinium cohnii*, J. Agric. Food Chem. 62 (2014) 12477–12484. doi:10.1021/jf503671m.

[138] H.Y. Ren, B.F. Liu, F. Kong, L. Zhao, G.J. Xie, N.Q. Ren, Enhanced lipid accumulation of green microalga *Scenedesmus* sp. by metal ions and EDTA addition, Bioresour. Technol. 169 (2014) 763–767. doi:10.1016/j.biortech.2014.06.062.

[139] X. Su, J. Xu, X. Yan, Lipidomic changes during different growth stages of *Nitzschia closterium f . minutissima*, Metabolomics. (2013) 300–310. doi:10.1007/s11306-012-0445-1.

[140] T. Melo, E. Alves, V. Azevedo, A. So, B. Neves, P. Domingues, R. Calado, M.H. Abreu, M. Rosário, Lipidomics as a new approach for the bioprospecting of marine macroalgae — Unraveling the polar lipid and fatty acid composition of *Chondrus crispus*, Algal Res. 8 (2015) 181–191. doi:10.1016/j.algal.2015.02.016.

[141] D. Yang, D. Song, T. Kind, Y. Ma, J. Hoefkens, O. Fiehn, Lipidomic Analysis of *Chlamydomonas reinhardtii* under Nitrogen and Sulfur Deprivation, PLoS ONE. 10 (2015) 1–16. doi:10.1371/journal.pone.0137948.

[142] N. Lu, D. Wei, F. Chen, S. Yang, Lipidomic profiling reveals lipid regulation in the snow alga *Chlamydomonas nivalis* in response to nitrate or phosphate deprivation, Process Biochem. 48 (2013) 605–613. doi:10.1016/j.procbio.2013.02.028.

[143] E. Peled, S. Leu, A. Zarka, M. Weiss, U. Pick, I. Khozin-Goldberg, S. Boussiba, Isolation of a novel oil globule protein from the green alga *Haematococcus pluvialis* (chlorophyceae), Lipids. 46 (2011) 851–861. doi:10.1007/s11745-011-3579-4.

[144] H. Goold, F. Beisson, G. Peltier, Y. Li-Beisson, Microalgal lipid droplets: composition, diversity, biogenesis and functions, Plant Cell Rep. 34 (2015) 545–555. doi:10.1007/s00299-014-1711-7.

[145] C.H. Tsai, K. Zienkiewicz, C.L. Amstutz, B.G. Brink, J. Warakanont, R. Roston, C. Benning, Dynamics of protein and polar lipid recruitment during lipid droplet assembly in *Chlamydomonas reinhardtii*, Plant J. 83 (2015) 650–660. doi:10.1111/tpj.12917.

[146] N.-L. Huang, M.-D. Huang, T.-L.L. Chen, A.H.C. Huang, Oleosin of subcellular lipid droplets evolved in green algae., Plant Physiol. 161 (2013) 1862–74. doi:10.1104/pp.112.212514.

[147] L. Davidi, A. Katz, U. Pick, Characterization of major lipid droplet proteins from *Dunaliella*, Planta. 236 (2012) 19–33. doi:10.1007/s00425-011-1585-7.

[148] H.M. Nguyen, M. Baudet, S. Cuiné, J.M. Adriano, D. Barthe, E. Billon, C. Bruley, F. Beisson, G. Peltier, M. Ferro, Y. Li-Beisson, Proteomic profiling of oil bodies isolated from the unicellular green microalga *Chlamydomonas reinhardtii*: With focus on proteins involved in lipid metabolism, Proteomics. 11 (2012) 4266–4273. doi:10.1002/pmic.201100114.

[149] I.P. Lin, P.L. Jiang, C.S. Chen, J.T.C. Tzen, A unique caleosin serving as the major integral protein in oil bodies isolated from *Chlorella* sp. cells cultured with limited nitrogen, Plant Physiol. Biochem. 61 (2012) 80–87. doi:10.1016/j.plaphy.2012.09.008.

[150] A. Vieler, S.B. Brubaker, B. Vick, C. Benning, A lipid droplet protein of *Nannochloropsis* with functions partially analogous to plant oleosins., Plant Physiol. 158 (2012) 1562–9. doi:10.1104/pp.111.193029.

[151] E.R. Moellering, C. Benning, RNA interference silencing of a major lipid droplet protein affects lipid droplet size in *Chlamydomonas reinhardtii*, Eukaryot. Cell. 9 (2010) 97–106. doi:10.1128/EC.00203-09.

[152] A. Ghosh, S. Khanra, M. Mondal, G. Halder, O.N. Tiwari, S. Saini, T.K. Bhowmick, K. Gayen, Progress toward isolation of strains and genetically engineered strains of microalgae for production of biofuel and other value added chemicals: A review, Energy Convers. Manag. 113 (2016) 104–118. doi:10.1016/j.enconman.2016.01.050.

[153] J.A. Gimpel, E.A. Specht, D.R. Georgianna, S.P. Mayfield, Advances in microalgae engineering and synthetic biology applications for biofuel production, Curr. Opin. Chem. Biol. 17 (n.d.) 489–495. doi:10.1016/j.cbpa.2013.03.038.

[154] T.G. Dunahay, E.E. Jaruis, P.G. Roessler, Genetic transformation of the diatoms *Cyclotella cryptzca*, J. Phycol. 31 (1995) 1004–1012.

[155] H. Schuhmann, D.K.Y. Lim, P.M. Schenk, Perspectives on metabolic engineering for increased lipid contents in microalgae, Biofuels. 3 (2016) 71-86.

[156] M.A. Scranton, J.T. Ostrand, F.J. Fields, S.P. Mayfield, *Chlamydomonas* as a model for biofuels and bio-products production, Plant J. 82 (2015) 523–531. doi:10.1111/tpj.12780.

[157] L. Wei, Y. Xin, Q. Wang, J. Yang, H. Hu, J. Xu, RNAi-based targeted gene knockdown in the model oleaginous microalgae *Nannochloropsis oceanica*, Plant J. 89 (2017) 1236–1250. doi:10.1111/tpj.13411.

[158] C. Wang, Y. Li, J. Lu, X. Deng, H. Li, Z. Hu, Effect of overexpression of LPAAT and GPD1 on lipid synthesis and composition in green microalga *Chlamydomonas reinhardtii*, J. Appl. Phycol. (2017) 1–9. doi:10.1007/s10811-017-1349-2.

[159] V.H. Work, R. Radakovits, R.E. Jinkerson, J.E. Meuser, L.G. Elliott, D.J. Vinyard, L.M.L. Laurens, G.C. Dismukes, M.C. Posewitz, Increased lipid accumulation in the *Chlamydomonas reinhardtii* sta7 - 10 starchless isoamylase mutant and increased carbohydrate synthesis in complemented strains, Eukarytotic Cell. 9 (2010) 1251–1261. doi:10.1128/EC.00075-10.

[160] E.M. Trentacoste, R.P. Shrestha, S.R. Smith, C. Glé, A.C. Hartmann, M. Hildebrand, Metabolic engineering of lipid catabolism increases microalgal lipid accumulation without compromising growth, PNAS. 110 (2013) 19748–19753. doi:10.1073/pnas.1309299110//DCSupplemental.www.pnas.org/cgi/doi/10.1073/pnas.1309299110.

[161] X. Fei, X. Li, P. Li, X. Deng, Involvement of *Chlamydomonas* DNA damage tolerence gene UBC2 in lipid accumulation, Algal Res. 22 (2017) 148–159. doi:10.1016/j.algal.2016.12.019.

[162] R. Margesin, F. Schinner, Potential of halotolerant and halophilic microorganisms for biotechnology, Extremophiles 5 (2001) 73–83.

[163] C. A. Popovich, C. Damiani, D. Constenla, A.M. Martínez, H. Freije, M. Giovanardi, S. Pancaldi, P.I. Leonardi, Neochloris oleoabundans grown in enriched natural seawater for biodiesel feedstock: Evaluation of its growth and biochemical composition, Bioresour. Technol. 114 (2012) 287–293. doi:10.1016/j.biortech.2012.02.121.

[164] S. Venkata Mohan, M.P. Devi, Salinity stress induced lipid synthesis to harness biodiesel during dual mode cultivation of mixotrophic microalgae, Bioresour. Technol. 165 (2014) 288–294. doi:10.1016/j.biortech.2014.02.103.

[165] L. Xia, J. Rong, H. Yang, Q. He, D. Zhang, C. Hu, NaCl as an effective inducer for lipid accumulation in freshwater microalgae Desmodesmus abundans, Bioresour. Technol. 161 (2014) 402–409. doi:10.1016/j.biortech.2014.03.063.

[166] A.F. Talebi, M. Tabatabaei, S. Kaveh, M. Tohidfar, F. Moradi, Comparative salt stress study on intracellular ion concentration in marine and salt-adapted freshwater strains of microalgae, Notulae Scientia Biologic. 5 (2013) 309–315.

[167] J. Trivedi, M. Aila, D.P. Bangwal, S. Kaul, M.O. Garg, Algae based biorefinery - How to make sense?, Renew. Sustain. Energy Rev. 47 (2015) 295–307. doi:10.1016/j.rser.2015.03.052.

[168] C. Chen, X. Zhao, H. Yen, S. Ho, C. Cheng, Microalgae-based carbohydrates for biofuel production, Biochem. Eng. J. 78 (2013) 1–10. doi:10.1016/j.bej.2013.03.006.

[169] J. Singh, S. Gu, Commercialization potential of microalgae for biofuels production, Renew. Sustain. Energy Rev. 14 (2010) 2596–2610. doi:10.1016/j.rser.2010.06.014.

[170] K. Tamura, G. Stecher, D. Peterson, A. Filipski, S. Kumar, MEGA6: Molecular evolutionary genetics analysis version 6.0, Mol. Biol. Evol. 30 (2013) 2725–2729. doi:10.1093/molbev/mst197.

[171] E. Bligh, W. Dyer, Canadian Journal of Biochemistry and Physiology, Can. J. Biochem. 37 (1959).

[172] A. Patel, D.K. Sindhu, N. Arora, R.P. Singh, V. Pruthi, P. a. Pruthi, Biodiesel production from Non-edible lignocellulosic biomass of *Cassia fistula* L. fruit pulp using oleaginous yeast *Rhodosporidium kratochvilovae* HIMPA1, Bioresour. Technol. (2015). doi:10.1016/j.biortech.2015.08.039.

[173] M. Dubois, K.A. Gilles, J.K. Hamilton, P.A. Rebers, F. Smith, Colorimetric method for determination of sugars and related substances, Anal. Chem. 28 (1956) 350–356. doi:10.1021/ac60111a017.

[174] H.K. Lichtenthaler, Chlorophylls and carotenoids: pigments of photosynthetic biomembranes, Methods Enzymol. 148 (1987) 350–382. doi:10.1016/0076-6879(87)48036-1.

[175] Z. Hu, Q. Zhong, Determination of thiobarbituric acid reactive substances in microencapsulated products, Food Chem. 123 (2010) 794–799. doi:10.1016/j.foodchem.2010.05.012.

[176] J. Tian, J. Yu, Journal of Photochemistry and Photobiology B : Biology Changes in ultrastructure and responses of antioxidant systems of algae (*Dunaliella salina*) during acclimation to enhanced ultraviolet-B radiation, J. Photochem. Photobiol. B Biol. 97 (2009) 152–160. doi:10.1016/j.jphotobiol.2009.09.003.

[177] L. Bates, R. Waldren, I. Teare, Rapid determination of free proline for water stress studies, Plant and Soil. 207 (1973) 205–207.

[178] A. Mishra, A. Mandoli, B. Jha, Physiological characterization and stress-induced metabolic responses of *Dunaliella salina* isolated from salt pan, J. Ind. Microbiol. Biotechnol. 35 (2008) 1093–1101. doi:10.1007/s10295-008-0387-9.

[179] K. Chokshi, I. Pancha, K. Trivedi, B. George, R. Maurya, A. Ghosh, S. Mishra, Biofuel potential of the newly isolated microalgae *Acutodesmus dimorphus* under temperature induced oxidative stress conditions, Bioresour. Technol. 180 (2015) 162–171. doi:10.1016/j.biortech.2014.12.102.

[180] I. Pancha, K. Chokshi, R. Maurya, K. Trivedi, S.K. Patidar, A. Ghosh, S. Mishra, Salinity induced oxidative stress enhanced biofuel production potential of microalgae *Scenedesmus* sp. CCNM 1077, Bioresour. Technol. 189 (2015) 341–348. doi:10.1016/j.biortech.2015.04.017.

[181] C.Y. Chen, J.S. Chang, H.Y. Chang, T.Y. Chen, J.H. Wu, W.L. Lee, Enhancing microalgal oil/lipid production from *Chlorella sorokiniana* CY1 using deep-sea water supplemented cultivation medium, Biochem. Eng. J. 77 (2013) 74–81. doi:10.1016/j.bej.2013.05.009 Regular article.

[182] B. Kim, R. Ramanan, Z. Kang, D. Cho, H. Oh, H. Kim, Biomass and Bioenergy *Chlorella sorokiniana* HS1 , a novel freshwater green algal strain , grows and hyperaccumulates lipid droplets in seawater salinity, Biomass and Bioenergy. 85 (2016) 300–305. doi:10.1016/j.biombioe.2015.12.026.

[183] U. Sabeela Beevi, R.K. Sukumaran, Cultivation of the fresh water microalga *Chlorococcum* sp. RAP13 in sea water for producing oil suitable for biodiesel, J. Appl. Phycol. (2014) 141–147. doi:10.1007/s10811-014-0340-4.

[184] A. Converti, A. A. Casazza, E.Y. Ortiz, P. Perego, M. Del Borghi, Effect of temperature and nitrogen concentration on the growth and lipid content of Nannochloropsis oculata and *Chlorella vulgaris* for biodiesel production, Chem. Eng. Process. Process Intensif. 48 (2009) 1146–1151. doi:10.1016/j.cep.2009.03.006.

[185] I. Pancha, K. Chokshi, T. Ghosh, C. Paliwal, R. Maurya, S. Mishra, Bicarbonate supplementation enhanced biofuel production potential as well as nutritional stress mitigation in the microalgae *Scenedesmus* sp. CCNM 1077, Bioresour. Technol. 193 (2015) 315–323. doi:10.1016/j.biortech.2015.06.107.

[186] D. Pal, I. Khozin-Goldberg, Z. Cohen, S. Boussiba, The effect of light, salinity, and nitrogen availability on lipid production by *Nannochloropsis* sp., Appl. Microbiol. Biotechnol. 90 (2011) 1429–1441. doi:10.1007/s00253-011-3170-1.

[187] L. Zhu, X. Zhang, L. Ji, X. Song, C. Kuang, Changes of lipid content and fatty acid composition of *Schizochytrium limacinum* in response to different temperatures and salinities, Process Biochem. 42 (2007) 210–214. doi:10.1016/j.procbio.2006.08.002.

[188] S.K. Hoekman, A. Broch, C. Robbins, E. Ceniceros, M. Natarajan, Review of biodiesel composition, properties, and specifications, Renew. Sustain. Energy Rev. 16 (2012) 143–169. doi:10.1016/j.rser.2011.07.143.

[189] H. Wu, X. Miao, Biodiesel quality and biochemical changes of microalgae *Chlorella pyrenoidosa* and *Scenedesmus obliquus* in response to nitrate levels, Bioresour. Technol. 170 (2014) 421–427. doi:10.1016/j.biortech.2014.08.017.

[190] T. Lee, C. Liu, Correlation of decreased calcium contents with proline accumulation in the marine green macroalga *Ulva fasciata* exposed to elevated NaCl contents in seawater, Journal of Experimental Botany. 50 (1999) 1855–1862.

[191] S.M. Dittami, A. Gravot, D. Renault, S. Goulitquer, A. Eggert, A. Bouchereau, C. Boyen, T. Tonon, Integrative analysis of metabolite and transcript abundance during the short-term response to saline and oxidative stress in the brown alga *Ectocarpus siliculosus*, Plant, Cell Environ. 34 (2011) 629–642. doi:10.1111/j.1365-3040.2010.02268.x.

[192] M. Choudhary, U.K. Jetley, M. Abash Khan, S. Zutshi, T. Fatma, Effect of heavy metal stress on proline, malondialdehyde, and superoxide dismutase activity in the cyanobacterium *Spirulina platensis*-S5, Ecotoxicol. Environ. Saf. 66 (2007) 204–209. doi:10.1016/j.ecoenv.2006.02.002.

[193] C.H. Tan, P.L. Show, J.S. Chang, T.C. Ling, J.C.W. Lan, Novel approaches of producing bioenergies from microalgae: A recent review, Biotechnol. Adv. 33 (2015) 1219–1227. doi:10.1016/j.biotechadv.2015.02.013.

[194] G.O. Kirst, Salinity Tolerance of eukaryotic marine algae, Annu. Rev. Plant Physiol. Plant Mol. Biol. 41 (1990) 21–53. doi:10.1146/annurev.pp.41.060190.000321.

[195] P.H. Yancey, Organic osmolytes as compatible , metabolic and counteracting cytoprotectants in high osmolarity and other stresses, (2005) 2819–2830. doi:10.1242/jeb.01730.

[196] J.M. Willey, J.B. Waterbury, E.P. Greenberg, Sodium-coupled motility in a swimming cyanobacterium, J. Bacteriol. 169 (1987) 3429–3434. doi:10.1128/jb.169.8.3429-3434.1987.

[197] W. Zhang, N.G.J. Tan, S.F.Y. Li, NMR-based metabolomics and LC-MS/MS quantification reveal metal-specific tolerance and redox homeostasis in *Chlorella vulgaris*, Mol. BioSyst. 10 (2014) 149–160. doi:10.1039/C3MB70425D.

[198] M.A. Fitzpatrick, C.M. McGrath, S.P. Young, Pathomx: An interactive workflow-based tool for the analysis of metabolomic data, BMC Bioinformatics. 15 (2014) 1–7. doi:10.1186/s12859-014-0396-9.

[199] J. Xia, N. Psychogios, N. Young, D.S. Wishart, MetaboAnalyst: A web server for metabolomic data analysis and interpretation, Nucleic Acids Res. 37 (2009) 652–660. doi:10.1093/nar/gkp356.

[200] J. Xia, I. V. Sinelnikov, B. Han, D.S. Wishart, MetaboAnalyst 3.0-making metabolomics more meaningful, Nucleic Acids Res. 43 (2015) W251–W257. doi:10.1093/nar/gkv380.

[201] M.A. Danielewicz, L.A. Anderson, A.K. Franz, Triacylglycerol profiling of marine microalgae by mass spectrometry, J. Lipid Res. 52 (2011) 2101–2108. doi:10.1194/jlr.D018408.

[202] K.J. Livak, T.D. Schmittgen, Analysis of relative gene expression data using real-time quantitative PCR and the $2^{-\Delta\Delta CT}$ method, Methods. 25 (2001) 402–408. doi:10.1006/meth.2001.1262.

[203] J. Fan, H. Xu, Y. Luo, M. Wan, Impacts of CO_2 concentration on growth , lipid accumulation , and carbon-concentrating-mechanism-related gene expression in oleaginous *Chlorella*, (2015) 2451–2462. doi:10.1007/s00253-015-6397-4.

[204] A. Krell, D. Funck, I. Plettner, U. John, G. Dieckmann, Regulation of proline metabolism under salt stress in the psychrophilic diatom *Fragilariopsis cylindrus* (Bacillariophyceae), J. Phycol. 43 (2007) 753–762. doi:10.1111/j.1529-8817.2007.00366.x.

[205] J. Liu, W. Hua, G. Zhan, F. Wei, X. Wang, G. Liu, H. Wang, Increasing seed mass and oil content in transgenic *Arabidopsis* by the overexpression of wri1 -like gene from *Brassica napus*, Plant Physiol. Biochem. 48 (2010) 9–15. doi:10.1016/j.plaphy.2009.09.007.

[206] J. Jia, D. Han, H.G. Gerken, Y. Li, M. Sommerfeld, Q. Hu, J. Xu, Molecular mechanisms for photosynthetic carbon partitioning into storage neutral lipids in *Nannochloropsis oceanica* under nitrogen-depletion conditions, Algal Res. 7 (2015) 66–77. doi:10.1016/j.algal.2014.11.005.

[207] H. Qian, G.D. Sheng, W. Liu, L. Yingcong, Z. Liu, F. Zhengwei, Inhibitory effects of atrazine on *Chlorella vulgaris* as assessed by real-time polymerase chain reaction, Environ. Toxicol. Chem. 27 (2008) 182–187. doi:10.1897/07-163.1.

[208] W. Liu, Y. Ming, P. Li, Z. Huang, Inhibitory effects of hypo-osmotic stress on extracellular carbonic anhydrase and photosynthetic efficiency of green alga *Dunaliella salina* possibly through reactive oxygen species formation, Plant Physiol. Biochem. 54

(2012) 43–48. doi:10.1016/j.plaphy.2012.01.018.

[209] J. Barber, Measurement of the membrane potential and evidence for active transport of ions in *Chlorella pyrenoidosa*, Biochemica et Biophysica Acta.150 (1907) 618–625.

[210] F. Alkayal, R.L. Albion, R.L. Tillett, L.T. Hathwaik, M.S. Lemos, J.C. Cushman, Expressed sequence tag (EST) profiling in hyper saline shocked *Dunaliella salina* reveals high expression of protein synthetic apparatus components, Plant Sci. 179 (2010) 437–449. doi:10.1016/j.plantsci.2010.07.001.

[211] A. Jacob, G.O. Kirst, C. Wiencke, H. Lehmann, Physiological responses of the antarctic green alga *Prasiola crispa* ssp. antarctica to salinity stress, J. Plant Physiol. 139 (1991) 57–62. doi:10.1016/S0176-1617(11)80165-3.

[212] J. Barber, Y.J. Shieh, Sodium transport in Na^+rich *Chlorella* cells, Planta. 111 (1973) 13–22. doi:10.1007/BF00386730.

[213] M. Kumar, P. Kumari, V. Gupta, C.R.K. Reddy, B. Jha, Journal of Experimental Marine Biology and Ecology Biochemical responses of red alga *Gracilaria corticata* (Gracilariales, Rhodophyta) to salinity induced oxidative stress, J. Exp. Mar. Bio. Ecol. 391 (2010) 27–34. doi:10.1016/j.jembe.2010.06.001.

[214] B. Geun, G. Baek, D. Jin, Y. Il, A. Synytsya, R. Bleha, D. Ho, C. Lee, J. Kweon, Characterization of a renewable extracellular polysaccharide from defatted microalgae *Dunaliella tertiolecta*, Bioresour. Technol. 129 (2013) 343–350. doi:10.1016/j.biortech.2012.11.077.

[215] F. Freitas, V.D. Alves, J. Pais, N. Costa, C. Oliveira, L. Mafra, L. Hilliou, R. Oliveira, M.A.M. Reis, Characterization of an extracellular polysaccharide produced by a *Pseudomonas* strain grown on glycerol, Bioresour. Technol. 100 (2009) 859–865. doi:10.1016/j.biortech.2008.07.002.

[216] A. Mishra, B. Jha, Isolation and characterization of extracellular polymeric substances from micro-algae *Dunaliella salina* under salt stress, Bioresour. Technol. 100 (2009) 3382–3386. doi:10.1016/j.biortech.2009.02.006.

[217] A. Bafana, Characterization and optimization of production of exopolysaccharide from *Chlamydomonas reinhardtii*, Carbohydr. Polym. 95 (2013) 746–752. doi:10.1016/j.carbpol.2013.02.016.

[218] M. Page-sharp, C.A. Behm, G.D. Smith, Involvement of the compatible solutes trehalose and sucrose in the response to salt stress of a cyanobacterial *Scytonema* species isolated from desert soils, Biochemica et Biophysica Acta.1472 (1999) 519–528.

[219] I. Ahmad, J.A. Hellebust, The relationship between inorganic nitrogen metabolism and proline accumulation in osmoregulatory responses of two euryhaline microalgae, Plant

Physiol. 88 (1988) 348–54. doi:10.1104/pp.88.2.348.

[220] H.D. Husic, N.E. Tolbert, Effect of osmotic stress on carbon metabolism in *Chlamydomonas reinhardtii*, Plant Physiol. 82 (1986) 594–596. http://www.plantphysiol.org/content/82/2/594.abstract%5Cnhttp://www.plantphysiol.org/content/82/2/594.full.pdf.

[221] L. Chen, D. Li, Y. Liu, Salt tolerance of *Microcoleus vaginatus* Gom., a cyanobacterium isolated from desert algal crust, was enhanced by exogenous carbohydrates, J. Arid Environ. 55 (2003) 645–656. doi:10.1016/S0140-1963(02)00292-6.

[222] A. Ghosh, S. Khanra, M. Mondal, G. Halder, O.N. Tiwari, S. Saini, T.K. Bhowmick, K. Gayen, Progress toward isolation of strains and genetically engineered strains of microalgae for production of biofuel and other value added chemicals: A review, Energy Convers. Manag. 113 (2016) 104–118. doi:10.1016/j.enconman.2016.01.050.

[223] G.O. Kirst, Ion composition of unicellular marine and fresh-water algae, with special reference to *Platymonas subcordiformis* cultivated in media with different osmotic strengths, Oecologia. 28 (1977) 177–189. doi:10.1007/BF00345253.

[224] G.R. Cramer, A. Lauchli, V.S. Polito, Displacement of Ca^{+2} by Na^+ from the Plasmalemma of Root Cells, Plant Physiol. 79, (1985) 207–211.

[225] M.E. Huflejt, A. Tremolieres, B. Pineau, J.K. Lang, J. Hatheway, L. Packer, F.- Gif, Y. Cedex, A.T. France, Changes in membrane lipid composition during saline growth of the fresh water cyanobacterium *Synechococcus* 63111, Plant Physiol. 94 (1990) 1512–1521.

[226] N. Lu, D. Wei, X.L. Jiang, F. Chen, S.T. Yang, Regulation of lipid metabolism in the snow alga *Chlamydomonas nivalis* in response to NaCl stress: An integrated analysis by cytomic and lipidomic approaches, Process Biochem. 47 (2012) 1163–1170. doi:10.1016/j.procbio.2012.04.011.

[227] T.C. Peeler, M.B. Stephenson, K.J. Einspahr, G.A. Thompson, Lipid characterization of an enriched plasma membrane fraction of *Dunaliella salina* grown in media of varying salinity, Plant Physiol. 89 (1989) 970–976.

[228] N. Arora, A. Patel, M. Sharma, J. Mehtani, P.A. Pruthi, V. Pruthi, K.M. Poluri, Insights into the Enhanced Lipid Production Characteristics of a Fresh Water Microalga under High Salinity Conditions, Ind. Eng. Chem. Res. 56 (2017) 7413–7421. doi:10.1021/acs.iecr.7b00841.

[229] K. Gounaris, J. Barber, Monogalactosyldiacylglycerol : the most abundant polar lipid in Nature, (1983) 378–381.

[230] B.H. Kim, R. Ramanan, Z. Kang, D.H. Cho, H.M. Oh, H.S. Kim, *Chlorella sorokiniana* HS1, a novel freshwater green algal strain, grows and hyperaccumulates lipid droplets in

seawater salinity, Biomass and Bioenergy. 85 (2016) 300–305.
doi:10.1016/j.biombioe.2015.12.026.

[231] C. Kavitha, A. Malarvizhi, S. Senthil Kumaran, M. Ramesh, Toxicological effects of arsenate exposure on hematological, biochemical and liver transaminases activity in an Indian major carp, Catla catla, Food Chem. Toxicol. 48 (2010) 2848–2854. doi:10.1016/j.fct.2010.07.017.

[232] S. Kumari, S. Roy, P. Singh, S. Singla-pareek, S. Kumari, S. Roy, P. Singh, S.L. Singla-pareek, A. Pareek, Cyclophilins : Proteins in search of function, Plant Signaling & Behavior. 8 (2018) e22734. doi:10.4161/psb.22734.

[233] S. Wienkoop, J. Weiß, P. May, S. Kempa, S. Irgang, L. Recuenco-Munoz, M. Pietzke, T. Schwemmer, J. Rupprecht, V. Egelhofer, W. Weckwerth, S.S. Merchant et al., Targeted proteomics for *Chlamydomonas reinhardtii* combined with rapid subcellular protein fractionation, metabolomics and metabolic flux analyses, Mol. Biosyst. 6 (2010) 1018. doi:10.1039/b920913a.

[234] B.K. Ndimba, R.J. Ndimba, T.S. Johnson, R. Waditee-Sirisattha, M. Baba, S. Sirisattha, Y. Shiraiwa, G.K. Agrawal, R. Rakwal, Biofuels as a sustainable energy source: An update of the applications of proteomics in bioenergy crops and algae, J. Proteomics. 93 (2013) 234–244. doi:10.1016/j.jprot.2013.05.041.

[235] T.A. Dempster, M.R. Sommerfeld, Effects of environmental conditions on growth and lipid accumulation in *Nitzschia communis* (Bacillariophyceae), J. Phycol. 34 (1998) 712–721. doi:10.1046/j.1529-8817.1998.340712.x.

[236] V. Krutkaew, T. Srirat, S. Tragoonrung, Cloning and Characterization of stearoyl – ACP desaturase gene (SAD) in oil palm (Elaeis guineensis Jacq .), Thai J. Genet. 6 (2013) 60–64.

[237] M. Azachi, A. Sadka, M. Fisher, P. Goldshlag, I. Gokhman, A. Zamir, B. Chemistry, M.A. Israel, Salt Induction of fatty acid elongase and membrane lipid modifications in the extreme halotolerant alga *Dunaliella salina*, Plant Physiol. 129 (2017) 1320-1329. doi:10.1104/pp.001909.1320.

[238] Y. Song, J. Gao, F. Yang, C. Kua, J. Liu, C.H. Cannon, Molecular Evolutionary Analysis of the Alfin-Like Protein Family in *Arabidopsis lyrata*, *Arabidopsis thaliana*, and *Thellungiella halophila*, PLoS ONE. 8 (2013) 1–10. doi:10.1371/journal.pone.0066838.

[239] H. Ullah, E.L. Scappini, A.F. Moon, L.V. Williams, D.L.E.E. Armstrong, Structure of a signal transduction regulator, RACK1, from *Arabidopsis thaliana*, Protein structure. 17 (2008) 1771–1780. doi:10.1110/ps.035121.108.4.

[240] M. Indorf, J. Cordero, G. Neuhaus, M. Rodrı, Salt tolerance (STO), a stress-related protein, has a major role in light signalling, The Plant Journal. 51 (2007) 563–574. doi:10.1111/j.1365-313X.2007.03162.x.

[241] L.M.L. Laurens, S. Van Wychen, J.P. Mcallister, S. Arrowsmith, T.A. Dempster, J. Mcgowen, P.T. Pienkos, Strain , biochemistry , and cultivation-dependent measurement variability of algal biomass composition, Anal. Biochem. 452 (2014) 86–95. doi:10.1016/j.ab.2014.02.009.

[242] T. Dong, E.P. Knoshaug, R. Davis, L.M.L. Laurens, S. Van Wychen, P.T. Pienkos, N. Nagle, Combined algal processing : A novel integrated biorefinery process to produce algal biofuels and bioproducts, Algal Res. 19 (2016) 316–323. doi:10.1016/j.algal.2015.12.021.

[243] I. BenMoussa-Dahmen, H. Chtourou, F. Rezgui, S. Sayadi, A. Dhouib, Salinity stress increases lipid, secondary metabolites and enzyme activity in *Amphora subtropica* and *Dunaliella* sp. for biodiesel production, Bioresour. Technol. 218 (2016) 816–825. doi:10.1016/j.biortech.2016.07.022.

[244] P.R. Pandit, M.H. Fulekar, M. Sri, L. Karuna, Effect of salinity stress on growth , lipid productivity, fatty acid composition, and biodiesel properties in *Acutodesmus obliquus* and *Chlorella vulgaris*, Environ. Sci. Pollut. Res. (2017). doi:10.1007/s11356-017-8875-y.

[245] T. Wang, H. Ge, T. Liu, X. Tian, Z. Wang, M. Guo, J. Chu, Y. Zhuang, Salt stress induced lipid accumulation in heterotrophic culture cells of *Chlorella protothecoides*: mechanisms based on the multi-level analysis of oxidative response, key enzyme activity and biochemical alteration, J. Biotechnol. 228 (2016) 18–27. doi:10.1016/j.jbiotec.2016.04.025.

[246] H. Pereira, K.N. Gangadhar, P.S.C. Schulze, T. Santos, C.B. de Sousa, L.M. Schueler, L. Custódio, F.X. Malcata, L. Gouveia, J.C.S. Varela, L. Barreira, Isolation of a euryhaline microalgal strain, *Tetraselmis* sp. CTP4, as a robust feedstock for biodiesel production, Sci. Rep. 6 (2016) 35663. doi:10.1038/srep35663.

[247] E.L. Sánchez-Alvarez, G. González-Ledezma, J.A. Bolaños Prats, J.L. Stephano-Hornedo, M. Hildebrand, Evaluating *Marinichlorella kaistiae* KAS603 cell size variation, growth and TAG accumulation resulting from rapid adaptation to highly diverse trophic and salinity cultivation regimes, Algal Res. 25 (2017) 12–24. doi:10.1016/j.algal.2017.03.027.

[248] S. Van Wychen, L.M.L. Laurens, [NREL] Determination of Total Solids and Ash in Algal Biomas, (2013) NREL/TP-5100-60956. doi:10.2172/1118077.

[249] S. Van Wychen, L.M.L. Laurens, Determination of total carbohydrates in algal biomass, Contract. 303 (2013) 275–3000. doi:10.2172/1118077.

[250] L.M.L. Laurens, M. Quinn, S. Van Wychen, D.W. Templeton, E.J. Wolfrum, Accurate and reliable quantification of total microalgal fuel potential as fatty acid methyl esters by in situ transesterification, Anal. Bioanal. Chem. 403 (2012) 167–178. doi:10.1007/s00216-012-5814-0.

[251] J.C. Batterton, C. Van Baalen, Growth responses of blue-green algae to sodium chloride concentration, Arch. Mikrobiol. 76 (1971) 151–165. doi:10.1007/BF00411789.

[252] K.K. Sharma, H. Schuhmann, P.M. Schenk, High lipid induction in microalgae for biodiesel production, Energies. 5 (2012) 1532–1553. doi:10.3390/en5051532.

[253] T. Ishika, N.R. Moheimani, P.A. Bahri, Sustainable saline microalgae co-cultivation for biofuel production: A critical review, Renew. Sustain. Energy Rev. 78 (2017) 356–368. doi:10.1016/j.rser.2017.04.110.

[254] A. Parvaiz, S. Satyawati, Salt stress and phyto-biochemical responses of plants – a review, Plant Soil Environ. 54 (2008) 89–99.

[255] G. Miller, N. Suzuki, S. Ciftci-Yilmaz, R. Mittler, Reactive oxygen species homeostasis and signalling during drought and salinity stresses, Plant, Cell Environ. 33 (2010) 453–467. doi:10.1111/j.1365-3040.2009.02041.x.

[256] A. Ben-Amotz, M. Avron, On the factors which determine massive beta-carotene accumulation in the halotolerant alga *Dunaliella bardawil*., Plant Physiol. 72 (1983) 593–7. doi:10.1104/PP.72.3.593.

[257] N. von Alvensleben, M. Magnusson, K. Heimann, Salinity tolerance of four freshwater microalgal species and the effects of salinity and nutrient limitation on biochemical profiles, J. Appl. Phycol. 28 (2016) 861–876. doi:10.1007/s10811-015-0666-6.

[258] D.W. Templeton, M. Quinn, S. Van Wychen, D. Hyman, L.M.L. Laurens, Separation and quantification of microalgal carbohydrates, J. Chromatogr. A. 1270 (2012) 225–234. doi:10.1016/j.chroma.2012.10.034.

[259] H.G. Gerken, B. Donohoe, E.P. Knoshaug, Enzymatic cell wall degradation of *Chlorella vulgaris* and other microalgae for biofuels production, Planta. 237 (2013) 239–253. doi:10.1007/s00425-012-1765-0.

[260] Z.A. Popper, G. Michel, C. Hervé, D.S. Domozych, W.G.T. Willats, M.G. Tuohy, B. Kloareg, D.B. Stengel, Evolution and diversity of plant cell walls: from algae to flowering plants, Annu. Rev. Plant Biol. 62 (2011) 567–590. doi:10.1146/annurev-arplant-042110-103809.

[261] D.G. Medcalf, Sulfated fucose-containing polysaccharides from brown algae: structural

features and biochemical implications, ACS Symp. Ser. 77 (1978) 225–244.

[262] M.R. Brown, The amino-acid and sugar composition of 16 species of microalgae used in mariculture, J. Exp. Mar. Bio. Ecol. 145 (1991) 79–99. doi:10.1016/0022-0981(91)90007-J.

[263] Y. Wang, S. Wang, P. Xu, C. Liu, M. Liu, Y. Wang, C. Wang, C. Zhang, Y. Ge, Review of arsenic speciation, toxicity and metabolism in microalgae, Rev. Environ. Sci. Biotechnol. 14 (2015) 427–451. doi:10.1007/s11157-015-9371-9.

[264] A. Jamers, R. Blust, W. De Coen, J.L. Griffin, O.A.H. Jones, An omics based assessment of cadmium toxicity in the green alga *Chlamydomonas reinhardtii*, Aquat. Toxicol. 126 (2013) 355–364. doi:10.1016/j.aquatox.2012.09.007.

[265] Y. Ge, Z. Ning, Y. Wang, Y. Zheng, C. Zhang, D. Figeys, Quantitative proteomic analysis of *Dunaliella salina* upon acute arsenate exposure, Chemosphere. 145 (2016) 112–118. doi:10.1016/j.chemosphere.2015.11.049.

[266] S. Pandey, R. Rai, L.C. Rai, Proteomics combines morphological, physiological and biochemical attributes to unravel the survival strategy of *Anabaena* sp. PCC7120 under arsenic stress, J. Proteomics. 75 (2012) 921–937. doi:10.1016/j.jprot.2011.10.011.

[267] E.J. Smith, W. Davison, J. Hamilton-taylor, Methods for preparing synthetic freshwaters, Water Res. 36 (2002) 1286–1296.

[268] W. Zhang, N.G.J. Tan, B. Fu, S.F.Y. Li, Metallomics and NMR-based metabolomics of *Chlorella* sp. reveal the synergistic role of copper and cadmium in multi-metal toxicity and oxidative stress, Metallomics. 7 (2015) 426–438. doi:10.1039/C4MT00253A.

[269] O. Beckonert, H.C. Keun, T.M.D. Ebbels, J. Bundy, E. Holmes, J.C. Lindon, J.K. Nicholson, Metabolic profiling, metabolomic and metabonomic procedures for NMR spectroscopy of urine, plasma, serum and tissue extracts., Nat. Protoc. 2 (2007) 2692–2703. doi:10.1038/nprot.2007.376.

[270] J. Xia, D.S. Wishart, Using metaboanalyst 3.0 for comprehensive metabolomics data analysis, Curr. Protoc. Bioinforma. 2016 (2016) 14.10.1-14.10.91. doi:10.1002/cpbi.11.

[271] S.S. Tripathy, A.M. Raichur, Enhanced adsorption capacity of activated alumina by impregnation with alum for removal of As (V) from water, 138 (2008) 179–186. doi:10.1016/j.cej.2007.06.028.

[272] A. Piotrowska-Niczyporuk, A. Bajguz, M. Talarek, M. Bralska, E. Zambrzycka, The effect of lead on the growth, content of primary metabolites, and antioxidant response of green alga *Acutodesmus obliquus* (Chlorophyceae), Environ. Sci. Pollut. Res. 22 (2015) 19112–19123. doi:10.1007/s11356-015-5118-y.

[273] O. Sytar, A. Kumar, D. Latowski, P. Kuczynska, K. Strzałka, M.N.V. Prasad, Heavy

metal-induced oxidative damage, defense reactions, and detoxification mechanisms in plants, Acta Physiol. Plant. 35 (2013) 985–999. doi:10.1007/s11738-012-1169-6.

[274] M.S. Podder, C.B. Majumder, Phycoremediation of arsenic from wastewaters by *Chlorella pyrenoidosa*, Groundw. Sustain. Dev. 1 (2015) 78–91. doi:10.1016/j.gsd.2015.12.003.

[275] Z.Y. Liu, G.C. Wang, B.C. Zhou, Effect of iron on growth and lipid accumulation in *Chlorella vulgaris*, Bioresour. Technol. 99 (2008) 4717–4722. doi:10.1016/j.biortech.2007.09.073.

[276] J.S. Yang, J. Cao, G.L. Xing, H.L. Yuan, Lipid production combined with biosorption and bioaccumulation of cadmium, copper, manganese and zinc by oleaginous microalgae *Chlorella minutissima* UTEX2341, Bioresour. Technol. 175 (2015) 537–544. doi:10.1016/j.biortech.2014.10.124.

[277] V.K. Sharma, M. Sohn, Aquatic arsenic: Toxicity, speciation, transformations, and remediation, Environ. Int. 35 (2009) 743–759. doi:10.1016/j.envint.2009.01.005.

[278] L. Pantoja Munoz, D. Purchase, H. Jones, A. Raab, D. Urgast, J. Feldmann, H. Garelick, The mechanisms of detoxification of As(III), dimethylarsinic acid (DMA) and As(V) in the microalga *Chlorella vulgaris*, Aquat. Toxicol. 175 (2016) 56–72. doi:10.1016/j.aquatox.2016.02.020.

[279] J.L. Levy, J.L. Stauber, M.S. Adams, W.A. Maher, J.K. Kirby, D.F. Jolley, Toxicity, biotransformation, and mode of action of arsenic in two freshwater microalgae (*Chlorella* sp and *Monoraphidium arcuatum*), Environ. Toxicol. Chem. 24 (2005) 2630–2639. doi:10.1897/04-580r.1.

[280] M. Srivastava, L.Q. Ma, J.A.G. Santos, Three new arsenic hyperaccumulating ferns, Sci. Total Environ. Sci. Total Environ. 364 (2006) 24–31. doi:10.1016/j.scitotenv.2005.11.002.

[281] J.Q. Xiong, M.B. Kurade, J.R. Kim, H.S. Roh, B.H. Jeon, Ciprofloxacin toxicity and its co-metabolic removal by a freshwater microalga *Chlamydomonas mexicana*, J. Hazard. Mater. 323 (2017) 212–219. doi:10.1016/j.jhazmat.2016.04.073.

[282] S. Jasrotia, A. Kansal, V.V.N. Kishore, Arsenic phyco-remediation by Cladophora algae and measurement of arsenic speciation and location of active absorption site using electron microscopy, Microchem. J. 114 (2014) 197–202. doi:10.1016/j.microc.2014.01.005.

[283] E. Afkar, H. Ababna, A.A. Fathi, Toxicological response of the green alga *Chlorella vulgaris*, to some heavy metals, Am. J. Environ. Sci. 6 (2010) 230–237. doi:10.3844/ajessp.2010.230.237.

[284] P. Kieffer, S. Planchon, M. Oufir, J. Ziebel, J. Dommes, L. Hoffmann, J.F. Hausman, J. Renaut, Combining proteomics and metabolite analyses to unravel cadmium stress-response in poplar leaves, J. Proteome Res. 8 (2009) 400–417. doi:10.1021/pr800561r.

[285] S. Gillet, P. Decottignies, S. Chardonnet, P. Le Maréchal, Cadmium response and redoxin targets in *Chlamydomonas reinhardtii*: A proteomic approach, Photosynth. Res. 89 (2006) 201–211. doi:10.1007/s11120-006-9108-2.

[286] H. Wu, X. Zhang, Q. Wang, L. Li, C. Ji, X. Liu, J. Zhao, X. Yin, A metabolomic investigation on arsenic-induced toxicological effects in the clam *Ruditapes philippinarum* under different salinities, Ecotoxicol. Environ. Saf. 90 (2013) 1–6. doi:10.1016/j.ecoenv.2012.02.022.